Fakultät für Medizin

Lehrstuhl für molekulare Allergologie

Multi-omics characterization of NSAID-exacerbated respiratory disease: Altered lipid metabolism and macrophage activation

Pascal Haimerl

Vollständiger Abdruck der von der Fakultät für Medizin der Technischen Universität München zur Erlangung des akademischen Grades eines

Doktors der Naturwissenschaften (Dr. rer. nat.)

genehmigten Dissertation.

Vorsitzender: Prof. Dr. Marc Schmidt-Supprian

Prüfer der Dissertation:

1. Prof. Dr. Carsten Schmidt-Weber

2. Prof. Dr. Matthias Feige

Die Dissertation wurde am 26.08.2019 bei der Technischen Universität München eingereicht und durch die Fakultät für Medizin am 11.02.2020 angenommen.

Declaration of content

Parts of Methods (3.2.1-3.2.3, 3.2.6-3.2.7, 3.2.9-3.2.13, 3.2.15-3.2.16, 3.3), Results (4.1, 4.3.2-4.3.4, 4.4) and Discussion (5.2, 5.3) in this thesis were adopted from our accepted manuscript “Inflammatory macrophage memory in NSAID-exacerbated respiratory disease” in the Journal of Allergy and Clinical Immunology and are described in more detail here.

月に聞て
蛙ながむる
田面かな

与謝蕪村

Table of Contents

List of Abbreviations

5-HT	5-hydroxytryptamine, serotonin	cysLT	cysteinyl leukotriene
A2M	α2 macroglobulin	CysLT1R	cysLT receptor 1
ABCA1	ATP-binding cassette sub-family A member 1	CysLT2R	cysLT receptor 2
ABCG1	ATP-binding cassette sub-family G member 1	DAMP	damage-associated molecular pattern
ACACA	acetyl-CoA carboxylase 1	DAPI	4′,6-diamidino-2-phenylindole
ACSL1	long-chain fatty acid-CoA ligase 1 (gene)	DC	dendritic cell
ADAM10	a disintegrin and metalloproteinase domain-containing protein 10	DEG	differentially expressed gene
AdipoR	adiponectin receptor	DHA	docosahexaenoic acid
ADIPOR2	adiponectin receptor 2 (gene)	dhCer	dihydroCer, sphinganine
AERD	aspirin-exacerbated respiratory disease	DMP	differentially methylated positions
AF488/568/647	Alexa Fluor 488/568/647	DMR	differentially methylated regions
AGRN	agrin	DMSO	dimethyl sulfoxide
AHR	airway hyperresponsiveness	DTT	dithiothreitol
aMDM	alveolar-like MDM	ECP	eosinophil cationic protein
AMP	adenosine monophosphate	EDTA	ethylenediaminetetraacetic acid
AMPK	AMP-activated protein kinase	EET	epoxyeicosatrienoic acid
ANOVA	analysis of variance	ELISA	enzyme-linked immunosorbent assay
APC	antigen-presenting cell	EM	electron microscopy
Apo	apolipoprotein	EMT	epithelial-mesenchymal-transition
AR	allergic rhinitis	ENT	ear, nose and throat
ASA	acetylsalicylic acid, aspirin	EP1-4	PGE_2 receptor 1-4
ASA-COX-2	aspirin-acetylated COX-2	EPA	eicosapentaenoic acid
AT	aspirin-tolerant	ESCRT	endosomal sorting complexes required for transport
ATP	adenosine triphosphate	ESI	electron spray ionization
BALF	bronchoalveolar lavage fluid	EV	extracellular vesicle
BEBM	bronchial epithelium basal medium	EXOC3L4	exocyst component 3-like protein 4
BEGM	bronchial epithelium growth medium	FACS	fluorescence-activated cell sorting
BMI	body mass index	FAO	fatty acid oxidation
C1P	ceramide-1-phosphate	FAT	fatty acid translocase
CACT	carnitine acylcarnite translocase	FBS	fetal bovine serum
CCL	CC motif chemokine ligand	FDR	false discovery rate
CCR	CC motif chemokine receptor	FESS	functional endoscopic sinus surgery
CD	cluster of differentiation	FFA	free fatty acid
CD200R1	CD200 receptor 1	FFAR	FFA receptor
CDase	ceramidase	FGF7	fibroblast growth factor 7
CEBPD	CCAAT/enhancer-binding protein delta	FIA	flow injection analysis
Cer	ceramide	FKBP5	FK506 binding protein 5
CERK	ceramide kinase	FLAP	5LO-activating protein
CerS	(dihydro)ceramide synthases	GalCDase	galactosylceramidase
CLEC	C-type lectin domain	GalCer	galactosylceramide
CoA	coenzyme A	GDF15	growth/differentiation factor 15
COL1A1	alpha-1 type I collagen	GGT	γ-glutamyl transpeptidase
COPD	chronic obstructive pulmonary disease	GluCDase	glucosylceramidase
COX	cyclooxygenase	GluCer	glucosylceramide
CPT	carnitine palmitoyl transferase	GM-CSF	granulocyte-macrophage colony-stimulating factor
CRS	chronic rhinosinusitis	GO term	gene ontology term
CRSwNP	CRS with nasal polyposis	GRCR	G protein-coupled receptors
CRTH2	chemoattractant receptor-homologous molecule expressed on Th2 cells	GUCY1A1	guanylate cyclase soluble subunit α1
CS	corticosteroid	GUCY1B1	guanylate cyclase soluble subunit β1
CXCL	CXC motif chemokine ligand	HADHA	3-hydroxyacyl-CoA dehydrogenase
CYP450	cytochrome P450	hBEC	human bronchial epithelial cell

HBSS	Hank's balanced salt solution	MRC1	mannose receptor C-type 1 (gene)
HDAC	histone deacetylase	MRM	multiple reaction monitoring
HDHA	hydroxyDHA	mRNA	messenger RNA
HDM	house dust mite	MSDC	myeloid-derived suppressor cells
HEPE	hydroxyeicosapentaenoic acid	MVB	multivesicular body
HETE	hydroxyeicosatetraenoic acid	MΦ	macrophage
HLA	human leukocyte antigen	N/A	no available
HODE	hydroxyoctadecadienoic acid	ND	not detected
HOME	hydroxyoctadecenoic acid	N-ERD	NSAID-exacerbated respiratory disease
HpETE	hydroxyperoxyeicosatetraenoic acid	NK cell	natural killer cell
HPGDS	hematopoietic PGD_2 synthase (gene)	NLF	nasal lining fluid
HPLC	high-performance LC	NLR	NOD-like receptors
HRP	horseradish peroxidase	NOD	nucleotide-binding oligomerization domain
HTR4	5-HT receptor 4, serotonin receptor 4	NP	nasal polyp
HUVEC	human umbilicial vein endothelial cells	NSAID	non-steroidal anti-inflammatory drug
ICS	inhaled corticosteroid	NTA	nanoparticle tracking analysis
IDO1	indoleamine-2,3-dioxygenase	OCS	oral corticosteroid
IF	immunofluorescence	ORMDL	orosomucoid-like
IFNγ	interferon γ	OXGR1	2-oxoglutarate receptor 1
IgE	immunoglobulin E	*p* adj.	adjusted *p*-value
IL	interleukin	PAMP	pathogen-associated molecular pattern
ILC2	group 2 innate lymphoid cells	PANK1	pantothenate kinase 1
ILV	intraluminal vesicle	PBMC	peripheral blood mononuclear cell
INCS	intranasal corticosteroid	PBS	phosphate-buffered saline
IRF4	interferon regulatory factor 4	PC	phosphatidylcholine
ITCH	itchy E3 ubiquitin protein ligase	PCA	principal component analysis
JAK	Janus kinase	PDE1A	phosphodiesterase 1A
KNN	k-nearest neighbors	PFA	paraformaldehyde
L/I/HMW	low, intermediate, high molecular weight	PG	prostaglandin
LA	linoleic acid	PGDS	PGD_2 synthase
LABA	long-acting adrenergic β_2 receptor agonist	PGFS	PGF_{2a} synthase
LacCer	lactosylceramide	PLS-DA	partial least squares-discriminant analysis
LAMA	long-acting muscarinic antagonist	PM	plasma membrane
LAMA5	laminin subunit alpha-5	PMN	polymorphonuclear leukocytes
LC-MS/MS	liquid chromatography-tandem mass spectrometry	POMC	pro-opiomelanocortin
LDHC	lactate dehydrogenase C	PPAR	peroxisome proliferator-activated receptor
LDS	lithium dodecyl sulfate	PPBP	pro-platelet basic protein, CXCL7
LEP	leptin (gene)	PRR	pattern recognition receptor
LO	lipoxygenase	PTGDS	PGD_2 synthase (gene)
LPIN1	lipin 1 (gene)	PTGER	PGE_2 receptor (gene)
LRP8	low-density lipoprotein receptor-related protein 8 (gene), ApoE receptor	PTGIS	prostacyclin synthase
LT	leukotriene	PTGS	COX (gene)
LTA4H	LTA_4 hydrolase	PUFA	polyunsaturated fatty acid
LTB	lymphotoxin-beta	PVDF	polyvinylidene fluoride
LTC4S	LTC_4 synthase	qPBS	0.2 µm-filtered PBS eluted from SEC
LX	lipoxin	RNAseq	RNA sequencing
LXR	liver-X-receptor	ROS	reactive oxygen species
lysoPC	lysophosphatidylcholine	RT	room temperature
M1 macrophage	classically-activated macrophage	S100B	S100 calcium-binding protein B
M2 macrophage	alternatively-activated macrophage	S1P	sphingosine-1-phosphate
MAPK	mitogen-activated protein kinase	$S1P_{1-5}$	S1P receptor 1-5
MDM	monocyte-derived macrophage	SABA	short-acting adrenergic β_2 receptor agonist
MeOH	Methanol	SBE	single base extension
MFI	mean fluorescence intensity	SCF	stem cell factor
MHC	major histocompatibility complex	SD	standard deviation
miRNA	microRNA	SDS	sodium dodecyl sulfate
MMP	matrix metalloproteinase	SEC	size-exclusion chromatography
mPGES-1	microsomal prostaglandin E synthase-1	SFA	saturated fatty acid

SGPP2	SPP2 (gene)
SIX5	SIX homeobox 5
SK	sphingosine kinase
SLIT	sublingual immunotherapy
SM	sphingomyelin
sMac	sputum macrophage
SMase	sphingomyelinase
SMPD3	SMase 3 (gene)
sMRM	scheduled MRM
SN	supernatant
SNOT22	sino-nasal outcome test with 22 questions
SPM	specialized pro-resolving mediator
SPP	S1P phosphatase
SPT	serine-palmitoyltransferase
STARD4	StAR-related lipid transfer protein 4
STAT	signal transducer and activator of transcription
TEI	total exosome isolation reagent
TEM	transmission electron microscopy
TGFβ	transforming growth factor β
Th1/2/17	T helper cell type 1/2/17
TLR	toll-like receptor
TNF	tumor necrosis factor α
tPA	tissue plasminogen
Treg	regulatory T cells
TSG101	tumor susceptibility gene 101
TSLP	thymic stromal lymphopoietin
TX	thromboxane
TXAS	TXA_2 synthase
VCAM1	vascular cell adhesion molecule 1
VL/I/L/HDL	very low, intermediate, low and high-density lipoproteins
ZAUM	Center of Allergy and Environment Munich
ZNF215	zinc finger protein 215
βME	β-mercaptoethanol

List of Figures

List of Tables

1 Introduction

1.1 Airway diseases

The importance and impact of airway diseases in and on modern society increases as the prevalence of allergies (rhinitis, asthma), chronic rhinosinusitis (CRS) and chronic obstructive pulmonary disease (COPD) rises worldwide (Beasley, 1998; Jean Bousquet & World Health Organization, 2007). Epidemiological studies indicate that this trend is strongly associated with the human exposome, implicating air pollution, respiratory infections, influences of the climate change on our environment and life style choices including urban living, smoking and obesity (Jean Bousquet & World Health Organization, 2007; Poole et al., 2019).

With treatment options that are often insufficient and/or expensive, and significant morbidity that negatively affects work productivity, airway diseases constitute a high social burden highlighting unmet needs for patients, health care systems and economies. Thus, the exploration of airway disease pathomechanisms and biomarkers might open new paths towards more efficient and patient-specific therapies (Bhattacharyya et al., 2019; Ivanova et al., 2012; Lewis et al., 2016; O'Neill et al., 2015).

1.1.1 Chronic Rhinosinusitis (with Nasal Polyps)

Affecting up to 12% of the Westernized population, one of the most common diseases of the upper airways is CRS (Hirsch et al., 2017; Jarvis et al., 2012; Hastan et al., 2011). Characterized by an inflammation of the nose and paranasal sinuses, CRS is diagnosed based on persistence of multiple nasal symptoms (nasal obstruction or discharge, facial pain/pressure, reduction or hyposmia) for more than 12 weeks. Severe forms of this disease involve the formation of nasal polyps (NP; termed CRSwNP), inflamed edematous tissue bulbs readily visible by nasal endoscopy and computed tomography (Figure 1.1). With the normal function of the nose disrupted and passages blocked by polypoid tissue, excess mucus cannot be drained. Nasal polyp tissue also forms a large array of pro-inflammatory mediators, resulting in the recruitment of multiple immune cell types. Chronic inflammation emerges and epithelial cells secrete additional mucus, further enhancing disease severity (Avila & Schleimer, 2008). Although CRS is a heterogenous disease and multiple endotypes exist, the most severe forms of CRSwNP are characterized by tissue eosinophilia and type 2 inflammation (Tomassen et al., 2016).

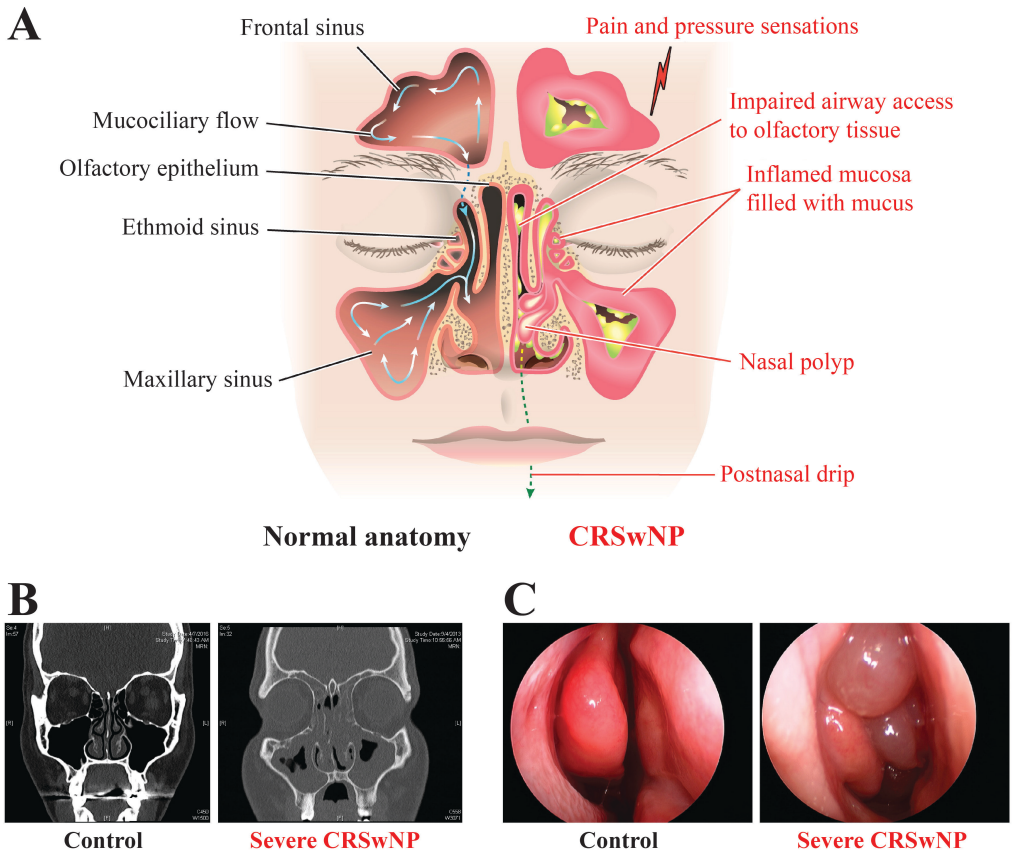

Figure 1.1 Clinical pathology of CRSwNP
A Schematic illustration of anatomical and CRSwNP-associated inflammatory features within the upper airways. Sinonasal mucosa inflammation and mucus hypersecretion impairs olfaction and nasal polyps develop, obstructing nasal airflow. **B** Computed tomography scan with inflamed mucosa (grey) and **C** endoscopical images of the nasal cavity showing the inferior turbinate and/or nasal polyps of healthy and severe CRSwNP individuals. This figure was adapted and reproduced with permission from "Immunophathogenesis of Chronic Rhinosinusitis and Nasal Polyposis" (Annual Review of Pathology: Mechanisms of Disease, Schleimer, 2017), Annual Reviews (Appendix I).

While the exact pathomechanisms are yet to be elucidated, an accepted model of CRS and nasal polyposis initiation involves epithelial injury by mechanical stressors and/or pathogens (Figure 1.2). Subsequent barrier-crossing of antigens and pathogen-associated molecular patterns (PAMPs), in conjunction with epithelial-derived damage-associated molecular patterns (DAMPs: thymic stromal lymphopoietin (TSLP), interleukin (IL)33, IL25) (Tao Liu et al., 2011; Nagarkar et al., 2013) rapidly activate group 2 innate lymphoid cells (ILC2s) (Miljkovic et al., 2014) and antigen-specific T cells with support of dendritic cells (DCs) (Hulse et al., 2013; Mechtcheriakova et al., 2011; Song et al., 2018). Epithelial cells and activated lymphocytes secrete type 2 cytokines (IL4, IL5, IL13), chemokines (e.g. eotaxins) (Stevens et al., 2015), and lipid mediators, promoting the recruitment, activation and survival of polymorphonuclear leukocytes (PMN) and

mast cells, further enhancing local inflammation (Mahdavinia et al., 2014; Takabayashi et al., 2012). Monocytes infiltrate the tissue following CC motif chemokine ligand (CCL)23 secretion by eosinophils (Poposki et al., 2011) and differentiate into alternatively-activated (M2) macrophages. A PMN- and mast cell-induced plasma leak reduces tissue plasminogen (tPa) and increases plasma-induced thrombin and fibrinogen levels in the NP tissue, enhancing an IL13-dependent crosslinking of fibrin by macrophages (via factor XIIIA), which thus contributes to fibrosis (Takabayashi, Kato, Peters, Hulse, Suh, Carter, Norton, Grammer, Cho, et al., 2013; Takabayashi, Kato, Peters, Hulse, Suh, Carter, Norton, Grammer, Tan, et al., 2013). However, a potential immune-regulatory role of macrophages in this chronic type 2 inflammation has not been described yet.

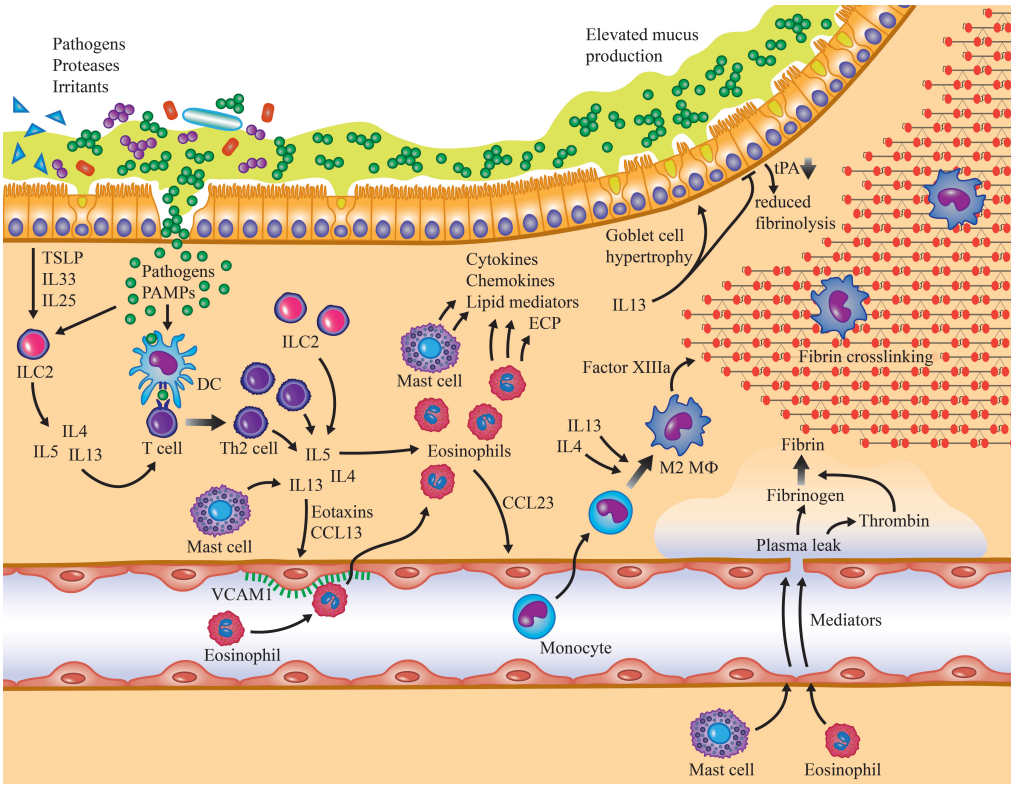

Figure 1.2 CRSwNP pathomechanism
Timeline illustration of the hypothetical model of nasal polyposis in type 2 inflammatory CRSwNP. **From left to right** External insults on the nasal epithelium activate several immune signaling cascades inducing a type 2 inflammation. T cells, eosinophils, mast cells and monocytes are recruited and secret mediators augmenting inflammation, edema and fibrosis. ECP, eosinophil cationic protein; MΦ, macrophage; Th2 cell, T helper cell type 2; VCAM1, vascular cell adhesion molecule 1. This figure was adapted and reproduced with permission from "Immunophathogenesis of Chronic Rhinosinusitis and Nasal Polyposis" (Annual Review of Pathology: Mechanisms of Disease, Schleimer, 2017), Annual Reviews (Appendix I).

Together with the upper airways, the lower airways are commonly affected by chronic type 2 inflammation. Indeed, the concept of united airways emerged in the 1990s (Passalacqua, 2000) and describes the functional unity of the upper and lower airways (Slavin, 2008; Stachler, 2015). This concept is based on the common histological and anatomical tissue characteristics and the functional dependencies between both sections of the airways, with the nose acting as guardian for the lung by filtering, heating and humidifying the inhaled air. In addition, immune phenotypes in airway inflammation are shared, as allergic rhinitis and rhinosinusitis can induce infiltration of proinflammatory leukocytes, including eosinophils, in the lung and *vice versa* (van Ree, Hummelshøj, Plantinga, Poulsen, & Swindle, 2014; Bhimrao, Wilson, & Howarth, 2011; Beeh et al., 2003; Ponikau et al., 2003). Indeed, epidemiological studies revealed comorbid diseases of upper and lower airways to be common, as 80% of allergic asthma patients have allergic rhinitis (AR) and up to 40% of AR patients suffer from allergic asthma (J. Bousquet et al., 2008). A similar linkage has been shown in European CRS patients, of which 25-70% have comorbid asthma (Bachert, Zhang, & Gevaert, 2015; Settipane & Chafee, 1977).

1.1.2 Asthma

Asthma is a chronic inflammatory disease of the lower airways and affects over 300 million individuals worldwide (Jean Bousquet & World Health Organization, 2007). It is characterized by recurrent events of wheezing, dyspnea/breathlessness, chest tightness and cough. Exposure to allergens, airway infection, lack of therapy-adherence and/or social economic stress can worsen symptoms and expiratory flow, evoking an acute asthma exacerbation that can even be life-threatening and demands intensive care (Murray, 2006; Pendergraft et al., 2004). Early treatment can revert symptoms, yet chronic inflammatory insults cause an irreversible remodeling of the lung (Pauwels et al., 2003; Reddel et al., 2015). Resembling CRS, this remodeling process is characterized by basal membrane and mucosal thickening, submucosal gland hypertrophy and collagen deposition which progressively enhances airflow obstruction and airway hyperresponsiveness (AHR) (Figure 1.3, bottom) (Ponikau et al., 2003).

Originally, asthma is initialized by allergens, microbes, irritants or pollutants that damage the epithelial barrier and/or are recognized by its pattern recognition receptors (PRRs). This induces various pro-inflammatory pathways, activating local and recruiting peripheral leukocytes (eosinophils, mast cells, macrophages, neutrophils, DCs, T cells) ultimately leading to chronic inflammation and tissue remodeling (Figure 1.3) (Fahy, 2015). Coinciding with CRS (Tomassen et al., 2016), two main endotypes of asthma exist. These can be distinguished by a non-type 2 inflammation, associated with tissue neutrophilia, and a type 2 inflammation, characterized by tissue eosinophilia. Both endotypes can advance into severe forms of asthma that are frequently resistant to CS treatment (Lachowicz-Scroggins et al., 2019; Lemanske & Busse, 2003; S. E. Wenzel et al., 1999; Yeh et al., 2018).

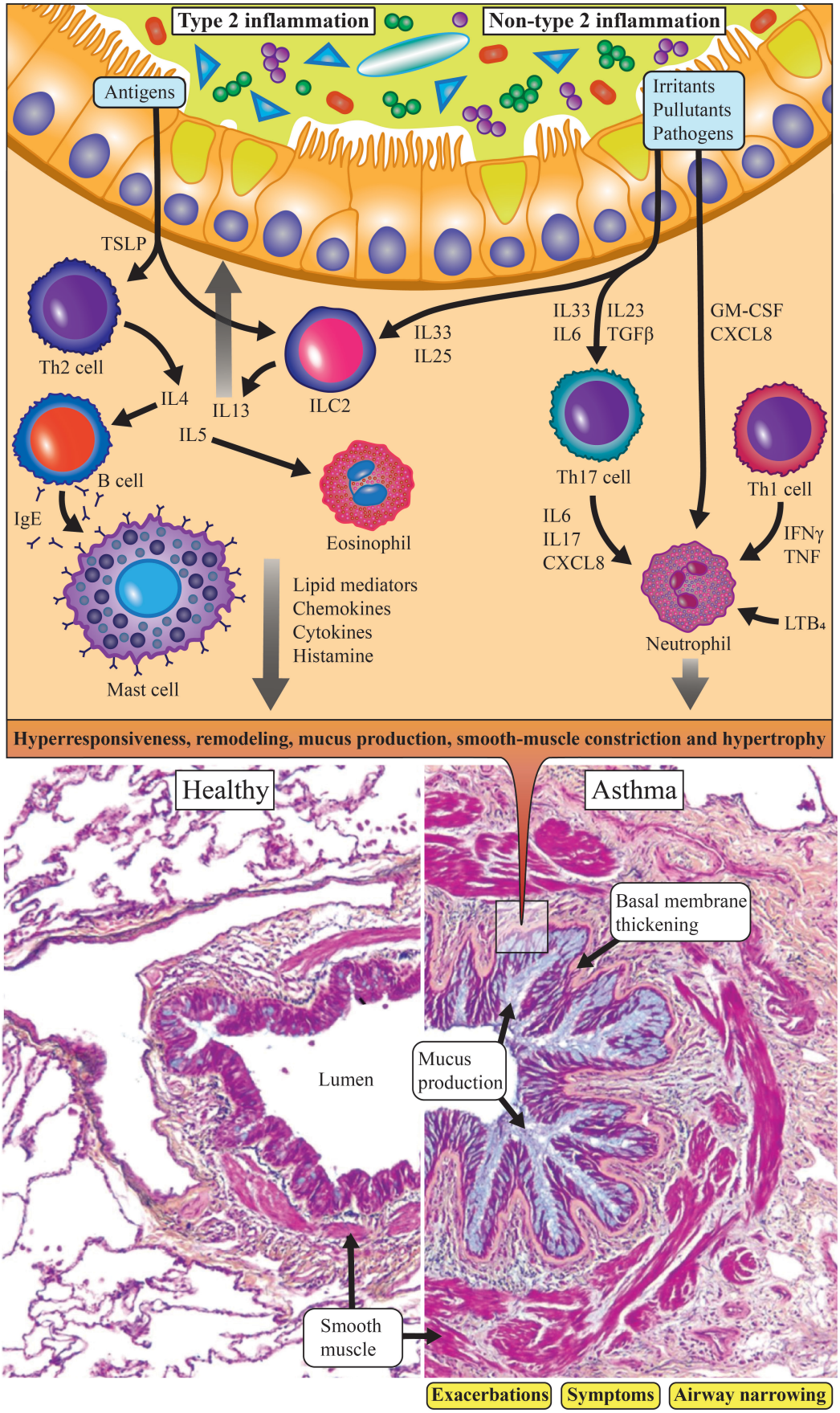
Type 2 inflammation
Non-type 2 inflammation
Antigens
Irritants
Pullutants
Pathogens
TSLP
Th2 cell
IL4
IL13
IL5
ILC2
IL33
IL25
IL33
IL6
IL23
TGFβ
GM-CSF
CXCL8
B cell
IgE
Eosinophil
Th17 cell
Th1 cell
IL6
IL17
CXCL8
IFNγ
TNF
LTB4
Neutrophil
Mast cell
Lipid mediators
Chemokines
Cytokines
Histamine
Hyperresponsiveness, remodeling, mucus production, smooth-muscle constriction and hypertrophy
Healthy
Asthma
Basal membrane thickening
Mucus production
Lumen
Smooth muscle
Exacerbations
Symptoms
Airway narrowing

Figure 1.3 Asthma pathology
Schematic illustration of type 2 and non-type 2 asthma-associated inflammatory features within a section of the lower airways. **Top left** Type 2 inflammation is initialized by antigen recognition and/or epithelial insult by irritants, pollutants or pathogens resulting in TSLP, IL33 and IL25 release. ILC2s and Th2 cells are activated and secrete type 2 cytokines (IL4, IL5, IL13), further eliciting the inflammatory cascade by recruiting and stimulating B cells, mast cells and eosinophils. Effector mediators (e.g. IL3, IL4, IL5, IL9, IL13, leukotrienes, prostaglandin (PG)D_2) amplify the type 2 inflammation and induce AHR, remodeling, mucus hyperproduction, airway smooth muscle constriction and hypertrophy. **Top right** Irritants, pollutants and pathogens can also initialize non-type 2 inflammation through IL33 and IL6 signaling that activate T helper cells type 17 (Th17). Th17-derived mediators recruit and activate T helper cells type 1 (Th1) and neutrophils. A neutrophilic inflammation is established and leads to AHR, remodeling, mucus hyperproduction, ASM constriction and hypertrophy. **Bottom** Severe asthma airway pathology that causes exacerbations, symptoms and airway obstruction is shown in histopathological sections of asthmatic bronchi **(right)** and compared to healthy control tissue **(left)**. CXCL8, CXC motif chemokine ligand 8; GM-CSF, granulocyte-macrophage colony-stimulating factor; IgE, immunoglobulin E; IFNγ, interferon γ; LTB_4, leukotriene B_4; TGFβ, transforming growth factor β; TNF, tumor necrosis factor α. This figure was adapted and reproduced with permission from "Severe and Difficult-to-Treat Asthma in Adults" (The New England Journal of Medicine, Israel & Reddel, 2017), Copyright Massachusetts Medical Society, and from "Clinical update on the use of biomarkers of airway inflammation in the management of asthma" (Journal of Asthma and Allergy, Wadsworth, Sin, & Dorscheid, 2011), Copyright Dove Medical Press Ltd. (Appendix II).

1.1.3 NSAID-exacerbated respiratory disease

Individuals with non-steroidal anti-inflammatory drug (NSAID)-exacerbated respiratory disease (N-ERD) suffer from a medical triad of both CRSwNP and asthma and show a severe hypersensitivity reaction after intake of NSAIDs, including aspirin (acetylsalicylic acid, ASA). First described in 1922 by Widal et al. (Widal, Abrami, & Lermoyez, 1987) and clinically characterized by Samter and Beers in 1968 (Samter & Beers, 1968), this disease is also known as Widal's triad, Samter's triad and aspirin-exacerbated respiratory disease (AERD).

N-ERD develops typically in the 3rd to 4th decade of life and begins with CRS, followed by nasal polyposis, asthma and NSAID-intolerance 1 to 5 years later (A. Szczeklik, Niżankowska, Duplaga, & the Aiane Investigators, 2000). Though risk factors for N-ERD including N-ERD family history, CRSwNP, asthma, atopy (S. Bavbek et al., 2012; Stevens et al., 2017) and (epi-)genetic modifications in the arachidonic acid (AA) metabolism (Dahlin & Weiss, 2016) are known, the initial cause and the underlying pathomechanisms remain incompletely understood.

The exact prevalence of N-ERD is unknown. However, 10% of adults with CRSwNP or asthma suffer from N-ERD (Rajan, Wineinger, Stevenson, & White, 2015) and prevalence surges to approximately 15% and 20% when individuals are subgrouped for

severe asthma (Mascia et al., 2005; Rajan et al., 2015) and NSAID hypersensitivity (C. Jenkins, Costello, & Hodge, 2004; Makowska et al., 2016), respectively. Hypersensitivity reactions towards NSAID develop fast. They begin in the upper airways (rhinorrhea, nasal congestion) about 30 minutes after intake and rapidly progress to the lower airways, eliciting an acute asthma exacerbation (wheezing, coughing, dyspnea) after 180 minutes the latest (Yoshimine et al., 2005). Severity and pace of progression are asthma control- and dose-dependent (Sevim Bavbek, Celik, Demirel, & Misirligil, 2003; Hope, Woessner, Simon, & Stevenson, 2009), as unstable asthmatics are more prone to develop drastic bronchospasm and might die during exacerbations (Yoshimine et al., 2005).

The N-ERD pathogenesis is similar to those of severe type 2 CRSwNP and asthma but shows an even more pronounced chronic tissue eosinophilia, which is related to abnormal changes in the AA metabolism that causes the NSAID-intolerance (A. Szczeklik et al., 2000). In brief, non-selective NSAIDs inhibit the cyclooxygenase 1 (COX-1) which processes AA to the potent anti-inflammatory lipid mediator prostaglandin (PG)E_2. Due to reduced levels of PGE_2, its immune-regulatory effects are overruled by proinflammatory responses, which are further enhanced by the shunting of excess AA into the 5-lipoxygenase (5-LO) pathway. Thus, robust inducers of inflammation, the cysteinyl leukotrienes (cysLTs), are produced and secreted, which enhance type 2 inflammatory responses in the airways and ultimately elicit an exacerbation (Figure 1.4) (Cahill & Boyce, 2017). This is accompanied by a general deficiency in PGE_2 synthesis and signaling as not only PGE_2 production is reduced due to lower expression of COX-2, but also PGE_2 receptor expression and functionality is impaired in N-ERD (Sang-Heon Kim et al., 2007; T. Liu, Laidlaw, Katz, & Boyce, 2013; Ying et al., 2006). In contrast, basal levels of the proinflammatory and stable cysLT leukotriene (LT)E_4 are increased in the sputum/exhaled breath condensate and urine and further elevated after aspirin intake (Antczak, Montuschi, Kharitonov, Gorski, & Barnes, 2002; Daffern, Muilenburg, Hugli, & Stevenson, 1999; Gaber et al., 2008; Mastalerz et al., 2014). The number of cells expressing the major pro-inflammatory cysLT receptor CysLT1R is increased in NPs of N-ERD patients as well (A. R. Sousa, Parikh, Scadding, Corrigan, & Lee, 2002).

The main type 2 cytokine IL4 has been implicated in the N-ERD-specific alterations of the arachidonic acid metabolism, as *in vitro* stimulations have shown that IL4 induces the expression of the CysLT1R and/or CysLT2R in mast cells (E. A. Mellor et al., 2003; Elizabeth A. Mellor, Austen, & Boyce, 2002), T cells, B cells, and eosinophils (Early et al., 2007). IL4 stimulation of monocytes enhanced the expression of both cysLT receptors as well (Thivierge, Stankova, & Rola-Pleszczynski, 2001), but also reduced COX-2 and microsomal prostaglandin E synthase-1 (mPGES-1) expression, major enzymes necessary for PGE_2 synthesis (Dworski & Sheller, 1997; Steinke, Payne, & Borish, 2012). Eosinophils and mast cells, key producers of cysLTs, are the drivers of tissue inflammation as their numbers are higher and they are more activated in N-ERD airway tissue in comparison to aspirin-tolerant (AT) controls (Mita et al., 2001; Nasser et al., 1996; Varga et al., 1999). Epithelial cells are not only the initiators of type 2 airway

inflammation by secreting TSLP and IL33 in response to external stimuli and tissue damage, they also actively contribute to the established inflammation with increased secretion of stem cell factor (SCF), a factor that recruits and activates mast cells (M. L. Kowalski et al., 2005). Indeed, mast cell-derived PGD_2 was abundant in the upper and lower airways in N-ERD (Buchheit et al., 2016). A pathogenic role of type 2 innate lymphoid cells (ILC2s) has recently been implicated as well, as they are recruited to the airways and further elicit the type 2 inflammation by secretion of IL4, IL5 and IL13 (White & Doherty, 2018).

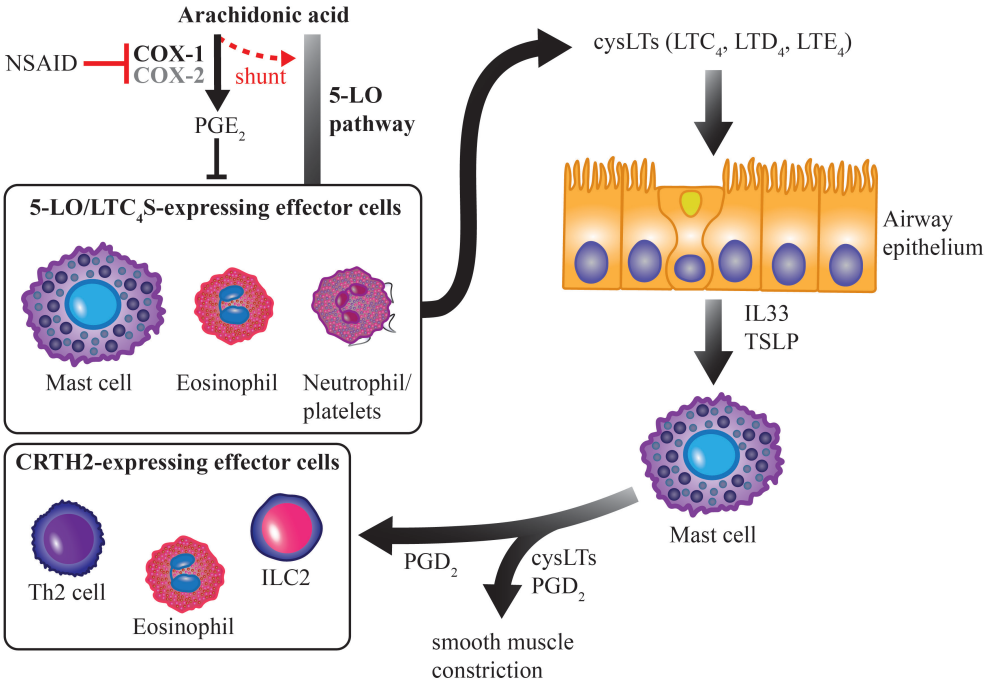

Figure 1.4 N-ERD insensitivity pathomechanism
NSAID inhibition of COX-1 in conjunction with lower expression of COX-2 diminishes PGE_2 production and thus effector cell inhibition in N-ERD patients. Arachidonic acid is shunted into the 5-LO pathway and converted to cysLTs by 5-LO/LTC_4 synthase (LTC_4S)-expressing effector cells, which act on the airway epithelium. IL33 and TSLP is secreted by epithelial cells and activate mast cells, which produce cysLTs and PGD_2. ILC2, Th2 cells and eosinophils are recruited via PGD_2/chemoattractant receptor-homologous molecule expressed on Th2 cells (CRTH2)-signaling and secreted cysLTs and PGD_2 induce airway smooth muscle constriction and thus asthma exacerbation. This figure was adapted and reproduced with permission from "Aspirin-exacerbated respiratory disease: Mediators and mechanisms of a clinical disease" (Journal of Allergy and Clinical Immunology, Cahill & Boyce, 2017), Elsevier (Appendix III).

1.1.4 Airway disease treatment – an unmet clinical need

Management of CRSwNP is difficult (Fokkens et al., 2012). All currently available therapeutic options described in the following section are summarized in Table 1.1. Standard therapy includes nasal saline irrigation and intranasal corticosteroids (INCS). Severe forms of CRSwNP are treated with short-term (4-weeks) oral corticosteroids (OCS, methylprednisolone). Though OCS reduce polyp size and symptoms dramatically, improvements often rapidly worsen after OCS treatment (Van Zele et al., 2010). Indeed, long-term treatment with OCS is contraindicated due to serious side-effects such as osteoporosis and Cushing's syndrome and is associated with increased mortality (Ekström et al., 2019; Sharma & Nieman, 2011). Conclusively, functional endoscopic sinus surgery (FESS) is the only option left. The removal of NP tissue has an immense impact on symptoms, restoring olfaction and minimizing the need for other medication (Senior et al., 1998). However, 80% of all patients experience a relapse over a period of 12 years, with 37% undergoing revision surgery (Benninger, Sindwani, Holy, & Hopkins, 2015). The development of biologicals introduced a new therapy regiment on top of classical treatment. Specifically targeting type 2 inflammation, omalizumab (anti-IgE), mepolizumab (anti-IL5) and dupilumab (anti-IL4/IL13) were the first of this new class of drugs to substantially improve symptom burden and reduce nasal polyp size (Bachert et al., 2016, 2017; Gevaert et al., 2013, 2011).

Asthma management is aiming for a long-term control of symptoms and effective treatment of acute exacerbations (Bateman et al., 2008; Reddel et al., 2015). As for CRSwNP, persistent asthma management is difficult and the treatment regimen changes with disease severity. Gold standard is the use of inhaled corticosteroids (ICS, such as fluticasone propionate) which significantly reduce asthma symptoms and the risk of exacerbations, increase lung function, quality of life and curtail asthma-related hospitalizations and death (Adams, Bestall, Malouf, Lasserson, & Jones, 2005; O'Byrne et al., 2001; Pauwels et al., 2003; Suissa, Ernst, Benayoun, Baltzan, & Cai, 2000). Most asthmatics can be controlled with ICS and the use of short-acting adrenergic β_2 receptor agonists (SABA, e.g. salbutamol) for mild or long-acting adrenergic β_2 receptor agonists (LABA, e.g. formoterol) for moderate and severe asthma, which induce a relaxation of the airway smooth muscles and diminish bronchoconstriction (Lemanske & Busse, 2003). However, steroid-insensitive and steroid-resistant subendotypes of asthma exist, which only take effect for high doses of ICS, OCS treatment or not at all, respectively (Barnes, 2013). Genetic and epigenetic alterations in glucocorticoid receptors, including binding affinity, nuclear translocation and expression on peripheral blood mononuclear cells (PBMCs), have been identified to be involved in steroid-insensitivity (Barnes, 2013). In addition, high ICS doses demanded by increased disease severity can cause steroid-insensitivity (Sher et al., 1994; Woodruff et al., 2007). The use of leukotriene receptor antagonists (montelukast) is less effective than ICS treatment, but recommended in case of adverse effects or insensitivity to ICS, comorbid AR or N-ERD (Chauhan & Ducharme, 2012; Philip et al., 2004).

Optional treatment choices for severe asthmatic and patients with a high risk of and/or frequent exacerbations are long-acting muscarinic antagonists (LAMA, e.g. tiotropium), invasive bronchothermoplasty, OCS and biologicals (Bateman et al., 2008). LAMA are inhibitors of airway smooth muscle contraction and show effects independent of atopy and ICS-resistance (Kerstjens et al., 2016).

In refractory and/or uncontrolled type 2 asthma with eosinophilia and CRSwNP, biologicals may be used and have a strong impact on disease pathology. Thus, quality of life and lung function increase significantly while the need for OCS and frequency of exacerbations decrease (S. Wenzel et al., 2016; Bleecker et al., 2016; Bjermer et al., 2016; Hanania et al., 2011).

The concept of united airways links not only pathomechanisms of upper and lower airway diseases together, but also local treatment approaches that influence the whole airways. The use of INCS in AR improves comorbid asthma (Lohia, Schlosser, & Soler, 2013). Indeed, sublingual immunotherapy (SLIT) in house dust mite (HDM) allergic patients improved disease severity in upper and lower airways and reduced the exacerbation frequency in mild and moderate asthmatics (Asamoah et al., 2017; Virchow et al., 2016). In addition, FESS of CRSwNP patients with comorbid asthma improved all symptom scores and lung function and reduced medication and number of hospitalizations (Benninger, Sindwani, Holy, & Hopkins, 2016; F. Chen et al., 2014; Rix, Håkansson, Larsen, Frendø, & von Buchwald, 2015). However, the major challenge in asthma management is to prevent airway remodeling by airway smooth muscles, which is only addressed by high doses of CS (Feltis et al., 2007; K. Wang, Liu, Wu, Feng, & Bai, 2008), but regularly accompanied by side effects and a lower quality of life (Sweeney et al., 2016).

N-ERD constitutes one of the most severe endotypes in both CRSwNP and asthma (J. Bousquet et al., 2008; Ta & White, 2015; Tomassen et al., 2016). Thus, treatment revolves around the use of INCS, ICS with LABA and cycles of OCS and recurrent FESS. In addition, leukotriene receptor antagonists (montelukast) and zileuton, an inhibitor of 5-LO, which is one of the key enzymes in LT synthesis, are used (S.-E. Dahlén et al., 2002; Tanya M. Laidlaw, Fuentes, & Wang, 2017; Ta & White, 2015). Adjunctive aspirin-desensitization therapy in combination with a low salicylate diet has been shown to improve symptom burden (after FESS) and is associated with reduced cysLT and IL4 levels (Berges-Gimeno, Simon, & Stevenson, 2003; Sommer et al., 2016). However, non-responding subendotypes exist, driving the demand for a detailed immuno-pathophysiological characterization and patient-specific therapeutic approaches (Bochenek et al., 2014; H. Y. Lee et al., 2017).

Improvement of airway disease management is imminent with the development of a wide variety of biologics, though treatment is limited for the most severe type 2 inflammatory endotypes as clinical trials are ongoing and treatment costs are high.

Table 1.1 Overview of current airway disease treatment options

Treatment	Drug	Mechanism of action	Indication	Endotype
saline irrigation	Sodium chloride solution	clearance of mucosa	CRSwNP N-ERD	all
non-sedating antihistamines	Cetirizine, Loratadine	histamine receptor H1 inhibition	CRSwNP N-ERD	mild atopy, uncontrolled
allergen immunotherapy	common aeroallergens	desensitization of immune system	CRSwNP Asthma (N-ERD)	(clear) seasonal/chronic atopy-related symptoms
corticosteroids (CS)	intranasal (INCS): Mometasone	immunosuppression	CRSwNP N-ERD	all
	inhaled (ICS): Fluticasone, Budesonide, Beclomethasone		Asthma N-ERD	all
	oral (OCS): Methylprednisolone		CRSwNP Asthma* N-ERD*	short-term or continuous* in severe and uncontrolled disease
β_2 agonists	short-acting (SABA): Salbutamol, Fenoterol	airway smooth muscle relaxation	Asthma	mild, intermittent
	long-acting (LABA): Formoterol, Salmeterol		Asthma N-ERD	moderate, severe
long-acting muscarinic-receptor agonists (LAMA)	Tiotropium	airway smooth muscle relaxation, reduction of mucus secretion	Asthma N-ERD	uncontrolled, severe
non-steroidal anti-inflammatory drugs (NSAIDs)	avoidance: Aspirin, Ibuprofen, Indomethacin, Diclofenac, Paracetamol, Naproxen, …	no NSAID-insensitivity reactions	N-ERD	all
	desensitization: Aspirin	unclear, positive effect on arachidonic acid metabolism		after FESS
leukotriene modifiers	Montelukast	CysLT1R-antagonist	CRSwNP Asthma N-ERD	uncontrolled, severe, steroid-resistance/ insensitivity
	Zileuton	inhibition of 5-LO		
biologicals	Omalizumab	FcεR-binding site on IgE	CRSwNP Asthma N-ERD	severe atopy
	Mepolizumab	circulating IL5		severe eosinophilia/ type 2 inflammation
	Reslizumab	circulating IL5		
	Benralizumab	IL5R on eosinophils, induces lysis		
	Dupilumab	common receptor subunit of IL4R and IL13R		
	Fevipiprant	CRTH2 (PGD_2 receptor)		
FESS	prior to surgery: OCS	NP tissue removal	CRSwNP N-ERD	uncontrolled, severe

1.2 Lipid mediators: the eicosanoid family

Intercellular communication and pathway activation in immune responses is not only mediated by classes of peptides and (glyco-)proteins, namely cytokines and chemokines, or soluble gases (NO, H_2S). Multiple lipid species have been shown to be specifically produced and secreted by several cell types in inflammation and exhibit a strong effect on their local cellular environment (T. Shimizu, 2009). Key lipid mediators are summarized in Table 1.2. The most prominent and functionally diverse lipid mediator family is the one of eicosanoids.

Table 1.2 Key lipid mediators and their functions

PUFA	Pathway	Lipid mediator	Physiological functions	References
AA	COX	PGD_2	chemotaxis lymphocytes ↑, PMN ↑ vascular permeability ↑ AHR ↓	Hirai et al., 2001; Johnston, Freezer, Ritter, O'Toole, & Howarth, 1995; Larsson, Hagfjärd, Dahlén, & Adner, 2011; Salimi et al., 2017; Smyth, Grosser, Wang, Yu, & FitzGerald, 2009; Xue et al., 2015
		PGE_2	anti-inflammatory macrophages ↑ chemotaxis + activation mast cells ↓, eosinophils ↓ airway remodeling ↓	Draijer et al., 2016; S. K. Huang et al., 2008; Peachell, MacGlashan, & Lichtenstein, 1988; Smyth et al., 2009; Sturm et al., 2008
		TXA_2	recruitment + activation platelets ↑ leukocyte extravasation ↑ bronchoconstriction ↑	Bureau, De Clerck, Lefort, Arreto, & Vargaftig, 1992; Ishizuka et al., 1998; Smyth et al., 2009
	5-LO	LTB_4	recruitment PMN ↑, monocytes ↑, macrophages ↑	Palmblad et al., 1981; M. J. Smith, Ford-Hutchinson, & Bray, 1980
		cysLTs: LTC_4 LTD_4 LTE_4	vascular permeability ↑ bronchoconstriction ↑ airway remodeling ↑ mucus secretion ↑ brush cell proliferation ↑	Bankova et al., 2018; Beller, Maekawa, Friend, Austen, & Kanaoka, 2004; Dahlen et al., 1983; Dahlén, Hedqvist, Hammarström, & Samuelsson, 1980; Henderson et al., 2002
	5-/12-/15-LO	LXA_4	efferocytosis, survival macrophages ↑ recruitment, function, survival PMN ↓	D. El Kebir et al., 2007; Driss El Kebir et al., 2009; Godson et al., 2000; Prieto et al., 2010
		LXB_4		
		15-HETE	anti-inflammatory macrophages ↑ function neutrophils ↓ LX synthesis ↑	J. T. Huang et al., 1999; Ricote, Welch, & Glass, 2000; C. N. Serhan & Reardon, 1989
LA		13-HODE	anti-inflammatory macrophages ↑	J. T. Huang et al., 1999; Ricote et al., 2000
DHA	15-LO	RvD1-6	phagocytosis macrophages ↑ activation + function T cells ↓ airway eosinophilia ↓ AHR ↓	Chiurchiù et al., 2016; Rogerio et al., 2012
EPA	CYP450, ASA-COX-2	RvE1-3	anti-inflammatory macrophages ↑ function, survival neutrophils ↓	D. El Kebir, Gjorstrup, & Filep, 2012; Isobe et al., 2012; Oh et al., 2012

PUFA, polyunsaturated fatty acid; AA, arachidonic acid; LA, linoleic acid; DHA, docosahexaenoic acid; EPA, eicosapentaenoic acid; CYP450, cytochrome P450; ASA-COX-2, aspirin-acetylated COX-2; TXA_2, thromboxane A_2; LXA_4/B_4, lipoxin A_4/B_4; RvD/E, resolvin D/E

1.2.1 The arachidonic acid metabolism: eicosanoid biosynthesis

Lipid mediators of the eicosanoid family derive from the 20-carbon polyunsaturated fatty acid (PUFA) AA. Numerous enzymes can metabolize AA into four eicosanoid subfamilies with distinct physiological functions: prostanoids, leukotrienes (LTs), hydroxyeicosatetraenoic acids (HETEs) and epoxyeicosatrienoic acids (EETs) (Figure 1.5) (T. Shimizu, 2009).

Prostanoids (prostaglandins (PGs), prostacyclins, thromboxanes (TXs)) are products of the COX pathway. They are involved in several physiological processes, contributing to inflammation and injury (fever, pain), uterine contraction, renal function and cardiovascular homeostasis (Smyth et al., 2009). Two isoforms of COX exist: COX-1, which is constitutively expressed in most cells, and the inducible COX-2, which is primarily expressed during inflammatory events (W. L. Smith & Langenbach, 2001). The COX enzymes metabolize AA to PGH_2, which is further converted by one of five isoform-specific synthases into PGD_2 (by PGD_2 synthase; PGDS), PGE_2 (mPGES-1), $PGF_{2\alpha}$ ($PGF_{2\alpha}$ synthase, PGFS), PGI_2 (prostacyclin synthase, PTGIS) and thromboxane TXA_2 (TXA_2 synthase, TXAS) (Figure 1.5). Both COX-isoforms are targets of inhibition by NSAIDs (T. Shimizu, 2009; W. L. Smith & Langenbach, 2001).

LTs derive from the 5-LO pathway and can be divided by structure and physiological function into cysLTs (LTC_4, LTD_4, LTE_4) and LTB_4 (Figure 1.5). AA is first converted by 5-LO to the common progenitor LTA_4, which can either be hydrolyzed to LTB_4 by the LTA_4 hydrolase (LTA_4H) (Maycock, Anderson, DeSousa, & Kuehl, 1982) or metabolized to LTC_4 by the glutathione transferase LTC_4 synthase (LTC_4S) (Jakschik, Harper, & Murphy, 1982). Consecutive cleavage of the peptide moiety by γ-glutamyl transpeptidase (GGT) and dipeptidase generates LTD_4 and LTE_4, respectively (Anderson, Allison, & Meister, 1982; C. W. Lee, Lewis, Corey, & Austen, 1983). LTs are predominantly produced by myeloid cells and are strong inducers of chemotaxis (LTB_4) and regulators of immune cell activation, vascular permeabilization and smooth muscle contraction (cysLTs) (Marc Peters-Golden & Henderson, 2007). Their effects are exerted locally, as they are short-lived (seconds to minutes) and rapidly metabolized by ω- and degraded by β-oxidation *in vivo* (R. C. Murphy & Gijón, 2007).

HETEs are another group of AA-derived immunoregulatory eicosanoids and are generated by the three lipoxygenases 5-/12-/15-LO (Figure 1.5) ((J. T. Huang et al., 1999; C. N. Serhan & Reardon, 1989). Cytochrome P450 epoxygenases can metabolize AA to EETs, which exert anti-inflammatory and vasodilatory effects (Figure 1.5) (Spector, 2009).

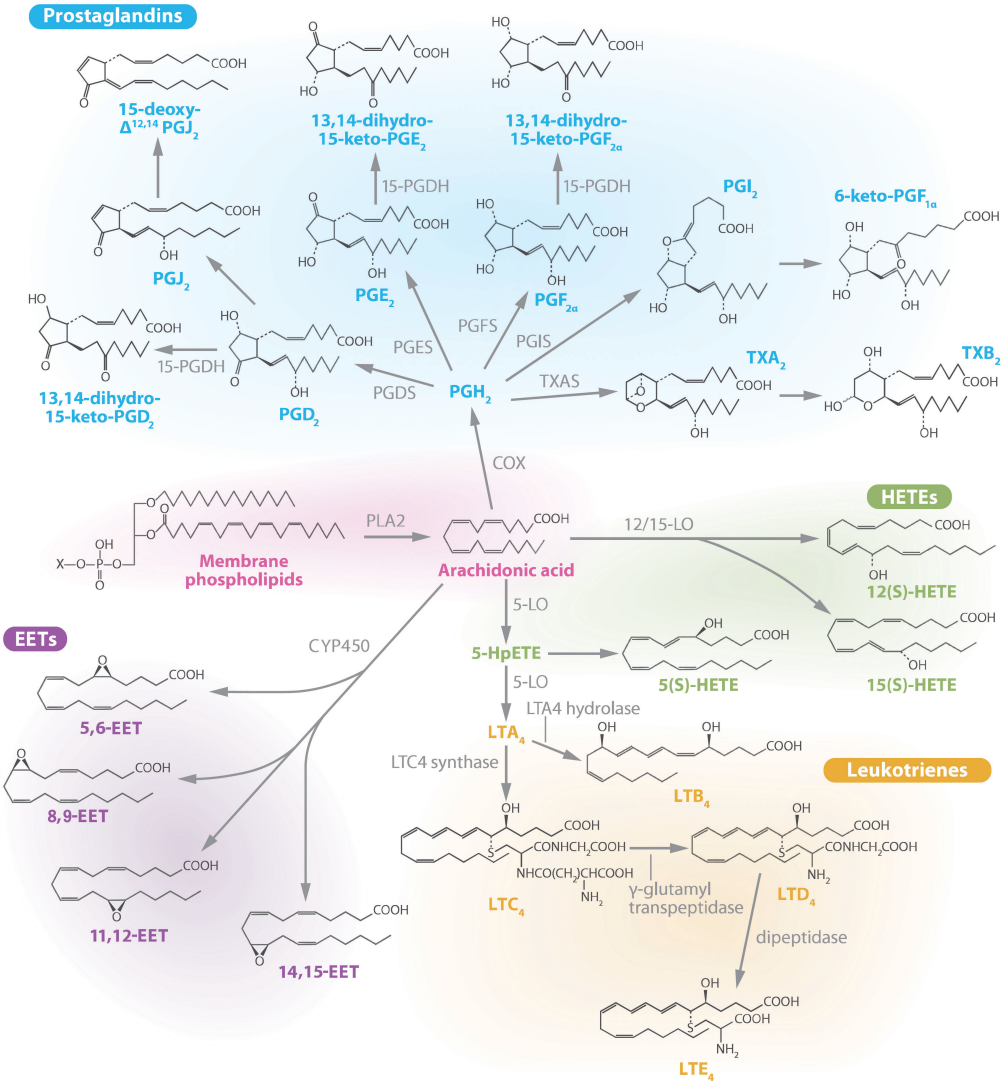

Figure 1.5 Eicosanoid biosynthesis pathways
Membrane phospholipid-derived arachidonic acid **(pink)** can be converted into several immunomodulatory prostaglandins **(blue)**, leukotrienes **(orange)**, HETEs **(green)** and EETs **(purple)** with physiological functions by several enzyme cascades. This figure was adapted and reproduced with permission from "Lipid Mediators in Health and Disease: Enzymes and Receptors as Therapeutic Targets for the Regulation of Immunity and Inflammation" (Annual Review of Pharmacology and Toxicology, T. Shimizu, 2009), Annual Reviews (Appendix IV).

1.2.2 Eicosanoids in type 2 airway inflammation

Eicosanoids are crucial in immune responses, as they are potent mediators that elicit, augment or resolve inflammation. A dysregulation of the AA metabolism is part of the pathogenesis of the type 2 airway diseases CRSwNP, asthma and especially N-ERD.

Increased levels of pro-inflammatory LTs were found in the bronchoalveolar lavage fluid (BALF) and urine of asthmatics and N-ERD patients (Gaber et al., 2008; Micheletto et al., 2010; S. E. Wenzel, Larsen, Johnston, Voelkel, & Westcott, 1990). Binding to their G protein-coupled receptors (GPCRs) CysLT1R and CysLT2R (Heise et al., 2000; Lynch et al., 1999), LTC_4 and LTD_4 enhance mucus secretion and induced bronchoconstriction and edema (S. E. Dahlén et al., 1983, 1980). Bronchoconstriction and binding capacities of LTE_4 to CysLT1R and CysLT2R are weak (Heise et al., 2000; Lynch et al., 1999). Recently, LTE_4 was demonstrated to bind with high affinity to the epithelial cell receptor CysLT3R (also known as 2-oxoglutarate receptor 1 (OXGR1) and GPR99) (Kanaoka, Maekawa, & Austen, 2013) and induce airway brush cell proliferation in a murine model of type 2 lung inflammation (Bankova et al., 2018). Murine models of airway inflammation also implicate a role of cysLTs in fibrosis and airway remodeling (Beller et al., 2004; Henderson et al., 2002), as treatment with the CysLT1R inhibitor montelukast was sufficient to block these remodeling processes in both mice and men (Henderson, Chiang, Tien, & Chi, 2006; Kelly et al., 2006). LTB_4 binds to its two GPCRs BLT1R and BLT2R and is one of the most potent inducers of chemotaxis of neutrophils, monocytes and macrophages (Palmblad et al., 1981; M. J. Smith et al., 1980).

The functions of the prostanoid PGD_2 resemble those of LTs. Binding of its stable metabolite $9\alpha11\beta\text{-}PGF_2$ to the thromboxane receptor (TP) induces bronchoconstriction (Johnston et al., 1995; Larsson et al., 2011), while the binding of PGD_2 to the PGD_2 receptor (CRTH2) on eosinophils and Th2 cells demonstrates strong chemoattractive properties (Hirai et al., 2001). PGD_2 is the main COX product of mast cells (Mita et al., 2001). Mast cells are present in elevated numbers in the upper (Takabayashi et al., 2012) and lower airways (Dougherty et al., 2010) and strongly drive type 2 inflammation in a TSLP-dependent manner (Buchheit et al., 2016). Mast cells, together with eosinophils, are particular sources of cysLTs (Mita et al., 2001; Nasser et al., 1996) and their effects are even more pronounced in N-ERD due to elevated COX-2 expression (A. Sousa et al., 1997), PGD_2 production (Buchheit et al., 2016), PGE_2 resistance (Tanya M. Laidlaw et al., 2014) and increased numbers of CysLT1R-expressing cells in NPs (A. R. Sousa et al., 2002). CysLTs and PGD_2 furthermore synergistically induce the infiltration and activation of ILC2s and Th2 cells, resulting in a profound production of type 2 cytokines (IL4, IL5, IL13) (Salimi et al., 2017; Xue et al., 2015). Recent studies have shown that macrophages and epithelial cells, including brush cells, are additional sources of LTs in airway inflammation (Dietz et al., 2017; Finney-Hayward et al., 2009; Shamsuddin, Hsueh, & Smith, 1992; Ualiyeva, Hallen, Kanaoka, Barrett, & Bankova, 2019).

TXA_2, a major AA metabolite of platelets and also produced by monocytes, mast cells and PMN, is a robust bronchoconstrictor (Bureau et al., 1992) and contributes to leukocyte recruitment by induction of cell adhesion molecules in the endothelium (Ishizuka et al., 1998). TXA_2 has been shown to be elevated in the BALF of N-ERD patients (Sladek et al., 1994). Platelets have also been demonstrated to adhere to neutrophils, eosinophils and monocytes in N-ERD, considerably augmenting cysLT production through transcellular conversion of excess LTA_4 into LTC_4 (T. M. Laidlaw et al., 2012).

Thus LTs, PGD_2 and TXA_2 are key lipid mediators that induce, enhance and perpetuate to type 2 inflammation and airway remodeling.

In contrast, immune homeostasis and resolution of inflammation are mediated by anti-inflammatory prostanoids: PGE_2 and the prostacyclin PGI_2. PGI_2 has been shown to counterregulate type 2 inflammation in a murine model of atopic asthma by inhibiting ILC2 function and strongly diminishing IL5 and IL13 expression (Zhou et al., 2016).

PGE_2 can bind to four different GPCR PGE_2 receptors (EP1-4). Of those, PGE_2 anti-inflammatory and airway protective functions are mainly mediated by EP2. PGE_2 blocks recruitment and activation of eosinophils and mast cells and prevents the induction of pro-inflammatory signaling cascades including LT production (Peachell et al., 1988; Sturm et al., 2008). EP2 signaling also inhibits fibroblast proliferation, resulting in less collagen deposition and thus protection against airway remodeling (S. K. Huang et al., 2008). These anti-inflammatory and bronchoprotective effects were confirmed by PGE_2 inhalation in challenged atopic asthma (Gauvreau, Watson, & O'Byrne, 1999) and N-ERD patients (Sestini et al., 1996) and in experimental airway inflammation models (T. Liu et al., 2012).

PGE_2 is primarily produced in cells co-expressing both COX-2 and mPGES-1, such as epithelial cells, fibroblasts and macrophages, and its production is enhanced during inflammatory responses (Uematsu, Matsumoto, Takeda, & Akira, 2002). In addition, PGE_2 induces an anti-inflammatory phenotype in macrophages, which show increased IL10 production and can prevent the development of atopic airway inflammation in mice (Draijer et al., 2016).

PGE_2 and its immune-regulatory functions are dysregulated in severe CRSwNP and asthma. Several studies have shown a decreased production of PGE_2 and impaired function of its synthesizing enzymes (COX-2, mPGES-1) in leukocytes, epithelial cells and fibroblasts in the upper and lower airways of affected patients (Adamjee et al., 2006; Cowburn et al., 1998; Marek L. Kowalski et al., 2000; CéSar Picado et al., 1999; Roca-Ferrer et al., 2011; Schäfer, Schmid, Göde, & Baenkler, 1999; Yoshimura, Yoshikawa, Otori, Haruna, & Moriyama, 2008). In addition, EP2 expression is decreased in eosinophils, mast cells, neutrophils and T cells in the nasal mucosa and lung (Corrigan et al., 2012; Ying et al., 2006) and NP-derived fibroblasts failed to induce EP2 upon *in vitro*

IL1β stimulation (Roca-Ferrer et al., 2011). Genetic and epigenetic differences are implied to contribute to disease pathology, as several polymorphisms of AA metabolism enzymes (5LO (S.-H. Kim et al., 2005), LTC_4S (Sanak, Pierzchalska, Bazan-Socha, & Szczeklik, 2000), COX-2 (W. Szczeklik, Sanak, & Szczeklik, 2004)) and receptors (CysLT1R (S.-H. Kim et al., 2006), CysLT2R (Pillai et al., 2004), EP2 (Jinnai et al., 2004), CRTH2 (Palikhe et al., 2010)) along with hypermethylation (PTGES) and hypomethylation (ALOX5AP, LTB4R, PGDS) in NPs (Cheong et al., 2011) were found in cells and tissues from N-ERD patients.

Collectively, lower expression of COX-2 and mPGES-1 and higher expression of 5LO and LTC_4S favor the shunt of AA into pro-inflammatory LTs, while the immune-regulatory functions of PGE_2 are diminished. These eicosanoid imbalances in type 2 airway diseases, particularly in N-ERD and in conjunction with reduced responsiveness of leukocytes, structural and smooth muscle cells due to altered receptor functionality (e.g. CysLT1R, CysLT2R, EP2, CRTH2), drive the inflammatory pathogenesis. The intake of NSAIDs and the inhibition of the COX-pathway in N-ERD causes an even more pronounced dysbalance and evokes an immediate and severe insensitivity reaction (Figure 1.4).

1.2.3 More lipid mediator families

Several additional lipid mediator species with immune regulatory functions exist, that are also products of LO and COX activity, but are biosynthesized from different PUFAs: linoleic acid (LA), eicosapentaenoic acid (EPA) and docosahexaenoic acid (DHA). 12-LO and 15-LO, expressed in monocytes (Conrad, Kuhn, Mulkins, Highland, & Sigal, 1992), macrophages (J. T. Huang et al., 1999; Ricote et al., 2000), eosinophils (Turk, Maas, Brash, Roberts, & Oates, 1982) and airway epithelial cells (Hunter, Finkbeiner, Nadel, Goetzl, & Holtzman, 1985), metabolize AA into HETEs (eicosanoids) and LA into hydroxyoctadecadienoic acids (HODEs) and hydroxyoctadecenoic acids (HOMEs) (Jostarndt et al., 2002; Zimmer et al., 2018). 15-HETE and 13-HODE induce an anti-inflammatory phenotype in macrophages via the peroxisome proliferator-activated receptor (PPAR)γ, which is enhanced in the presence of the key type 2 cytokine IL4 (J. T. Huang et al., 1999; Ricote et al., 2000). 15-HETE also acts on neutrophils, inhibiting superoxide and LTB_4 production and inducing lipoxin (LX) synthesis (C. N. Serhan & Reardon, 1989).

LXs are part of the family of specialized pro-resolving mediators (SPMs) and are secreted by neutrophils, macrophages (Freire-de-Lima et al., 2006) and platelets (C N Serhan & Sheppard, 1990). They are synthesized from the AA pathway intermediate products LTA_4 and 15-hydroxyperoxyeicosatetraenoic acid (HpETE) by 5-/12-/15-LO and are termed LXA_4 and LXB_4 (C. N. Serhan, Hamberg, & Samuelsson, 1984; C N Serhan & Sheppard, 1990). Acetylation of COX-2 by ASA (ASA-COX-2) forms 15(R)-HETE, which is converted into the epi-lipoxins 15-epi-LXA_4 and 15-epi-LXB_4 (Claria & Serhan, 1995).

Lipoxins diminish neutrophil recruitment (Jozsef, Zouki, Petasis, Serhan, & Filep, 2002), function and survival (D. El Kebir et al., 2007; Driss El Kebir et al., 2009), while macrophage efferocytosis is enhanced (Godson et al., 2000) and apoptosis is blocked (Prieto et al., 2010), thus initiating the resolution of inflammation. Administration of 15-epi-LXA_4 sufficiently reduced AHR and airway inflammation in a murine model of asthma (Levy & Serhan, 2003). However, there might be a minor relevance for LXs in asthma as oxidative stress and elevated soluble epoxide hydrolase activity may lead to their rapid degradation *in vivo* (Ono et al., 2014).

Resolvins constitute another group of SPMs and are subgrouped based on the PUFA they derive from. The six D-series resolvins (RvD1-6) are biosynthesized from 17-hydroxyDHA (HDHA), an intermediate 15-LO product of DHA (Hong, Gronert, Devchand, Moussignac, & Serhan, 2003). The resolvins of the E-series derive from the CYP450 and/or ASA-COX-2 intermediate product 18-hydroxyeicosapentaenoic acid (HEPE) of EPA (Charles N. Serhan et al., 2000). Resolvins can inhibit (Isobe et al., 2012) and induce apoptosis in PMN (D. El Kebir et al., 2012), elicit a regulatory macrophage phenotype with an enhanced IL10 production and phagocytosis (Oh et al., 2012), reduce airway eosinophilia and AHR (Rogerio et al., 2012) and diminish T cell responses (Chiurchiù et al., 2016), thus contributing to the resolution of inflammation.

1.3 Metabolomics

Biological processes degrade, transform and produce a broad variety of low molecular weight metabolites (e.g. fatty acids, lipids, steroids, small peptides, amino acids, sugars, vitamins). The compilation of all metabolites of an organism, tissue, cell type or single cell defines a specific biochemical fingerprint – the metabolome (Idle & Gonzalez, 2007). The study of metabolomes, called "metabolomics", reveals the metabolic status, e.g. in respect of genetic diversity, gene expression or extrinsic stimuli (Idle & Gonzalez, 2007). Differences of current physiologies between pheno- and endotypes, for example in disease, can be identified by metabolomics, while common genomics to proteomics approaches solely illustrate processes that might be happening in a cell (Idle & Gonzalez, 2007).

1.3.1 Obesity, metabolic changes and their implications in airway diseases

Several epidemiological studies suggest a link between obesity and airway disease (severity), as obesity is common in asthmatics (Beuther & Sutherland, 2007; Ding, Martin, & Macklem, 1987; Holguin, Bleecker, et al., 2011; Moore et al., 2010; Rizk, Lavoie, Pepin, Wright, & Bacon, 2012; Telenga et al., 2012). Obese asthmatics respond more poorly to standard controller therapy (M. Peters-Golden, 2006; Savas et al., 2017) and a cellular CS resistance is implicated in comparison to asthmatics with a lower body mass index (BMI) (Sutherland, Goleva, Strand, Beuther, & Leung, 2008). Though the mechanisms remain obscure, the impact of obesity-induced metabolic alterations on airway diseases is object of investigation.

With over 1.9 billion overweight (BMI 25-30) and obese (BMI >30) people in the world (World Health Organization, 2018) and the development of metabolic syndrome (including diabetes mellitus, sleep apnea, osteoarthritis and cardiovascular disease) (Saklayen, 2018), this epidemic increase in body weight and fat has a high impact on health costs due to severe comorbidities and significantly reduced life expectancy (Saklayen, 2018). Main cause of obesity is the modern lifestyle in Western countries with an abundance of inexpensive high energy density foods and declining levels of physical activity (Saklayen, 2018; World Health Organization, 2018). Weight gain is also a common side-effect of CS therapy in asthmatics (Rizk et al., 2012; Wung et al., 2008). Excess energy is stored as fat in adipocytes, which enlarge and proliferate, and deposited ectopically throughout the body (Halberg, Wernstedt-Asterholm, & Scherer, 2008). Both, enlarged adipocytes in adipose tissue (Alvarez-Llamas et al., 2007; Kratchmarova et al., 2002) and ectopic fat tissue (Neeland et al., 2013), secrete several mediators that create an inflammatory environment, causing a detrimental metabolic change that is thought to be the origin of the metabolic syndrome (Saklayen, 2018; Stępień et al., 2014). Macrophages massively accumulate in adipose tissue and are the main drivers of inflammation (Lumeng, Bodzin, & Saltiel, 2007; Odegaard et al., 2007; Weisberg et al., 2006). In healthy adipose tissue, resident M2 macrophages mediate tissue homeostasis by

suppressing inflammation and promoting tissue remodeling and repair through IL10 and arginase-1 (Lumeng et al., 2007; Odegaard et al., 2007). The accumulation of lipids in both adipocytes and macrophages induces an infiltration and polarization of macrophages into a pro-inflammatory, classical-activated phenotype (M1) (Lumeng et al., 2007; Odegaard et al., 2007; Prieur et al., 2011). Indeed, obesity is a risk factor for the development of late onset non-atopic asthma (Beuther & Sutherland, 2007) which is characterized by a more type 1 inflammatory (immune) state, neutrophilia (Moore et al., 2010; Telenga et al., 2012) and increased AHR induced by low volume breathing due to mechanical hindrance (Ding et al., 1987). Vice versa, early onset asthma (Holguin, Bleecker, et al., 2011) contributes to obesity development, possibly as a result of reduced physical activity, and may be affected by the altered secretome due to metabolic changes.

Adipokines (1.3.2), sphingolipids (1.3.3), apolipoproteins (1.3.4) and aberrant fatty acid oxidation (FAO, 1.3.5) have been shown to be involved in the link between obesity, airway disease and lipid metabolism alterations.

1.3.2 Adipokines – adiponectin and leptin

Multiple adipokines with metabolic and immune regulatory functions exist, of which leptin and adiponectin are the most prominent.

Leptin is an adipocyte-derived peptide hormone and it induces satiety after food intake by binding to the leptin receptor in the hypothalamus (Satoh et al., 1998). Leptin levels increase with adipose mass and can lead to leptin resistance, as increased levels do not generate the feeling of satiety in obesity (Considine et al., 1996). Leptin has several pro-inflammatory effects on the innate and adaptive immune system. It activates and induces chemotaxis of PMN, monocytes, macrophages and DCs (Caldefie-Chezet, Poulin, & Vasson, 2003; Gruen, Hao, Piston, & Hasty, 2007; Mattioli, Straface, Quaranta, Giordani, & Viora, 2005; Santos-Alvarez, Goberna, & Sánchez-Margalet, 1999; Wong, Cheung, & Lam, 2007). Thus, multiple pro-inflammatory and immune-regulatory mediators are secreted by monocytes and macrophages in response to leptin: IL1β, IL6, TNF, CCL2, PGE_2, cysLTs and LTB_4 (Acedo, Gambero, Cunha, Lorand-Metze, & Gambero, 2013; Mancuso, Canetti, Gottschalk, Tithof, & Peters-Golden, 2004; Raso et al., 2002; Santos-Alvarez et al., 1999). Neutrophils, macrophages and endothelial cells also produce reactive oxygen species (ROS), further augmenting inflammation (Bouloumie, Marumo, Lafontan, & Busse, 1999; Caldefie-Chezet et al., 2003; Raso et al., 2002). Eosinophils from obese asthmatics show enhanced adhesion and chemotactic sensitivity towards CCL5 and eotaxin, correlating with higher leptin levels in the serum of these patients (Grotta et al., 2013). In addition, leptin increases the proliferation of T and B cells and the secretion of IL2 and IFNγ, while the numbers of regulatory T cells (Tregs) are reduced *in vivo* (Claycombe, King, & Fraker, 2008; De Rosa et al., 2007; Lord et al., 1998). Leptin may contribute to airway inflammation, as leptin levels are increased in the airways of asthmatics and positively correlate with plasma levels and BMI (Holguin, Rojas, Brown,

& Fitzpatrick, 2011) and airway leptin receptors are downregulated in asthma and associated with remodeling processes (Bruno et al., 2009).

Adiponectin is predominantly produced in adipocytes but exerts anti-inflammatory functions in comparison to leptin (Combs et al., 2002). High blood levels of adiponectin are found in healthy individuals, which are negatively correlated with adipose mass and decrease in obesity (Ryo et al., 2004). Obesity-associated changes in the microenvironment, such as the type 1 milieu (IL6, TNF), hypoxia and oxidative stress, reduce the production of adiponectin (Hosogai et al., 2007), while PPARγ enhances adiponectin production and adipocyte proliferation (Combs et al., 2002; J. Zhang et al., 2004). Adiponectin is a complex peptide molecule that can form low, intermediate and high molecular weight (L/I/HMW) complexes which activate the adenosine monophosphate (AMP)-activated protein kinase (AMPK), PPARα and PPARγ through binding to the adiponectin receptor 1 and 2 (AdipoR1, AdipoR2) on immune cells and in tissues (Chinetti, Zawadski, Fruchart, & Staels, 2004; Yamauchi et al., 2003). Most of the anti-inflammatory function of adiponectin is mediated by M2 macrophages. Adiponectin promotes M2 polarization of monocytes, reducing the production of IL6, TNF and ROS, while the expression of M2 markers, IL10 and efferocytosis is upregulated (Lovren et al., 2010; Ohashi et al., 2010; Takemura et al., 2007). Adiponectin further induces apoptosis in T cells, limiting T cell proliferation and cytokine production (Wilk et al., 2011). Adiponectin knockout mice show an emphysematous lung phenotype with an abnormal augmentation of airway spaces and activated, TNF and matrix metalloproteinase (MMP)12-producing alveolar macrophages (Summer et al., 2008). Adiponectin serum levels were shown to be reduced in asthmatic women (Sood et al., 2008). Indeed, adiponectin mediates immune-regulatory effects in the airways as lung epithelial cells express AdipoR1 (Miller, Cho, Pham, Ramsdell, & Broide, 2009) and adiponectin reduced airway inflammation in an atopic asthma model in mice (Shore, Terry, Flynt, Xu, & Hug, 2006).

While both leptin and adiponectin show immune regulatory functions, their levels are altered in obesity and asthma. Despite several links between altered adipokine levels and airway inflammation, their exact role in airway diseases remain unclear.

1.3.3 Sphingolipids – biosynthesis and role in immunity and inflammatory diseases

Besides PUFA-derived lipid mediators (see 1.2), the complex and diverse, saturated fatty acid (SFA)-derived sphingolipids represent another group of bioactive lipids with distinct functions in membrane biology and cell activity. The complex sphingolipid metabolism and biosynthesis involve numerous regulatory enzymes and metabolites, giving rise to hundreds of unique lipids (Hannun & Obeid, 2018). Both are described in Figure 1.6.

Sphingosine-1-phosphate (S1P) is the most studied sphingolipid and exhibits auto- and paracrine functions, acting as first and secondary messenger through binding to one of five GPCR S1P receptors ($S1P_{1-5}$) (Payne, Milstien, & Spiegel, 2002) or by epigenetic modifications through intracellular binding to histone deacetylases (HDACs) (Hait et al., 2009). S1P plays a major role in T cell homeostasis and inflammation by mediating the egress from lymphoid and infiltration into peripheral tissue through a S1P gradient in tissue and plasma (Allende, Dreier, Mandala, & Proia, 2004; Benechet et al., 2016). S1P and ceramide-1-phosphate (C1P) share pro-survival properties and together with sphingosine and ceramide (Cer), which have strong pro-apoptotic functions, are part of a fine balance of cell viability (Gómez-Muñoz et al., 2005; Obeid, Linardic, Karolak, & Hannun, 1993; P. Xia et al., 2002). Sphingomyelinase (SMase)-activity, catalyzing the hydrolysis of sphingomyelins (SMs) into Cers, has been shown to contribute to sustained inflammation by upregulating CCL5 and IL6 in response to IL1β and TNF (R. W. Jenkins et al., 2011). Sphingolipids, especially Cers and SMs, have been implicated in cell membrane domain formation, possibly affecting signaling by GPCRs (Carreira, Ventura, Varela, & Silva, 2015). Indeed, elevated SM content of membranes in erythrocytes of asthmatics indicate alterations in lipid rafts that might contribute to disease pathophysiology (Gupta, Vijayan, & Bansal, 2010).

Orosomucoid-like (ORMDL) proteins negatively regulate the *de novo* biosynthesis of sphingolipids through inhibition of serine-palmitoyltransferase (SPT) (Siow & Wattenberg, 2012) and genome-wide association studies revealed ORMDL3 to be a risk factor for asthma-development (Moffatt et al., 2007). Recent metabolomic studies confirmed sphingolipid alterations to correlate with AHR and disease severity in asthma and N-ERD (Kowal, Żebrowska, & Chabowski, 2019; Reinke et al., 2017; Trinh et al., 2016; Worgall et al., 2013). First therapeutic approaches targeting S1P function revealed promising effects of synthetic S1P receptor antagonist FTY420 and sphingosine kinase (SK) inhibitors in murine models of allergic airway inflammation, reducing AHR, mucus production, T cell-mediated responses, ORMDL3 expression and thus, inflammation (Oyeniran et al., 2015; Price et al., 2013; Sawicka et al., 2003).

While several associations to diseases and biological functions of sphingolipids have been identified in recent years, their explicit mechanisms of action and the effects of fatty acid residue chain length and saturation are yet to be elucidated.

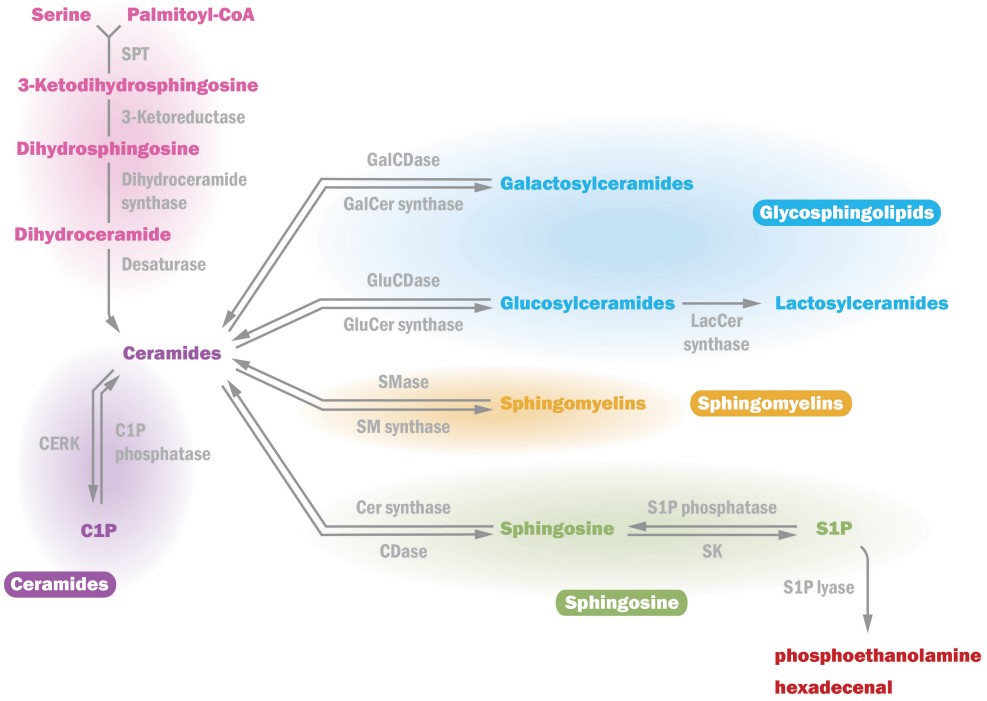

Figure 1.6 Sphingolipid biosynthesis and metabolism
De novo biosynthesis **(pink)** is initiated by the condensation of the amino acid serine and palmitoyl-coenzyme A (CoA) to form 3-ketodihydrosphingosine through serine palmitoyltransferase (SPT) activity. Subsequent reduction forms dihydrosyphingosines followed by acetylation by one of six different (dihydro)ceramide synthases (CerS) to dihydroceramide (dhCer, sphinganine). Each dihydroceramide synthase exhibits affinities for specific fatty acyl chain lengths, forming various dhCers (e.g. CerS6 synthesizes C16-dhCer, CerS1 C18-dhCer). Desaturases introduce a double bond between C4 and C5 of the palmitate, catalyzing the formation of the corresponding ceramide (Cer), the precursor of all complex sphingolipids. Sphingomyelins (SM) **(orange)**, Cers with phosphatidylcholine-residue, and the glycosphingolipids **(blue)** glucosylceramides (GluCers, glucose-residue), lactosylceramides (LacCers, lactose-residue) and galactosylceramides (GalCers, galactose-residue) can be hydrolyzed into Cers by several hydrolases (SMases, GluCeramidase (GluCDase), GalCDase) or synthesized with Cers through synthases (SM synthase, GluCer synthase, LacCer synthase, GalCer synthase). Sphingosine is produced in the salvage pathway **(green)** by the same hydrolases and can directly derive from Cer by ceramidase (CDase) activity. Sphingosine can either be metabolized (back) to Cer by CerS or phosphorylated into the highly bioactive S1P by sphingosine kinases (SK). S1P can be reverted to sphingosine by S1P phosphatases (SPPs) or irreversibly degraded into phosphoethanolamine and hexadecenal by S1P lyase **(red)**. Like sphingosine, Cer can be phosphorylated into Cer-1-phosphate (C1P) through ceramide kinase (CERK) action and the reaction can be reverted by C1P phosphatase **(purple)**. This figure was adapted and reproduced with permission from "Sphingolipids and their metabolism in physiology and disease" (Nature Reviews Molecular Cell Biology, Hannun & Obeid, 2018), Springer Nature (Appendix V).

1.3.4 Apolipoproteins – lipid transporters with immune regulatory functions

Apolipoproteins and acylcarnitines constitute two more metabolite classes that play central roles in fatty acid transport and are part of the interconnection between the fatty acid metabolism, obesity and airway diseases.

Apolipoproteins form the outer scaffold of lipoproteins, particles with hydrophobic content (triglycerides, cholesterol esters) and more hydrophilic outer layer (phospholipids, free cholesterol) and mediate their functions through receptor binding (Brown & Goldstein, 1986; Rigotti, Miettinen, & Krieger, 2003). Lipoproteins are fatty acid shuttles between the intestine (intestinal uptake of processed food), the periphery (muscles, heart, adipose tissues) and liver (excretion via bile or feces) through lymph and plasma. They are discriminated by their hydrated density into very low, intermediate, low and high-density lipoproteins (VL/I/L/HDL) (Dominiczak & Caslake, 2011).

Macrophages play a major role in the control of lipoproteins and cholesterol in the periphery, including adipose tissue (see 1.3.1), as they are taking up cholesterol from their surroundings and remove excess amounts by reverse cholesterol transport to the liver. Accumulation of intracellular cholesterol induces the anti-inflammatory transcription factor liver-X-receptor (LXR) (Yvan-Charvet et al., 2008), which increases the expression of the adenosine triphosphate (ATP)-binding cassette sub-family A member 1 (ABCA1) and ABCG1 that promote cholesterol efflux onto HDL together with apolipoprotein A1 (ApoA1) (X. Wang et al., 2007). However, modified LDL also acts as toll-like receptor (TLR) agonist on macrophages, inducing inflammation that can be enhanced by elevated intracellular cholesterol levels through inflammasome activation (Duewell et al., 2010; Sheedy et al., 2013; Yvan-Charvet et al., 2008). Adipose tissue macrophages in obesity have also been shown to be further activated by ceramides and SFAs binding to TLRs and nucleotide-binding oligomerization domain (NOD)-like receptors (NLRs), eliciting chronic inflammation (Vandanmagsar et al., 2011) as TLR-signaling represses LXR activity (Castrillo et al., 2003). High LXR expression together with ApoE-promoted cholesterol efflux in hematopoietic stem cells and myeloid progenitors in the bone marrow have been shown to curtail the generation of pro-inflammatory leukocytes through reduced responsiveness towards IL3 and GM-CSF signaling (A. J. Murphy et al., 2011), a regulation that is presumably reverted in obesity and metabolic syndrome (Herishanu, Rogowski, Polliack, & Marilus, 2006; Y.-J. Lee et al., 2010). Other immunoregulatory functions of ApoE were demonstrated in murine macrophages, that switched to a M2 phenotype and showed downregulated type 1 responses (Baitsch et al., 2011). Interestingly, corticosteroid treatment induced ApoE expression and M2 phenotype as well (Trusca et al., 2017). LDL receptor-signaling by an ApoE mimetic was sufficient to reduce airway inflammation in a murine model of allergic asthma (Yao et al., 2010).

1.3.5 Acylcarnitines and fatty acid oxidation in inflammation

In comparison to apolipoproteins, which transport lipids throughout the organism, acylcarnitines mediate the intracellular transport of fatty acids into the mitochondria for FAO. FAO represents an essential source of energy by providing ATP, particularly when glucose and glycogen stores are low (e.g. during fasting or prolonged/extensive exercise) and when glycolysis is diminished. After hydrolyzing triglycerides, free fatty acids (FFAs) are released into the blood by adipose tissue and enter cells through fatty acid transport systems (fatty acid translocase (FAT)/cluster of differentiation 36 (CD36)) (Bartlett & Eaton, 2004). FFAs are activated by esterification into acyl-CoAs and while medium chain acyl-CoAs can freely diffuse into the mitochondria, long-chain acyl-CoAs have to be transported by the carnitine shuttle (Bartlett & Eaton, 2004). Long-chain acyl-CoAs are converted into acylcarnitines through exchange of the CoA group with carnitine by carnitine palmitoyl transferase (CPT) 1, imported into the mitochondrion via carnitine acylcarnite translocase (CACT) and reconverted into acyl-CoAs by CPT2 (Bartlett & Eaton, 2004). Subsequent β-oxidation involves a cascade of several enzymes and intermediate metabolites, ultimately resulting in the production of ATP (Bartlett & Eaton, 2004).

Metabolic alterations define the polarization of macrophages as M1 macrophages are dependent on the glycolytic metabolism, while M2 macrophages capitalize on FAO (S. C.-C. Huang et al., 2014; Jha et al., 2015). Disease-associated alterations of the energy metabolism in myeloid cells, especially in macrophages and myeloid-derived suppressor cells (MSDCs), towards an enhanced FAO are common in chronic inflammatory diseases (e.g. parasitic infections and cancer) and necessary to sustain their pathogenic functions (Hossain et al., 2015; S. C.-C. Huang et al., 2014). Indeed, acylcarnitines can induce the expression of pro-inflammatory enzymes and mediators (COX-2, CXCL2, CCL5, IL1β, IL6, TNF) in a dose-dependent manner (Rutkowsky et al., 2014). An elevated FAO was shown in a murine model of allergic asthma with increased levels of CPT1 and 3-hydroxyacyl-CoA dehydrogenase (HADHA) (Al-Khami et al., 2017), an enzyme catalyzing the final steps during FAO (Bartlett & Eaton, 2004). The pharmacological inhibition of key FAO enzymes with etomoxir (CPT1-inhibitor) and ranolazine (HADHA-inhibitor) improved both anti-cancer responses (Hossain et al., 2015) and significantly reduced HDM-induced airway inflammation (Al-Khami et al., 2017).

Thus, the metabolism of both PUFAs (see 1.2) and SFAs (see 1.3) play a central role and are frequently altered in inflammatory airway diseases, strengthening the need to further elaborate the complex network and functions of lipids and their regulators. While the focus of this study is on type 2 airway pathology, several diseases may benefit from our results as well, e.g. coronary heart diseases, atherosclerosis, metabolic disease, cancer, COPD and arthritis.

1.4 Exosomes - Intercellular signaling by small lipid vesicles

1.4.1 Extracellular vesicles – exosomes and microparticles

Intercellular communication by extracellular vesicles (EVs) moved into the focus of research in recent years after the discovery of RNA and miRNA as on part of their diverse cargo in 2007 (Valadi et al., 2007).

EVs are small lipid vesicles that can derive from almost all cell types and organisms (including bacteria, archeae, parasites, fungi and plants) (Albuquerque et al., 2008; An, Huckelhoven, Kogel, & van Bel, 2006; Ellen et al., 2009; Rivera et al., 2010; Silverman et al., 2010)) and EVs have been isolated from several body fluids (e.g. plasma, breast milk, saliva, urine, nasal lining fluid (NLF), BALF) (Lässer, O'Neil, et al., 2011; Lässer, Seyed Alikhani, et al., 2011; Levänen et al., 2013; Wiggins, Glatfelter, Kshirsagar, & Brukman, 1986)). They are classified by their biosynthesis into two types: endosomal pathway-derived EVs, called exosomes, (30 - 150 nm in diameter) and larger microvesicles that are shed from the cell membrane (30 - 1.000 nm in diameter, Figure 1.7) (Abels & Breakefield, 2016).

Exosomes are of particular interest since their cargo, a mixture of various proteins (enzymes, cytokines), lipids (including lipid mediators) and nucleic acids (small non-coding RNAs, messenger (m)RNAs), largely mimic the content of their cell of origin, which can however be specifically enriched (Abels & Breakefield, 2016). Inward budding of late endosomes forms intraluminal vesicles (ILVs), resulting in a multivesicular body (MVB). MVBs are either degraded by fusion with lysosomes or transported to the cell membrane, where they fuse and release ILVs as exosomes into the extracellular space (Figure 1.7) (Abels & Breakefield, 2016). This transport is primarily mediated by the four endosomal sorting complexes required for transport (ESCRT-0-III), but an ESCRT-independent pathway involving Cers and SMase activity has been described as well (Trajkovic et al., 2008). EV secretion changes in response to cellular activation, stress, injury or microenvironmental alterations like hypoxia or pH changes (Esser et al., 2010; Kulshreshtha, Ahmad, Agrawal, & Ghosh, 2013; Mittelbrunn et al., 2011; Parolini et al., 2009). The definite mechanism of (cell-specific) EV uptake remains obscure, though several mechanisms including micropinocytosis, clathrin-dependent and clathrin-independent uptake have been described (Abels & Breakefield, 2016).

Exosomes have been implicated in the pathogenesis of many diseases, including airway inflammation.

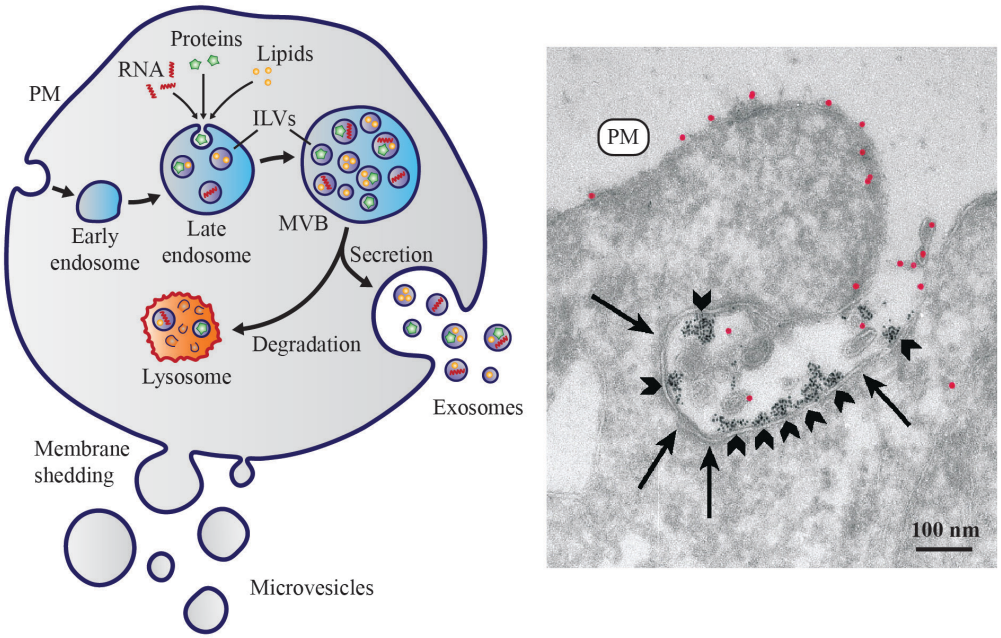

Figure 1.7 Extracellular vesicle biosynthesis
Left Schematic illustration of the release of extracellular vesicles. Microvesicles are shed from the plasma membrane (PM). Exosomes derive from the endosomal pathway as intraluminal vesicles (ILVs), with a diverse cargo of different types of RNA, proteins and lipids, form multivesicular bodies (MVBs). MVBs are either degraded by fusion with lysosomes or release their ILVs as exosomes by fusion with the PM. **Right** Electron microscopy image of a fusion between a MVB and the PM **(arrows)** in an Epstein-Barr virus-transformed B cell. Small bovine serum albumin (BSA)-gold particles were internalized into MVB **(arrowheads)**. Major histocompatibility complex (MHC) class II at the PM and on ILVs was labeled with large gold particles **(pseudocolored in red)**. This figure was adapted and reproduced with permission from "Biogenesis, Secretion, and Intercellular Interactions of Exosomes and Other Extracellular Vesicles" (Annual Review of Cell and Developmental Biology, Colombo, Raposo, & Théry, 2014), Annual Reviews (Appendix VI).

1.4.2 Exosomes in airway inflammation

Since exosomes are present in biological fluids, several investigations were performed to study exosomes in NLF and BALF of CRSwNP and asthmatic patients.

Altered levels of cystatin-SN, peroxiredoxin-5 and glycoprotein VI were detected in both NLF-derived exosomes and nasal tissue of CRSwNP patients in comparison to healthy controls and were highly accurate predictors of disease, suggesting NLF-derived exosomes as useful non-invasive biomarkers (Mueller et al., 2019). Functional associations with exosomes were found in two other studies: in the first, CRSwNP NLF-derived exosomes contained higher levels of a disintegrin and metalloproteinase domain-containing protein 10 (ADAM10) in comparison to healthy controls. Stimulation of human umbilicial vein endothelial cells (HUVECs) resulted in enhanced proliferation and

increased permeability, implicating a potential function of exosomes to promote angiogenesis and vascular permeability in CRSwNP (W. Zhang et al., 2018). In the second study, NLF-derived exosomes from CRSwNP patients with and without comorbid asthma demonstrated increased chemotactic properties for monocytes, neutrophils and natural killer (NK) cells, while levels of anti-microbial and barrier-related proteins were decreased in comparison to healthy NLF-derived exosomes (Lässer et al., 2016). Though the exact cellular sources are unknown, these studies indicate a pathogenic role of exosomes in CRSwNP.

In asthmatics, the quantity of exosomes is increased in the BALF, correlates with blood eosinophilia and IgE levels (Hough et al., 2018) and asthmatic eosinophils also secrete more exosomes (Mazzeo et al., 2015). BALF-derived exosomes from asthmatics have been shown to contain cargo that mediates multiple functions associated with disease pathogenesis. Micro ribonucleoic acids (miRNAs) associated with mitogen-activated protein kinase (MAPK) and Janus kinase (JAK)-signal transducer and activator of transcription (STAT) signaling pathways and targeting IL6, IL8, IL10 and IL13 were altered in comparison to exosomes from healthy BALF (Levänen et al., 2013). Indeed, exosomal miRNAs have a strong impact on gene expression as demonstrated by the miRNA transfer between T cells and antigen-presenting cells *in vitro* immune synapses (Mittelbrunn et al., 2011), while BALF-derived exosomes also demonstrated to mimic DC-functions and induce antigen-specific activation of T cells by surface expression of MHC-I, MHC-II and co-stimulatory CD54 and CD86 (Admyre et al., 2003).

Furthermore, exosomes have effects on the epithelial barrier. Asthmatic fibroblast-derived exosomes have been shown to induce an abnormal enhanced proliferation of human bronchial epithelial cells (hBECs) of both healthy and asthmatic individuals by reduced TGFβ-signaling in comparison to healthy-derived BALF exosomes (Haj-Salem, Plante, Gounni, Rouabhia, & Chakir, 2018). Exosome numbers increased significantly within the BALF of an experimental model of allergic asthma and after IL-13 treatment of hBECs *in vitro*, which were associated with macrophages numbers *in vivo* as well as with increased chemotaxis and proliferation of monocytes *in vitro* (Kulshreshtha et al., 2013). Macrophage- and DC-derived exosomes further induce chemotaxis of PMN and contain functional LTA_4H and LTC_4S capable of forming LTB_4 and LTC_4, which shifts towards LTB_4 production upon TGFβ-stimulation of their cells of origin (Esser et al., 2010). Indeed, exosomal LTB_4 was demonstrated to mediate neutrophil chemotaxis in an auto- and paracrine fashion (Majumdar, Tameh, & Parent, 2016) and BALF-derived exosomes were shown to contain enzymes for LT biosynthesis and induce LTC_4 and IL8 secretion by hBECs *in vitro*, with elevated responses from asthmatic patients compared to those from healthy controls (Torregrosa Paredes et al., 2012). Furthermore, inhibition of SMase significantly reduced exosome production and improved disease severity in a murine model of allergic asthma (Kulshreshtha et al., 2013) and intranasal application of BALF-derived exosomes from allergen-tolerized mice upregulated TGFβ and were

sufficient to protect from allergic sensitization and thus airway inflammation (Prado et al., 2008).

Collectively, exosomes have been shown to be altered in numbers and cargo in upper and lower airway inflammation. They have multiple cellular origins and show diverse functions, thus contributing to disease pathogenesis. However, a potential contribution of exosomes to N-ERD has not been studied.

2 Aim of study

Inflammatory airway diseases are on the rise and constitute a significant burden for patients, but also society. The type 2 NSAID-exacerbated respiratory disease (N-ERD), characterized by chronic rhinosinusitis with nasal polyps (CRSwNP), asthma and robust insensitivity-reactions towards NSAID due to a dysregulated arachidonic acid (AA) metabolism, represents one of the most severe forms of airway inflammation. Together with other severe endotypes that are refractory towards corticosteroid (CS) therapy and due to an incomplete understanding of the pathomechanisms, treatment options for these diseases are often limited. Thus, there is an urgent need for further mechanistic investigation and improved treatment options for these unmet clinical needs.

The aim of the study at hand was to characterize N-ERD by multi-omics approaches to gain new insights into the upper and lower airway pathogenesis and to determine novel targets suitable for disease intervention and/or therapy that might contribute to the resolution of nasal polyposis and CS resistance.

In the first part of this study, we sought to investigate the resistance towards the anti-inflammatory lipid mediator prostaglandin (PG)E_2 in polymorphonuclear cells (PMN) in depth (e.g. lipid mediatory analysis by LC-MS/MS) and explore similar characteristics as well as phenotype-defining imprintings in *in vitro*-generated alveolar-like monocyte-derived macrophages (aMDM) of N-ERD individuals in comparison to NT CRSwNP and healthy controls (e.g. RNA sequencing, targeted/genome-wide methylomics).

We performed RNAseq analyses of nasal brushings, isolated macrophages from induced sputum and aMDM of the same N-ERD and healthy individuals to further distinguish functional aspects of local inflammatory environments in (CS-treated) upper and lower airways and assert a pathogenic contribution of macrophages, a highly immune regulatory cell that has yet been neglected in N-ERD research.

As a strong link between airway inflammation, obesity and (lipid) metabolism alterations has been indicated by several studies, we quantified a broad metabolic profile including several lipid species (e.g. phosphatidylcholines, sphingolipids, acylcarnitines) in a multi-fluid approach (plasma, sputum, nasal lining fluid (NLF)) as well as plasma adipokines, which were correlated to body mass index (BMI) and disease burden.

Lastly, with the emerging role of nano-sized extracellular vesicles (exosomes) in intercellular signaling in homeostasis and disease, we attempted to isolate exosomes from *in vitro* whole blood-derived cell and airway tissue cultures and body fluids. aMDM and human bronchial epithelial cells (hBECs) were stimulated with purified exosomes to evaluate their functional capacities.

3 Materials and Methods

3.1 Materials

3.1.1 Chemicals

Chemical	Company
Acetone for HPLC >99.8%	Sigma-Aldrich, Merck, Darmstadt, Germany
Aqua ad iniectabilia	Berlin-Chemie, Berlin, Germany
β-mercaptoethanol	Carl Roth, Karlsruhe, Germany
Calciumchloride ($CaCl_2$)	Sigma-Aldrich, Merck, Darmstadt, Germany
Dimethyl sulfoxide (DMSO) for cell culture	Applichem, Darmstadt, Germany
Disodium phospate (Na_2PO_4)	Merck, Darmstadt, Germany
Ethanol absolute for analysis	Merck, Darmstadt, Germany
Formvar-carbon	Serva Electrophoresis, Heidelberg, Germany
Glucose D-(+)	Sigma-Aldrich, Merck, Darmstadt, Germany
Glutaraldehyde	Electron Microscopy Sciences, Hatfield, PA, USA
Glycerol	Merck, Darmstadt, Germany
Isopropanol for synthesis >99.5%	Carl Roth, Karlsruhe, Germany
Methanol for preparative chromatography	Merck, Darmstadt, Germany
Methanol gradient grade for liquid chromatography	Merck, Darmstadt, Germany
Monopotassium phosphate (KH_2PO_4)	Merck, Darmstadt, Germany
Non-fat dried milk powder	Applichem, Darmstadt, Germany
Paraformaldehyde, reagent grade, crystalline	Sigma-Aldrich, Merck, Darmstadt, Germany
Potassium chloride (KCl)	Merck, Darmstadt, Germany
Roticlear	Carl Roth, Karlsruhe, Germany
Roti-Histokitt II	Carl Roth, Karlsruhe, Germany
Sodium chloride (NaCl)	Roth, Karlsruhe, Germany
Sodium dodecyl sulfate (SDS)	Sigma-Aldrich, Merck, Darmstadt, Germany
Trisodium citrate dihydrate	Sigma-Aldrich, Merck, Darmstadt, Germany
Triton-X 100	Sigma-Aldrich, Merck, Darmstadt, Germany
Trizma base	Sigma-Aldrich, Merck, Darmstadt, Germany
Trizma hydrochloride (Trizma HCl)	Sigma-Aldrich, Merck, Darmstadt, Germany
Tween-20	Sigma-Aldrich, Merck, Darmstadt, Germany
UltraPure DEPC-Treated Water	Thermo Fisher Scientific, Waltham, MA, USA
Uranylacetate	Serva Electrophoresis, Heidelberg, Germany
Xylenes, histological grade	Sigma-Aldrich, Merck, Darmstadt, Germany

3.1.2 Reagents and enzymes

Reagent / enzyme	Company
Adenosine deaminase Streptococcus thermophilus, recombinant	Sigma-Aldrich, Merck, Darmstadt, Germany
Alexa Fluor 488 C5 Maleimide	Thermo Fisher Scientific, Waltham, MA, USA
BD Pharm Lyse 10X	BD Biosciences, Heidelberg, Germany
Calcium ionophore A23187	Sigma-Aldrich, Merck, Darmstadt, Germany
CD14 MicroBeads, human	Miltenyi Biotec, Bergisch Gladbach, Germany
Cytochalasin B from Drechslera dematioidea	Sigma-Aldrich, Merck, Darmstadt, Germany
Donkey Serum	Sigma-Aldrich, Merck, Darmstadt, Germany
Fc Receptor Binding Inhibitor Polyclonal Antibody	Thermo Fisher Scientific, Waltham, MA, USA
Fluoroshield with DAPI	GeneTex, Irvine, CA, USA
Forskolin	Cayman Chemical, Ann Arbor, MI, USA
Giemsa's azur eosin methylene blue solution	Merck, Darmstadt, Germany
human GM-CSF, premium grade	Miltenyi Biotec, Bergisch Gladbach, Germany
human IL4, premium grade	Miltenyi Biotec, Bergisch Gladbach, Germany
human TGFβ1 Recombinant (CHO derived)	Peprotech, Hamburg, germany
human TNF, research grade	Miltenyi Biotec, Bergisch Gladbach, Germany
Live/Dead Fixable Aqua Dead Cell Stain Kit	Thermo Fisher Scientific, Waltham, MA, USA
LymphoPrep	Alere Technologies AS, Oslo, Norway
MaxBlock Autofluorescence Reducing Reagent Kit	MaxVision Biosciences, Washington, CO, USA
May-Gruenwald's Solution	Carl Roth, Karlsruhe, Germany
N-Formyl-Met-Leu-Phe (fMLP) >97% (HPLC)	Sigma-Aldrich, Merck, Darmstadt, Germany
NuPAGE LDS Sample Buffer 4X	Thermo Fisher Scientific, Waltham, MA, USA
NuPAGE MOPS SDS Running Buffer 20X	Thermo Fisher Scientific, Waltham, MA, USA
NuPAGE Sample Reduction Reagent 10X	Thermo Fisher Scientific, Waltham, MA, USA
NuPAGE Transfer Buffer 10X	Thermo Fisher Scientific, Waltham, MA, USA
Polymorphprep	Alere Technologies AS, Oslo, Norway
Prostaglandin E2	Cayman Chemical, Ann Arbor, MI, USA
Restore Western Blot Stripping Buffer	Thermo Fisher Scientific, Waltham, MA, USA
RLT Buffer	Qiagen, Hilden, Germany
RNAprotect	Qiagen, Hilden, Germany
RosetteSep Human Monocyte Enrichment Cocktail	Stemcell Technologies, Vancouver, Canada
SeeBlue Plus2 Pre-stained Protein Standard	Thermo Fisher Scientific, Waltham, MA, USA
Sodium chloride 5.85% solution (NaCl)	B-Braun, Melsungen, Germany
Sputolysin Reagent (DTT)	Calbiochem, Merck, Darmstadt, Germany
SuperSignal West Femto Maximum Sensitivity Substrate	Thermo Fisher Scientific, Waltham, MA, USA
Total Exosome Isolation Reagent (from cell culture media)	Thermo Fisher Scientific, Waltham, MA, USA
Trypan Blue Solution 0.4%	Thermo Fisher Scientific, Waltham, MA, USA
Trypsin-EDTA (0.05%), phenol red	Thermo Fisher Scientific, Waltham, MA, USA

3.1.3 Buffers

Buffer	Chemicals and reagents
4X SDS sample buffer	0.25 M Trizma HCl, 8% SDS, 40% glycerol, pH 6.8
Antibody dilution buffer Immunofluorescence	PBS, 3% BSA
Blocking solution Immunofluorescence	PBS, 3% BSA, 10% donkey serum
Blocking solution Western Blot (MTBS-T)	TBS-T, 5% non-fat dried milk powder
Cytospin buffer	PBS, 5% BSA
FACS buffer with EDTA (FB_{EDTA})	PBS, 1% FBS, 0.5 mM EDTA
Phosphate-buffered saline (PBS) buffer 20X	8 g KCl, 8 g KH2PO4, 46.4 g NaHPO4, 320 g NaCl, pH 7.0
Sodium citrate buffer	1 L H_2O, 2.94 g trisodium citrate dihydrate, pH 6.0
TBS buffer	1 L H_2O, 60.55 g Trizma base, 87.66 g NaCl, pH 7.6
TBS-T washing buffer	TBS, 0.02% Tween-20
Transfer buffer	NuPAGE Transfer Buffer, 10% MeOH

3.1.4 Media and components

Medium components	Company
Antibiotic-Antimycotic 100X	Thermo Fisher Scientific, Waltham, MA, USA
Bovine Serum Albumin (BSA)	Sigma-Aldrich, Merck, Darmstadt, Germany
Bronchial Epithelium Basal Medium (BEBM)	Lonza, Basel, Switzerland
Bronchial Epithelium Growth Medium (BEGM)	Lonza, Basel, Switzerland
DMEM-F12 Medium	Thermo Fisher Scientific, Waltham, MA, USA
Dulbecco's PBS, no calcium, no magnesium	Thermo Fisher Scientific, Waltham, MA, USA
Fetal Bovine Serum (FBS), exosome-depleted	Thermo Fisher Scientific, Waltham, MA, USA
Gentamicin (50 mg/mL)	Thermo Fisher Scientific, Waltham, MA, USA
Hank's Balanced Salt Solution (HBSS), no calcium, no magnesium, no phenol red	Thermo Fisher Scientific, Waltham, MA, USA
Hyclone Research Grade Fetal Bovine Serum (FBS)	GE Healthcare Life Science, Chicago, IL, USA
L-Glutamine (200 mM)	Thermo Fisher Scientific, Waltham, MA, USA
Penicillin-Streptomycin (10.000 U/mL)	Thermo Fisher Scientific, Waltham, MA, USA
RPMI-1640 Medium	Thermo Fisher Scientific, Waltham, MA, USA
UltraPure 0.5M EDTA, ph 8.0	Thermo Fisher Scientific, Waltham, MA, USA

Medium	Medium components
BEBM starving medium	BEBM, 1% antibiotic-antimycotic, 1 µg/mL gentamicin
BEGM medium	BEGM, 1% antibiotic-antimycotic, 1 µg/mL gentamicin
Complete exosome-free medium	RPMI-1640, 10% exosome-free FBS, 1% penicillin-streptomycin, 1 µg/mL gentamicin
Complete medium	RPMI-1640, 10% FBS, 1% penicillin-streptomycin, 1 µg/mL gentamicin
Erythrocyte lysis buffer	PBS, 1X BD Pharm Lyse
Freezing medium	50% DMEM-F12, 40% FBS, 10% DMSO
$HBSS_{CaCl2}$	HBSS, 1.6 mM CaCl2
MACS buffer	PBS, 0.5% BSA, 0.5 mM EDTA
PBS_{EDTA}	PBS, 0.5 mM EDTA
PGC	PBS, 1 mg/mL glucose D-(+), 1 mM CaCl2

3.1.5 Antibodies

Method	Antigen	Clone / ID	Fluorophore / enzyme	Host	Dilution	Company
FACS	CCR3	5E8	PE	mouse	1:5-50	BD Biosciences, Heidelberg, Germany
	CD11b	ICRF44	Pacific Blue	mouse	1:10-50	BD Biosciences, Heidelberg, Germany
	CD14	M5E2	V500	mouse	1:10	BD Biosciences, Heidelberg, Germany
	CD16	B73.1	PE-Cy7	mouse	1:5-50	BioLegend, San Diego, CA, USA
	CD45	2D1	APC-H7	mouse	1:10	BD Biosciences, Heidelberg, Germany
	CD61	VI-PL2	APC	mouse	1:10-50	Thermo Fisher Scientific, Waltham, MA, USA
	CRTH2	BM16	PE-CF594	rat	1:50	BD Biosciences, Heidelberg, Germany
	Siglec-8	7C9	PerCP-Cy5.5	mouse	1:50	BioLegend, San Diego, CA, USA
IF	ApoE	poly		rabbit	1:50	Atlas Antibodies, Bromma, Sweden
	β-actin	I-19, poly		goat	1:50	Santa Cruz Biotechnology, Dallas, TX, USA
	HTR4	poly		rabbit	1:50	OriGene Technologies, Rockville, MD, USA
	CD81	D-4, mono		mouse	1:50	Santa Cruz Biotechnology, Dallas, TX, USA
	TSG101	C-2, mono		mouse	1:50	Santa Cruz Biotechnology, Dallas, TX, USA
	anti-rabbit	poly	AF488	donkey	1:500	Thermo Fisher Scientific, Waltham, MA, USA
	anti-goat	poly	AF568	donkey	1:500	Thermo Fisher Scientific, Waltham, MA, USA
	anti-mouse	poly	AF647	donkey	1:500	Thermo Fisher Scientific, Waltham, MA, USA
Western blot	CD63	H-193, poly		rabbit	1:500	Santa Cruz Biotechnology, Dallas, TX, USA
	CD81	D-4, mono		mouse	1:250	Santa Cruz Biotechnology, Dallas, TX, USA
	TSG101	C-2, mono		mouse	1:500	Santa Cruz Biotechnology, Dallas, TX, USA
	anti-rabbit	poly	HRP	goat	1:10.000	Santa Cruz Biotechnology, Dallas, TX, USA
	anti-mouse	poly	HRP	goat	1:2.000	Santa Cruz Biotechnology, Dallas, TX, USA

IF, immunofluorescence; AF488/568/647, Alexa Fluor 488/568/647; HRP, horseradish peroxidase; poly, polyclonal; mono, monoclonal

3.1.6 Oligonucleotides

Gene	Size	Primer	Sequence	Anneal. temp. °C	Number of CpGs analyzed
HPGDS	126	forward PCR	TATGATTTATTTGTGTTATGTTTTT	58.8	
		reverse PCR	Biotin-AAATTACCTATCCTCTCACTAACTC		
		pyrosequencing	GTTTTGGGTTTATATG		2
LTB4R	213	forward PCR	Biotin-GGATTTTTTTTGTTTTTATGTATTGG	52	
		reverse PCR	CAAAACCCCCACTTATTCTACTTAA		
		pyrosequencing	AAAAACTTCCTAACC		2
			AAAAACCAAAACAAAAAT		2
ALOX5AP	106	forward PCR	TTTTTGGGGAGTTTGAAGTAAATAT	64	
		reverse PCR	Biotin-AAACTTTCCTTACCATTCTAAACCA		
		pyrosequencing	AATGTTGTTTTGTTGGTTAT		2
PTGES	262	forward PCR	GTGTTTGGGGTTTTTTTGTATTTT	64	
		reverse PCR	Biotin-AAAATTCCCAACTCCTAACAAATATC		
		pyrosequencing	AAGTTTAGTTTATGATTTT		10

3.1.7 Commercial Kits

Kit	Company
AbsoluteIDQ p180 Kit	Biocrates Life Sciences AG, Innsbruck, Austria
Elute, Prime, Fragment Mix	Illumina, San Diego, CA, USA
EpiTect 96 Fast Bisulfite kit	Qiagen, Hilden, Germany
EZ-96 DNA Methylation Kit	Zymo Research, Irvine, CA, USA
Phusion U Hot Start PCR Master Mix	Thermo Fisher Scientific, Waltham, MA, USA
Pierce BCA Protein Assay Kit	Thermo Fisher Scientific, Waltham, MA, USA
PyroGold SQA Reagent Kit	Qiagen, Hilden, Germany
Quant-iT PicoGreen dsDNA Assay Kit	Thermo Fisher Scientific, Waltham, MA, USA
Quick-DNA Microprep Plus Kit	Zymo Research, Irvine, CA, USA
Quick-RNA Microprep Kit	Zymo Research, Irvine, CA, USA
RNA 6000 Nano Kit	Agilent, Santa Clara, CA, USA
TruSeq Stranded Total RNA Library Prep Kit with Ribo-Zero	Illumina, San Diego, CA, USA

3.1.8 Commercial Assays

Assay type	Analyte(s)	Company
ELISA, human	adiponectin	Cusabio Technology LLC, Houston, TX, USA
ELISA, human	ECP	Thermo Fisher Scientific, Waltham, MA, USA
ELISA, human	leptin	Bertin Pharma, Montigny Le Bretonneux, France
ELISA, human	total IgE	Bertin Pharma, Montigny Le Bretonneux, France
immunoCAP	ECP	Thermo Fisher Scientific, Waltham, MA, USA
immunoCAP	total IgE	Thermo Fisher Scientific, Waltham, MA, USA
17-Multiplex, human	CXCL1, CXCL2, CXCL8, CXCL9, CXCL10, CXCL11, CCL5, CCL11, CCL17, TNF, IL1β, IL6, IL12p70, IL18, IL33, IL10, IL27	R&D Systems, Minneapolis, MN, USA
4-Multiplex, human	CXCL1, CXCL2, PPBP, CCL18	R&D Systems, Minneapolis, MN, USA
2-Multiplex, human	CXCL8, CCL20	R&D Systems, Minneapolis, MN, USA
8-Multiplex, human	CCL2, CCL26, CXCL8, GM-CSF, IL25, IL33, Periostin, TSLP	R&D Systems, Minneapolis, MN, USA

3.1.9 Commercial human bronchial epithelial cells

TAN	Age	Sex	Race	Alcoholism	Smoker	Group	Company
32332	42 Y	M	B	N	N	Healthy	Lonza, Basel, Switzerland
32254	19 Y	F	B	N	N	Healthy	Lonza, Basel, Switzerland
32484	16 Y	F	C	N	N	Healthy	Lonza, Basel, Switzerland
29132	19 Y	F	C	N	N	Healthy	Lonza, Basel, Switzerland
28706	37 Y	M	H	N	N	Healthy	Lonza, Basel, Switzerland

Age: Y, years; sex: M, male; F, female; race: B, Black; C, Caucasian; H, Hispanic; alcoholism/smoker: N, no

3.1.10 Consumables

Item	Company
12 Well Chamber Slide, removable grid	ibidi, Gräfelfing, Germany
96-well plate tissue culture treated, flat/round	Sarstedt, Nümbrecht, Germany
Amicon Ultra-4, PLGC Ultracel-PL Membrane, 10 kDa	Merck, Darmstadt, Germany
BD Falcon 6-/12-/24-/48-/96-well plate (non-) tissue culture treated, flat	BD Biosciences, San Diego, CA, USA
BD Falcon Cell Strainer 70 µm	BD Biosciences, San Diego, CA, USA
Cell Scraper S/M/L	TPP Techno Plastic Products, Trasadingen, Switzerland
Cellstar Tubes 15/50 mL	Greiner Bio-One, Frickenhausen, Germany
Costar Spin-X centrifuge tube, pore size 0.22 µm	Corning, Corning, NY, USA
CryoPure Tube 1.8 mL, white	Sarstedt, Nümbrecht, Germany
Electron microscopy grid	Plano, Wetzlar, Germany
Exosome Spin Columns (MW 3000)	Thermo Fisher Scientific, Waltham, MA, USA
Extra Thick Western Blotting Filter Paper	Thermo Fisher Scientific, Waltham, MA, USA
Filtropure V50, 500 mL, 0.2 µm	Sarstedt, Nümbrecht, Germany
Immobilon-P Membrane, PVDF, 0.45 µm	Merck, Darmstadt, Germany
Infinium MethylationEPIC BeadChip	Illumina, San Diego, CA, USA
Leukosorb	Pall, New York, NY, USA
Menzel-Gläser Cover Slips, 20x20/24x50	Thermo Fisher Scientific, Waltham, MA, USA
Micro tube 2mL, with screw lid with rubber ring	Sarstedt, Nümbrecht, Germany
NuPAGE 4-12% Bis-Tris Protein Gels, 12-well	Thermo Fisher Scientific, Waltham, MA, USA
qEVoriginal, 70nm, 10 mL	Izon Science, Christchurch, New Zealand
Rhino-Pro Curette	Arlington Scientific, Springville, UT, USA
SafeSeal SurPhob Tips 10/200/1250 µL	Biozym Scientific, Hessisch Oldendorf, Germany
SafeSeal tube 1.5/2 mL	Sarstedt, Nümbrecht, Germany
Serological Pipettes 5/10/25 mL, graduated	Greiner Bio-One, Frickenhausen, Germany
Shandon Cytoclip	Thermo Fisher Scientific, Waltham, MA, USA
Shandon Filter Cards, white	Thermo Fisher Scientific, Waltham, MA, USA
Shandon TPX Single Chamber	Thermo Fisher Scientific, Waltham, MA, USA
S-Monovette EDTA blood collection tube	Sarstedt, Nümbrecht, Germany
Strata-X 96-well plates	Phenomenex, Aschaffenburg, Germany
SuperFrost Plus Adhesion Slides	Thermo Fisher Scientific, Waltham, MA, USA
SurPhob Low Binding Tips 10/200/1250 µL	Biozym Scientific, Hessisch Oldendorf, Germany
T-25/75 cell culture flasks	Greiner Bio-One, Frickenhausen, Germany
Whatman paper filter papers grade 1, 90 mm	GE Healthcare Life Science, Chicago, IL, USA

3.1.11 Devices

Device	Company
1200/1260 Series HPLC	Agilent, Waldbronn, Germany
Agilent 2100 BioAnalyzer	Agilent, Santa Clara, CA, USA
Analytical Balance ALJ	Kern & Sohn, Bailingen-Frommern, Germany
API 4000 triple quadrupole system	Sciex, Darmstadt, Germany
Axiovert 25/40C Microscope	Zeiss, Oberkochen, Germany

Device	Company
BCV control vacuum pump	Vacuubrand, Wertheim, Germany
BD LSR Fortessa	BD Biosciences, Heidelberg, Germany
Bio Plex 200 System	Bio-Rad, Munich, Germany
CM120 Phillips electron miscroscope	FEI Company, Hillsboro, Oregon, USA
Cytospin 4 Cytocentrifuge	Thermo Fisher Scientific, Waltham, MA, USA
ECL ChemoCam Imager	Intas Science Imaging Instruments, Göttingen, Germany
ELGA Purelab flex	Veolia Water Technologies, Celle, Germany
Epoch Microplate Specrophotometer	BioTek, Winooski, USA
EVOS FL Auto Cell Imaging System	Thermo Fisher Scientific, Waltham, MA, USA
Hamilton Microlab STARTM robot	Hamilton, Bonaduz, Switzerland
Heracell CO_2 Incubators	Heraeus, Hanau, Germany
HERAFreeze -80 °C Freezer	Thermo Fisher Scientific, Waltham, MA, USA
Herasafe (KS) Biological Safety Cabinets	Heraeus, Hanau, Germany
HTC PAL autosampler	CTC Analytics, Zwingen, Switzerland
HydroSpeed Microplate Washer	Tecan, Münnedorf, Switzerland
Illumina HiSeq4000 platform	Illumina, San Diego, CA, USA
Illumina iScan platform	Illumina, San Diego, CA, USA
inoLab pH7110 pH meter	WTW, Weilheim, Germany
Kinetex C18 reversed phase column	Phenomenex, Aschaffenburg, Germany
Leica SP5 confocal microscope	Leica Microsystems, Wetzlar, Germany
Megafuge 1.0R	Heraeus, Hanau, Germany
Megafuge 40R	Thermo Fisher Scientific, Waltham, MA, USA
Microlab STAR robot	Hamilton Bonaduz AG, Bonaduz, Switzerland
Mini Blot Module	Thermo Fisher Scientific, Waltham, MA, USA
NanoDrop ND-1000	NanoDrop Technologies Inc., Wilmington, DE, USA
NanoPhotometer N60	Implen, Munich, Germany
NanoSight LM10	Malvern Instruments, Malvern, UK
Pari Boy SX nebulizer	Pari, Starnberg, Germany
Neubauer improved counting chamber	Marienfeld Superior, Lauda Königshofen, Germany
Olympus SIS Keen View G2 camera	Olympus, Hamburg, Germany
PerfectSpin 24R Refrigerated microfuge	PeqLab Biotechnology, Erlangen, Germany
PowerEase 90W Power Supply	Thermo Fisher Scientific, Waltham, MA, USA
PSQ 96 MD system	Qiagen, Hilden, Germany
Sciex QTRAP 5500 mass spectrometer	Sciex, Darmstadt, Germany
SecurityGuard Ultra Cartridge C18	Phenomenex, Aschaffenburg, Germany
SenTix 81 pH meter electrode	WTW, Weilheim, Germany
Sigma 1-15 Microfuge	Sigma Laborzentrifugen, Osterode am Harz, Germany
Stuart Digital Tube Roller SRT9D	Cole-Parmer, Stone, Staffordshire, UK
SW21 shaking water bath	Julabo, Seelbach, Germany
Thermomixer 5437	Eppendorf, Hamburg, Germany
Transferpipette (2.5-25/5-50/20-200/30-300 µL)	Brand, Wertheim, Germany
Ultravap nitrogen evaporator	Porvair Sciences, Leatherhead, UK
Unitwirst RT Shaker	UniEquip, Martinsried, Germany
Vortex Genie2	Bender + Hobein, Bruchsal, Germany
Zorbax Eclipse Plus C18 UHPLC column	Agilent, Waldbronn, Germany

3.1.12 Deposited Data

Type of analysis	Data set	Database	Database ID
Total RNA sequencing	Nasal brushings	EMBL-EBI	E-MTAB-7962
mRNA sequencing	sMac and aMDM	EMBL-EBI	E-MTAB-7965
Genome-wide methylomics	Monocytes and aMDM	EMBL-EBI	E-MTAB-8065

Data is openly accessible upon acceptance of our submitted manuscript at: https://www.ebi.ac.uk/

3.1.13 Software

Software / R package	Company / accessibility
Adobe Illustrator v23.0.1	Adobe Systems Incorporated, San Jose, CA, USA
AmiGO 2	http://amigo.geneontology.org/amigo
Analyst Software 1.6.2-3	Sciex, Darmstadt, Germany
biomaRt v2.38.0	https://www.ensembl.org/info/data/biomart/biomart_r_package.html
DEBrowser v1.11.9	https://bioconductor.org/packages/release/bioc/html/debrowser.html
DMRcate v1.18.0	http://bioconductor.org/packages/release/bioc/html/DMRcate.html
EnhancedVolcano v1.1.3	https://bioconductor.org/packages/release/bioc/html/EnhancedVolcano.html
featureCounts v1.6.2	http://subread.sourceforge.net/
Fiji v2.0.0-re-69/1.52n	https://fiji.sc/
FlowJo v10	Tree Star, Ashland, OR, USA
GenomeStudio v2011.1	Illumina, San Diego, CA, USA
GraphPad Prism 6	GraphPad Software, La Jolla, CA, USA
GSNAP v2018-07-04	http://research-pub.gene.com/gmap/
Htseq-count v0.6.0	https://htseq.readthedocs.io/en/release_0.11.1/count.html
Limma v3.38.3	https://bioconductor.org/packages/release/bioc/html/limma.html
MetaboAnalyst 4.0	https://ww.metaboanalyst.ca
Methylation Module v1.9.0	Illumina, San Diego, CA, USA
Microsoft Office 365	Microsoft, Redmond, WA, USA
Minfi v1.28.4	https://bioconductor.org/packages/release/bioc/html/minfi.html
MultiQuant Software v3.0.1-2	Sciex, Darmstadt, Germany
PyroMark CpG software v1.0.11.14	Qiagen, Hilden, Germany
R v3.5.0-3.5.3	https://www.r-project.org/
R Studio v1.2.1335	https://www.rstudio.com/
STAR aligner v2.4.2a	https://github.com/alexdobin/STAR
ToppGene suite	https://toppgene.cchmc.org
VennDiagram v1.6.20	https://cran.r-project.org/web/packages/VennDiagram/index.html
yapima	https://github.com/xpastor/yapima

3.2 Methods

3.2.1 Study cohort recruitment

This study was approved by the local ethics committee at the Klinikum rechts der Isar, Technical University of Munich (internal reference: 422/16). Written informed consent in accordance with the Declaration of Helsinki was obtained from all study participants. Two cohorts of thirty-five (cohort I) and nine (cohort II) individuals were recruited and classified according to their clinical characteristics at the ear, nose and throat (ENT) clinic of the Klinikum rechts der Isar (Munich, Germany). MALM score was determined for all patients by nasal endoscopy. Healthy controls had no history of chronic rhinosinusitis, nasal polyposis, asthma or intolerance to NSAID. NSAID-tolerant controls with chronic rhinosinusitis with nasal polyps (NT CRSwNP) had taken NSAIDs within the previous 6 months without any adverse reaction. N-ERD was diagnosed based on physician-diagnosed chronic asthma, CRSwNP and a history of respiratory reactions to oral NSAIDs. Exclusion criteria were acute airway infections, other systemic immune disorders, pregnancy, cancer and use of antibiotics, 5-LO inhibitor zileuton, biologics (omalizumab, benralizumab, reslizumab, mepolizumab, dupilumab) and/or OCS four weeks prior to the study. Clinical data of both cohorts are summarized in Table 4.2. For *in vitro* stimulations with exosomes, an additional eight healthy individuals without any diagnosed chronic inflammatory airway disease (all female, mean age: 31.5 (27 – 41) years) were recruited at the Center of Allergy and Environment Munich (ZAUM).

3.2.2 Collection of NLF and nasal brushings

NLF was obtained by placing a filter paper strip (Leukosorb, Pall) on NP of N-ERD and NT CRSwNP patients and inferior turbinates of healthy controls under anterior rhinoscopy for 5 minutes as previously described (Chawes et al., 2010). The paper strips were transferred into a 0.22 µm filter spinning tube (Corning Costar Spin-X, Merck) and centrifuged for 5 minutes at 6.000 x g at 4 °C. Filter units were discarded and cohort I samples were stored at -80 °C until metabolomics analysis (see 3.2.12). For cohort II, the NLF volume was determined prior to dilution with a -20 °C cold 1:1 (V/V) phosphate-buffered saline (PBS)-Methanol (MeOH, Merck) solution to achieve a final MeOH concentration of 40-50% (V/V) before storage at -80 °C for lipid mediator analysis (see 3.2.11). Nasal brushing samples from N-ERD NP and inferior turbinates of healthy individuals of cohort II were collected under anterior rhinoscopy using the Rhino-Pro Curette (Arlington Scientific) as described previously (Dhariwal et al., 2017; Proud, Sanders, & Wiehler, 2004). Nasal brushing samples were directly transferred into RNAprotect (Qiagen) and stored at -80 °C until RNA isolation for RNAseq (see 3.2.16).

3.2.3 Plasma, PBMC and PMN from whole blood

Whole venous blood was drawn randomly between 8:00 and 13:00 in the morning in ethylenediaminetetraacetic acid (EDTA) blood collection tubes (S-Monovette, Sarstedt) without following any specific period of fasting or dietary preparation. For cohort I and PMN isolation, blood was layered on Polymorphprep (Alere Technologies AS) within 2 h of collection and centrifuged at 500 x g for 35 minutes without brake at room temperature (RT), respectively. Plasma was aliquoted and stored at -80 °C for metabolomics analysis (see 3.2.12, 3.2.13) and enzyme-linked immunosorbent assay (ELISA, see 3.2.9). PBMC and PMN layers were transferred into separated 50 mL falcons with PBS. LymphoPrep (Alere Technologies AS) was used for PBMC isolation from blood samples of cohort II.

3.2.4 *In vitro* stimulation of PMN

Erythrocytes were lysed with BD Lysis Buffer (BD Biosciences) for 10-15 min at RT. PGE_2 resistance testing was performed as described previously (Flamand, 2002; Tanya M. Laidlaw et al., 2014). Briefly, $2x10^6$ PMN were short-term cultured in 200 µL Ca^{2+}- and Mg^{2+}-free HBSS (Thermo Fisher Scientific) supplemented with 1.6 mM $CaCl_2$ (Sigma-Aldrich) ($HBSS_{CaCl2}$) in 48-well plates and primed with 700 pM GM-CSF and 1.2 nM TNF (both Miltenyi Biotec) for 30 min, 10 µM cytochalasin B for 20min and 0.1 U/mL adenosine deaminase (both Sigma-Aldrich) for 5 min prior stimulation with PBS (Thermo Fisher Scientific), 100 nM PGE_2 or 50 µM forskolin (both Cayman Chemical) for 30 min. A subsequent stimulation with 1 µM fMLP (Sigma-Aldrich) for 10 min was stopped with 200 µL ice-cold $HBSS_{CaCl2}$. After centrifugation for 2 min at 2.000 x g, 4 °C, supernatant (SN) were aliquoted and, for lipid mediator analysis (see 3.2.11), diluted 1:1 (V/V) with -20 °C cold MeOH (Merck) and stored at -80 °C.

PMN SN generation for exosome isolations was performed as previously described (Majumdar et al., 2016). Briefly, $10x10^6$ PMN were primed in 1 mL RPMI-1640 (Thermo Fisher Scientific) supplemented with 5 ng/mL GM-CSF for 30 min, centrifuged for 5 min at 1.600 rpm, 4 °C and resuspended in ice-cold PBS for 30 min to reduce basal exocytosis levels. Cells were resuspended in PBS supplemented with 1 mg/mL glucose (Sigma-Aldrich) and 1 mM $CaCl_2$ and stimulated with 2 nM fMLP for 30 min at 37 °C. After centrifugation, SN was stored at -80 °C until exosomes isolation by precipitation or size-exclusion chromatography (SEC) (see 3.2.17).

3.2.5 FACS of whole blood and isolated PMN

For flow cytometry analysis, also known as fluorescence-activated cell sorting (FACS), 20 µL of whole peripheral blood were incubated with fluorophore-conjugated, 1:10 diluted anti-human CD45, CD11b, CD14 (all BD Biosciences), CD61 (Thermo Fisher Scientific) and 1:5 diluted anti-human CD16 (BioLegend), CC motif chemokine receptor type 3 (CCR3, BD Biosciences) antibodies for 20 min at RT and then fixed in 1% paraformaldehyde (PFA, Sigma-Aldrich) for 10 minutes at RT. Erythrocytes were lysed for 15 minutes at RT by addition of 200 µL erythrocyte lysis buffer (BD Pharm Lyse, BD Biosciences). Cells were washed with 1 mL FACS buffer (FB, PBS with 1% FBS (GE Healthcare Life Science)) supplemented with 5 mM EDTA (Thermo Fisher Scientific) (FB_{EDTA}), centrifuged at 2.000 rpm, RT for 2 min and resuspended in ice-cold FB_{EDTA}.

For isolated PMN FACS analysis, $2x10^6$ PMN were resuspended and incubated in FB_{EDTA} with Fc block (1:50 dilution, Thermo Fisher Scientific) for 10 min at RT to block unspecific antibody-binding before staining the cells with 1:50 diluted anti-human CD11b, CD16, CCR3, CD61, Siglec-8 (Biolegend) and CRTH2 (BD Biosciences) for 30 min at 4 °C. Cells were washed, centrifuged at 2.000 rpm, RT for 2 min and resuspended in ice-cold FB_{EDTA}. FACS analysis was performed on a BD LSR Fortessa (BD Biosciences) and data were analyzed with FlowJo v10 (Tree Star).

3.2.6 *In vitro* generation and stimulation of alveolar-like macrophages

$CD14^+$ monocytes were isolated from PBMC using CD14 MACS beads (Miltenyi Biotec) according to manufacturer's instructions, transferred in T-75 and/or T-25 flasks and differentiated into aMDM in the presence of 10 ng/mL GM-CSF and 2 ng/mL TGFβ1 (Peprotech) in complete medium (RPMI-1640 supplemented with 10% FBS, 100 units/mL penicillin, 100 µg/mL streptomycin (Penicillin-Streptomycin, Thermo Fisher Scientific) and 1 µg/mL gentamicin (Thermo Fisher Scientific) at a concentration of $0.5x10^6$ monocytes/mL for seven days as described previously (Dietz et al., 2017; Esser et al., 2010). FBS was exchanged for 10% exosome-free FBS (Thermo Fisher Scientific) for exosome-free conditions. $2x10^5$ or $1x10^6$ aMDM were seeded in 96-well or 6-well plates and stimulated for 24 h with following conditions: (q)PBS as control, 10 ng/mL IL4 (Miltenyi Biotec), 100 nM PGE_2 or sputum exosomes equaling $2x10^5$ sputum cells from N-ERD or healthy individuals. PBS, IL4 and PGE_2 stimulations with $2x10^5$ aMDM were further stimulated with the calcium ionophore A23187 (5 µM, Sigma-Aldrich) for 10 min at 37 °C to enhance lipid mediator production (Capasso, Tavares, Tsang, & Bennett, 1985). SN were aliquoted and, for lipid mediator analysis (see 3.2.11), diluted 1:1 (V/V) with -20 °C cold MeOH and stored at -80 °C. aMDM were washed once with PBS, lysed in RLT Buffer (Qiagen) with 1% β-mercaptoethanol (βME, Carl Roth) and stored at -80 °C until RNA or deoxyribonucleic acid (DNA) isolation (see 3.2.16 or 3.2.14-3.2.15, respectively).

3.2.7 Sputum induction and sMac isolation

Sputum induction was performed as previously described (Zissler et al., 2018). Patients inhaled increasing concentrations of hypertonic saline solutions (3, 4, 5% NaCl V/V) in three consecutive 7-minute inhalation steps. After each step, patients were asked to expectorate sputum. Samples were kept and processed on ice in the first 60 minutes after sputum induction. Sputum plugs were selected, pooled, weighed ($w_{sputum\ plugs}$) and homogenized with 4:1 ($V/w_{sputum\ plugs}$) of 0.1% dithiothreitol (DTT, Sputolysin Reagent, Calbiochem) and incubated under motion for 15 min at 4 °C. An aliquot of the homogenate was stored at -80 °C for metabolomic analysis (see 3.2.12). The homogenate was diluted 2:1 ($V/w_{sputum\ plugs}$) with PBS and filtrated through a 70 µm cell filter (BD Biosciences). After centrifugation for 10 min at 790 x g, 4 °C without break, SN were aliquoted and, for lipid mediator analysis (see 3.2.11), diluted 1:1 (V/V) with -20 °C cold MeOH and stored at -80 °C. The sputum cell pellet was resuspended in ice-cold PBS, counted and 50.000 cells were transferred in 5% BSA (V/V, in PBS) on SuperFrost Plus Adhesion Slides (Thermo Fisher Scientific) by centrifugation at 300 rpm for 5 min, RT in a Cytospin 4 cytocentrifuge (Thermo Fisher Scientific). Differential cell counts were performed by counting at least 400 non-squamaous cells as described previously (Zissler et al., 2018). Briefly, air-dried slides were fixed with MeOH for 5 min and stained using the Pappenheim method (8 min May-Gruenwald (Carl Roth) followed by 35 min Giemsa (Merck) staining) and analyzed at 40x magnification. The sputum cell pellet was resuspended in ice-cold PBS and highly purified sputum macrophages (sMac) were obtained as described previously (Frankenberger et al., 2011). Briefly, sputum cells were co-incubated with erythrocytes from the same donor and RosetteSep human monocyte enrichment cocktail (Stemcell Technologies) for 20 min at RT. A subsequent density gradient centrifugation at 1.500 rpm for 15 min, RT without brake on LymphoPrep generated a mononuclear layer with sMac. sMac purity and viability were determined by cell counting with trypan blue (Thermo Fisher Scientific) and were >90% for all individuals. sMac were lysed in RLT Buffer with 1% βME and stored at -80 °C until RNA isolation for RNAseq (3.2.16).

3.2.8 Immunofluorescence (IF)

Inferior turbinate or NP tissues were collected from healthy or N-ERD individuals undergoing rhinosurgery. Prior to FESS, N-ERD patients have taken oral glucocorticoids in accordance to common guidelines (Fokkens et al., 2012; Pundir et al., 2016). Tissue specimens were fixed in 4% PFA and embedded in paraffin wax. Sections (4 µm) on SuperFrost Plus Adhesion Slides were dewaxed at 65 °C for 30 min and rehydrated in roticlear (Carl Roth), isopropanol (Carl Roth), 96% ethanol (EtOH, V/V, Merck) and 70% EtOH (V/V). Autofluorescence was blocked with MaxBlock reagent A (MaxVision Biosciences) for 5 min at RT followed by 60% EtOH (V/V) for 1 min and H_2O. Antigens were retrieved by boiling in sodium citrate buffer with 0.05% Tween-20 (Sigma-Aldrich)

for three times with 20 min cool downs in between. Tissues were permeabilized with 0.2% Triton-X 100 (V/V, Sigma-Aldrich) for 45 min at RT and blocked with 10% donkey serum (V/V, Sigma-Aldrich) in 3% BSA (V/V, in PBS) for 1 h at RT. Primary 1:50 diluted anti-human ApoE (Atlas Antibodies), HTR4 (OriGene Technologies), CD81, TSG101 (both Santa Cruz Biotechnology) antibodies in blocking solution were added and incubated over night at 4 °C with subsequent 1 h incubation with fluorescence-conjugated donkey anti-rabbit/mouse (AF488/AF647) antibodies (all Thermo Fisher Scientific) in 3% BSA (V/V, in PBS) for detection. Autofluorescence post-conditioner (MaxBlock reagent B, MaxVision Biosciences) for 5 min at RT and tissues were stained and mounted with 4′,6-diamidino-2-phenylindole (DAPI)-containing Fluoroshield (GeneTex) for 5 min at RT and stored at 4 °C. Images were recorded on a Leica SP5 confocal microscope (Leica Microsystems) and processed with Fiji v2.0.0-re-69/1.52n (Schindelin et al., 2012).

3.2.9 Enzyme-linked immunosorbent assay (ELISA)

ELISAs for human ECP (Cusabio), total IgE (Invitrogen, Thermo Fisher Scientific), adiponectin and leptin (both Bertin Pharma) were performed according to the manufacturer's instructions with plasma samples of cohort I. ECP and total IgE were measured by immunoCAP (Thermo Fisher Scientific) for cohort II at the Klinikum rechts der Isar. Total IgE unit kU/L results were converted into ng/mL for consistency (Amarasekera, 2011).

3.2.10 Chemokine/cytokine multiplex assays

Multiplex chemokine/cytokine assays (Magnetic Luminex Assay 17-plex, 4-plex, 2-plex, 8-plex, all R&D Systems: see 3.1.8 for a detailed list of analytes) of aMDM SN, hBECs SN and exosome preparations were performed according to the manufacturer's instructions on a Bio Plex 200 System (Bio-Rad).

3.2.11 Lipid mediator analysis – LC-MS/MS

The following method description has been provided by the Genome Analysis Center (GAC) Metabolomics Core Facility of the Helmholtz Zentrum München, Munich, Germany:

Lipid mediator analysis was performed as described previously (Henkel et al., 2018). Automated solid phase extractions were performed with a HamiltoFn Microlab STAR robot (Hamilton Bonaduz AG). Prior to extraction all samples (cell culture SN, sputum SN, NLF) were diluted with H_2O to a MeOH content of 15% and 10 µl of IS stock solution was added. Samples were extracted using Strata-X 96-well plates (30 mg,

Phenomenex) and eluted with MeOH. Samples were evaporated to dryness under nitrogen stream and redissolved in 100 µl MeOH/H_2O (1:1).

Chromatographic separation of eicosanoids was achieved with a 1260 Series HPLC (Agilent Technologies Deutschland GmbH) using a Kinetex C18 reversed phase column (2.6 µm, 100 x 2.1 mm, Phenomenex) with a SecurityGuard Ultra Cartridge C18 (Phenomenex) precolumn. The Sciex QTRAP 5500 mass spectrometer (Sciex), equipped with a Turbo-VTM ion source, was operated in negative ionization mode. Samples were injected via HTC PAL autosampler (CTC Analytics), set to 4 °C. Metabolites were identified via retention time and scheduled multiple reaction monitoring (sMRM). Unique Q1/Q3 transitions were selected for each analyte by using single analyte injections and comparison with the literature (Dumlao, Buczynski, Norris, Harkewicz, & Dennis, 2011). Analytes with identical sMRM transitions were differentiated by retention time. Acquisition of liquid chromatography-tandem mass spectrometry (LC-MS/MS) data was performed using Analyst Software 1.6.3 followed by quantification with MultiQuant Software 3.0.2 (both Sciex).

3.2.12 Metabolomics (I) – Metabolite Quantification

The following method description has been provided by the Genome Analysis Center (GAC) Metabolomics Core Facility of the Helmholtz Zentrum München, Munich, Germany and has been previously published elsewhere (e.g. Y. Yang et al., 2019):

The targeted metabolomics approach was based on LC-electron spray ionization (ESI)-MS/MS and flow injection analysis (FIA)-ESI-MS/MS measurements and the AbsoluteIDQ p180 Kit (Biocrates Life Sciences AG). The assay allows simultaneous quantification of 188 metabolites out of 10 µL plasma, 2.5 µL NLF or 5 µL sputum homogenate and includes free carnitine, 39 acylcarnitines (Cx:y), 21 amino acids (19 proteinogenic + citrulline + ornithine), 21 biogenic amines, hexoses (sum of hexoses – about 90-95% glucose), 90 glycerophospholipids (14 lysophosphatidylcholines (lysoPC) and 76 phosphatidylcholines (PC)), and 15 sphingolipids (SMx:y). The abbreviations Cx:y are used to describe the total number of carbons and double bonds of all chains, respectively (for more details see (Römisch-Margl et al., 2012)). For the LC-part, compound identification and quantification were based on sMRM measurements. The method of AbsoluteIDQ p180 Kit has been proven to be in conformance with the EMEA-Guideline "Guideline on bioanalytical method validation (July 21st 2011)" (European Medicines Agency (EMA), 2011), which implies proof of reproducibility within a given error range. Plasma, NLF and sputum preparation samples were applied directly and undiluted to the assay. The limits of detection (LODs) were set to three times the values of the zero samples (PBS, for all three materials). The assay procedures of the AbsoluteIDQ p180 Kit as well as the metabolite nomenclature have been described in detail previously (Römisch-Margl et al., 2012; Zukunft, Sorgenfrei, Prehn, Möller, & Adamski, 2013). Sample handling was performed by a Hamilton Microlab STARTM

robot (Hamilton Bonaduz AG) and a Ultravap nitrogen evaporator (Porvair Sciences), beside standard laboratory equipment. Mass spectrometric analyses were done on an API 4000 triple quadrupole system (Sciex) equipped with a 1200 Series high-performance (HP)LC (Agilent Technologies Deutschland GmbH) and HTC PAL auto sampler (CTC Analytics) controlled by the software Analyst (v1.6.2). Data evaluation for quantification of metabolite concentrations and quality assessment was performed with the software MultiQuant (v3.0.1, Sciex) and the MetIDQ software package, which is an integral part of the AbsoluteIDQ Kit. Metabolite concentrations were calculated using internal standards and reported in µM. Previously trials with NLF and sputum preparations have been performed to determine assay performance, quality and sample input quantity.

3.2.13 Metabolomics (II) – Sphingolipid Metabolite Quantification

The following method description has been provided by the pharmazentrum Frankfurt/ZAFES of the Goethe University Frankfurt, Frankfurt, Germany and has been previously published elsewhere (e.g. Koch et al., 2017):

For the quantification of sphingolipids, 10 µL plasma were mixed with 200 µL extraction buffer (citric acid 30 mM, disodium hydrogen phosphate 40 mM) and 20 µL of the internal standard solution containing sphingosine-d7, sphinganine-d7, sphingosine-1-phosphate-d7, C17:0 Cer, C16:0 Cer-d7, C18:0 Cer-d3, C17:0 LacCer, C18:0 dhCer-d3, C16:0 LacCer-d3, C18:0 GluCer-d5, C24:0 Cer-d7 (all avanti polar lipids) and C24:0 Cer-d4 (Chiroblock GmbH). The mixture was extracted once with 600 µL MeOH/chloroform/hydrochloric acid (15:83:2, V/V/V). The lower organic phase was evaporated at 45 °C under a gentle stream of nitrogen and reconstituted in 100 µL of tetrahydrofuran/water (9:1, V/V) with 0.2 formic acid and 10 mM ammonium formate.

For the preparation of calibration standards and quality control samples, 20 µL of a working solution were processed as stated instead of 10 µL sample. Working solutions for the generation of calibrator and quality control samples were prepared as a mixture of all analytes by serial dilution using a mixture of tetrahydrofuran and chloroform.

Amounts of sphingolipids were analyzed by liquid chromatography coupled to tandem mass spectrometry. An Agilent 1260 series binary pump (Agilent technologies) equipped with a Zorbax Eclipse Plus C18 UHPLC column (50 mm x 2.1 mm ID, 1.8 µm, Agilent Technologies Deutschland GmbH) was used for chromatographic separation. The column temperature was 55 °C. The HPLC mobile phases consisted of water with 0.2% formic acid and 2 mM ammonium formate (mobile phase A) and acetonitrile/isopropanol/acetone (50:30:20, V/V/V) with 0.2% formic acid (mobile phase B). For separation, a gradient program was used at a flow rate of 0.4 mL/min. The initial buffer composition 65% (A)/35% (B) was held for 0.6 min and then within 0.4 min, linearly changed to 35% (A)/65% (B) and held for 0.5 min. Within 3 min, (B) was further increased to 100% and held for 6.5 min. Subsequently, the composition was linearly

changed within 0.5 min to 65% (A)/35% (B) and then held for another 2.5 min. The total running time was 14 min, and the injection volume was 10 µL. To improve ionization, isopropyl alcohol was infused post-column using an isocratic pump at a flow rate of 0.1 mL/min. After every sample, sample solvent was injected for washing and re-equillibrating the analytical column using two short runs (4 min each).

The MS/MS analyses were performed using a triple quadrupole mass spectrometer QTrap 5500 (Sciex) equipped with a Turbo V Ion Source operating in positive electrospray ionization mode. The MS parameters were set as follows: Ionspray voltage 5500 V, source temperature 450 °C, curtain gas 35 psi, collision gas 12 psi, nebulizer gas 45 psi and heating gas 65 psi. The analysis was done in MRM mode. Data acquisition was done using Analyst Software (v1.6.2) and quantification was performed with MultiQuant Software (v3.0.2, both Sciex), employing the internal standard method (isotope dilution mass spectrometry). Variations in the accuracy of the calibration standards were less than 15% over the whole range of calibration, except for the lower limit of quantification, where a variation in accuracy of 20% was accepted.

3.2.14 Targeted methylomics – Bisulfite pyrosequencing

The following method description has been provided by the CEA-Institut de Génomique of the Centre National de Génotypage, Evry Cedex, France and has been previously published elsewhere (e.g. Yaghi et al., 2016):

Quantitative DNA methylation analysis was performed by pyrosequencing of bisulfite treated DNA (Tost & Gut, 2007). One µg of DNA was bisulfite converted using the EpiTect 96 Fast Bisulfite kit (Qiagen) according to the manufacturer's instructions. Regions of interest (ALOX5AP, LTB4R, HPGDS, PTGES) for validation were amplified using 30 ng of bisulfite treated human genomic DNA and 4 pmol of forward and reverse primer, one of them being biotinylated. Sequences for oligonucleotides for PCR amplification and pyrosequencing are shown in 3.1.6. Primers were added to the 1X Phusion U Hot Start PCR Master Mix (ThermoFisher Scientific) in a final volume of 25 µl. The PCR program consisted of a denaturing step of 15 min at 95 °C followed by 50 cycles of 30 seconds at 95 °C, 30 seconds at the respective annealing temperature (see 3.1.6) and 15 seconds at 72°C, with a final extension of 5 min at 72 °C. 10 µl of PCR product were rendered single-stranded as previously described (Tost & Gut, 2007) and 4 pmol of the respective sequencing primer were used for analysis. Quantitative DNA methylation analysis was carried out on a PSQ 96 MD system with the PyroGold SQA Reagent Kit (Qiagen) and results were analyzed using the PyroMark CpG software (v1.0.11.14, Qiagen).

3.2.15 Genome-wide methylomics

Genomic DNA was extracted according to the manufacturer's instructions (Zymo Research). Genomic DNA quality and quantity was assessed by NanoPhotometer N60 (Implen).

The following method description has been provided by the Genome Analysis Center (GAC) Genotyping Core Facility of the Helmholtz Zentrum München, Munich, Germany:

Genomic DNA (750 ng) was bisulfite converted using the EZ-96 DNA Methylation Kit (Zymo Research). Subsequent methylation analysis was performed on an Illumina (San Diego) iScan platform using the Infinium MethylationEPIC BeadChip according to standard protocols provided by Illumina. GenomeStudio software version 2011.1 with Methylation Module version 1.9.0 was used for initial quality control of assay performance and for generation of methylation data export files.

3.2.16 Whole transcriptome analysis – RNA sequencing

Total RNA was extracted according to the manufacturer's instructions (Zymo Research). Total RNA quality and quantity was assessed by NanoDrop ND-1000 (NanoDrop Technologies Inc.) or NanoPhotometer N60 (Implen). RNA integrity number (RIN) was determined with the Agilent 2100 BioAnalyzer (RNA 6000 Nano Kit, Agilent).

The following method description has been provided by the Institute of Human Genetics Next-Generation Sequencing Core Facility of the Helmholtz Zentrum München, Munich, Germany and has been previously published elsewhere (e.g. Fischer et al., 2019):

For library preparation using the TruSeq Stranded Total RNA Library Prep Kit with Ribo-Zero (Illumina) for total RNAseq (nasal brushings), 1 µg of RNA was depleted for cytoplasmatic ribosomal (r)RNAs, fragmented, and reverse transcribed with the Elute, Prime, Fragment Mix. For sMac and aMDM, strand specific, polyA-enriched RNA sequencing was performed as described earlier (Haack et al., 2013). Briefly, 300 ng of RNA was poly(A) selected, fragmented, and reverse transcribed with the Elute, Prime, Fragment Mix (Illumina). A-tailing, adaptor ligation, and library enrichment were performed as described in the High Throughput protocol of the TruSeq RNA Sample Prep Guide (total RNAseq) and in the TruSeq Stranded mRNA Sample Prep Guide (stranded mRNAseq) (both Illumina). RNA libraries were assessed for quality and quantity with the Agilent 2100 BioAnalyzer and the Quant-iT PicoGreen dsDNA Assay Kit (Invitrogen, Thermo Fisher Scientific).

RNA libraries were sequenced as 150 bp paired-end runs on an Illumina HiSeq4000 platform resulting in ~50-118 Million single end reads per library. The STAR aligner (v2.4.2a) (Dobin et al., 2013) with modified parameter settings (--twopassMode=Basic) was used for split-read alignment against the human genome assembly hg19 (GRCh37)

and UCSC knownGene annotation. To quantify the number of reads mapping to annotated genes we used HTseq-count (v0.6.0) (Anders, Pyl, & Huber, 2015). FPKM (Fragments Per Kilobase of transcript per Million fragments mapped) values were calculated using custom scripts.

3.2.17 Exosome isolation

For first trials with cell and NP tissue culture SN, exosomes were isolated by either precipitation or SEC, while sputum exosomes from cohort I were isolated by precipitation and subsequently purified by SEC as suggested by guidelines (Coumans et al., 2017). SN samples were thawed on ice and larger protein aggregates, microvesicles and debris were removed by centrifugation for 10 min at 2.000 x g, 4 °C and 30 min at 10.000 x g, 4 °C. Debris-free SN were mixed with 1:2 (V/V) total exosome isolation reagent (TEI, Thermo Fisher Scientific) and incubated overnight at 4 °C. Exosome pellets (TEI exosomes) were retrieved after centrifugation for 1 h at 10.000 x g, 4 °C and resuspended in 0.2 µm-filtered PBS (qPBS). For sputum samples, exosomes of each study group were resuspended and pooled in a total of 500 µL qPBS. For SEC, 500 µL SN, TEI exosomes or qPBS as control were transferred onto qEV columns (Izon Science) and purified exosomes were eluted in a total of 1.5 mL qPBS according to manufacturer's instructions. Sputum exosomes were concentrated by centrifugation with Amicon Ultra-4 10 kDa columns with regenerated cellulose (Merck) to normalize the exosome preparations to initial sputum cell counts ($10x10^6$ cells/mL). Exosome preparations were aliquoted in low protein-binding screw-cap tubes with rubber-ring (Sarstedt), snap-frozen in liquid nitrogen and stored at -80 °C according to guidelines (Coumans et al., 2017).

3.2.18 Western blot

TEI- or SEC-isolated exosomes from cell or NP tissue culture SN and crude NLF were analyzed by Western Blot. 27 µL sample were mixed with either 4X lithium dodecyl sulfate (LDS) sample buffer (Thermo Fisher Scientific) or 4X in-house sodium dodecyl sulfate (SDS) sample buffer (see 3.1.3) and optional with either 10X reducing agent (DTT, Thermo Fisher Scientific) or 3.2 µL βME. Samples were heated for 10 min at 95 °C before loading into 40 µL pockets of 4-12% Bis-Tris protein gels (Thermo Fisher Scientific). One to two pockets were used for 5 µL of a pre-stained protein standard (SeeBlue Plus 2, Thermo Fisher Scientific). Proteins were separated at 125 V for 60-90 min, RT in MOPS buffer (Thermo Fisher Scientific) and transferred onto a polyvinylidene fluoride (PVDF) membrane (Merck) using a Mini Blot Module (Thermo Fisher Scientific) at 20 V for 90 min, RT in transfer buffer (Thermo Fisher Scientific) with 10% MeOH. The PVDF membrane was shortly washed in tis-buffered saline (TBS) with 0.02% Tween-20 (TBS-T, V/V) and blocked in 5% non-fat dried milk in TBS-T (MTBS-T) for 1 h, RT and subsequently incubated with a primary anti-human antibody

solution (CD63, CD81 or tumor susceptibility gene 101 (TSG101); for dilution and details see 3.1.5) in MTBS-T overnight at 4 °C while in motion. Washed with TBS-T, the PVDF membrane was incubated with a secondary anti-rabbit/mouse IgG HRP-conjugated antibody solution (for dilutions and details see 3.1.5) in MTBS-T for 1 h, RT. The PVDF membrane was washed with TBS-T and transferred into TBS before adding the detection substrate (SuperSignal West Femto Maximum Sensitive Substrate, Pierce, Thermo Fisher Scientific) according to manufacturer's instructions. Images were recorded with an ECL ChemoCam Imager (Intas). For the detection of multiple proteins, antibodies were removed from the PVDF membrane with stripping buffer (Thermo Fisher Scientific) for 30 min, RT before incubation with a different primary antibody.

3.2.19 Nanoparticle Tracking Analysis (NTA)

Concentration and size distribution of exosome preparations or qPBS were analyzed with a NanoSight LM10 (Malvern Instruments) microscope operated at RT with camera level set to 11, detection threshold set to 3 and automatic configuration for blur size and max jump distance. Exosome preparations were diluted 1:10 to 1:100 (V/V) with H_2O to achieve >50 particles per frame for tracking. Each sample was measured in triplicates for 30 seconds.

3.2.20 Transmission Electron Microscopy (TEM)

TEM analyses of exosome preparations were performed at the Electron Microscopy Core Facility of the European Molecular Biology Laboratory (EMBL) in Heidelberg, Germany. 5 µL of exosome preparations or qPBS were deposited on in-house Formvar-carbon (Serva) coated electron microscopy (EM) grids (Plano) for 20 min at RT. EM grids were washed with PBS, stained with 1% glutaraldehyde (V/V, Electron Microscopy Sciences) in PBS, washed with H_2O and embedded in 3% uranylacetate (w/V, Serva) in H_2O for 1 min at RT. Air-dried EM grids were analyzed on a CM120 Phillips electron microscope equipped with an Olympus SIS Keen View G2 camera (Olympus) operated at 100 kV with a magnification of 24.500x.

3.2.21 Culture and stimulation of hBECs

Human bronchial epithelial cells (hBECs, passage 1) from five healthy donors were obtained from Lonza (see 3.1.9 for donor characteristics), expanded in bronchial epithelium growth medium (BEGM, Lonza) supplemented with 1% antibiotic-antimycotic (100 units/mL penicillin, 100 µg/mL streptomycin, 250 ng/mL amphotericin B, Thermo Fisher Scientific) and 1 µg/mL gentamicin (Thermo Fisher Scientific) and stored à $6x10^5$ cells in 1 mL freezing medium (5:4:1 (V/V) DMEM-F12 (Thermo Fisher Scientific)/FBS/DMSO (Applichem)) in 1.8 mL screw-cap cryo tubes (Sarstedt) in liquid

nitrogen (passage 2). Cells were thawed in a lukewarm water bath, washed with 37 °C warm BEGM, cultured for one more passage (passage 3) and seeded in 6-well plates at a density of $150x10^4$ hBECs/2 mL BEGM or in 12-well chamber slides (ibidi) at a density of $7x10^4$ hBECs/200 µL BEGM (passage 4). After reaching 80-85% confluency, hBECs were washed with PBS and serum-deprived in 1 mL (6-well plates) or 200 µL (chamber slides) bronchial epithelium basal medium (BEBM, Lonza) with 1% antibiotic-antimycotic and 1 µg/mL gentamicin overnight (16-17 h). hBECs in chamber slides were used for exosome uptake experiments (see 3.2.22). hBECs in 6-well plates were stimulated with qPBS, healthy and N-ERD sputum-derived exosomes equaling $800x10^5$ initial sputum cells for 24 h. 6-well plates were then centrifuged for 2 min at 2.000 x g, 4 °C and SN was aliquoted and stored at -80 °C for multiplex analysis (see 3.2.10). hBECs were washed with ice-cold PBS, lysed in RLT buffer (Qiagen) with 1% βME (Carl Roth) and stored at -80 °C.

3.2.22 Exosome-uptake cultures

An sputum exosome equivalent (100 µL) of $1x10^6$ initial sputum cells of N-ERD or healthy individuals or qPBS were labeled with 500 ng C5-maleimide AF488 (Thermo Fisher Scientific) in 2.5 µL cell-culture grade DMSO for 60 min, RT in the dark as described previously (Roberts-Dalton et al., 2017). Excess dye was removed and labeled exosomes were eluted by qPBS-rehydrated ExoSpin columns (Thermo Fisher Scientific) for 3 min at 750 x g, RT, aliquoted à 20 µL in low protein-binding screw-cap tubes with rubber ring and stored at -80 °C. Labeled exosomes or qPBS were thawed at 37 °C and transferred into chamber slides with $200x10^5$ aMDM in 200 µL exosome-free complete medium or 80-85% confluent, starved hBECs (see 3.2.21) in 200 µL BEBM. Live cell images of AF488-fluorescence were taken prior stimulation and 30 min, 1 h, 2 h and 24 h after the addition of labeled exosomes. SN was aliquoted and stored at -80 °C. Cells were washed with PBS, fixated with 4% PFA for 15 min at RT, permeabilized with -20 °C cold acetone (Sigma-Aldrich) for 10 minutes and blocked in blocking solution (PBS, 10% donkey serum (V/V), 3% BSA (V/V)) for 1 h, RT. Cells were stained with primary 1:50 diluted goat anti-human β-actin antibody (Santa Cruz Biotechnology) at 4 °C overnight, secondary donkey anti-goat AF568 (Thermo Fisher Scientific) for 1h, RT and DAPI for 5 minutes, RT with Fluoroshield. Images were recorded on a Leica SP5 confocal microscope and processed with Fiji v2.0.0-re-69/1.52n (Schindelin et al., 2012).

3.3 Bioinformatical analysis and statistics

3.3.1 Genome-wide transcriptomics – RNAseq

Raw reads were mapped to the human genome (hg38) with GSNAP (version 2018-07-04) (Wu & Nacu, 2010) and splice-site information from Ensembl release 87 (Zerbino et al., 2018). Uniquely mapped reads and gene annotations from Ensembl were used as input for featureCounts (v1.6.2) (Liao, Smyth, & Shi, 2014) to create counts per gene and cell. All non-protein coding genes were removed.

Differential expression analysis was performed with R (v3.5.0) (R Core Team, 2017) and the R package DEBrowser (v1.11.9) (Kucukural, Yukselen, Ozata, Moore, & Garber, 2019). Count and metadata were uploaded and low coverage features with a maximum count of < 10 were removed. Normalization and differential expression analysis were performed utilizing the implemented R package DESeq2 (Love, Huber, & Anders, 2014). For the nasal brushing and aMDM dataset, significance thresholds were set to adjusted *p*-value (*p* adj.) ≤ 0.05 (Benjamini-Hochberg false discovery rate, Benjamini & Hochberg, 1995) and log2 Fold Change ≥ 1 / ≤ -1. For the sMac vs. aMDM dataset, the *p* adj. threshold was set to ≤ 0.01. To remove epithelial signatures in the sMac dataset, AmiGO 2 (Ashburner et al., 2000; Carbon et al., 2009; Mi et al., 2017; The Gene Ontology Consortium, 2019) search results of Homo sapiens protein-coding genes associated with the gene ontology (GO) term “epithelial”, but not “macrophage”, were excluded from the dataset. To further reduce dimensionality, differential expressed genes were matched with the search term results of “carnitine”, “sphingo”, “cytokine”, “chemokine” and “icosanoid” through the biomaRt package (v2.38.0) (S. Durinck et al., 2005; Steffen Durinck, Spellman, Birney, & Huber, 2009). Enrichment and pathway analysis of differentially expressed genes (DEGs) was performed with the online platform ToppGene suite (J. Chen, Bardes, Aronow, & Jegga, 2009). Volcano plots were created using the differential expression data with standard R packages and EnhancedVolcano (v1.1.3) (Blighe K, 2019). For consistency with metabolomics data (see 3.3.3), heatmaps were created with MetaboAnalyst 4.0 (Chong et al., 2018). RNA sequencing data have been deposited in the ArrayExpress database at EMBL-EBI (Kolesnikov et al., 2015) under accession number E-MTAB-7962 (nasal brushing) and E-MTAB-7965 (sMac and aMDM).

3.3.2 Genome-wide epigenetics – Methylome sequencing

The methylation arrays were processed and analysed using a modified version of yapima (commit: 01c41aeadf6c4f97a7afecbf9e69ff08604594d9). The array data were loaded into the R environment (R version 3.5.1 ‘Feather Spray’, 2018-07-02) using the minfi package (Aryee et al., 2014) and cross-reactive probes (McCartney et al., 2016) were flagged. Probes with single base extension (SBE) position-overlapping single nucleotide polymorphisms (SNPs) with allele frequency higher than 0.005 in European populations

(McCartney et al., 2016) were also flagged (n = 339887). Measurements with detection p-values higher than 0.01, as estimated by minfi and typically of low quality, were masked. Probes with low quality in at least 50% of the samples were also flagged. The intensities were adjusted with the minfi package (Aryee et al., 2014). The background signal was corrected using Noob (Triche, Weisenberger, Van Den Berg, Laird, & Siegmund, 2013), with an offset of 15 and dye bias correction without a reference sample, and normalized with SWAN (Maksimovic, Gordon, & Oshlack, 2012). The analysis of differentially methylated positions (DMP) was done on the M-values of the reliable probes (not flagged) using the biconductor limma package (Ritchie et al., 2015). The interaction between the cell type and the disease status was analysed, using as covariates the patient identifier, the smoking status, the gender and the presence of atopy (a detailed protocol is described in the limma userguide: bioconductor.org/packages/3.1/bioc/vignettes/limma/inst/doc/usersguide.pdf).

Benjamini-Hochberg false discovery rate (Benjamini & Hochberg, 1995) was applied to correct for multiple testing. Probes with an adjusted p-value lower than 0.05 where taken as the significant subset. Volcano plots of DMPs were created with standard R packages and EnhancedVolcano (v1.1.3) (Blighe K, 2019). The detection of differentially methylated regions (DMR) was done using the bioconductor DMRcate package (Peters et al., 2015). The t statistics from the DMP analysis was used and the beta log fold change was computed running the standard limma workflow on the beta values. All the other parameters were left as default. When necessary, the beta-values were derived from the M-values as described by Du et al. (Du et al., 2010). For functional analyses of DMRs, a significance threshold was set to Stouffer $\leq$ 0.05. Significant DMR-derived genes were subjected to enrichment and pathway analysis by ToppGene suite (J. Chen et al., 2009) and compared by cell type and with aMDM-derived DEGs (RNAseq data) in a Venn Diagram created with the VennDiagram package (H. Chen & Boutros, 2011). Genome-wide methylomics data have been deposited in the ArrayExpress database at EMBL-EBI (Kolesnikov et al., 2015) under accession number E-MTAB-8065.

3.3.3 Targeted metabolomics – Multi-fluid analyses

Based on the exploratory study design, values below LOD were included in subsequent analyses. Metabolomics data of all measurements were imported into the online platform MetaboAnalyst 4.0 (Chong et al., 2018) for statistical analysis.

Plasma metabolomics data from both metabolomics approaches were pooled. The final dataset included 204 quantified metabolites after the removal of 9 features with > 20% missing values. Remaining missing values (24, 0.3% of total values) were estimated with the k-nearest neighbors (KNN) algorithm. Data were normalized by sum, cube root transformed and auto-scaled. The unsupervised principal component analysis (PCA) and hierarchical clustering were used to identify 4 outliers (3x N-ERD, 1x healthy) in the combined plasma data set (J. Xia & Wishart, 2011). These have been excluded from

subsequent data analysis. Maximum variance between all three groups was visualized by PCA. Subsequent data processing included the supervised partial least squares-discriminant analysis (PLS-DA) and analysis of variance (ANOVA). Hierarchical clustering (distance measurement "Euclidean", clustering algorithm "Ward") with group averages was deployed to depict group-specific metabolite clusters.

The sputum data from cohort I and NLF data from cohort II were analyzed respectively. Prior to upload to MetaboAnalyst, both data sets were normalized on sample protein concentrations to account for matrix and patient-specific differences. Patient numbers were lower compared to plasma samples (NLF n = 8/8/11 Healthy, NT CRSwNP, N-ERD; sputum n = 3/0/5) and no outliers were present in both data sets.

Metabolomics pathway analysis was performed with the plasma data set on the MetaboAnalyst 4.0 platform. Data were processed and normalized identically to the statistical analysis. 211 of 213 metabolites were successfully denoted with Human Metabolome Database (HMDB) IDs. Of those, a total of 55 distinct Kyoto Encyclopedia of Genes and Genomes (KEGG) IDs could be identified. KEGG IDs sum up all metabolites of one compound group (e.g. SM) by not taking into account differences in lipid chain residues (e.g. length, double bonds). Thus, the sums of all metabolites sharing the same KEGG ID were used when applicable. Pathway analysis was performed using the "Homo sapiens (KEGG)" library with "Global Test" and "Relative Betweenness Centrality" specified as the algorithms for pathway enrichment and topological analysis.

3.3.4 Statistics

Non-parametric statistical analyses were performed using GraphPad Prism 6 (GraphPad Software). Differences between two or three groups with single conditions were tested by Chi-square test, Mann-Whitney-Wilcoxon test or Kruskal-Wallis test with Dunn's correction, respectively. Differences between three groups with multiple conditions were tested by 2-way ANOVA with Dunnett's correction. Linear regression and two-tailed Spearman correlation were used for BMI, sinonasal outcome test (SNOT)22 score and adipokine comparisons. NLF eicosanoid data were normalized on NLF sample volume; sputum eicosanoid data were normalized on total sputum cell numbers. All heatmaps of non-metabolomics data were created with MetaboAnalyst 4.0 for consistency. Auto-scaled data were visualized without any further normalization by distance measurement "Euclidean" and no clustering algorithms were applied. For all tests, (adjusted) p-values < 0.05 were considered significant. All data are shown as mean ± standard deviation (SD) if not explicitly stated otherwise.

4 Results

4.1 Characterization of N-ERD patient cohorts

A total of two cohorts were recruited during the course of this study. The larger cohort included 15 N-ERD and 10 NT CRSwNP patients as well as 10 healthy controls and was used for *in vitro* PMN and aMDM experiments and for plasma and NLF metabolite characterization of N-ERD (cohort I). A smaller cohort consisted of 5 N-ERD and 4 healthy individuals and was recruited to analyze local tissue milieus and immune cells in N-ERD (cohort II). Performed experiments and analyses are summarized in Table 4.1.

Table 4.1 Study design and experimental overview

Cohort	Sample type	Sample subtype	Experiment	Subchapter
I	whole blood	PMN, aMDM	PGE_2 resistance	4.2
			lipid mediator analysis	4.2
			chemokine/cytokine analysis (only aMDM)	4.2.2, 4.3.3
		PMN, monocytes, aMDM	targeted methylomics of AA metabolism genes	4.3.1
		monocytes, aMDM	genome-wide methylomics	4.3.3
		plasma	metabolomics	4.4.3
			adipokine analysis	4.4.4
	NLF		metabolomics	4.4.1
II	whole blood	aMDM	RNAseq	4.3.2
	nasal brushing		RNAseq	4.3.5
	induced sputum	sputum macrophages (sMac)	RNAseq	4.3.4
		homogenate	metabolomics	4.4.1
		SN	exosome isolation	4.5.2
			lipid mediator analysis	4.4.2
	NLF		lipid mediator analysis	4.4.2

Recruited individuals were age- and sex-matched and the mean age revolved around the 5th decade of life with the tendency towards a higher percentage of female patients in the N-ERD group, as typically seen for this disease (Table 4.2) (A. Szczeklik et al., 2000). Only females were included in cohort II to obviate any sex-bias in RNA sequencing (RNAseq) data. Individuals in both cohorts did not differ in BMI, smoking/ever smoked status or atopy, but in disease-specific parameters. N-ERD and NT CRSwNP patients differed from healthy controls in Malm score, SNOT22 score, total IgE and INCS use, with N-ERD showing slightly higher scores in comparison to NT CRSwNP. Higher prevalence of asthma (100% *vs.* 40%), lower sniffing test scores and the use of ICS further distinguished N-ERD from NT CRSwNP patients. All recruited individuals did not take any OCS, biologics or the 5-LO inhibitor zileuton up to 6 weeks prior to study enrollment to preclude any systemic and local alterations that might interfere with our read-outs.

Table 4.2 Patient characterization

Parameter	Cohort I			Cohort II	
group	Healthy	NT CRSwNP	N-ERD	Healthy	N-ERD
number of individuals	10	10	15	4	5
age (years)	54 (30-76)	52 (28-79)	57 (31-82)	50 (31-64)	52 (35-69)
sex (female)	7/10 (70%)	5/10 (50%)	13/15 (87%)	4/4 (100%)	5/5 (100%)
BMI	23.8 (19.8-28)	26.1 (20.4-32.7)	25.5 (19.3-32.9)	n.d.	n.d.
smoking / ever smoked	1/10 (10%)	0/10 (0%)	2/15 (13.3%)	0/4 (0%)	1/5 (20%)
atopy	5/10 (50%)	7/10 (70%)	7/15 (47%)	1/4 (25%)	1/5 (20%)
asthma	0/10 (0%)	4/10 (40%)	15/15 (100%)*	0/4 (0%)	5/5 (100%)*
MALM score (0-6)	0	2.8 (1-6)*	3.1 (1-6)*	0	2.6 (1-6)*
SNOT22 score (0-110)	0.8 (0-8)	24.9 (0-62)*	33.4 (6-73)*	4.0 (3-7)	25.8 (14-37)*
sniffing test score (0-16)	13.5 (10-16)	10.1 (4-14)	4.9 (0-15)*	n.d.	n.d.
total IgE (ng/mL)	91 (32-318)	254 (90-771)*	193 (50-540)*	15 (11-21)	112 (72-172)*
ECP (ng/mL)	4.4 (1.6-7.7)	6.5 (2.6-12.4)	6.0 (0.2-13.0)	9.1 (3.0-13.9)	27.3 (3.5-53.7)
corticosteroids					
oral	0/10 (0%)	0/10 (0%)	0/15 (0%)	0/4 (0%)	0/5 (0%)
inhaled	0/10 (0%)	4/10 (40%)	11/15 (73%)*	0/4 (0%)	5/5 (100%)*
nasal	0/10 (0%)	10/10 (100%)*	14/15 (93%)*	0/4 (0%)	4/5 (80%)*
LABA	0/10 (0%)	3/10 (30%)	9/15 (60%)*	0/4 (0%)	2/5 (40%)
biologics	0/10 (0%)	0/10 (0%)	0/15 (0%)	0/4 (0%)	0/5 (0%)
zileuton	0/10 (0%)	0/10 (0%)	0/15 (0%)	0/4 (0%)	0/5 (0%)
montelukast	0/10 (0%)	0/10 (0%)	2/15 (13%)	0/4 (0%)	0/5 (0%)

NT CRSwNP, non-steroidal anti-inflammatory drug (NSAID)-tolerant chronic rhinosinusitis with nasal polyps; N-ERD, NSAID-exacerbated respiratory disease; BMI, body mass index; MALM polyp scoring, range 0-3 per nostril; SNOT22, sino-nasal outcome test with 22 questions; ECP, eosinophilic cationic protein; LABA, long-acting beta-2 agonist; biologics include Omalizumab, Benralizumab, Reslizumab, Mepolizumab, Dupilumab; n.d., not determined. Data are shown as mean (min-max) and count (percentage). Data were analyzed with the Chi-square test, Kruskal-Wallis test with Dunn's correction or Mann-Whitney-Wilcoxon test: *$p < 0.05$. This table was adapted from our submitted manuscript (see Declaration of content).

4.2 PGE_2 resistance in N-ERD

Laidlaw et al. demonstrated a PGE_2 resistance in granulocytes isolated from the blood of N-ERD patients, which resulted in a diminished anti-inflammatory response and elevated LT production in comparison to NT asthmatics and healthy controls (Tanya M. Laidlaw et al., 2014). LT production was suggested to be further enhanced by increased numbers of granulocyte-adherent platelets via transcellular LT biosynthesis (T. M. Laidlaw et al., 2012; Tanya M. Laidlaw et al., 2014). We sought to reproduce these findings and further characterize the phenotype of N-ERD PMN and the mechanisms involved. The same group further showed that fibroblasts isolated from N-ERD NPs were resistant to PGE_2 treatment and highly proliferative in comparison to NT controls (Cahill et al., 2016). This resistance was mediated by a reduced EP2 expression, possibly due to histone acetylation (H3K27ac). Thus, we wanted to verify if a PGE_2 resistance is also present in macrophages from N-ERD patients and if this altered responsiveness to PGE_2 might play a role in type 2 immunopathology (Varga et al., 1999).

4.2.1 N-ERD and CRSwNP PMN show no features of PGE_2 resistance

Isolated PMN from all individuals of cohort I were analyzed by FACS for the presence of cell-adherent platelets ($CD61^+$) and the surface protein expression of CCR3, Siglec-8, CRTH2 and CD11b. Siglec-8 was a marker of interest due to its immune regulatory function in eosinophils by inducing apoptosis upon ligation (Nutku, 2003). We found no differences in the surface expression of CCR3, CRTH2, Siglec-8 or CD11b on $CCR3^+$ SSC^{hi} eosinophils as well as CD11b on $CCR3^-$ neutrophils of N-ERD PMN in comparison to those of NT CRSwNP and healthy individuals (Figure 4.1).

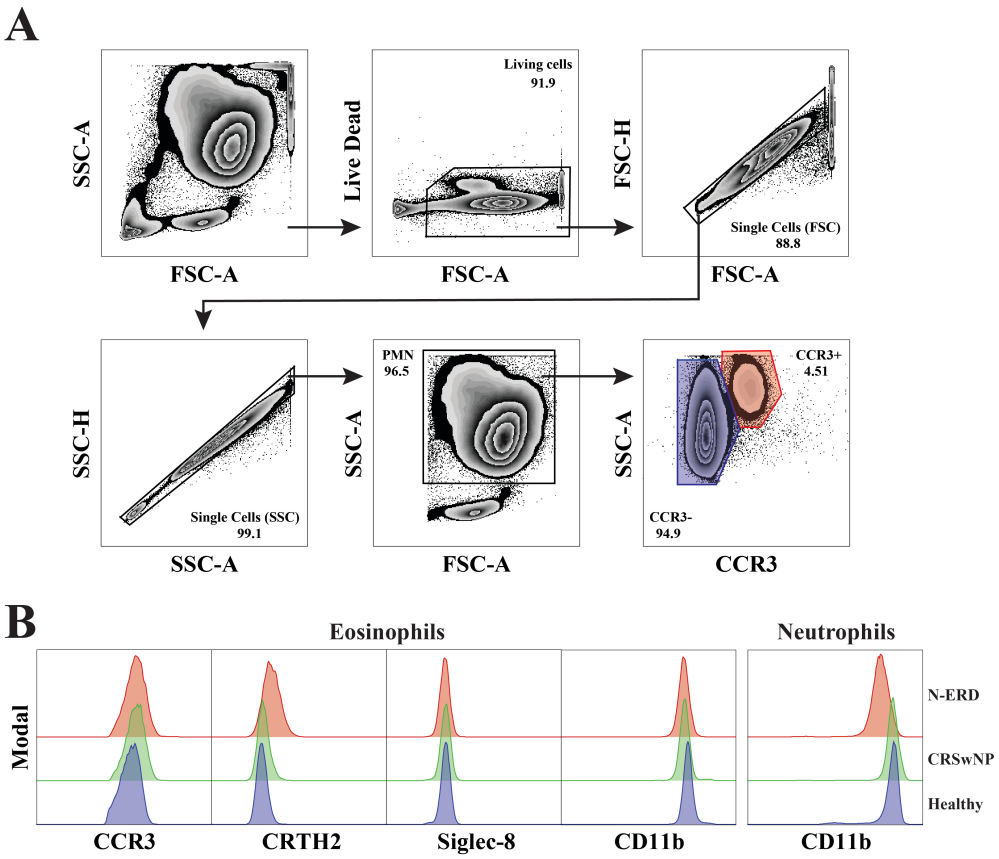

Figure 4.1 PMN surface marker do not differ between patient groups
A FACS gating strategy for living single cell $CCR3^-$ neutrophils and $CCR3^+$ SSC^{hi} eosinophils in PMN. **B** Mean fluorescence intensity (MFI) comparison of cell surface marker (CCR3, CRTH2, Siglec-8, CD11b) of $CCR3^+$ SSC^{hi} eosinophils and $CCR3^-$ neutrophils between N-ERD (red), CRSwNP (green) and healthy (blue) individuals. Data shown as histograms. Representative plots for N-ERD (n = 15), NT CRSwNP (n = 10) and healthy (n = 10) are shown.

No evidence of cell-adherent platelets on eosinophils or neutrophils was found in PMN of all groups (Figure 4.2 A, B). To test if the collection of venous blood with EDTA instead of heparin (Tanya M. Laidlaw et al., 2014) and isolation via density gradient centrifugation resulted in a loss of cell-adherent platelets, we stained whole blood from

twelve cohort I individuals and additional healthy volunteers. While ~10% of all $CD45^+$ $CCR3^-$ neutrophils and $CD45^+$ $CCR3^+$ SSC^{hi} eosinophils were positive for CD61, there was no difference between N-ERD, NT CRSwNP and healthy individuals (Figure 4.2 C, D) as well as no differences between heparinized and EDTA-anticoagulated blood (data not shown).

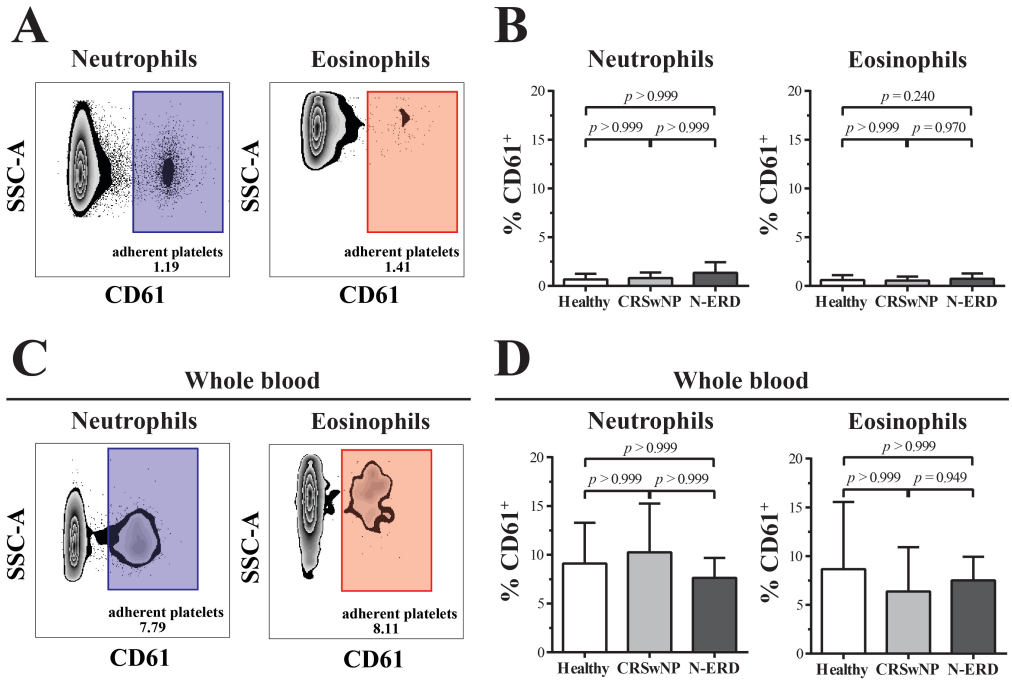

Figure 4.2 No cell-adherent platelets found in N-ERD and NT CRSwNP PMN
A and C FACS blots of isolated PMN and whole blood showing CD61 staining of ($CD45^+$) $CCR3^-$ neutrophils and ($CD45^+$) $CCR3^+$ SSC^{hi} eosinophils. A representative individual is shown. **B and D** Quantification of $CD61^+$ neutrophils and eosinophils of N-ERD (n = 15/7), NT CRSwNP (n = 10/4) and healthy (n = 10/3) individuals. Data are shown as mean ± SD and were analyzed with the Kruskal-Wallis test with Dunn's correction: $p < 0.05$.

Similar to Laidlaw et al. (Tanya M. Laidlaw et al., 2014), we cultured and stimulated PMN with PGE_2 and Forskolin and quantified a total of 12 lipid mediators in the SN by LC-MS/MS instead of ELISAs. No differences in lipid mediator levels were found between N-ERD, NT CRSwNP and healthy individuals in baseline PMN SN (Table 4.3). While our stimulation with Forskolin failed (data not shown), the inhibitory effects of PGE_2 were weaker and no differences were found between all three groups for LTB_4 and cysLTs contrary to Laidlaw et al. (Tanya M. Laidlaw et al., 2014) (Figure 4.3). Similar results (no differences) were obtained for all other measured lipid mediators (data not shown). Thus, we decided to discontinue further investigations in this direction.

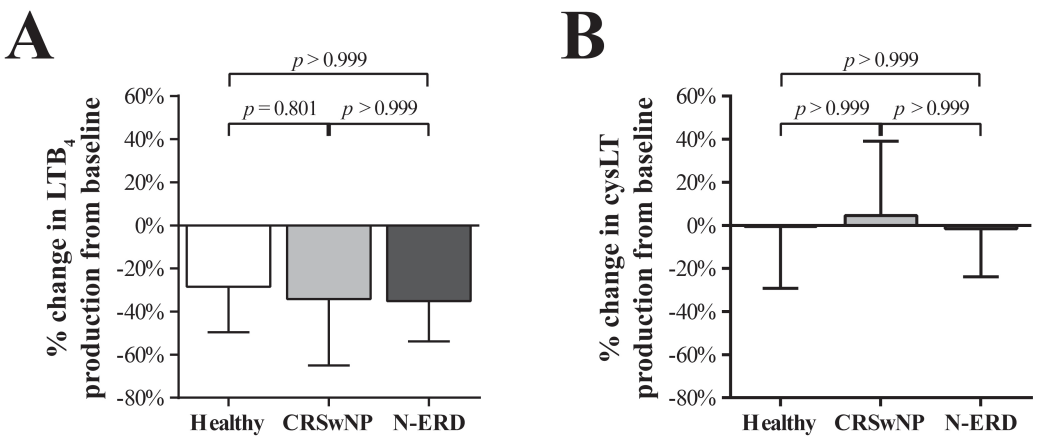

Figure 4.3 No PGE_2 resistance found in N-ERD and NT CRSwNP PMN
% change of **A** LTB_4 and **B** cysLT concentrations in PMN SN of healthy (n = 8), NT CRSwNP (n = 10) and N-ERD (n = 15) individuals after stimulation with 100 nM PGE_2. Data are shown as mean ± SD and were analyzed with the Kruskal-Wallis test with Dunn's correction: $p < 0.05$.

Table 4.3 PMN lipid mediator profile

Lipid mediator	Concentration (ng/mL)			p value			log2 Fold Change		
	Healthy	CRSwNP	N-ERD	N *vs.* H	N *vs.* C	C *vs.* H	N *vs.* H	N *vs.* C	C *vs.* H
11-HETE	0.0280	0.0472	0.0321	0.999	0.725	0.495	0.195	-0.557	0.752
12-HETE	0.1325	0.1194	0.1177	0.999	0.999	0.999	-0.170	-0.020	-0.150
12,13-DiHOME	0.1346	0.1422	0.1599	0.999	0.999	0.999	0.249	0.169	0.080
5-HETE	0.5095	0.4175	0.5585	0.999	0.909	0.901	0.133	0.420	-0.287
5-oxoETE	0.0669	0.0622	0.0622	0.999	0.999	0.999	-0.106	-0.001	-0.105
9-HETE	0.0425	0.0601	0.0440	0.999	0.999	0.632	0.049	-0.451	0.500
LTB_4	2.0093	2.2997	2.2306	0.999	0.999	0.999	0.151	-0.044	0.195
cysLTs	0.7254	0.3681	0.7065	0.734	0.999	0.524	-0.038	0.941	-0.979
$PGF_{2\alpha}$	0.0260	0.0248	0.0250	0.999	0.999	0.999	-0.060	0.010	-0.071
TXB_2	0.1238	0.1823	0.1697	0.824	0.999	0.820	0.455	-0.104	0.559

Baseline lipid mediator concentrations in PMN SN of N-ERD (n = 15), NT CRSwNP (n = 10) and healthy (n = 8) individuals. cysLTs, sum of LTC_4, LTD_4 and LTE_4; H, healthy; C, NT CRSwNP; N, N-ERD. Data were analyzed with the Kruskal-Wallis test with Dunn's correction: $p < 0.05$.

4.2.2 aMDM from N-ERD, CRSwNP and healthy individuals are equally sensitive to PGE_2 and IL4 treatment

In vitro-generated aMDM from isolated $CD14^+$ monocytes of cohort I individuals were stimulated with PGE_2 or IL4 to investigate a potential altered responsiveness to PGE_2 or to a key type 2 cytokine and modulator of macrophage activation. SN of 24 h-stimulated aMDM were subjected to lipid mediator analysis and chemokine/cytokine multiplex assay. 16 different lipid mediators were quantified but showed no consistent significant differences of PGE_2- or IL4-stimulated aMDM between N-ERD, NT CRSwNP and healthy individuals (Table 8.1, Table 8.3). At baseline, an enhanced production of 5-LO metabolites (LTB_4, 5-HEPE, 5-HETE, 5-oxoETE) and auto-oxidation products of DHA (11-HDHA, 13-HDHA) was measured in N-ERD aMDM in comparison to those from

NT CRSwNP and healthy controls (Figure 4.4 A-D, Table 8.1). CysLTs, PGD_2, TXB_2 (the stable metabolite of TXA_2) and LXA_4 also tended to be increased in N-ERD aMDM (Table 8.1).

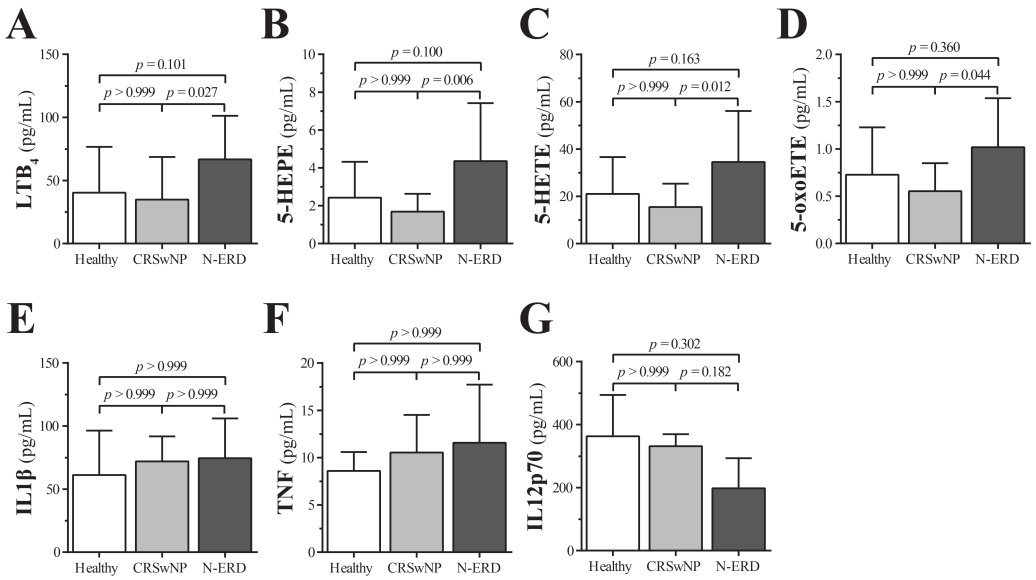

Figure 4.4 Elevated baseline 5-LO metabolite production and minor cytokine tendencies in N-ERD aMDM
Baseline lipid mediator concentrations of **A** LTB_4, **B** 5-HEPE, **C** 5-HETE and **D** 5-oxoETE in aMDM SN of healthy (n = 10), NT CRSwNP (n = 10) and N-ERD (n = 13) individuals. Baseline concentrations of **E** IL1β, **F** TNF and **G** IL12p70 in aMDM SN of healthy (n = 3), NT CRSwNP (n = 3) and N-ERD (n = 3) individuals. Data were analyzed with Kruskal-Wallis test with Dunn's correction: $p < 0.05$.

17 chemokines/cytokines were quantified in the aMDM SN of three individuals with the highest SNOT22 scores for N-ERD and NT CRSwNP patients and lowest SNOT22 scores for healthy controls. Similar to the lipid mediator analysis, no coherent differences were found between stimulations and patient groups (Table 8.4). Baseline levels of IL1β and TNF tended to be elevated and IL12 to be reduced in N-ERD aMDM (Figure 4.4 E-G, Table 8.2). Thus, mediator profiles do not differ between patient groups after stimulations with PGE_2 or IL4, however baseline levels of pro-inflammatory mediators tend to be increased in N-ERD aMDM in comparison to NT CRSwNP and healthy controls.

4.3 Transcriptomics and methylomics

4.3.1 Targeted bisulfite sequencing of AA metabolism genes reveals no differences in PMN, monocytes and aMDM of N-ERD, CRSwNP and healthy individuals

In 2011, Cheong et al. showed significant differences in the genome-wide methylation profile of NP tissues from Korean N-ERD and NT CRSwNP with asthma individuals, that were not present in a comparison of cells isolated from buffy coats (Cheong et al., 2011). Particularly, genes of key proteins in the AA metabolism pathway were found to be differentially methylated. PGDS, LTB4R (BLT1R) and ALOX5AP, the gene of the 5LO-activating protein FLAP which is essential for 5-LO activity (Dixon et al., 1990), were hypomethylated, while PTGES (mPGES-1) was hypermethylated. Since Cheong et al. analyzed whole buffy coat DNA but not DNA from separated cell types, we hypothesized that differentially methylated genes in NP tissues might be derived from infiltrating and accumulating immune cells, which only make up a small percentage of total cells in buffy coats, and that these cells may have an altered methylation profile prior to tissue infiltration. Thus, we isolated DNA from cohort I PMN, monocytes and aMDM and performed targeted bisulfite sequencing of PGDS, LTB4R, ALOX5AP and PTGES. We also included aMDM stimulated with PGE_2 or IL4 to investigate possible changes in gene methylation induced by type 2 *in vitro* settings, as they can occur as early as 6 h *post* stimulation (Vento-Tormo et al., 2016). However, no significant methylation differences for single CpG sites or whole gene regions were detected between groups for each cell type and aMDM stimulations (Table 8.5-Table 8.8).

4.3.2 N-ERD aMDM transcriptome differs from those of healthy aMDM

Since no major differences in PGE_2 resistance and type 2 stimulations were found in blood-derived PMN, monocytes and aMDM (see 4.2 and 4.3.1), we focused on local airway samples and decided to perform whole transcriptome analysis. Thus, we sampled nasal brushings and isolated macrophages from induced sputum (sMac) from cohort II individuals, a smaller cohort only consisting of female N-ERD patients and healthy controls (Table 4.2). We further generated aMDM from the same individuals to compare the aMDM phenotype to those of sMac and explore the differences to our alveolar-like *in vitro* model.

Prior to the comparison of sMac to aMDM, we compared the transcriptome of N-ERD and healthy aMDM. We identified 86 down- and 19 upregulated genes in aMDM from N-ERD patients in comparison to healthy controls (Figure 4.5 A). Functional and pathway analyses revealed genes involved in chemotaxis (CXCL1-3, pro-platelet basic protein (PPBP, CXCL7), CXCL8, CCL18, CCL20) to be upregulated and genes associated with host defense (CD1A-C, C-type lectin domain family 10 member A (CLEC10A), CLEC18B) to be downregulated (Figure 4.5, Table 4.4). ToppGene pathway analysis indicated an alteration of “Interleukin-4 and 13 signaling”-associated genes including an

upregulation of CXCL8, PTGS2 (COX-2) and downregulation of macrophage-inhibiting transcription factor CCAAT/enhancer-binding protein delta (CEBPD, Banerjee et al., 2013; Hsiao et al., 2013) (Figure 4.5, Table 4.4). Thus, the transcriptome of N-ERD aMDM indicates a pre-activated, pro-inflammatory phenotype in comparison to those of healthy controls.

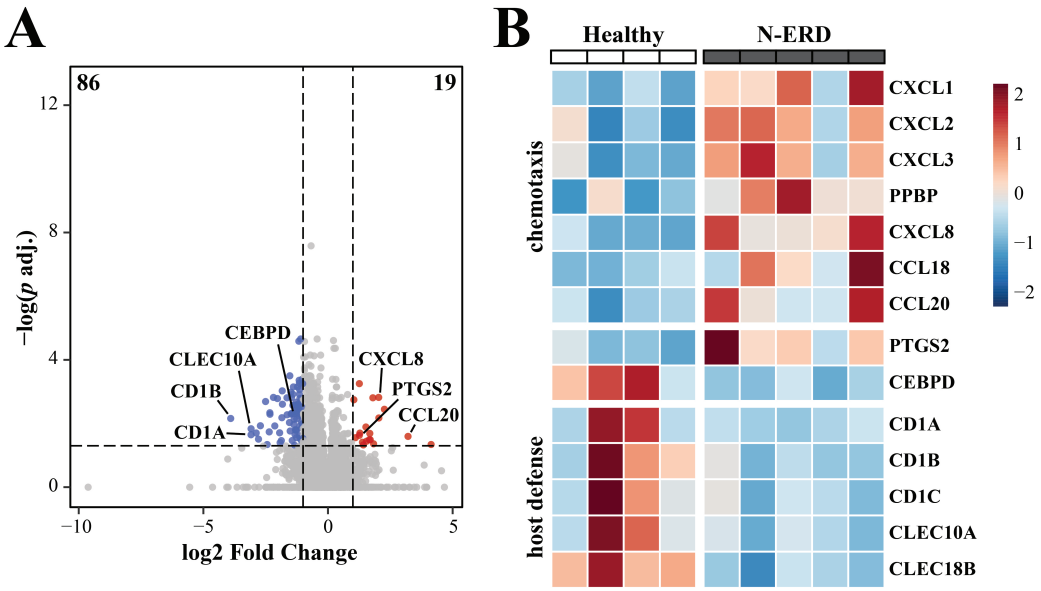

Figure 4.5 Aberrant aMDM activation in N-ERD patients
Transcriptome analysis of aMDM from N-ERD (n = 5) and healthy (n = 4) individuals. **A** Volcano plot of DEGs; significant changes shown in blue (down) or red (up); thresholds were set to p adj. ≤ 0.05 and log2 Fold Change ≥ +1 / ≤ -1. **B** Heatmap of selected DEGs (z-score) between patients. See 3.1.12 Deposited Data for the complete list of DEGs. This figure was adapted from our submitted manuscript (see Declaration of content).

Table 4.4 Selected pathways dysregulated in N-ERD aMDM

Pathway	*q* value Bonferroni	DEGs in pathway	Total genes in pathway	Pathway DEGs in N-ERD aMDM
Chemokine receptors bind chemokines	**< 0.001**	6	48	↑: PPBP, CXCL1, CXCL2, CXCL3, CCL20, CXCL8
IL-17 signaling pathway	**< 0.001**	7	93	↑: CXCL1, CXCL2, CXCL3, PTGS2, CCL20, CXCL8
				↓: MMP9
Genes encoding secreted soluble factors	**< 0.001**	10	344	↑: PPBP, CXCL1, CXCL2, CXCL3, CCL18, CCL20, CXCL8
				↓: GDF15, LTB, S100B
Interleukin-10 signaling	**< 0.001**	5	49	↑: CXCL1, CXCL2, PTGS2, CCL20, CXCL8
Ensemble of genes encoding extracellular matrix and extracellular matrix-associated proteins	**0.002**	16	1028	↑: PPBP, CXCL1, CXCL2, CXCL3, CCL18, CCL20, CXCL8
				↓: CLEC18B, GDF15, LAMA5, S100B, MMP9, CLEC10A, LTB, AGRN, COL1A1
TNF signaling pathway	**0.003**	6	108	↑: CXCL1, CXCL2, CXCL3, PTGS2, CCL20
				↓: MMP9
Interleukin-4 and 13 signaling	**0.004**	6	114	↑: PTGS2, CXCL8
				↓: CEBPD, POMC, LAMA5, MMP9
Chemokine signaling pathway	**0.006**	7	182	↑: PPBP, CXCL1, CXCL2, CXCL3, CCL18, CCL20, CXCL8

Selected ToppGene pathway analysis results of DEGs between N-ERD and healthy aMDM as revealed by RNAseq. GDF15, growth/differentiation factor 15; LTB, lymphotoxin-beta; S100B, S100 calcium-binding protein B; LAMA5, laminin subunit alpha-5; AGRN, agrin; COL1A1, alpha-1 type I collagen; POMC, pro-opiomelanocortin. Significance threshold by Bonferroni: $q < 0.05$

4.3.3 Genome-wide methylomics reveal slight alterations of FAO, chemokines and host defense in N-ERD aMDM and monocytes

Since changes in gene expression in N-ERD aMDM were apparent even after 7 days of *in vitro* differentiation, we next studied whether DEGs were associated with epigenetic modifications.

Genome-wide DNA methylation analysis of cohort I aMDM and monocyte DNA revealed 3930 lower and 211 higher differentially methylated positions (DMPs) in N-ERD aMDM and 2574 lower and 186 higher DMPs in N-ERD monocytes compared to those from healthy controls (Figure 4.6). Functional analysis of significant differentially methylated regions (DMRs) of aMDM identified chemotaxis (CXCL2, platelet factor 4 (PF4, CXCL4)) and carnitine transport (CPT1A, CPT1B, acetyl-CoA carboxylase 1 (ACACA)) as major hits (Table 4.5). The DMR of CPT1B was methylated to a greater extent in N-ERD aMDM, while CPT1A, ACACA, CXCL2 and PF4 were less methylated (Table 8.9). Identical DMR differences were present in monocytes for CPT1B and PF4 (Table 8.9).

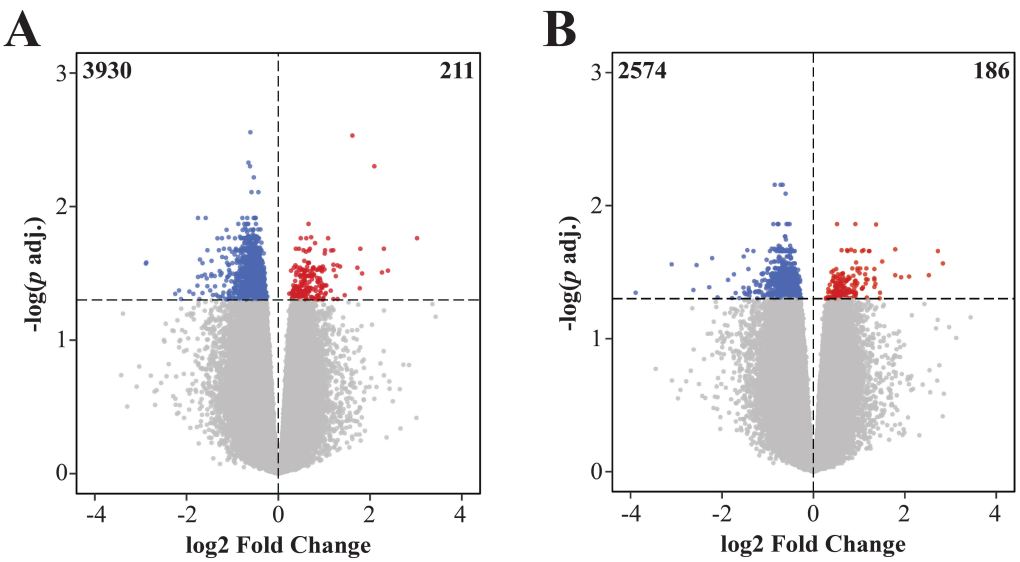

Figure 4.6 N-ERD and healthy aMDM and monocytes differ in their methylation profile
Genome-wide methylome analysis of aMDM and monocytes from N-ERD (n = 15) and healthy (n = 8) individuals. **A and B** Volcano plot of DMPs from **A** monocytes and **B** aMDM; significantly changed DMPs shown in blue (down) or red (up); a threshold was set to p adj. ≤ 0.05. See 3.1.12 Deposited Data for the complete list of DMPs. This figure was adapted from our submitted manuscript (see Declaration of content).

Table 4.5 Selected functional pathways associated with N-ERD DMRs in aMDM

Pathway	Analysis	q value Bonferroni	DMR-genes in pathway	Total genes in pathway	Pathway DMRs in N-ERD aMDM
carnitine O-palmitoyl-transferase activity	Molecular function	1.000	2	4	↑: CPT1B ↓: CPT1A
CXCR chemokine receptor binding		1.000	3	17	↓: PF4, ITCH, CXCL2
carnitine shuttle	Biological process	0.777	3	9	↑: CPT1B ↓: ACACA,CPT1A
carnitine transmembrane transport		1.000	3	12	↑: CPT1B ↓: ACACA,CPT1A

Selected ToppGene molecular function and biological process analysis results of DMR-derived genes between N-ERD and healthy aMDM as revealed by RNAseq. ITCH, itchy E3 ubiquitin protein ligase. Significance threshold b Bonferroni: $q < 0.05$

To verify if gene expression alterations are linked to changes in methylation patterns, we compared aMDM DEGs (cohort II) with DMR-derived genes from aMDM and monocytes (cohort I) of N-ERD *vs.* healthy. A total of three aMDM DEGs overlapped with genes of aMDM DMRs (CXCL2, SIX homeobox 5 (SIX5), zinc finger protein 215 (ZNF215)) and none for monocyte DMR-derived genes or the combination of all three datasets (Figure 4.7 A). Although DMRs only partially overlapped between aMDM and

monocytes, N-ERD *vs.* healthy-specific differences in methylation were stable as DMRs did not differ between both cell types after *in vitro* differentiation (Figure 4.7 B). Fibroblast growth factor 7 (FGF7), involved in anti-bacterial effector functions (Gardner et al., 2016), was one of the DMRs with the highest difference in methylation shared by N-ERD aMDM and monocytes (mean Δβ Fold Change = -0.161; -0.161, Table 8.9).

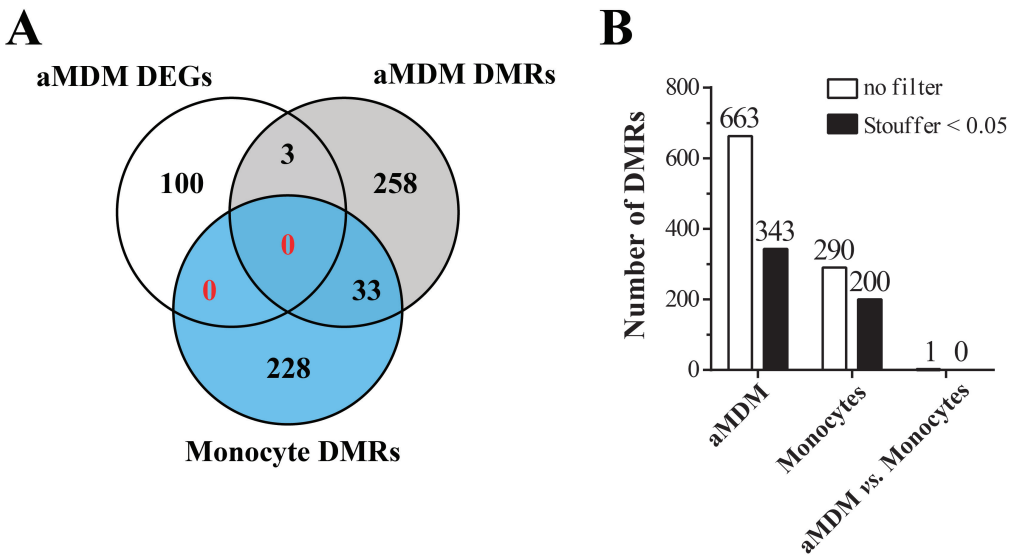

Figure 4.7 N-ERD aMDM DEGs are independent of DMRs
Genome-wide methylome analysis of aMDM and monocytes from N-ERD (n = 15) and healthy (n = 10) individuals. **A** Venn diagram of significant aMDM DEG- and DMR-, and monocyte DMR-derived genes of N-ERD *vs.* healthy comparisons. **B** Comparison of all and Stouffer-filtered (< 0.05) DMRs of aMDM, monocytes and aMDM *vs.* monocytes between N-ERD and healthy individuals. See 3.1.12 Deposited Data for the complete lists of DMRs. This figure was adapted from our submitted manuscript (see Declaration of content).

To validate the increased pro-inflammatory activation of N-ERD aMDM as revealed by RNAseq (Figure 4.5 B, see 4.3.2), we quantified the chemotaxis-associated DEGs (CXCL1-2, PPBP, CXCL8, CCL18, CCL20) by multiplex analysis of aMDM SN from cohort I. However, no significant differences between N-ERD, NT CRSwNP and healthy individuals were detected for all chemokines measured. Indeed, only CCL20 levels tended to be elevated in N-ERD aMDM (Figure 4.8).

Thus, transcriptomics, methylomics and mediator analysis together suggested that N-ERD was associated with a systemic pro-inflammatory activation of monocytes/macrophages and a dysregulated lipid metabolism.

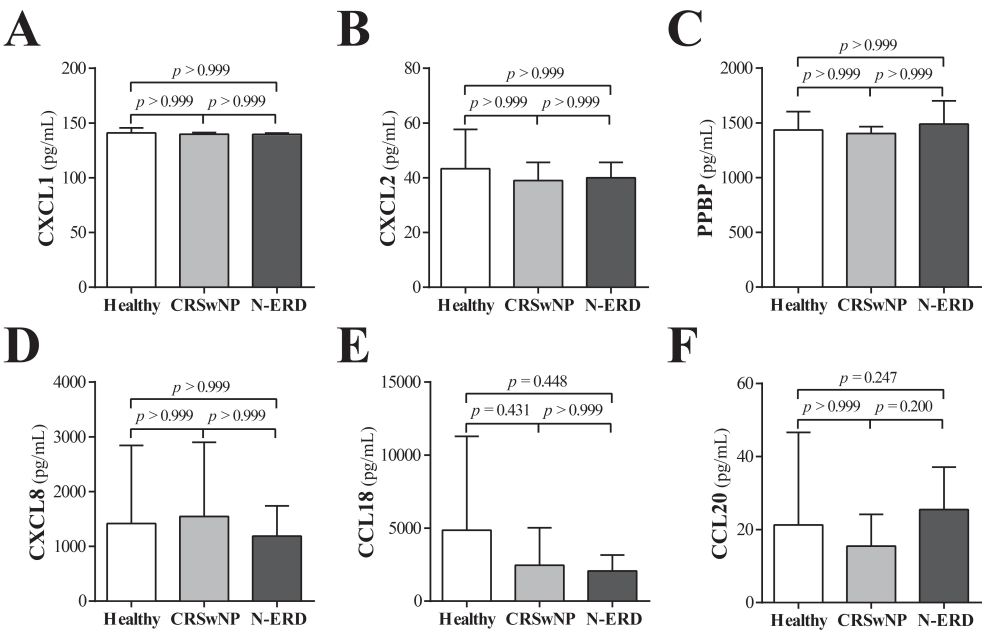

Figure 4.8 Chemokines do not differ from healthy controls in N-ERD and NT CRSwNP aMDM

Chemokine multiplex analysis of baseline aMDM SN from N-ERD (n = 15), NT CRSwNP (n = 10) and healthy (n = 10) individuals to validate RNA-seq results. Data are shown as mean values with SD for **A** CXCL1, **B** CXCL2, **C** PPBP, **D** CXCL8, **E** CCL18 and **F** CCL20. Data were analyzed with Kruskal-Wallis test with Dunn's correction: $p < 0.05$.

4.3.4 RNA sequencing reveals a strong activation of sMac in comparison to aMDM in N-ERD

Next, we sought to compare the transcriptomes of isolated sMac from N-ERD and healthy individuals. However, we failed to obtain sufficient numbers of sMac from age-matched healthy controls, which produced significantly less sputum than younger healthy volunteers in our trials. Thus, we instead compared sMac with *in vitro*-generated aMDM of the same N-ERD patients. As expected in a comparison of different cell types, RNAseq identified a large number of DEGs with a total of 984 genes being down- and 1869 genes being upregulated in sMac as compared to aMDM (Figure 4.9 A).

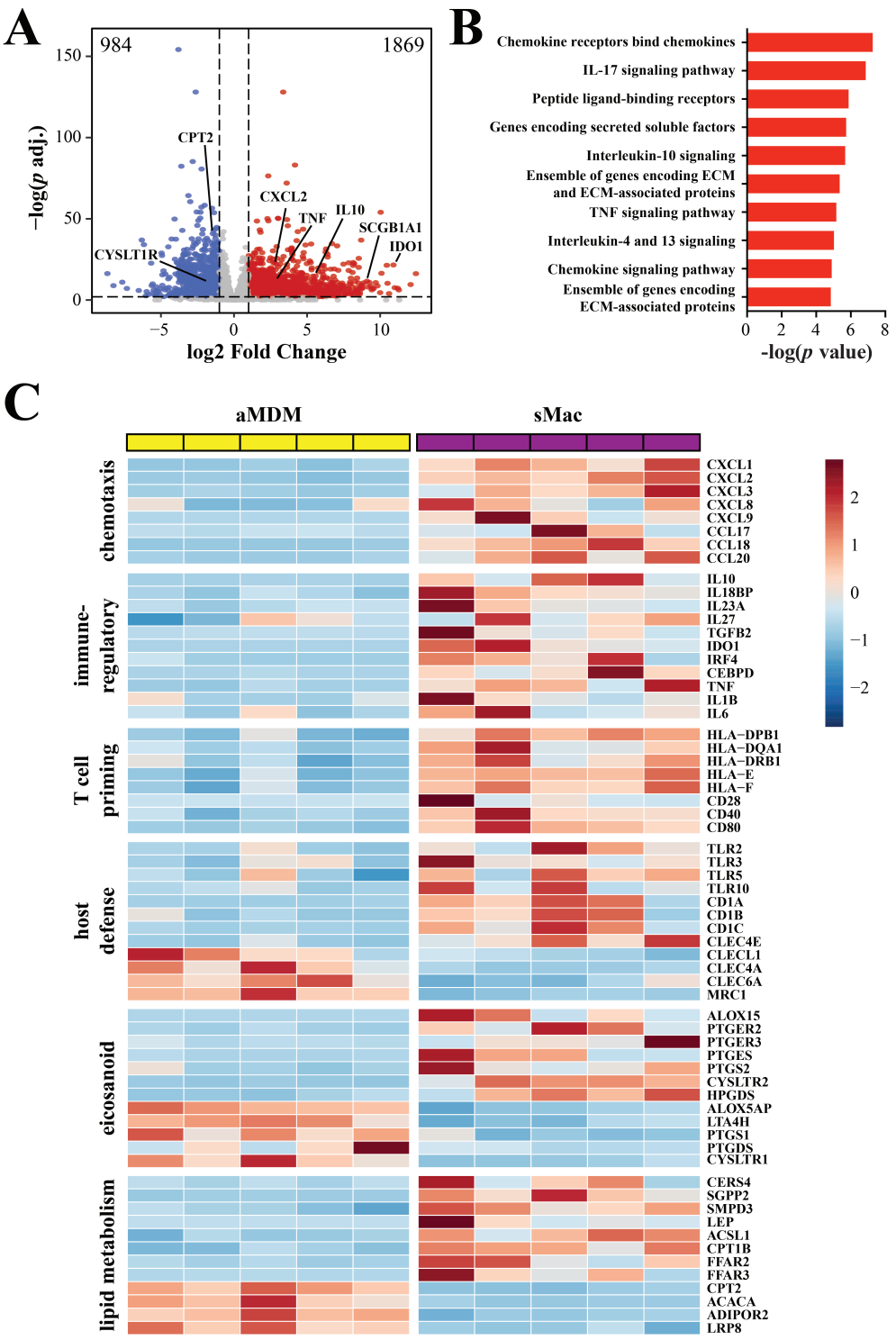

Figure 4.9 Transcriptome analysis reveals significant differences between N-ERD sMac and aMDM

Transcriptome analysis of sMac *vs.* aMDM from N-ERD ($n = 5$) patients. **A** Volcano plot of DEGs; significant changes shown in blue (down) or red (up); thresholds were set to p adj. ≤ 0.01 and log2 Fold Change ≥ +1 / ≤ -1. **B** Top 10 significant pathways obtained by ToppGene analysis. **C** Heatmap of selected DEGs (z-score) between cell types. See 3.1.12 Deposited Data for the complete list of DEGs. IDO1, indoleamine-2,3-dioxygenase; IRF4, interferon regulatory factor 4; HLA, human leukocyte

antigen; MRC1, mannose receptor C-type 1; PTGER2-3, EP2-3; HPGDS, hematopoietic prostaglandin D synthase; PTGS1-2, COX-1/2; PTGDS, PGD_2 synthase; CERS4, ceramide synthase 4; SGPP2, S1P phosphatase 2; SMPD3, SMase-3; LEP, leptin; ACSL1, long-chain fatty acid-CoA ligase 1; FFAR2-3, FFA receptor 2-3; ADIPOR2, adiponectin receptor 2; LRP8, low-density lipoprotein receptor-related protein 8. This figure was adapted from our submitted manuscript (see Declaration of content).

Functional and pathway analyses revealed the majority of DEGs to be associated with immune regulation, host defense and lipid metabolism (Figure 4.9 B, Table 8.10). We further filtered all DEGs for GO terms associated with immune responses and the eicosanoid and lipid metabolism (Figure 4.9 C, see 3.3.1). sMacs demonstrated a high expression of genes associated with chemotaxis (CXCL1-3, 8, 9, CCL17, 18, 20), immune regulation (IDO1, IL10, IL23A, IL27, IRF4, CEBPD), T-cell priming (HLA, CD28, CD40, CD80) and host defense (TLR2, 5, 10, CD1A-C), suggestive of an activated, highly responsive phenotype in comparison to aMDM (Figure 4.9 C). In addition, both cell types exhibited distinct eicosanoid gene expression signatures, with a 5-LO dominant profile of aMDM (ALOX5AP, CYSLTR1, LTA4H, PTGS1, PTGDS) and a potentially immune regulatory profile of sMac (ALOX15, CYSLTR2, PTGS2, HPGDS, PTGER2-3, PTGES). Multiple genes of the lipid metabolism associated with pro- and anti-inflammatory functions (CERS4, SGPP2, SMPD3, LEP, LRP8, ADIPOR2), were significantly altered between sMac and aMDM as well (Figure 4.9 C).

4.3.5 Nasal brushings of N-ERD NP show a macrophage signature and an altered lipid metabolism in comparison to healthy turbinate controls

We collected nasal brushings primarily consisting of multiple epithelial layers (Pipkorn & Karlsson, 1988) from N-ERD NP and healthy turbinate tissues and subjected isolated RNA to RNAseq. A total of 19 down- and 28 upregulated genes were found in N-ERD tissue (Figure 4.10 A). Enrichment and pathway analysis revealed the most significant DEGs to be associated with the lipid metabolism (APOE, APOC1, APOB) (Figure 4.10, Table 4.6). Elevated expression of receptors implicated in the release of immune regulatory cytokines and eicosanoids (5-hydroxytryptamine (5-HT) receptor 4 (HTR4), PTGER3) were found in N-ERD NPs, while exocyst component 3-like protein 4 (EXOC3L4) expression, a gene involved in epithelial integrity (Martin-Urdiroz, Deeks, Horton, Dawe, & Jourdain, 2016), was downregulated (Figure 4.10 B). Possibly as a result of INCS use (Table 4.2), N-ERD tissues also showed increased expression of the corticosteroid-induced gene FK506 binding protein 5 (FKBP5, Singhania et al., 2017). RNAseq further revealed immune regulatory genes predominantly expressed by macrophages (α2 macroglobulin (A2M, Hovi, Mosher, & Vaheri, 1977), CD200 receptor 1 (CD200R1, Hoek et al., 2000), HLA-DQB2) to be downregulated, which might indicate the presence and phenotype alteration of macrophages in nasal brushings from N-ERD NP and healthy turbinates (Figure 4.10 B).

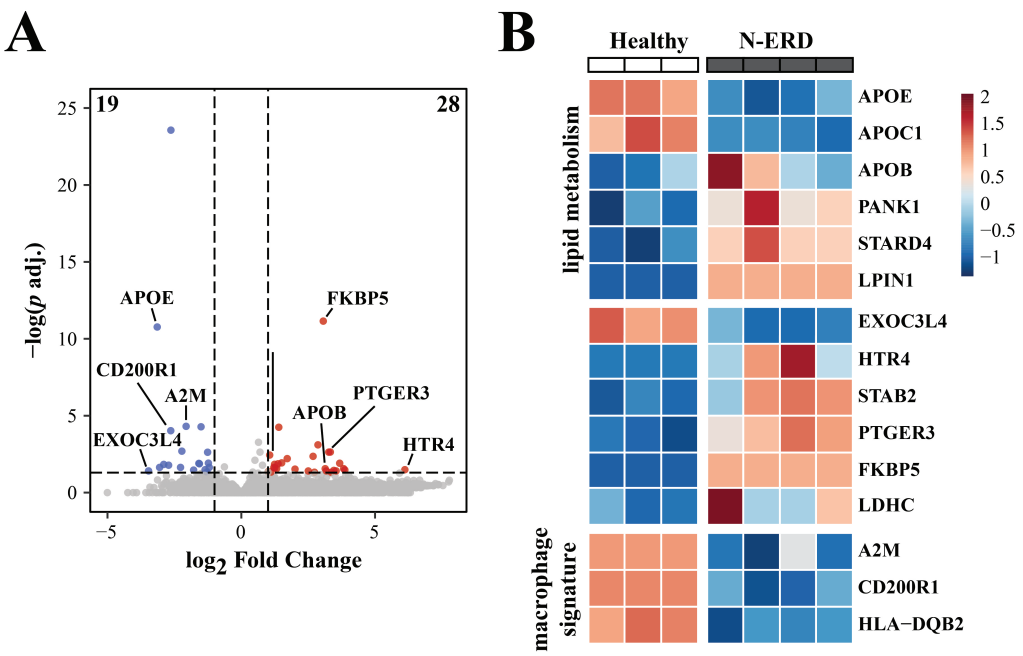

Figure 4.10 Altered lipid metabolism and macrophage signature in N-ERD NPs
Transcriptome analysis of N-ERD NP (n = 4) and healthy turbinate (n = 3) nasal brushings. **A** Volcano plot of DEGs; significant changes shown in blue (down) or red (up); thresholds were set to p adj. ≤ 0.05 and log2 Fold Change ≥ +1 / ≤ -1. **B** Heatmap of selected DEGs (z-score) between patients. PANK1, pantothenate kinase 1; STARD4, StAR-related lipid transfer protein 4; LPIN1, lipin 1; STAB2, stabilin 2; LDHC, lactate dehydrogenase C. See 3.1.12 Deposited Data for the complete list of DEGs. This figure was adapted from our submitted manuscript (see Declaration of content).

Table 4.6 Selected pathways dysregulated in nasal brushings of N-ERD NPs

Pathway	q value Bonferroni	DEGs in pathway	Total genes in pathway	Pathway DEGs in N-ERD aMDM
altered lipoprotein metabolic	**< 0.001**	3	7	↑: APOB
				↓: APOC1, APOE
lipoprotein metabolic	**0.002**	3	13	↑: APOB
				↓: APOC1, APOE
Lipoprotein metabolism	**0.021**	4	74	↑: APOB
				↓: A2M, APOC1, APOE
VLDL biosynthesis	**0.027**	2	5	↑: APOB
				↓: APOC1
Platelet homeostasis	**0.047**	4	91	↑: PDE1A, APOB, GUCY1A1, GUCY1B1
Lipid digestion, mobilization, and transport	0.115	4	115	↑: APOB
				↓: A2M, APOC1, APOE

Selected ToppGene pathway analysis results of DEGs between N-ERD and healthy aMDM as revealed by RNAseq. PDE1A, phosphodiesterase 1A; GUCY1A1, guanylate cyclase soluble subunit α1; GUCY1B1, guanylate cyclase soluble subunit β1. Significance threshold by Bonferroni: $q < 0.05$.

We further obtained intact N-ERD NP and healthy turbinate tissues from volunteers undergoing FESS and were able to confirm reduced levels of ApoE and elevated levels of HTR4 in N-ERD NP tissue by IF stainings (Figure 4.11). Collectively, this indicated that N-ERD is associated with an aberrant lipid metabolism and dysregulated activation of epithelial cells and macrophages in upper airway tissue.

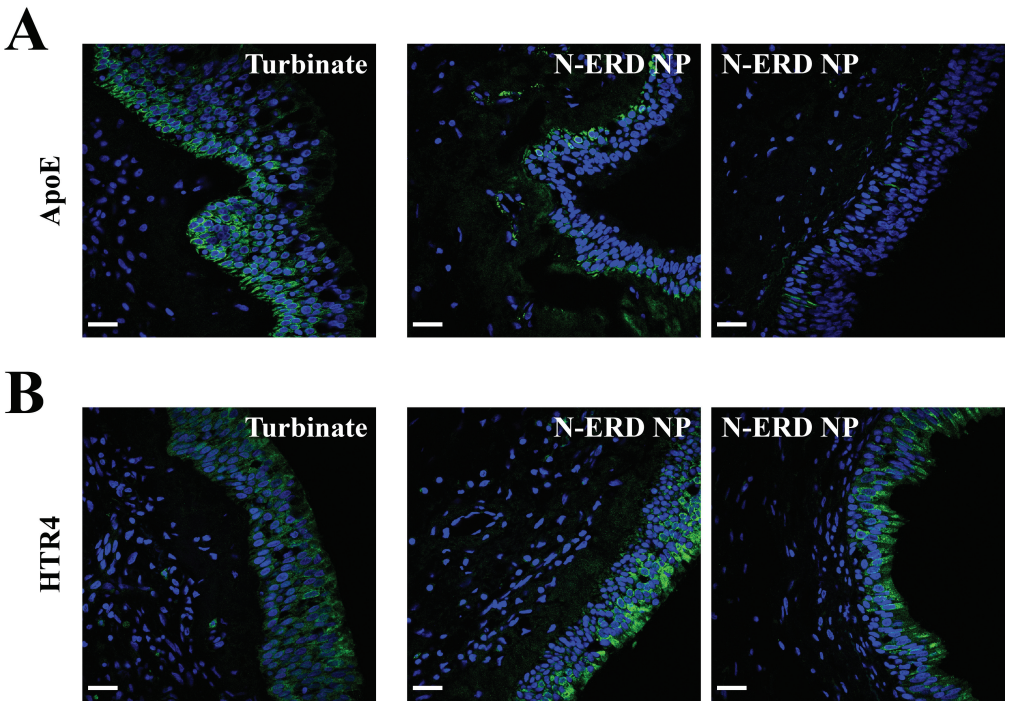

Figure 4.11 ApoE and HTR4 are dysregulated in N-ERD NP epithelium
Representative IF pictures of **A** ApoE and **B** HTR4 (both green) and DAPI (blue) in N-ERD NP (n = 2) and healthy turbinate (n = 1) tissue. Scale bars (white): 25 µm. This figure was adapted from our submitted manuscript (see Declaration of content).

4.4 Lipidomics: metabolome and lipid mediators

Based on our findings by RNAseq and genome-wide methylomics (see 4.3) that metabolic pathways might be altered, and several studies demonstrating a strong link between airway inflammation, obesity and an aberrant (lipid) metabolism (see 1.3), we decided to perform targeted metabolomics analyses of airway lining fluids (sputum, NLF) and plasma to examine the local and systemic metabolic status in N-ERD and/or NT CRSwNP. In addition, a lipid mediator analysis of the lower and upper airway lining fluids (sputum, NLF) was performed to obtain an even broader lipid profile in these body fluids.

4.4.1 Acylcarnitines are slightly associated with N-ERD in sputum and NLF

Sputum from cohort II and NLF from cohort I were subjected to targeted metabolomics analysis. We measured a total of 188 metabolites which included acylcarnitines, amino acids, biogenic amines, phosphatidylcholines (PC), lysoPCs, SMs and the sum of hexoses.

Principal component analysis (PCA) revealed an overlapping metabolite profile of N-ERD and healthy sputum with a low overall variance between samples and metabolites (Figure 4.12 A). Subsequent supervised partial least squares-discriminant analysis (PLS-DA), a supervised clustering model to enhance group separation, had a low predictive capability (accuracy = 0.63, R^2 = 0.45) and robustness (Q^2 = -0.14, p = 1.000) and no significantly different metabolites were found with ANOVA (data not shown). Thus, we chose a hierarchical clustering approach to explore metabolite clusters that may be associated with N-ERD, despite the absence of significant differences. Indeed, three metabolite clusters were identified and all acylcarnitine metabolites were present in cluster II, which was associated with N-ERD and demonstrated elevated acylcarnitine levels in comparison to healthy controls (Figure 4.12 B, Table 8.11).

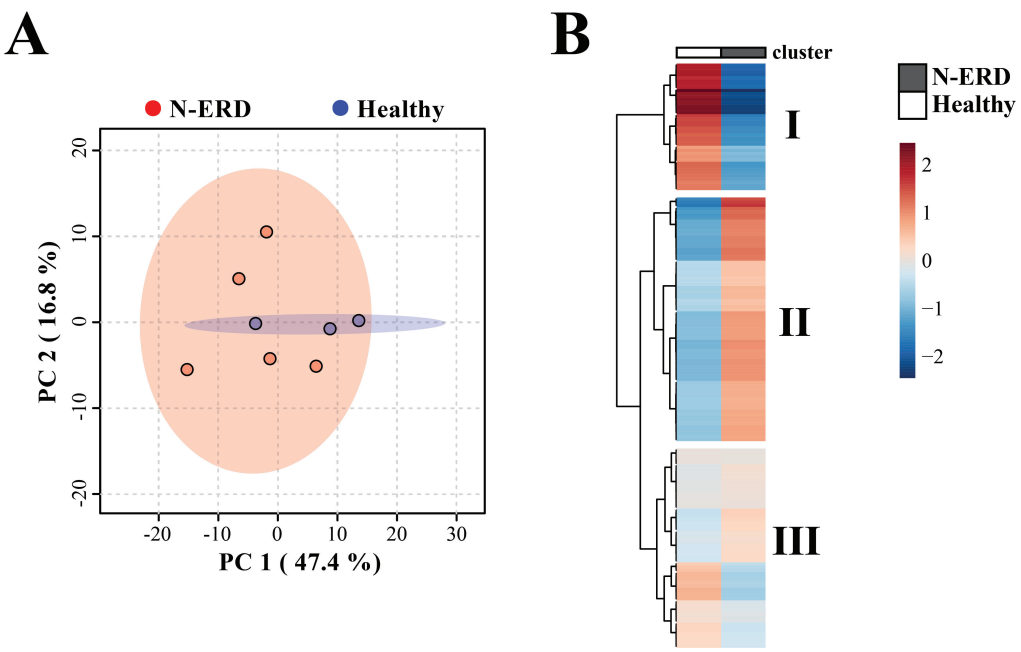

Figure 4.12 Sputum acylcarnitines are associated with N-ERD
Targeted metabolomics of sputum from N-ERD (n = 5) and healthy (n = 3) individuals. **A** PCA comparing N-ERD (red) patients and healthy controls (blue). Colored areas show 95% confidence intervals for each group. **B** Heatmap of metabolites assigned to clusters. Rows represent metabolites, columns show normalized, auto-scaled mean group concentrations. Concentration differences between patient groups are shown as z-score in blue (low) and red (high). See Table 8.11 for a detailed analyte group distribution in all clusters. This figure was adapted from our submitted manuscript (see Declaration of content).

Similar results were obtained for NLF of cohort I. A low variance between N-ERD, NT CRSwNP and healthy individuals was revealed by PCA (Figure 4.13 A) and PLS-DA (accuracy = 0.36, R^2 = 0.23; Q^2 = 0.04; p = 0.458) and ANOVA identified no significant differences in metabolite levels between the patient groups (data not shown). Despite the absence of significant differences, hierarchical clustering identified four metabolite clusters (Figure 4.13 B). The most prominent cluster I was associated with N-ERD and characterized by elevated levels of acylcarnitines in comparison to NLF obtained from NT CRSwNP and healthy individuals (Table 8.11). The majority and highest concentrations of SM metabolites (11 out of 15 measured) were present in cluster III, which was predominantly associated with the healthy control group (Figure 4.13 B, Table 8.11).

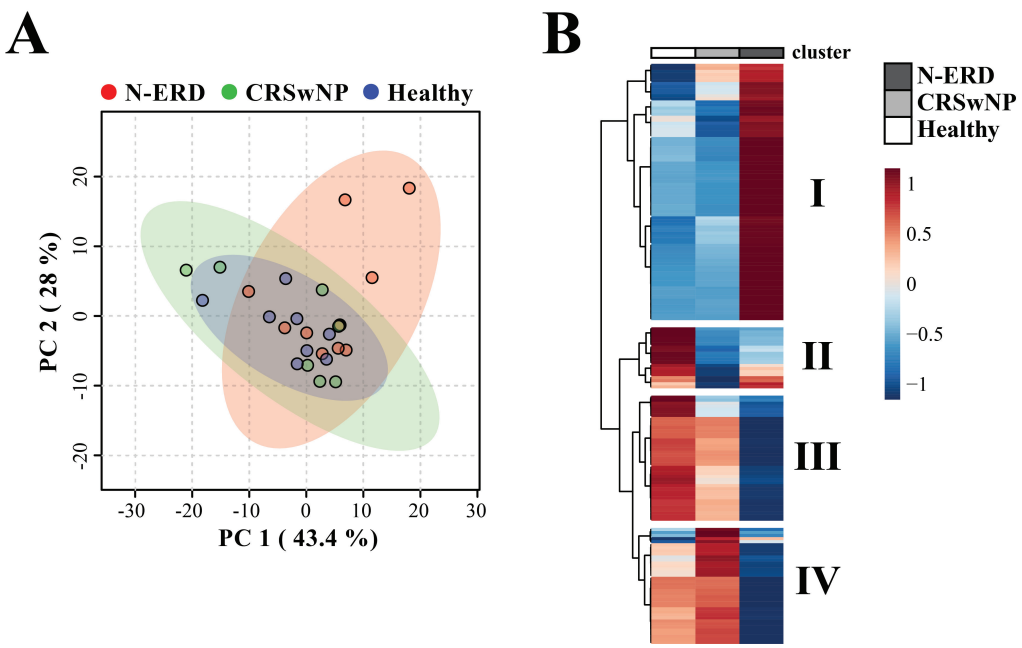

Figure 4.13 Targeted metabolomics reveal lipid metabolism aberrations in N-ERD NLF
Targeted metabolomics of NLF from N-ERD (n = 11), NT CRSwNP (n = 8) and healthy (n = 8) individuals. **A** PCA comparing N-ERD (red), NT CRSwNP (green) and healthy (blue) individuals. Colored areas show 95% confidence intervals for each group. **B** Heatmap of metabolites assigned to clusters. Rows represent metabolites, columns show normalized, auto-scaled mean group concentrations. Concentration differences between patient groups are shown as z-score in blue (low) and red (high). See Table 8.11 for a detailed analyte group distribution in all clusters. This figure was adapted from our submitted manuscript (see Declaration of content).

4.4.2 Lipid mediator analysis of sputum and NLF reveals distinct AA metabolism profiles in N-ERD patients

To characterize the local lipid mediator profile in the airways of N-ERD patients, we performed LC-MS/MS analysis of cohort II sputum and NLF.

Only 4 out of 54 PUFA metabolites could be quantified in induced sputum and included the 5-LO metabolites LTB_4, 5-HEPE, 5-oxoETE and the airway protective PGE_2 (Figure 4.14 A). While there were no differences for the 5-LO metabolites, PGE_2 tended to be reduced (p = 0.057, log2 Fold Change = -2.37) in N-ERD in comparison to healthy sputum (Figure 4.14 A).

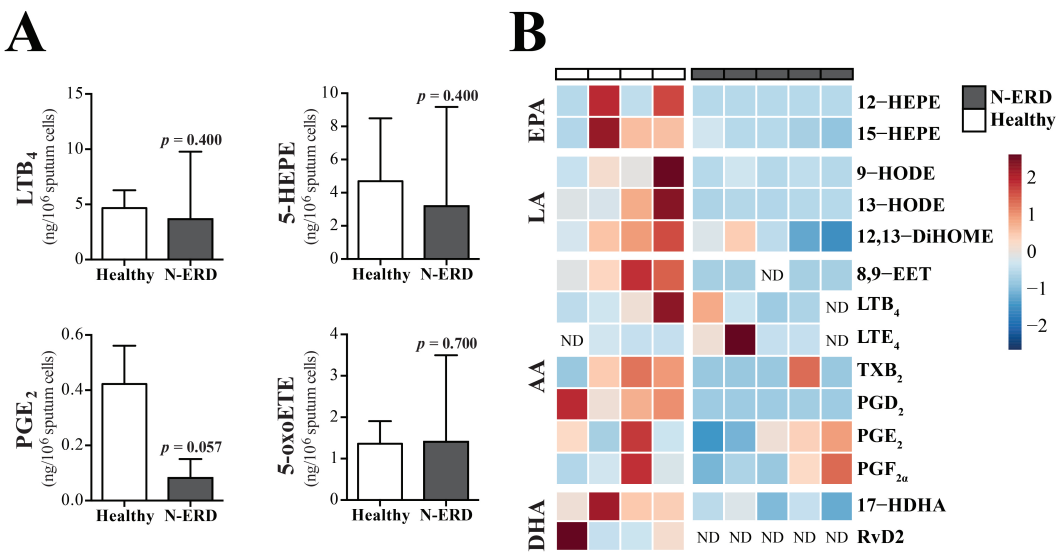

Figure 4.14 N-ERD patients exhibit distinct lipid mediator profiles in sputum and NLF

A Concentrations of LTB_4, PGE_2, 5-HEPE and 5-oxoETE normalized to $1x10^6$ sputum cells of N-ERD ($n = 4$) and healthy ($n = 3$) individuals. **B** Heatmap showing profiles (z-score) of selected PUFA metabolites, grouped according to their progenitor (eicosapentaenoic acid, EPA; linoleic acid, LA; arachidonic acid, AA; docosahexaenoic acid, DHA) in NLF of N-ERD ($n = 5$) and healthy ($n = 4$) individuals. See Table 8.12 for a detailed list of lipid mediators measured in NLF. ND, not detected. Data are shown as mean ± SD and were analyzed with Mann-Whitney test: $p < 0.05$. This figure was adapted from our submitted manuscript (see Declaration of content).

In contrast to sputum, 21 PUFA metabolites were detected in NLF by LC-MS/MS analysis. Elevated levels of EPA-, LA-, AA- and DHA-derived metabolites (significant for 12-HEPE, 9-HODE, 13-HODE, 8,9-EET, PGD_2, 17-HDHA) were identified in NLF from healthy controls, apart from LTE_4, which was increased in two out of five N-ERD patients (Figure 4.14 B, Table 8.12). Only low levels of 17-HDHA, precursor of all D-series resolvins (see 1.2.3), were detected in N-ERD NLF, while we failed to measure RvD2, which could only be detected in NLF from healthy individuals (Figure 4.14 B, Table 8.12).

Together, these data suggest that increased nasal cysLT production accompanied by lower levels of SPMs and reduced lower airway PGE_2 might contribute to nasal polyposis and NSAID-sensitive asthma in N-ERD.

4.4.3 Aberrant sphingolipid metabolism in N-ERD and CRSwNP patient plasma

To study whether local changes in metabolite profiles in N-ERD are reflected systemically, we additionally performed metabolomics analysis of plasma from N-ERD, NT CRSwNP and healthy individuals from cohort I. This analysis was appended by a targeted metabolomics approach for additional 26 sphingolipids including sphingosine, S1P, sphinganines, sphinganine-1-phosphat (SA1P), Cers, GluCers and lactosylCers (LacCers). Similar to NLF and sputum metabolomic analyses, PCA revealed a low variance between all three groups (Figure 4.15 A) and PLS-DA (accuracy = 0.42, R^2 = 0.97; Q^2 = -0.30; p = 0.441) and ANOVA identified no significant differences in metabolite levels (data not shown). Hierarchical clustering differentiated N-ERD, NT CRSwNP and healthy plasma metabolomes into five partially overlapping clusters (Figure 4.15 B).

Clusters I and II mainly comprised amino acids with elevated levels in healthy controls, while clusters III and IV were characterized by high concentrations of sphingolipids and S1P in NT CRSwNP and N-ERD, with the highest plasma levels of S1P, sphingosine and sphinganine in NT CRSwNP (Figure 4.15 B, Table 8.11). All quantified sphingomyelins and the highest concentrations of long-chain acylcarnitines were associated with N-ERD (cluster V, Figure 4.15 B, Table 8.11).

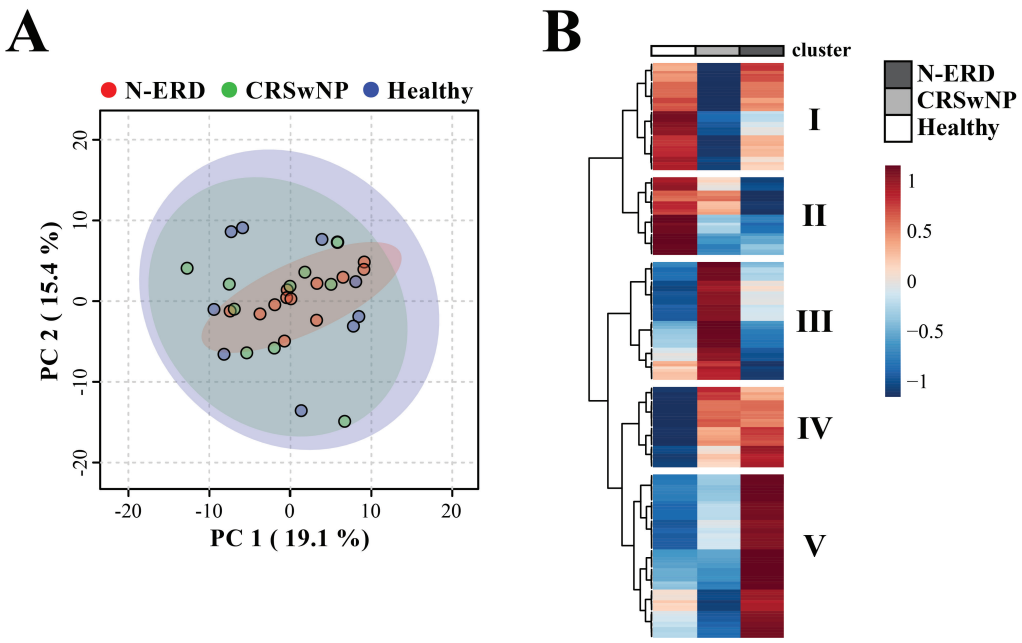

Figure 4.15 Sphingolipids are elevated in N-ERD and NT CRSwNP plasma
Targeted metabolomics of plasma from N-ERD (n = 12), NT CRSwNP (n = 10) and healthy (n = 9) individuals. **A** PCA comparing N-ERD (red), NT CRSwNP (green) and healthy (blue) individuals. Colored areas show 95% confidence intervals for each group. **B** Heatmap of metabolites assigned to clusters. Rows represent metabolites, columns show normalized, auto-scaled mean group concentrations. Concentration differences between patient groups are shown as z-score in blue (low) and red (high). See Table 8.11 for a detailed analyte group distribution in all clusters. This figure was adapted from our submitted manuscript (see Declaration of content).

We subsequently performed two-group pathway analyses of the plasma metabolome data with several limitations (see 3.3.3). Consistent with hierarchical clustering, all three comparisons revealed distinct sphingolipid metabolism profiles despite not reaching significance (Table 4.7). Other top pathways were associated with the amino acid metabolism and can be neglected since we did not obtain any dietary information of our patients and there was no fasting prior to blood collection (Table 4.7).

Thus, together with the sputum and NLF metabolomes and LC-MS/MS analyses, the plasma metabolome suggested that N-ERD was characterized by aberrations in signaling lipids (lipid mediators 4.4.2 and sphingolipids) and acylcarnitines, indicative of a broad dysregulation of the lipid metabolism in this disease.

Table 4.7 Top 5 plasma pathway analysis results

Group comparison	Pathway	*p* value Holm	Metabolite hits in pathway	Total metabolites in pathway	FDR	Pathway impact
N-ERD *vs.* Healthy	Alanine, aspartate and glutamate metabolism	1.00	5	24	0.881	0.751
	Sphingolipid metabolism	1.00	9	25	0.881	0.610
	Arginine and proline metabolism	1.00	13	77	0.881	0.573
	Glycine, serine and threonine metabolism	1.00	5	48	0.881	0.420
	Taurine and hypotaurine metabolism	1.00	2	20	0.881	0.363
N-ERD *vs.* CRSwNP	Alanine, aspartate and glutamate metabolism	1.00	5	24	0.925	0.751
	Sphingolipid metabolism	1.00	9	25	0.680	0.610
	Arginine and proline metabolism	1.00	13	77	0.925	0.573
	Glycine, serine and threonine metabolism	1.00	5	48	0.925	0.420
	Taurine and hypotaurine metabolism	1.00	2	20	0.925	0.363
CRSwNP *vs.* Healthy	Alanine, aspartate and glutamate metabolism	1.00	5	24	0.885	0.751
	Sphingolipid metabolism	1.00	9	25	0.832	0.610
	Arginine and proline metabolism	1.00	13	77	0.832	0.573
	Glycine, serine and threonine metabolism	1.00	5	48	0.832	0.420
	Taurine and hypotaurine metabolism	1.00	2	20	0.964	0.363

Top 5 pathway impact results of plasma pathway analysis by MetaboAnalyst 4.0. Results are shown for each two-group comparison. FDR, false discovery rate. Significance threshold by Holm: $p < 0.05$.

4.4.4 Adipokines do not correlate with disease severity in N-ERD and CRSwNP patients

Several studies describe a link between obesity, adipokines and airway inflammation (see 1.3). Thus, we assessed plasma adiponectin and leptin levels and correlated them with BMI and clinical symptom scores of cohort I.

BMI was similar throughout all patient groups (Table 4.2). N-ERD, but not NT CRSwNP patients, showed a weak positive correlation between BMI and SNOT22 scores ($r = 0.25$, $p = 0.37$, Figure 4.16 A). As leptin levels were demonstrated to be pro-inflammatory and adiponectin to be airway-protective (see 1.3.2), we next assessed and compared both adipokines in study individuals (Figure 4.16 B, C). Leptin levels were slightly, however not significantly elevated in N-ERD and NT CRSwNP plasma (Figure 4.16 B). While adiponectin plasma concentrations did not differ between NT CRSwNP and healthy individuals, concentrations were increased in N-ERD in comparison to NT CRSwNP (Figure 4.16 C).

No correlations were found for adiponectin and BMI or SNOT22 scores in NT CRSwNP and N-ERD patients (Figure 4.16 D, E). Coherent with current literature (see 1.3.2), leptin levels increased with higher BMI, which was significant for N-ERD (Figure 4.16 F). In addition, leptin showed a weak positive correlation with SNOT22 scores in both N-ERD and NT CRSwNP groups (Figure 4.16 G).

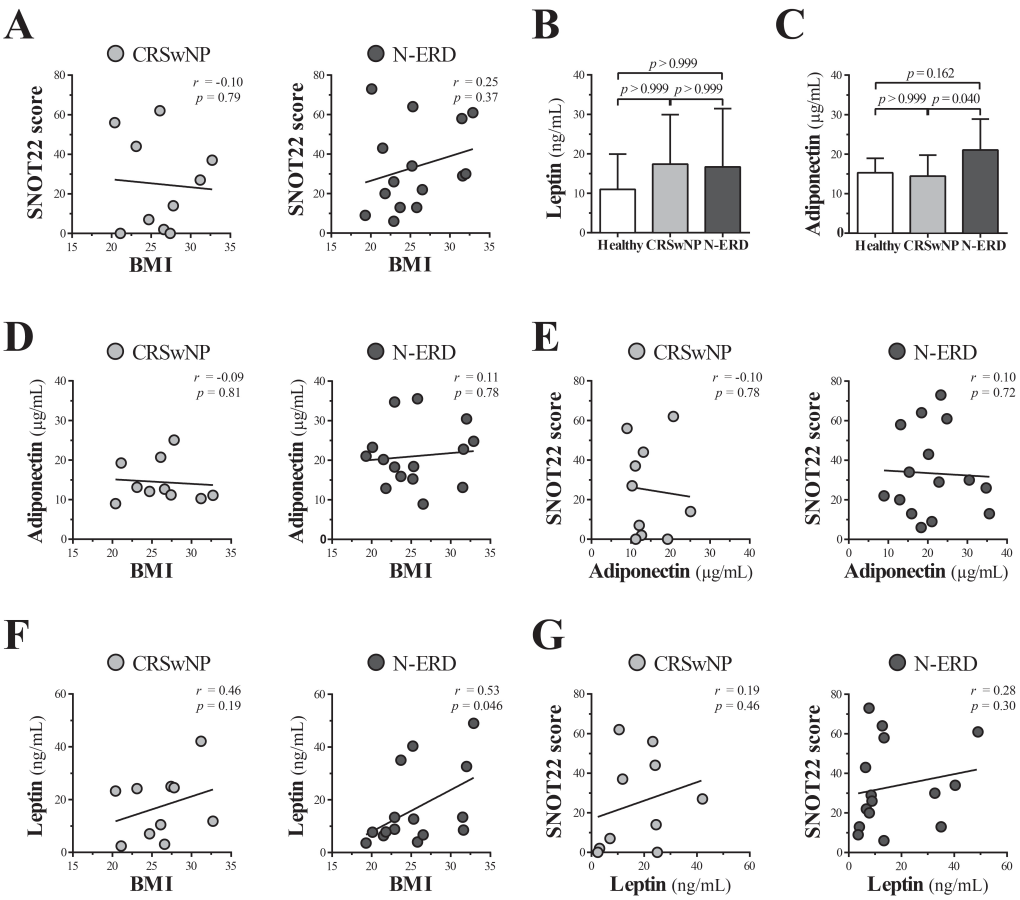

Figure 4.16 BMI slightly correlates with N-ERD but not NT CRSwNP disease severity

A, D-G Correlations between **A** BMI-SNOT22, **D** BMI-adiponectin plasma concentrations, **E** SNOT22-adiponectin, **F** BMI-leptin plasma concentrations and **G** SNOT22-leptin of NT CRSwNP (grey, n = 10) and N-ERD (dark grey, n = 15) patients. **B, C** plasma concentrations of **B** leptin and **C** adiponectin of N-ERD (n = 15), NT CRSwNP (n = 10) and healthy (n = 10) individuals. Data are shown as mean ± SD and were analyzed with Kruskal-Wallis test with Dunn's correction: $p < 0.05$. This figure was adapted from our submitted manuscript (see Declaration of content).

4.5 Extracellular vesicles: upper and lower airway exosomes

4.5.1 Exosomes can be isolated from nasal tissue culture SN and sputum

Generation, isolation and handling of exosomes is challenging as they are nano-sized particles (e.g. not easily observable by FACS or microscope, Coumans et al., 2017). Initially, we cultured PMN (fMLP-stimulated) and aMDM of healthy and N-ERD individuals (in exosome-free medium) for 24-48 h and isolated exosomes via precipitation. However, we failed to reproducibly detect exosome-associated proteins (TSG101, CD63, CD81) in highly material-consuming western blots (Figure 4.17 A) and particles in NTA analysis (Figure 4.17 B). Since lipid mediator and transcriptomic analyses revealed only minor differences in blood-derived immune cells between N-ERD and healthy individuals and exosomes were successfully isolated from nasal lavages and BALF by others (see 1.4.2), we decided to focus on local airway samples.

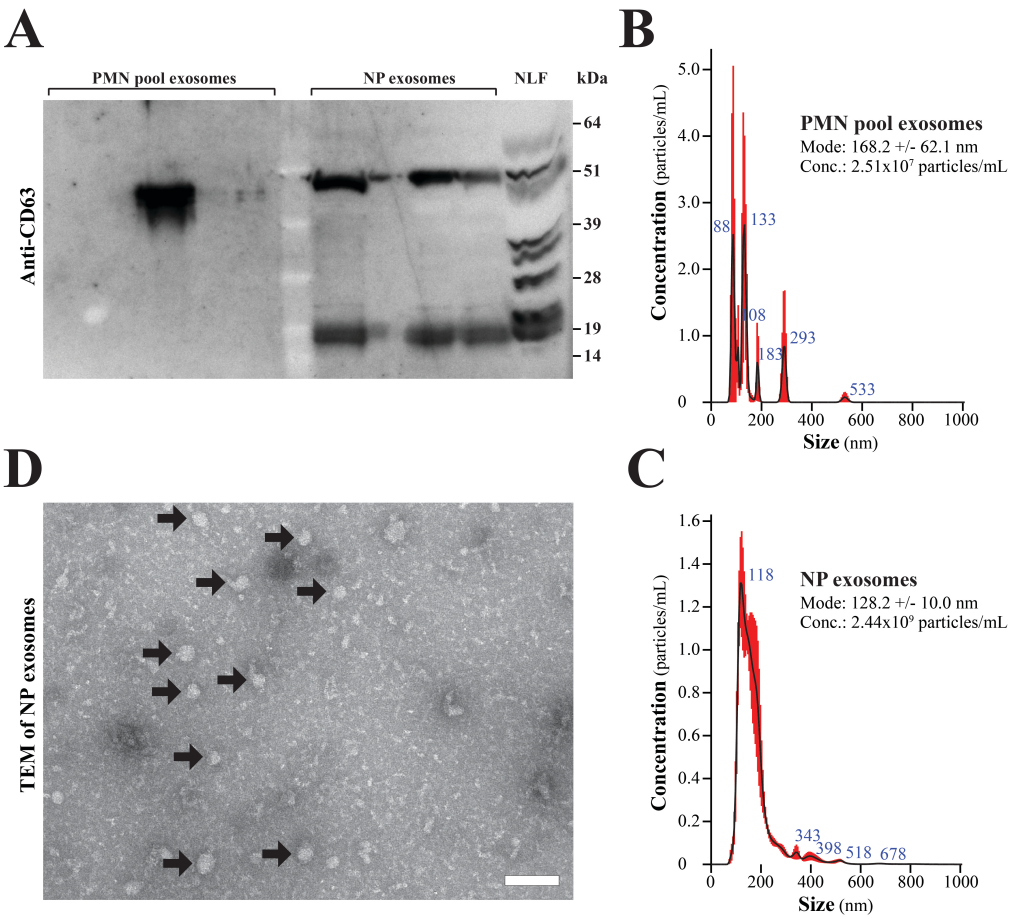

Figure 4.17 Exosomes can be readily isolated from nasal tissue cultures, but not from PMN SN

A Anti-CD63 Western blot of exosomes isolated from pooled SN of N-ERD PMN treated with fMLP (n = 4, total cells: 50x10^6, left) and exosomes isolated from CRSwNP NP tissue culture SN (n = 1, right). kDa, kilodalton. **B and C** NTA of exosomes isolated from **B** pooled SN sputum SN of N-ERD PMN and **C** CRSwNP

NP tissue culture SN. Particle size and concentration distributions with the SEM (red) for three measurements of each sample are shown. **D** TEM picture of exosomes (round-shaped structures, examples indicated by black arrows) isolated from CRSwNP NP tissue culture SN. Magnification: 24.500x, scale-bar (white): 100 nm.

We cultured NP tissue obtained from the clinic (in exosome-free medium) and used the SN to isolate exosomes by precipitation. The presence of exosomes was successfully determined by NTA, western blot and TEM (Figure 4.17 A, C, D), though material was very limited, and preparations were not yet purified of contaminant proteins. IF stainings of the exosome-markers CD81 and TSG101 in N-ERD and NT CRSwNP NPs as well as turbinate tissue from healthy individuals revealed elevated exosome markers in the N-ERD NP epithelium, that suggest an increased exosome secretion (Figure 4.18). Since we were not able to obtain an adequate quantity of nasal tissues from N-ERD, NT CRSwNP (both NPs) and healthy (turbinates) individuals during this study, the nasal tissue-derived exosome study was put on a halt.

However, we decided to further pursue exosomes isolated from sputum which was successfully achieved in first pilot experiments (data not shown).

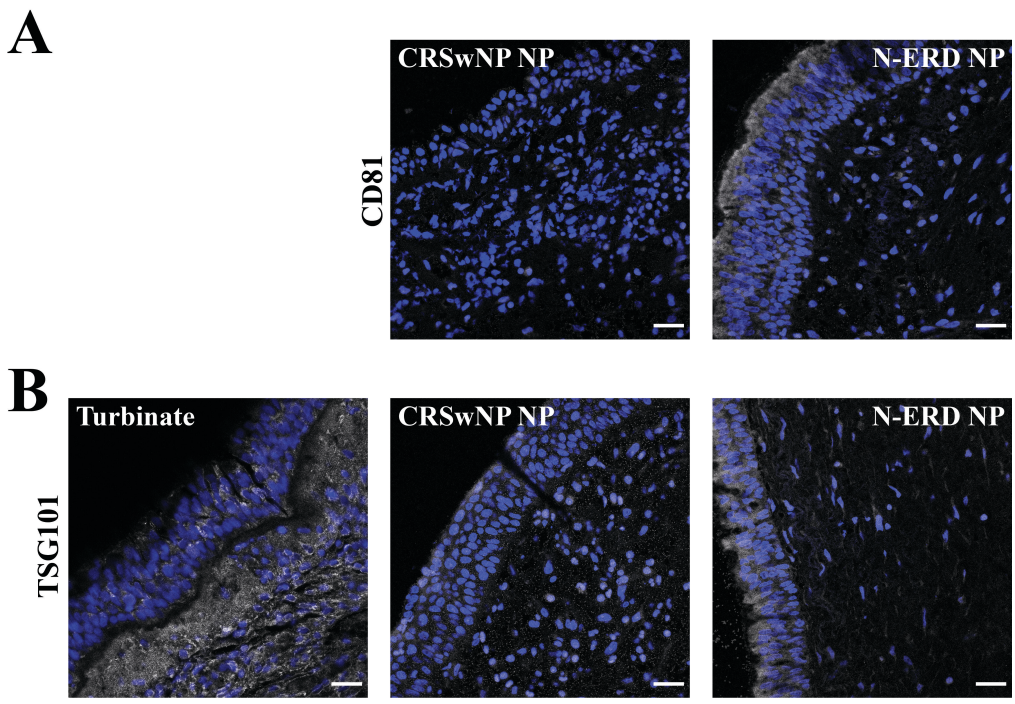

Figure 4.18 Exosome markers CD81 and TSG101 are elevated in the epithelium of N-ERD NP
Representative IF pictures of **A** CD81 and **B** TSG101 (both grey) and DAPI (blue) in N-ERD NP (n = 2), CRSwNP NP (n = 2) and healthy turbinate (n = 1, only TSG101) tissue. Scale bars (white): 25 µm.

4.5.2 Sputum-derived exosomes from N-ERD and healthy individuals induce distinct responses in aMDM and hBECs

Sputum SN from cohort II was used to isolate exosomes for *in vitro* stimulations of aMDM and commercially available human bronchial epithelial cells (hBECs) from healthy individuals. Since unphysiological amounts of exosomes are often used in *in vitro* stimulations (Sverdlov, 2012), we decided to normalize our exosome concentrations by initial sputum cell count and stimulate cells in a 1:1 ratio (e.g. stimulate $0.2x10^6$ aMDM with an exosome-equivalent isolated from $0.2x10^6$ sputum cells). Sputum samples were pooled to obtain one exosome isolation per group (N-ERD and healthy). As sputum yield of healthy individuals was low, additional sputum SN material was kindly provided by Dr. Ulrich Zissler but resulted in the loss of age matching (mean: 52.4 *vs.* 33.0, $p = 0.020$, Table 4.8).

Differential sputum cell counting revealed elevated numbers of sputum neutrophils (mean: 52.4% *vs.* 33.0%, $p = 0.004$) in N-ERD, while the percentage of macrophages (mean: 38.0% *vs.* 84.8%, $p = 0.004$) was highest in sputum from healthy controls (Table 4.8). Eosinophil ($p = 0.221$) and lymphocyte ($p = 0.565$) counts did not differ between both groups.

Table 4.8 Sputum characterization

Donor	Group	Age	Sex	Differential sputum cell count (%)						% of exosome pool
				Total living leukocytes	sMac	neutrophils	lymphocytes	eosinophils	basophils	
#1	N-ERD	35	female	3.18	32	66	1	1	0	22.8
#16	N-ERD	65	female	6.04	28	67	2	4	0	27.5
#71	N-ERD	69	female	2.58	31	68	0	0	0	18.8
#75	N-ERD	53	female	3.41	25	71	5	0	0	24.9
#76	N-ERD	40	female	0.87	74	24	1	1	0	6.0
#36	healthy	31	female	0.50	84	16	1	0	0	4.0
#38	healthy	53	female	0.43	N/A	N/A	N/A	N/A	N/A	2.3
#109	healthy	51	female	0.15	outlier, too much epithelial cells					0
#110	healthy	64	female	0.80	41	55	1	4	0	5.7
AM_023#	healthy	23	female	8.12	99	0	1	0	0	11.0
AM_036#	healthy	25	female	19.02	100	0	0	0	0	18.5
AM_070#	healthy	29	female	12.46	96	3	1	0	0	15.2
AM_048#	healthy	24	female	6.27	97	1	3	0	0	9.3
AM_033#	healthy	21	female	3.54	99	1	0	0	0	5.7
LL_033#	healthy	21	female	3.35	70	29	1	0	0	5.5
LL_069#	healthy	21	female	5.98	77	22	1	0	0	22.9

Characterization of cohort II and additionally supplied (#) sputum donors and samples.

Highly purified exosomes were isolated by precipitation followed by subsequent SEC (in line with Coumans et al., 2017) and characterized by NTA (Figure 4.19 A). Sputum exosomes were used to stimulate aMDM and serum-starved hBECs in exosome-free medium for 24 h. 0.2 µm-filtered PBS eluted from qEV SEC columns (qPBS) was used as negative control. Eight epithelial cell-derived immune regulatory mediators (GM-CSF,

periostin, CXCL8, CCL2, CCL26, IL25, IL33, TSLP) were quantified in sputum exosome preparations and hBEC SN (Table 8.13). No TSLP was measured in all stimulations and periostin, IL33 and CCL2 did not differ between all conditions (Table 8.13). Stimulation with N-ERD exosomes resulted in increased secretion of GM-CSF, CXCL8 and CCL26 by hBECs, while healthy sputum exosomes showed only minor effects (Figure 4.19 B, Table 8.13). Very low levels of CXCL8 were exclusively detected in N-ERD exosomes but is assumed to be not responsible for the high CXCL8 production by hBECs after stimulation (Figure 4.19 B, Table 8.13).

aMDM SN was subjected to chemokine/cytokine multiplex (17 analytes) and lipid mediator analyses. Sputum exosomes from healthy individuals contained IL33, IL27, IL12p70 and low levels of IL18, CXCL10 and CXCL11, while N-ERD exosomes solely contained minor levels of IL33, IL12p70, IL18 and CXCL10 (Figure 4.19 C, Table 8.14). Despite lower CXCL10 content, N-ERD sputum exosomes induced higher, but not significant, levels of CXCL10 in aMDM than those isolated from sputum of healthy individuals. In contrast, healthy sputum exosomes strongly induced nearly all other analytes (Figure 4.19 C, Table 8.14).

To not overrule minor effects of sputum exosomes on the lipid mediator profile of stimulated aMDM, we did not perform an additional stimulation with the ionophore A23187, which strongly enhances eicosanoid production (Borgeat & Samuelsson, 1979). Thus only 6 of 54 lipid mediators could be quantified, which all belonged to the COX-pathway (Figure 4.20). Healthy sputum exosomes strongly upregulated the synthesis of COX-metabolites (8-iso-$PGF2_{\alpha}$, TXB_2, $PGF_{2\alpha}$, PGE_2, PGD_2), while N-ERD-derived sputum exosomes only slightly increased $PGF_{2\alpha}$, TXB_2 and PGE_2 production (Figure 4.20).

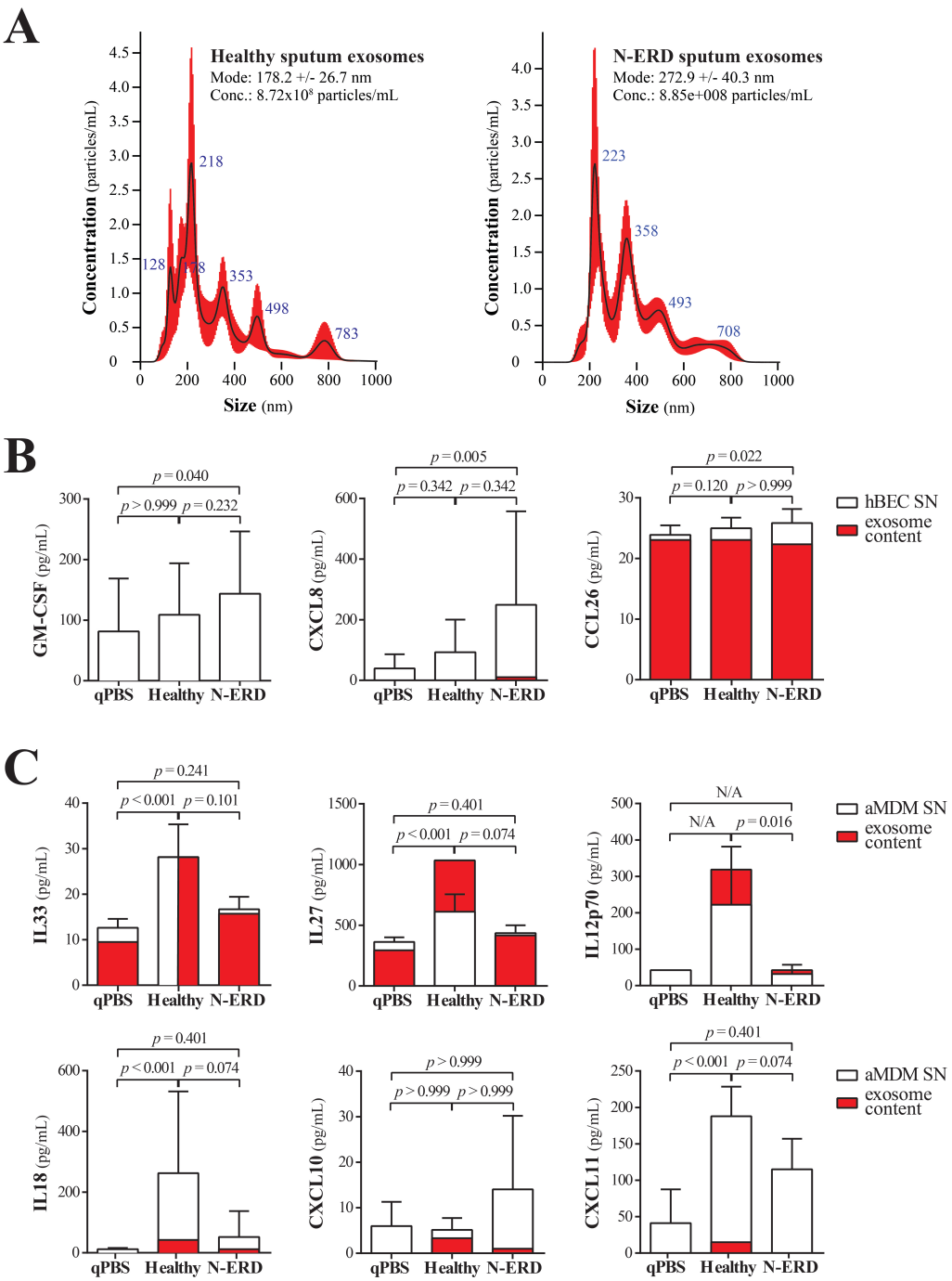

Figure 4.19 Exosomes isolated from healthy and N-ERD sputum elicit distinct chemokine/cytokine responses in hBECs and aMDM

A NTA of purified sputum exosomes from sputum SN of healthy (n = 10) and N-ERD (n = 5) individuals. Particle size and concentration distributions with the SEM (red) for three measurements of the same sample are shown. **B and C** Chemokine/cytokine multiplex measurements in SN of hBEC (n = 5) and aMDM (n = 8) cultures of healthy donors (white) and the sputum exosome preparations they were stimulated with for 24 h (red). N/A, not available (due to not detectable analytes in some conditions); qPBS, qEV SEC-processed PBS. Data are shown as mean ± SD and were analyzed with Friedman test with Dunn's correction or Mann-Whitney-Wilcoxon test (IL12p70 Healthy *vs.* N-ERD): $p < 0.05$.

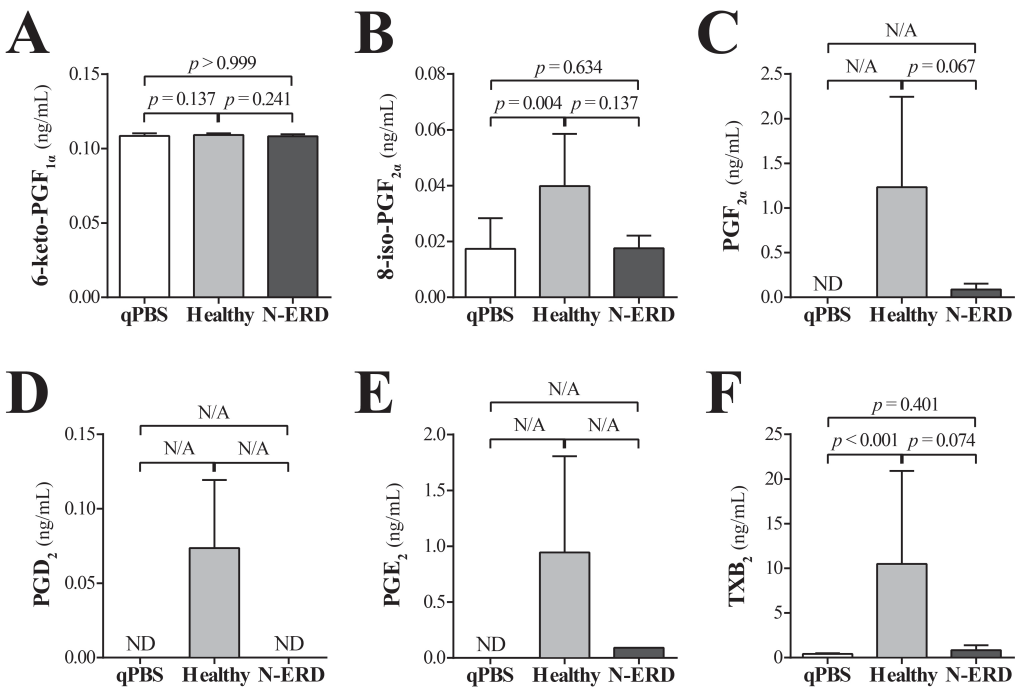

Figure 4.20 Sputum exosomes from healthy but not N-ERD individuals induce COX metabolites in aMDM

Lipid mediators **A** 6-keto-$PGF_{2\alpha}$, **B** 8-iso-$PGF_{2\alpha}$, **C** $PGF_{2\alpha}$, **D** PGD_2, **E** PGE_2 and **F** TXB_2 measured in the SN of aMDM from healthy donors (n = 8) stimulated with sputum-derived exosomes (without ionophore A23187). ND, not detected; N/A, not available (due to not detectable analytes in some conditions); qPBS, qEV SEC-processed PBS. Data are shown as mean ± SD and were analyzed with the Friedman test with Dunn's correction or Mann-Whitney-Wilcoxon test ($PGF_{2\alpha}$: Healthy *vs.* N-ERD): $p < 0.05$.

Finally, to verify the uptake of exosomes in hBECs and aMDM, we transferred cells into chamber slides, stimulated them with C5-maleimide AF488-stained sputum exosomes (Roberts-Dalton et al., 2017) and assessed fluorescence signals at six different time points after stimulation for 24 h (see 3.2.22). However, we were not able to detect any specific staining in hBECs (n = 2) and aMDM (n = 2) (data not shown).

Collectively these data suggest that sputum exosomes are potent and cell-specific activators that themselves contain several chemokines/cytokines and can induce the production of several immune regulatory mediators in aMDM and hBECs.

5 Discussion

N-ERD remains a major clinical need, particularly due to recurrent and therapy-resistant nasal polyposis. To identify new mechanisms and potential therapeutic targets of N-ERD, we combined transcriptomics (RNAseq) and methylomics with multi-fluid metabolomics and lipid mediator analysis (LC-MS/MS) approaches. N-ERD patients showed distinct gene expression, DNA methylation and metabolite profiles both locally (in nasal tissue, NLF and sputum) as well as systemically (in plasma and monocyte-derived macrophages), with major aberrations in lipid metabolism and host defense.

5.1 N-ERD PMN and aMDM exhibit no PGE_2 resistance in an European population

Several pro- and anti-inflammatory cascades are altered in inflammatory diseases and thus influence cell compositions and phenotypes at local sites. The origin of these alterations is commonly based on genetic and/or epigenetic alterations of specific key immunoregulatory enzymes and/or mediators.

Laidlaw et al. postulated granulocytes from N-ERD patients to produce higher levels of pro-inflammatory LTB_4 and cysLTs, which are further elevated by granulocyte-adhering platelets, and to resist the anti-inflammatory effects of PGE_2 in comparison to NT asthmatics and healthy controls (T. M. Laidlaw et al., 2012; Tanya M. Laidlaw et al., 2014). However, we could not confirm the presence of platelets adhering to blood PMN by repeating the experiments described by Laidlaw et al. (Figure 4.2). To test if the anti-coagulation agent EDTA (heparin was used by the authors) and/or our PMN isolation protocol resulted in the loss of adhering platelets, we analyzed whole blood with EDTA or heparin of study participants and additional healthy volunteers. Again, we were not able to detect any differences between patient groups, while the $CD61^+$ signal diminished after PMN isolation (10% *vs.* 1%, Figure 4.2).

In addition to the missing platelet-adherence of PMN, we also were not able to detect an enhanced production of LTB_4, cysLTs or other lipid mediators, which have not been analyzed by Laidlaw et al. before, in PMN of our study cohort (Table 4.3). We further were not able to confirm any PGE_2 resistance in N-ERD, as we detected no differences in lipid mediator concentrations between PMN from N-ERD, NT CRSwNP and healthy individuals after stimulation with PGE_2 (Figure 4.3). Though both study populations are (presumably) largely Caucasian, there might be differences between North American and European patients that might be responsible for the different results obtained by Laidlaw et al. and in our study. Such differences might be due to different lifestyles or different treatment regimens (e.g. use of different anti-inflammatory drugs) and it would be interesting to address this issue in a future multi-center cohort study across different continents.

Besides PMN, fibroblasts isolated from N-ERD NP have been demonstrated to exhibit a PGE_2 resistance as well, which was shown to be mediated by reduced expression of EP_2. We stimulated aMDM with PGE_2 and IL4 to analyze PGE_2 resistance and responsiveness to a key cytokine in type 2 inflammation and macrophage polarization. However, we found no differences in the lipid mediator and chemokine/cytokine profile between N-ERD, NT CRSwNP and healthy aMDM for both stimulations (Table 8.1, Table 8.3, Table 8.4). While there might indeed be no PGE_2 resistance in N-ERD aMDM, another explanation for this observation might be that the used concentration of 100 nM was not sufficient to elicit any effects, since lipid mediators (e.g. LTB_4 and cysLTs) were not reduced (Table 8.1, Table 8.3) In the literature, common PGE_2 concentrations for *in vitro* stimulations of MDM range between 1 nM to 10 µM (Sanin et al., 2018; Tang et al., 2017). Since limited amounts of aMDM precluded us from a titration, we decided to use a moderate concentration of 100 nM PGE_2, which also prevents an overstimulation that might have abrogated subtle differences in PGE_2 responses between patient group aMDM.

Another plausible explanation for the observation of no differences of PGE_2- but also IL4-stimulated aMDM is the cellular *in vitro* model we used. While the differentiation of monocytes with GM-CSF and TGFβ1 induces an alveolar-like M2 phenotype, the presence of TGFβ1 also suppresses the responsiveness to external stimuli. In one of our studies, which was performed after the recruitment of cohort I, we could demonstrate that MDM differentiated without TGFβ1 are more responsive to IL4 treatment than aMDM (Henkel et al., 2018). In conjunction with studies demonstrating TGFβ1, IL4 and PGE_2 to regulate each other in a dose-dependent manner that leads to common or distinct functional phenotypes (Hart et al., 1989; McCartney-Francis & Wahl, 2001; Ramirez-Yañez, Hamlet, Jonarta, Seymour, & Symons, 2006; Remes Lenicov et al., 2018; F. Zhang et al., 2016), GM-CSF differentiated MDM could have been a more suitable cell type to study PGE_2 and IL4 treatment-induced responses between N-ERD, NT CRSwNP and healthy individuals.

However, N-ERD aMDM exhibited elevated levels of pro-inflammatory 5-LO and COX metabolites (e.g. LTB_4, 5-HETE, cysLTs, PGD_2, TXB_2) in comparison to aMDM from NT CRSwNP patients and healthy controls at baseline (Figure 4.4, Table 8.1). In addition, type 1 cytokine concentrations (e.g. IL12p70) tended to be reduced in N-ERD, while IL1β and TNF levels were slightly elevated (Figure 4.4, Table 8.2). Thus, the lipid mediator and chemokine/cytokine profiles of N-ERD aMDM indicate a more pro-inflammatory phenotype in comparison to NT controls. In future studies, it would be intriguing to confirm and elucidate the molecular basis of these systemic differences in the activation of macrophages (both MDM and aMDM). In particular, transcriptome and cellular metabolome analyses of precursor populations (e.g. $CD34^+$ cells) might reveal (novel) pathways related to factors in the circulation or in the bone marrow that determine the pro-inflammatory (pre-)activation of N-ERD monocytes/macrophages.

5.2 Transcriptomics and methylomics indicate a pro-inflammatory aMDM phenotype with aberrant lipid metabolism in N-ERD

Cheong et al. postulated differences in AA metabolism genes, specifically a hypomethylation of PGDS, LTB4R and ALOX5AP, while PTGES was hypermethylated in NP of N-ERD in comparison to NT CRSwNP asthmatic patients (Cheong et al., 2011). They also compared the DNA methylation profiles in cells isolated from buffy coats and found no differences between both study groups. However, buffy coats do not contain PMN and the percentage of monocytes generally revolves around 10% of all cells in buffy coats. Thus, since these major drivers of type 2 inflammation were not specifically analyzed in this study, we hypothesized that PMN and monocytes/aMDM show differences in the methylation of PGDS, LTB4R, ALOX5AP and PTGES prior the influx into NP tissue.

We could not confirm our hypothesis, as methylation levels did not differ between PMN, monocytes and aMDM from N-ERD, NT CRSwNP and healthy individuals (Table 8.5-Table 8.8, see 4.3.1). Together with studies that demonstrated changes in mediator production and receptor expression in N-ERD airways and the alterations in DNA methylation of whole NP tissue by Cheong et al., we likewise suggest that the local inflammatory environment drives alterations in DNA methylation of infiltrating cells disease-specifically as the cellular composition of the tissue environment was similar between study groups (Cahill & Boyce, 2017; Cheong et al., 2011; Sang-Heon Kim et al., 2007; T. Liu et al., 2013; A. R. Sousa et al., 2002; Ying et al., 2006).

We found several differences in the transcriptome of N-ERD aMDM in comparison to healthy controls. Despite the reduction in potentially host-protective molecules (CD1a-c, CLEC10A, CLEC18A), N-ERD aMDM showed an increased expression of pro-inflammatory chemokines (CXCL1-3, PPBP, CXCL8, CCL20) (Figure 4.5, see 4.3.2). Together with an enhanced expression of PTGS2 (Eliopoulos, 2002; Tang et al., 2017) and reduced expression of the immunosuppressive transcription factor CEBPD (Hsiao et al., 2013), this profile was indicative of a pre-activated, pro-inflammatory state that is common for airway macrophages as compared to MDM in healthy individuals (Tomlinson et al., 2012).

Notably, these alterations in gene expression in N-ERD aMDM were evident even after 7 days of *in vitro* differentiation in the presence of GM-CSF and TGFβ1. This suggested that an altered immunological profile was indeed imprinted on the level of bone marrow precursors or monocytes (see 5.1).

While the differentiation of monocytes into aMDM introduces extensive changes in DNA methylation (Vento-Tormo et al., 2016), DMRs between N-ERD and healthy individuals were stable as no differences were found in a comparison of both cell types (Figure 4.7, see 4.3.3). Though the number of DMPs and DMRs differed greatly between monocytes and aMDM and only partially overlapped, a group-specific, stable DNA methylation

phenotype was indicated by taking into account the differences between N-ERD *vs.* healthy in this analysis. With only CXCL2 overlapping between DEGs and DMRs, the relatively small methylation differences between N-ERD and healthy monocytes/aMDM likely play a minor role in the pro-inflammatory expression phenotype identified by RNAseq (Figure 4.7). Besides DNA methylation, several other epigenetic mechanisms (e.g. histone modifications, non-coding RNA-mediated regulation) could not be analyzed in this study and should be addressed in the future to further characterize the pro-inflammatory imprinting of N-ERD monocytes/aMDM (Z. Chen, Li, Subramaniam, Shyy, & Chien, 2017).

Functional analysis of DMR-derived genes of aMDM revealed CPT1A, CPT1B and ACACA to be differentially methylated in N-ERD (Table 4.5). These differences in DNA methylation of acylcarnitine transport-related genes indicate alterations in FAO. While CPT1 is involved in acylcarnitine transport for FAO (Bartlett & Eaton, 2004), ACACA catalyzes the carboxylation of acetyl-CoA to malonyl-CoA and thus is a key enzyme in the fatty acid synthesis (Wakil, Stoops, & Joshi, 1983). Fatty acid synthesis has only recently been shown to be essential for the pro-inflammatory activation of T cells and macrophages (Carroll et al., 2018; J. Lee et al., 2014). Thus, it would be interesting to further explore potential differences in FAO in aMDM from N-ERD patients and healthy individuals, but also disease-controls (e.g. NT CRSwNP) in live cell metabolic assays (e.g. Seahorse).

In conjunction with a hypomethylation of FGF7, previously implicated in macrophage-dependent host defense in the airways (Gardner et al., 2016) and found to be slightly elevated in our aMDM RNAseq analysis (log2 Fold Change: 0.5, see 3.1.12 Deposited Data), a moderate trend towards pro-inflammatory mediators (IL1β, TNF, CCL20, eicosanoids, Figure 4.4, Table 8.2, see 4.2.2) as well as immunoregulatory and lipid metabolism alterations in the transcriptome (CXCL1-3, PPBP, CXCL8, PTGS2, CEBPD, Figure 4.5, see 4.3.2) and methylome (CXCL2, PF4, CPT1A, CPT1B, ACACA, Table 4.5, see 4.3.3), N-ERD aMDM appear to exhibit a predisposition towards an enhanced responsiveness that may fully unfold in peripheral tissues (e.g. nasal and/or lung mucosa) upon inflammatory challenge.

Since low numbers of recovered sMac from healthy individuals precluded a comparison of the transcriptome from local macrophages of the lower airways between N-ERD and healthy controls, we compared sMac with aMDM from the same N-ERD patients. sMac demonstrated a distinct expression profile that was functionally linked to chemokine, IL17, IL10, IL4 and IL13 as well as TNF signaling pathways (Figure 4.9 B, Table 8.10). Indeed, in line with previous studies (Saradna, Do, Kumar, Fu, & Gao, 2018; Tomlinson et al., 2012), several pro-inflammatory chemokines (e.g. CXCL and CCL family) and immunoregulatory enzymes (e.g. IDO1, PTGS2 (COX-2), PTGES (mPGES-1)) and cytokines (e.g. IL10, IL18BP, IL23A, IL27, IL1β, IL6, TNF, TGFβ2) were increased in sMac (Figure 4.9). An elevated expression of PRRs (e.g. TLR family) and T cell priming-

associated genes (e.g. HLA family, CD1a-c, CD28, CD40, CD80) further indicated altered host defense activity, while type 1 cytokine expression did not differ in comparison to aMDM (Figure 4.9). Together with an immune regulatory eicosanoid profile (ALOX15 (15-LO), PTGS2, PTGES, PTGER2-3) in comparison to aMDM, which were characterized by higher expression of 5-LO pathway genes (ALOX5AP, LTA4H), and an enrichment in alternative activation markers (e.g. IL10, TGFβ2, IRF4, CCL17, CEBPD), the sMac transcriptome suggests a M2 phenotype that might be the result of active type 2 inflammation in the airways of N-ERD patients (Figure 4.9).

Accordingly, N-ERD sMac exhibited a distinct FAO-associated expression profile in comparison to aMDM, indicating a demand for FFAs for FAO with elevated expression of FFA receptors (FFAR2-3), CPT1B and ACSL1, an enzyme that catalyzes long-chain fatty acids to acyl-CoA esters and mediates inflammatory functions in macrophages (Figure 4.9) (Al-Khami et al., 2017; S. C.-C. Huang et al., 2014; Jha et al., 2015; Rubinow et al., 2013). Lower expression of CPT2 might result in an accumulation of acylcarnitines that can induce COX-2, CXCL2, IL1β, IL6 and TNF (Rutkowsky et al., 2014), pro-inflammatory mediators elevated in N-ERD sMac in comparison to aMDM (Figure 4.9). ACACA, one of the genes differentially methylated in aMDM (Table 4.5), was potentially downregulated due to excess fatty acid availability by higher expression of FFARs (Figure 4.9).

The higher expression of CERS4, SMase-3 (SMPD3) and SPP2 (SGPP2) indicates a shift from sphingolipid to ceramide synthesis by catalyzing the dephosphorylation of S1P and formation of ceramide (Figure 4.9, Figure 1.6). Thus, pro-inflammatory effects of S1P are likely to be diminished in N-ERD sMac in comparison to aMDM. In contrast, the receptors for anti-inflammatory ApoE (LRP8) and adiponectin (ADIPOR2) were downregulated in sMac (Baitsch et al., 2011; Lovren et al., 2010; Ohashi et al., 2010), while the expression of leptin, which can induce the production of several pro-inflammatory mediators (e.g. IL1β, TNF, IL6, cysLTs, LTB_4), was elevated (Figure 4.9) (Acedo et al., 2013; Mancuso et al., 2004; Raso et al., 2002). These observations match dysregulations of ApoE, adiponectin and leptin that are associated with inflammatory airway diseases (Bruno et al., 2009; Holguin, Rojas, et al., 2011; Shore et al., 2006; Summer et al., 2008; Yao et al., 2010) and suggest that lipid metabolism alterations in sMac contribute to N-ERD pathogenesis.

Induced sputum is a strong, non-invasive tool facilitating the access to lower airway cell populations including sMac. Though cell yield is donor-dependent and low ($0.2\text{-}1.5\text{x}10^5$ sMac per donor in this study), new tools such as single cell RNAseq could provide important insights into sMac subpopulations of N-ERD patients. Thus, it would be interesting to compare the sMac single cell transcriptomes of N-ERD, NT CRSwNP with/without asthma, asthmatics without CRSwNP and healthy individuals in future studies.

Nasal brushings of N-ERD patients also exhibited an altered lipid metabolism expression profile (APOE, APOC1 and LPIN1), which has been implicated in macrophage-mediated immune responses (Figure 4.10). In particular, ApoE, which can suppress the pro-inflammatory activation of macrophages and reduce allergic airway inflammation to HDM (Baitsch et al., 2011; Yao et al., 2010), was downregulated in N-ERD NP as shown by RNAseq and IF (Figure 4.10, Figure 4.11). Coherently, the expression of CD200R1 and A2M, which also regulate macrophage activation (Hoek et al., 2000; Hoffman, Pizzo, & Weinberg, 1988), was reduced in N-ERD nasal polyps (Figure 4.10). In contrast, LPIN1, expressed by macrophages and involved in TLR signaling and inflammatory responses (Meana et al., 2014; Navratil et al., 2015), was upregulated in N-ERD (Figure 4.10) and might indicate a predominance of pro-inflammatory macrophages. Indeed, a massive influx of macrophages was previously shown in nasal polyps of CRSwNP patients, underlining their potential pathological relevance (Varga et al., 1999). Thus, macrophage (metabolic) phenotypes and functions represent an important subject of research into the patho-mechanisms of N-ERD. However, the presence of macrophages in nasal scapings has to be confirmed since MHC-II genes (HLA-DQB2) are expressed by all antigen-presenting cells (APCs; macrophages, DCs, B cells) and CD200R1 was shown to be expressed in T and B cells as well (Rijkers et al., 2008). Single cell RNAseq of whole NP and turbinate tissues could thus provide an important insight in NP pathogenesis by specifically identifying and analyzing all cell types involved in N-ERD and NT CRSwNP inflammation of the upper airways.

Information about the roles of EXOC proteins (e.g. EXOC3L4), which was the most downregulated gene in nasal brushings from N-ERD patients (Figure 4.10), is scarce. As the exocyst complex is involved in epithelial membrane trafficking and integrity, impaired expression of exocyst components might contribute to the aberrant differentiation and barrier function of the nasal epithelium in N-ERD (Martin-Urdiroz et al., 2016). In contrast, lactate dehydrogenase C (LDHC) was upregulated in N-ERD nasal brushings (Figure 4.10). High expression of LDHC is implicated in cancer, correlates with poor prognosis and can induce epithelial-mesenchymal-transition (EMT) (Hua et al., 2017), an important process of epithelial barrier repair and dysregulated in nasal polyps and airway remodeling in asthma (Hackett, 2012; H.-W. Yang, Lee, Shin, Park, & Lee, 2017). Interestingly, LDHC levels increased in nasal brushings of asthmatic children responding well to OCS treatment, suggesting that the upregulation in LDHC expression might be INCS-induced (X. Zhang et al., 2017). However, potential roles of LDHC in nasal polyposis and EMT remain elusive. We also found an upregulation of the CS-induced gene FKBP5 in N-ERD NP (Mostafa et al., 2019), which has been associated with poor responsiveness to corticosteroids in asthmatics and to aberrant lipid and glucose metabolism (Figure 4.10) (Sidibeh et al., 2018; Woodruff et al., 2007). It would thus be important to assess the expression of potentially CS-induced genes (LDHC and FKBP5) in tissues from untreated patients and to correlate expression of these genes with the clinical response to OCS and INCS. A recruitment of untreated patients or volunteers

stopping their INCS and/or ICS medication could further elaborate the mode of action of and resistance to CS treatment and identify novel targets for therapy in single cell RNAseq analyses of nasal tissues and/or sputum/sMac.

Finally, the expression of the three receptors HTR4, PTGER3 and STAB2 was elevated in N-ERD nasal brushings in comparison to healthy controls (Figure 4.10, Figure 4.11). Serotonin (5-HT) signaling has been demonstrated to induce cysLT production and to be a risk factor for COPD (Soler Artigas et al., 2011; Y. Wang et al., 2004), while EP3 signaling facilitates wound healing, M2 recruitment and was shown to be airway-protective in a murine model of allergic airway inflammation (Hosono, Isonaka, Kawakami, Narumiya, & Majima, 2016; Kunikata et al., 2005). Enhanced expression of the scavenger receptor STAB2 may suggest an increased ability of the nasal epithelium from N-ERD patients to engulf apoptotic cells, thus contribute to the resolution of inflammation (S.-Y. Park et al., 2008).

Conclusively, the transcriptomes of N-ERD NP nasal brushings indicate a heterogenous expression profile characterized by altered levels of pro-inflammatory, immune regulatory and tissue repair genes, which may be linked to an aberrant lipid metabolism and contribute to the chronic type 2 inflammation that is typical for N-ERD. It was beyond the scope of this thesis to investigate any of the identified N-ERD signature genes in detail, but such research should be carried out in the future. Indeed, as the pathogenesis of N-ERD is incompletely understood and therapeutic options are unsatisfactory, the genes identified in the frame of our study could serve as novel targets for the treatment of N-ERD and related pathologies.

5.3 Dysregulated sphingolipid metabolism and elevated levels of acylcarnitines in N-ERD body fluids might contribute to disease pathogenesis

With several findings indicating alterations in the transcription and DNA methylation of lipid metabolism pathways (see 4.3), we performed targeted metabolomics analyses of airway lining fluids (sputum, NLF) and plasma to examine the local and systemic metabolic status in N-ERD and/or NT CRSwNP (see 4.4).

Plasma metabolomics revealed the sphingolipid metabolism to be altered in NT CRSwNP and N-ERD in comparison to healthy individuals, which had lower sphingolipid levels (Figure 4.15, Table 8.11). Indeed, serum sphingolipids, especially sphingosine and S1P, were shown to be increased in N-ERD individuals in comparison to NT asthmatics and correlated with AHR in a Korean study by Trinh et al. (Trinh et al., 2016). Interestingly, our analysis revealed the opposite with plasma concentrations of S1P, sphingosine and sphinganine being the highest in the NT CRSwNP group (Figure 4.15, Table 8.11). Though our study cohort was smaller and differences between groups did not reach significance, these results might be due to a distinct systemic metabolome of NT CRSwNP and NT asthmatics or indicate ethnicity-specific alterations between Caucasian and Asian patients suffering from N-ERD and NT CRSwNP or AT asthma. Trinh et al. further demonstrated that SM levels did not differ between N-ERD and NT asthmatics, but decreased after ASA-challenge in the serum of N-ERD patients and correlated with methacholine-induced AHR (Trinh et al., 2016). In our study cohort, plasma SM were associated with N-ERD (Figure 4.15, Table 8.11), which is in line with a previous study that showed SM levels to be elevated in erythrocyte membranes of asthmatics, but not healthy controls (Gupta et al., 2010). SM levels might thus be lower in NT CRSwNP patients as compared to N-ERD since only 40% suffered from comorbid asthma, whilst all N-ERD patients were asthmatic (Table 4.2). While elevated concentrations of SM in N-ERD might indicate alterations in signal transduction (Carreira et al., 2015; Gupta et al., 2010), SM could also be capitalized as a source for Cer generation during (acute) inflammatory events (e.g. response to NSAID as shown by Trinh et al. (Trinh et al., 2016)) and thus further promote disease severity by promoting inflammation (R. W. Jenkins et al., 2011). Indeed, while we could not perform the additional targeted sphingolipid analysis (including e.g. sphingosine, S1P) for our sputum and NLF samples due to sample limitations and missing method optimization for more complex sample matrices, we detected high levels of SM in the NLF of healthy, but not NT CRSwNP and N-ERD individuals (Figure 4.13, Table 8.11), which might indicate a chronic reduction of SM due to Cer generation and thus ongoing inflammation in the nasal mucosa of NT CRSwNP and N-ERD patients. Thus, it would be interesting to assess the sphingolipid profiles of body fluids and airway tissues of well-characterized endotypes of asthma and CRSwNP (e.g. N-ERD, NT CRSwNP with and without asthma, asthmatics without CRSwNP) in a multi-center cohort study across different continents to include different ethnicities (e.g. Caucasian, Hispanic, Asian, African) and validate the relevance of

sphingolipid metabolism alterations in these diseases (Kowal et al., 2019; Oyeniran et al., 2015; Price et al., 2013; Reinke et al., 2017; Sawicka et al., 2003; Trinh et al., 2016; Worgall et al., 2013).

Whilst alterations in sphingolipid metabolism in N-ERD have been reported previously, there is no literature on a potential dysregulation of acylcarnitines in N-ERD. However, previous studies had suggested aberrant levels of acylcarnitines in chronic inflammatory conditions (e.g. obesity-associated inflammation) (Enooku et al., 2019; Sampey et al., 2012). Indeed, the highest concentrations of (long-chain) acylcarnitines were exclusively found in plasma, sputum and NLF in N-ERD, but not in NT CRSwNP and healthy individuals (Figure 4.12, Figure 4.13, Figure 4.15, Table 8.11). In keeping with recent studies revealing elevated levels of acylcarnitines to be associated with increased FAO and airway inflammation in a murine model of allergic asthma, this suggested an involvement of acylcarnitines in type 2 inflammation (Al-Khami et al., 2017). Acylcarnitines were also shown to elicit a pro-inflammatory state in macrophages by inducing CXCL2, IL1β, IL6, TNF and PTGS2 expression (Rutkowsky et al., 2014). These findings indicate a possible link between increased plasma and sputum acylcarnitine concentrations and the pro-inflammatory state of aMDM and sMac seen in N-ERD individuals (see 4.3). Thus, local and systemic changes in lipid metabolic pathways and macrophage effector functions may converge and contribute to the pathogenesis of N-ERD and should be addressed by further studies exploring the effects of acylcarnitines on e.g. PMN, mast cells, macrophages and/or epithelial cells.

As the classical bioactive lipid pathway to be involved in the pathogenesis of N-ERD, we further analyzed eicosanoids in NLF and sputum N-ERD patients. To the best of our knowledge, this is the first lipid mediator profile analysis by LC-MS/MS in NLF of N-ERD individuals. Most N-ERD studies focus on urinary eicosanoid levels and/or exclusively assume local lipid mediator alterations in the upper airways on the basis of tissue histology/immunohistochemistry stainings and gene expression analyses (Daffern et al., 1999; Gaber et al., 2008; T. M. Laidlaw et al., 2012; Micheletto et al., 2010; Sestini et al., 1996; Ying et al., 2006), while studies including NLF are scarce (Ferreri, Howland, Stevenson, & Spiegelberg, 1988; C. Picado et al., 1992; S. Shimizu, Ogawa, Seno, Kouzaki, & Shimizu, 2013). In these previous studies, lipid mediators were measured by radioimmunoassay or ELISA in nasal lavages and differences between N-ERD, NT and healthy controls were only detected after provocation with ASA (Ferreri et al., 1988; C. Picado et al., 1992). In contrast, we chose to sample pure NLF from N-ERD NP or healthy turbinate tissue by filter paper strips (see 3.2.2), which enabled us to analyze the tissue-specific baseline lipid mediator fingerprint in the upper airways. LC-MS/MS analysis of NLF revealed a high heterogeneity and low concentrations of eicosanoids involved in N-ERD (e.g. LTB_4, PGD_2, PGE_2, TXB_2, Figure 4.14, see 1.1.3, 1.2.2), that might be explained by dilution due to increased nasal drainage (samples were normalized to the volume of sampled NLF) or INCS treatment. The cysLT LTE_4 was the only lipid mediator that tended to be elevated in N-ERD NLF and might be linked to enhanced

HTR4 signaling, which is implicated by upregulated HTR4 expression in N-ERD NP tissue (Figure 4.10, Figure 4.11) and can induce (serotonin-driven) cysLT production (Y. Wang et al., 2004). Potentially, epithelial brush cells, which expand in response to LTE_4, may also represent an important source of cysLTs in NP tissue that is relatively resistant to INCS treatment (Bankova et al., 2018; Dietz et al., 2017). Although no changes in anti-inflammatory PGE_2 levels could be observed in NLF of N-ERD patients, lower concentrations of 17-HDHA and non-detectable RvD2 might contribute to tissue eosinophilia, T cell activation and diminished numbers of regulatory macrophages observed in N-ERD (Chiurchiù et al., 2016; Rogerio et al., 2012). Indeed, a recent study demonstrated an IL10-deficiency of M2 macrophages in eosinophilic NP tissue of CRSwNP patients in comparison to non-eosinophilic controls (Z.-C. Wang et al., 2018). Thus, it would be interesting to analyze the NLF lipid mediator profile in a larger study cohort, including more CRSwNP endotypes, and to elaborate their cellular sources and impact on cell composition and function in NP tissue. In addition, the recruitment of patients without any CS treatment could improve our understanding of CS-induced alterations and therapy-resistance in CRSwNP and N-ERD.

Presumably due to the extensive processing time of sputum samples and low sample input (most SN was used for exosome isolation), we could only measure four lipid mediators in sputum of N-ERD and healthy individuals (Figure 4.14). Of those, PGE_2 strongly tended to be reduced in N-ERD, suggesting a less anti-inflammatory eicosanoid profile in the lung. In contrast, previous studies have shown cysLTs to be elevated in N-ERD sputum in comparison to NT asthmatics, while LTB_4 and PGE_2 levels were unaltered at baseline (Gaber et al., 2008; Mastalerz et al., 2014). Lipid mediator profile comparisons between N-ERD and healthy individuals are missing for sputum. However, one study demonstrated no differences for PGE_2 in exhaled breath condensates between N-ERD, NT asthmatics and healthy cohorts and further showed that CS treatment reduced cysLTs levels but did not alter LTB_4 and PGE_2 production (Antczak et al., 2002). While this suggests ICS to be not accountable for reduced PGE_2 concentrations in our N-ERD sputum samples, further studies with higher sample input (to detect more lipid mediators) and asthmatic (NT CRSwNP with/without asthma, asthmatics without NT CRSwNP), CS therapy (with/without ICS) and healthy controls are needed to accurately characterize their sputum lipid mediator profiles and identify N-ERD specific alterations at baseline.

With recent advances in technology, the suggested future studies could be performed, complemented and expanded in an international multi-cohort, multi-fluid study of several airway disease endotypes (with and without CS treatment) by utilizing the novel lipidomics platform Lipidizer, which quantifies over 1.000 lipid species from 13 different lipid classes in a single sample (Ubhi et al., 2016).

Obesity and airway inflammation, especially asthma, have been shown to be interlinked and adipokines, peptide hormones with lipid metabolism and immune regulatory

functions, have been implicated in the mechanistic link between these disorders (see 1.3.2). There was a slight, non-significant positive correlation between disease burden and BMI for N-ERD, but not NT CRSwNP individuals (Figure 4.16 A). This may be explained by a reduction in physical activity with increasing disease burden in N-ERD individuals, that all suffer from asthma in contrast to NT CRSwNP controls in our study cohort (Table 4.2). Reduced physical activity may then cause weight gain and elevated availability of FFAs in individuals with higher BMI can fuel pro-inflammatory effector functions through elevated FAO as demonstrated in asthma (Al-Khami et al., 2017). Thus, lipid metabolism alterations revealed by our RNAseq and genome-wide methylomics results (see 4.3), may contribute to increased disease severity. Interestingly, there was no correlation between disease burden and adipokines (adiponectin, leptin, Figure 4.16 E, G). Adiponectin, which was shown to be anti-inflammatory and bronchoprotective (Shore et al., 2006) and reduced in obesity and asthma (Ryo et al., 2004; Sood et al., 2008), was elevated in N-ERD plasma (Figure 4.16 C). However, beneficial effects might be reduced due to lower expression of adiponectin receptor LRP8 in sMac (Figure 4.9), which matches previous observations in experimental airway inflammation (Shore et al., 2006). In addition, adiponectin signaling influences multiple lipid metabolism pathways, including S1P production, providing a potential link to lipid mediators which are strong drivers of inflammation (Holland et al., 2011). Thus, it would be necessary to confirm systemic, but also local differences in adiponectin levels and adiponectin receptor expression in N-ERD and adequate controls and to characterize the effects of adiponectin on major effector cell types (PMN, mast cells, macrophages, epithelial cells) to elaborate its role in hallmark inflammatory responses of N-ERD.

5.4 Airway-derived exosomes elicit cell type-specific immune regulatory responses *in vitro*

Exosomes, nano-sized extracellular vesicles with specifically enriched content (e.g. proteins, mRNA, miRNA), have been shown to play a substantial role in intercellular communication and were demonstrated to be altered in and contribute to CRSwNP and asthma in recent studies (see 1.4.2).

After initial trials, we decided to focus on sputum-derived exosomes and to stimulate aMDM and hBECs with a physiological number of exosomes that are normalized by initial sputum cell count (see 4.5.2). As sputum yield differed greatly between study individuals, we decided to pool N-ERD and healthy sputum exosomes into single samples with the latter being appended by additional sputum SN to acquire a sufficient amount of exosomes to perform *in vitro* stimulations (see 4.5.2). Interestingly, NTA analysis revealed a heterogenous size distribution in purified sputum exosomes from healthy and N-ERD individuals (Figure 4.19 A). While the presence of microvesicles can be excluded due to several purification steps including SEC, exosomes might have agglomerated in pure water during NTA measurements (Coumans et al., 2017; Zabeo et al., 2016). TEM analyses of isolated sputum exosomes are yet to be performed to assess the purity, vesicle size and presence of agglomerates. Sputum exosome stimulations were carried out with aMDM and hBECs from young healthy donors to ensure optimal responses by minimizing e.g. epigenetic alterations and accumulated mutations acquired by aging, which might interfere with our analyses (see 3.2.1, 3.1.9). We used qPBS, 0.2 µm-filtered PBS that was eluted from qEV SEC columns, as negative and baseline control to preclude external contaminations introduced during the isolation process.

Sputum exosomes of healthy individuals contained higher levels of chemokines/cytokines (IL33, IL27, IL12p70, IL18, CXCL10, CXCL11) than those of N-ERD patients (Figure 4.19 C, Table 8.14). Indeed, aMDM stimulated with healthy sputum exosomes showed elevated levels of IL33, IL27 and IL12p70 in comparison to N-ERD exosomes, which might be explained by the differences in exosome content of those cytokines. However, sputum exosomes from healthy individuals strongly activated and induced pro-inflammatory (CXCLs, CCLs, TNF, IL1β, IL6, IL12p70, IL18, IL33) and anti-inflammatory (IL10, IL27) chemokines/cytokines in aMDM that indicated no clear tendency towards M1 or M2 polarization (Table 8.14). Healthy sputum exosomes also elicited COX metabolites (8-iso-$PGF_{2\alpha}$, $PGF_{2\alpha}$, PGD_2, PGE_2, TXB_2) in aMDM of healthy individuals (Figure 4.20). With the exception of higher concentrations of CXCL10, N-ERD sputum exosomes induced only minor changes of secreted mediator levels in aMDM in comparison to those isolated from healthy sputum (Figure 4.19 C, Figure 4.20, Table 8.14). While the significant effects of healthy sputum exosomes presumably mirror a homeostatic and/or host defense milieu in the lung, exosomes from N-ERD sputum were not capable to induce such a strong aMDM activation, which indicates a distinct exosome cargo profile. While we could not measure lipid mediators

in sputum exosomes directly due to sample limitations, our chemokine/cytokine analysis suggests a mediator-independent cargo (e.g. enzymes, mRNA, miRNA) to be responsible for the observed mediator inductions in aMDM. Indeed, BALF exosomes isolated from asthmatics have been shown to contain functional eicosanoid pathway enzymes which induced cysLT production upon uptake by hBECs (Torregrosa Paredes et al., 2012), while tumor-derived exosomes were demonstrated to contain miRNAs capable of contributing to M2 polarization and promoting FAO in BMDM (J. E. Park et al., 2019). Since the exosomal cargo is highly dependent on the cellular activity of their cells of origin, and thus the tissue microenvironment (Kulshreshtha et al., 2013; J. E. Park et al., 2019; Torregrosa Paredes et al., 2012), our results may suggest that the reduced capability of N-ERD sputum exosomes to elicit aMDM activation results from immunosuppressive effects of ICS therapy rather than from chronic lower airway inflammation (Figure 4.19 C, Figure 4.20).

In contrast, N-ERD exosomes elicited a more pronounced response in hBECs by (exosomal chemokine/cytokine content-independently) inducing GM-CSF, CXCL8 and CCL26 in comparison to sputum exosomes from healthy individuals, which only induced minor changes (Figure 4.19 B, Table 8.13). Interestingly, while healthy sputum exosomes more strongly elevated CXCL8 in aMDM in comparison to N-ERD sputum exosomes, CXCL8 levels were higher in the SN of hBECs stimulated with sputum exosomes from N-ERD individuals (Figure 4.19 B, Table 8.13, Table 8.14). This is in line with a previous study of hBECs stimulated with BALF exosomes from allergic asthmatics (Torregrosa Paredes et al., 2012). Thus, our data indicate cell type-specific responses to sputum exosomes albeit the molecular mechanisms remain obscure. One explanation could be different surface proteins on the exosomes that mediate cargo-independent cell activation and/or alter exosome uptake. Presumably due to low sample input, we were not able to confirm (differences in) the uptake of labeled exosomes (data not shown).

Further studies exploring the cargo of sputum-derived exosomes (e.g. proteomics, mRNA/miRNA sequencing) from N-ERD, NT asthmatic (with and without CRSwNP) and healthy controls and additional functional *in vitro* tests could provide insight into the pathogenesis of airway diseases. The acquisition of sputum from patients with and without ICS treatment could further help to specify mechanisms of CS treatment as well as to identify exosome cargo (e.g. enzymes, miRNAs) that might mediate CS resistance in non-responders. An expansion to the upper airways and the analysis of INCS-treated and naive NP-derived exosomes might result in the discovery of signaling pathways that are involved in CS-resistant NP pathogenesis.

5.5 Clinical implication of an aberrant lipid metabolism in N-ERD pathogenesis

N-ERD constitutes one of the most severe forms of chronic type 2 airway inflammation with limited therapy options and its definite pathomechanisms yet to be uncovered. In this study, we sought to explore the metabolomes of body fluids (NLF, sputum, plasma; see 4.4), elaborate the link between obesity and airway inflammation (see 4.4.4) as well as to unravel novel alterations in PMN, macrophages and NP (see 4.2, 4.3) and if those are mediated by exosomes (see 4.5) in N-ERD patients in comparison to NT CRSwNP and healthy controls. Though our results require confirmation by larger cohort studies, we observed several interesting differences: targeted metabolomics suggested plasma sphingolipids to be elevated in N-ERD and NT CRSwNP and acylcarnitines, key metabolites in FAO, to be specifically enhanced in all body fluids of N-ERD individuals (see 4.4). While we did not find any evidence of PGE_2 resistance and/or hypersensitivity towards IL4 in PMN and aMDM (see 4.2), secretome, transcriptome and methylome analyses implicated an imprinted, pro-inflammatory phenotype in N-ERD aMDM that is associated with elevated lipid mediator production and FAO metabolism alterations (see 4.2.2, 4.3.1-4.3.3). Indeed, RNAseq of sMac (*vs.* aMDM, both N-ERD) indicated a highly immune regulatory and pro-inflammatory profile with several modifications in lipid pathways (e.g. eicosanoid, sphingolipid, FAO; see 4.3.4) and the nasal scraping transcriptomes of N-ERD NP and healthy turbinate tissues further identified local lipid metabolism changes associated with macrophage functions, thus corroborating the findings in aMDM (see 4.3.5). We also demonstrated that sputum-derived exosomes are potent, cell-specific activators (aMDM, hBECs), but their definite functions in N-ERD pathogenesis remain obscure as functional analyses are limited by sample availability and presumably strong effects of ICS treatment on the exosome cargo (see 4.5.2).

Conclusively, our study implicates an aberrant lipid metabolism (e.g. eicosanoid, sphingolipid, FAO) in conjunction with a pro-inflammatory macrophage phenotype in the pathogenesis of N-ERD. These results append and link together several previous studies that have demonstrated ApoE (mimetics) (Yao et al., 2010), sphingosine pathway inhibitors (S1P receptor antagonist FTY420, SK inhibitors) (Oyeniran et al., 2015; Price et al., 2013; Sawicka et al., 2003) and FAO inhibitors (CPT1-inhibitor etomoxir, HADHA-inhibitor ranolazine) (Al-Khami et al., 2017) to alleviate (murine) airway type 2 inflammation *in vivo* by targeting pathways that are specifically implicated to be increased in N-ERD. (Pharmacological) modification of these metabolic pathways to reinstate lipid homeostasis and normal macrophage function might provide a viable therapeutic approach to balance mediator profiles and reduce airway inflammation in patients with N-ERD as well as related type 2 inflammatory conditions. In addition, lowering the BMI and withdrawing excess FFAs that fuel FAO, and thus inflammatory pathogenesis, may improve quality of life of N-ERD patients (Al-Khami et al., 2017). Thus, our study provides a basis for future studies into new pharmacological- and life style interventions for the management of chronic type 2 airway inflammation.

6 Scientific summary

6.1 English version

Chronic inflammatory airway diseases like chronic rhinosinusitis with nasal polyps (CRSwNP) and asthma affect over 300 million individuals globally and represent debilitating diseases with a high impact on healthcare systems and economies. Treatment options are limited and/or expensive, can elicit serious side effects (e.g. osteoporosis, Cushing's syndrome) and severe endotypes are often refractory, highlighting unmet needs for patients and societies. Non-steroidal anti-inflammatory drug (NSAID)-exacerbated respiratory disease (N-ERD) represents a particularly severe CRSwNP endotype, which is characterized by a strong type 2 inflammation of the upper and lower airways (CRSwNP and asthma) accompanied by an insensitivity towards NSAIDs due to a dysregulated arachidonic acid (AA) metabolism. As the pathogenesis of N-ERD remains incompletely understood, the aim of this study was to thoroughly characterize immune cells (granulocytes, macrophages) and (local) body fluids in comparison to NSAID-tolerant (NT) CRSwNP and/or healthy controls to confirm, validate and elaborate disease-specific alterations by a multi-omics approach.

By combining chemokine/cytokine multiplex, LC-MS/MS lipid mediator, RNA sequencing (RNAseq) and whole-genome methylomics analyses, we show that N-ERD macrophages displayed a persistent, (pre-)activated, pro-inflammatory phenotype that might be linked to alterations in fatty acid oxidation (FAO). Transcriptomics of sputum macrophages (sMac) and nasal brushings from N-ERD patients implicated immune regulatory functions of macrophages in local inflammatory tissue environments and also highlighted lipid metabolism alterations that were linked to FAO. Indeed, targeted multi-fluid metabolomics (plasma, sputum, nasal lining fluid (NLF)) revealed elevated concentrations of acylcarnitines, key metabolites in FAO and involved in inflammatory responses, in all analyzed body fluids of N-ERD patients. Plasma sphingolipid profiles of N-ERD and NT CRSwNP were increased in comparison to healthy controls but distinct from each other, confirming a potential involvement of further signaling lipids in N-ERD. However, we could not confirm a previously reported prostaglandin (PG)E_2 resistance in granulocytes from N-ERD patients and N-ERD macrophages did not exhibit altered responsiveness to PGE_2 or interleukin-4 stimulation.

Conclusively, our study reveals a broadly dysregulated lipid metabolism, an aberrant macrophage activation and altered immune regulatory functions of extracellular vesicles (EVs) as potential pathomechanisms of N-ERD. Thus, our work provides a basis for future mechanistic studies to investigate the roles of metabolic reprogramming and EVs in the severe and chronic type 2 inflammation of N-ERD. Restoring normal macrophage function and homeostatic lipid metabolism might provide a new therapeutic approach to balance mediator profiles and reduce airway inflammation in patients with N-ERD and related type 2 inflammatory conditions.

6.2 Deutsche Fassung

Mit weltweit über 300 Millionen betroffenen Patienten stellen chronisch-entzündliche Atemwegserkrankungen, wie zum Beispiel die chronische Rhinosinusitis mit *Polyposis nasi* (engl. *chronic rhinosinusitis with nasal polyps* (CRSwNP)) oder das *Asthma bronchiale*, eine hohe Belastung für die Patienten sowie Gesundheitssysteme und Wirtschaft dar. Effiziente Therapiemöglichkeiten sind limitiert oder teuer und können schwere Nebenwirkungen hervorrufen (z.B. Osteoporose, *Morbus Cushing*). Schwere Krankheitsverläufe gehen häufig mit Therapieresistenzen einher. Um die Behandlung zu verbessern sind neue Ansätze nötig. Die *Samter Trias* (engl. *non-steroidal anti-inflammatory drug* (NSAID)-*exacerbated asthma* (N-ERD)) stellt einen besonders schweren Endotyp der CRSwNP dar. Dieser ist durch eine robuste Entzündung des Typs 2 in den oberen und unteren Atemwegen (CRSwNP und *Asthma bronchiale*), sowie einer Hypersensibilität gegenüber nichtsteroidale Antirheumatika/Analgetika (NSAR, engl. NSAID) charakterisiert. Diese Hypersensibilität basiert auf einem fehlregulierten Stoffwechsel der Arachidonsäure (engl. *arachidonic acid*, AA).

Die detaillierte Pathogenese von N-ERD ist unvollständig aufgeklärt. Ziel dieser Studie war es Immunzellen (Granulozyten, Makrophagen) und Körperflüssigkeiten (Plasma, Sputum, Nasensekret (engl. *nasal lining fluid*, (NLF)) von N-ERD Patienten detailliert zu charakterisieren und mit denen von NSAID-toleranten (NT) CRSwNP und/oder gesunden Probanden zu vergleichen. Damit sollten neue Erkenntnisse zu krankheitsspezifischen Veränderungen anhand von Multi-Omics-Ansätzen gewonnen werden. Mittels einer Kombination von Chemokin/Zytokin-Multiplex-, LC-MS/MS-Lipidmediatoren-, RNA-Sequenzierungs (RNAseq)- und genomweiten Methylom-Analysen zeigen wir, dass *in vitro*-generierte Makrophagen von N-ERD Patienten einen stabilen, (vor-)aktivierten, entzündlichen Phänotyp aufweisen, welcher mit Veränderungen in der Fettsäureoxidation (engl. *fatty acid oxidation*, FAO) in Verbindung gebracht werden konnte. Die Transkriptomanalysen von Sputummakrophagen (sMac) und nasalen Kürettagen von N-ERD Patienten legen immunregulatorische Funktionen von Makrophagen in der lokalen Atemwegsentzündung nahe und identifizierten Veränderungen im Lipidstoffwechsel, welche ebenfalls mit einer fehlgeleiteten FAO verknüpft sind. Eine gezielte, multi-fluide Metabolomanalyse (Plasma, Sputum, NLF) zeigte erhöhte Konzentrationen von Acylcarnitinen in allen untersuchten Körperflüssigkeiten von N-ERD Patienten. Diese stellen Schlüsselmetabolite in der FAO dar und sind an Entzündungsreaktionen beteiligt. Plasmakonzentrationen von Sphingolipiden waren im Vergleich zu gesunden Kontrollen in N-ERD und NT CRSwNP Probanden erhöht. Sie unterschieden sich jedoch zwischen beiden Erkrankungen und bestätigten damit eine mögliche, spezifische Beteiligung dieser Signallipide an der N-ERD Pathogenese. Wir konnten allerdings weder eine bereits aufgezeigte Prostaglandin (PG)E_2-Resistenz in Granulozyten von N-ERD Patienten bestätigen, noch einen Hinweis auf eine veränderte Reaktivität von N-ERD Makrophagen auf eine PGE_2 oder Interleukin-4 Stimulation finden.

Zusammenfassend zeigt unsere Studie einen vielfältig veränderten Lipidstoffwechsel, eine fehlgeleitete Aktivierung von Makrophagen und ein immunregulatorisches Potential von extrazellulären Vesikeln (engl. *extracellular vesicles* (EVs)) als mögliche Pathomechanismen von N-ERD auf. Diese Arbeit bietet somit eine Grundlage für zukünftige, mechanistische Studien zur Untersuchung der Rollen von EVs und der metabolischen Reprogrammierung in der schweren, chronischen Typ 2 Entzündung bei N-ERD. Die damit gewonnenen Erkenntnisse können neue therapeutische Ansätze für Patienten mit N-ERD und anderen entzündlichen Erkrankungen des Typs 2 ermöglichen. Insbesondere könnte die Wiederherstellung einer normalen Makrophagen- und Lipidstoffwechselfunktion zu einer Reduktion der Entzündungsmediatoren und folglich der chronischen Atemwegsentzündung führen.

7 Bibliography

Abels, E. R., & Breakefield, X. O. (2016). Introduction to Extracellular Vesicles: Biogenesis, RNA Cargo Selection, Content, Release, and Uptake. *Cellular and Molecular Neurobiology*, *36*(3), 301–312. https://doi.org/10.1007/s10571-016-0366-z

Acedo, S. C., Gambero, S., Cunha, F. G. P., Lorand-Metze, I., & Gambero, A. (2013). Participation of leptin in the determination of the macrophage phenotype: An additional role in adipocyte and macrophage crosstalk. *In Vitro Cellular & Developmental Biology - Animal*, *49*(6), 473–478. https://doi.org/10.1007/s11626-013-9629-x

Adamjee, J., Suh, Y.-J., Park, H.-S., Choi, J.-H., Penrose, J., Lam, B., … Sampson, A. (2006). Expression of 5-lipoxygenase and cyclooxygenase pathway enzymes in nasal polyps of patients with aspirin-intolerant asthma. *The Journal of Pathology*, *209*(3), 392–399. https://doi.org/10.1002/path.1979

Adams, N. P., Bestall, J. C., Malouf, R., Lasserson, T. J., & Jones, P. (2005). Beclomethasone versus placebo for chronic asthma. *Cochrane Database of Systematic Reviews*. https://doi.org/10.1002/14651858.CD002738.pub2

Admyre, C., Grunewald, J., Thyberg, J., Gripenbäck, S., Tornling, G., Eklund, A., … Gabrielsson, S. (2003). Exosomes with major histocompatibility complex class II and co-stimulatory molecules are present in human BAL fluid. *European Respiratory Journal*, *22*(4), 578–583. https://doi.org/10.1183/09031936.03.00041703

Albuquerque, P. C., Nakayasu, E. S., Rodrigues, M. L., Frases, S., Casadevall, A., Zancope-Oliveira, R. M., … Nosanchuk, J. D. (2008). Vesicular transport in Histoplasma capsulatum: An effective mechanism for trans-cell wall transfer of proteins and lipids in ascomycetes. *Cellular Microbiology*, *10*(8), 1695–1710. https://doi.org/10.1111/j.1462-5822.2008.01160.x

Al-Khami, A. A., Ghonim, M. A., Del Valle, L., Ibba, S. V., Zheng, L., Pyakurel, K., … Ochoa, A. C. (2017). Fuelling the mechanisms of asthma: Increased fatty acid oxidation in inflammatory immune cells may represent a novel therapeutic target. *Clinical & Experimental Allergy*, *47*(9), 1170–1184. https://doi.org/10.1111/cea.12947

Allende, M. L., Dreier, J. L., Mandala, S., & Proia, R. L. (2004). Expression of the Sphingosine 1-Phosphate Receptor, S1P 1 , on T-cells Controls Thymic Emigration. *Journal of Biological Chemistry*, *279*(15), 15396–15401. https://doi.org/10.1074/jbc.M314291200

Alvarez-Llamas, G., Szalowska, E., de Vries, M. P., Weening, D., Landman, K., Hoek, A., … Vonk, R. J. (2007). Characterization of the Human Visceral Adipose Tissue Secretome. *Molecular & Cellular Proteomics*, *6*(4), 589–600. https://doi.org/10.1074/mcp.M600265-MCP200

Amarasekera, M. (2011). Immunoglobulin E in health and disease. *Asia Pacific Allergy*, *1*(1), 12. https://doi.org/10.5415/apallergy.2011.1.1.12

An, Q., Huckelhoven, R., Kogel, K.-H., & van Bel, A. J. E. (2006). Multivesicular bodies participate in a cell wall-associated defence response in barley leaves attacked by the pathogenic powdery mildew fungus. *Cellular Microbiology*, *8*(6), 1009–1019. https://doi.org/10.1111/j.1462-5822.2006.00683.x

Anders, S., Pyl, P. T., & Huber, W. (2015). HTSeq—A Python framework to work with high-throughput sequencing data. *Bioinformatics*, *31*(2), 166–169. https://doi.org/10.1093/bioinformatics/btu638

Anderson, M. E., Allison, R. D., & Meister, A. (1982). Interconversion of leukotrienes catalyzed by purified gamma-glutamyl transpeptidase: Concomitant formation of leukotriene D4 and gamma-glutamyl amino acids. *Proceedings of the National Academy of Sciences*, *79*(4), 1088–1091. https://doi.org/10.1073/pnas.79.4.1088

Antczak, A., Montuschi, P., Kharitonov, S., Gorski, P., & Barnes, P. J. (2002). Increased Exhaled Cysteinyl-Leukotrienes and 8-Isoprostane in Aspirin-induced Asthma. *American Journal of Respiratory and Critical Care Medicine*, *166*(3), 301–306. https://doi.org/10.1164/rccm.2101021

Aryee, M. J., Jaffe, A. E., Corrada-Bravo, H., Ladd-Acosta, C., Feinberg, A. P., Hansen, K. D., & Irizarry, R. A. (2014). Minfi: A flexible and comprehensive Bioconductor package for the analysis of Infinium DNA methylation microarrays. *Bioinformatics*, *30*(10), 1363–1369. https://doi.org/10.1093/bioinformatics/btu049

Asamoah, F., Kakourou, A., Dhami, S., Lau, S., Agache, I., Muraro, A., … Sheikh, A. (2017). Allergen immunotherapy for allergic asthma: A systematic overview of systematic reviews. *Clinical and Translational Allergy*, *7*(1). https://doi.org/10.1186/s13601-017-0160-0

Ashburner, M., Ball, C. A., Blake, J. A., Botstein, D., Butler, H., Cherry, J. M., … Sherlock, G. (2000). Gene Ontology: Tool for the unification of biology. *Nature Genetics*, *25*(1), 25–29. https://doi.org/10.1038/75556

Avila, P., & Schleimer, R. P. (2008). Airway epithelium. In *Kay, AB Kaplan, AP Bousquet, J., Holt, PG., editors: Allergy and Allergic Diseases. 2nd. Vol. 1* (pp. 366–397). Hoboken, NJ: Wiley-Blackwell.

Bachert, C., Mannent, L., Naclerio, R. M., Mullol, J., Ferguson, B. J., Gevaert, P., … Sutherland, E. R. (2016). Effect of Subcutaneous Dupilumab on Nasal Polyp Burden in Patients With Chronic Sinusitis and Nasal Polyposis: A Randomized Clinical Trial. *JAMA*, *315*(5), 469. https://doi.org/10.1001/jama.2015.19330

Bachert, C., Sousa, A. R., Lund, V. J., Scadding, G. K., Gevaert, P., Nasser, S., … Fokkens, W. J. (2017). Reduced need for surgery in severe nasal polyposis with mepolizumab: Randomized trial. *Journal of Allergy and Clinical Immunology*, *140*(4), 1024-1031.e14. https://doi.org/10.1016/j.jaci.2017.05.044

Bachert, C., Zhang, L., & Gevaert, P. (2015). Current and future treatment options for adult chronic rhinosinusitis: Focus on nasal polyposis. *Journal of Allergy and Clinical Immunology*, *136*(6), 1431–1440. https://doi.org/10.1016/j.jaci.2015.10.010

Baitsch, D., Bock, H. H., Engel, T., Telgmann, R., Müller-Tidow, C., Varga, G., … Nofer, J.-R. (2011). Apolipoprotein E Induces Antiinflammatory Phenotype in Macrophages. *Arteriosclerosis, Thrombosis, and Vascular Biology*, *31*(5), 1160–1168. https://doi.org/10.1161/ATVBAHA.111.222745

Banerjee, S., Xie, N., Cui, H., Tan, Z., Yang, S., Icyuz, M., … Liu, G. (2013). MicroRNA let-7c Regulates Macrophage Polarization. *The Journal of Immunology*, *190*(12), 6542–6549. https://doi.org/10.4049/jimmunol.1202496

Bankova, L. G., Dwyer, D. F., Yoshimoto, E., Ualiyeva, S., McGinty, J. W., Raff, H., … Barrett, N. A. (2018). The cysteinyl leukotriene 3 receptor regulates expansion of

IL-25–producing airway brush cells leading to type 2 inflammation. *Science Immunology*, *3*(28), eaat9453. https://doi.org/10.1126/sciimmunol.aat9453

Barnes, P. J. (2013). Corticosteroid resistance in patients with asthma and chronic obstructive pulmonary disease. *Journal of Allergy and Clinical Immunology*, *131*(3), 636–645. https://doi.org/10.1016/j.jaci.2012.12.1564

Bartlett, K., & Eaton, S. (2004). Mitochondrial beta-oxidation. *European Journal of Biochemistry*, *271*(3), 462–469. https://doi.org/10.1046/j.1432-1033.2003.03947.x

Bateman, E. D., Hurd, S. S., Barnes, P. J., Bousquet, J., Drazen, J. M., FitzGerald, M., … Zar, H. J. (2008). Global strategy for asthma management and prevention: GINA executive summary. *European Respiratory Journal*, *31*(1), 143–178. https://doi.org/10.1183/09031936.00138707

Bavbek, S., Yılmaz, I., Çelik, G., Aydın, ö., Erkekol, F. ö., Orman, A., … Mısırlıgil, Z. (2012). Prevalence of aspirin-exacerbated respiratory disease in patients with asthma in Turkey: A cross-sectional survey. *Allergologia et Immunopathologia*, *40*(4), 225–230. https://doi.org/10.1016/j.aller.2011.05.015

Bavbek, Sevim, Celik, G., Demirel, Y. S., & Misirligil, Z. (2003). Risk factors associated with hospitalizations for asthma attacks in Turkey. *Allergy and Asthma Proceedings*, *24*(6), 437–442.

Beasley, R. (1998). Worldwide variation in prevalence of symptoms of asthma, allergic rhinoconjunctivitis, and atopic eczema: ISAAC. *The Lancet*, *351*(9111), 1225–1232. https://doi.org/10.1016/S0140-6736(97)07302-9

Beeh, K. M., Beier, J., Kornmann, O., Meier, C., Taeumer, T., & Buhl, R. (2003). A single nasal allergen challenge increases induced sputum in¯ammatory markers in non-asthmatic subjects with seasonal allergic rhinitis: Correlation with plasma interleukin-5. *Clinical and Experimental Allergy*, 8.

Beller, T. C., Maekawa, A., Friend, D. S., Austen, K. F., & Kanaoka, Y. (2004). Targeted Gene Disruption Reveals the Role of the Cysteinyl Leukotriene 2 Receptor in Increased Vascular Permeability and in Bleomycin-induced Pulmonary Fibrosis in Mice. *Journal of Biological Chemistry*, *279*(44), 46129–46134. https://doi.org/10.1074/jbc.M407057200

Benechet, A. P., Menon, M., Xu, D., Samji, T., Maher, L., Murooka, T. T., … Khanna, K. M. (2016). T cell-intrinsic S1PR1 regulates endogenous effector T-cell egress dynamics from lymph nodes during infection. *Proceedings of the National Academy of Sciences*, *113*(8), 2182–2187. https://doi.org/10.1073/pnas.1516485113

Benjamini, Y., & Hochberg, Y. (1995). Controlling the false discovery rate: A practical and powerful approach to multiple testing. *Journal of the Royal Statistical Society Series B*, *57*(1), 289–300.

Benninger, M. S., Sindwani, R., Holy, C. E., & Hopkins, C. (2015). Early versus Delayed Endoscopic Sinus Surgery in Patients with Chronic Rhinosinusitis: Impact on Health Care Utilization. *Otolaryngology–Head and Neck Surgery*, *152*(3), 546–552. https://doi.org/10.1177/0194599814565606

Benninger, M. S., Sindwani, R., Holy, C. E., & Hopkins, C. (2016). Impact of medically recalcitrant chronic rhinosinusitis on incidence of asthma: Asthma in ongoing chronic rhinosinusitis. *International Forum of Allergy & Rhinology*, *6*(2), 124–129. https://doi.org/10.1002/alr.21652

Berges-Gimeno, M. P., Simon, R. A., & Stevenson, D. D. (2003). Long-term treatment with aspirin desensitization in asthmatic patients with aspirin-exacerbated respiratory disease. *Journal of Allergy and Clinical Immunology*, *111*(1), 180–186. https://doi.org/10.1067/mai.2003.7

Beuther, D. A., & Sutherland, E. R. (2007). Overweight, Obesity, and Incident Asthma: A Meta-analysis of Prospective Epidemiologic Studies. *American Journal of Respiratory and Critical Care Medicine*, *175*(7), 661–666. https://doi.org/10.1164/rccm.200611-1717OC

Bhattacharyya, N., Villeneuve, S., Joish, V. N., Amand, C., Mannent, L., Amin, N., … Khan, A. (2019). Cost burden and resource utilization in patients with chronic rhinosinusitis and nasal polyps. *The Laryngoscope*. https://doi.org/10.1002/lary.27852

Bhimrao, S. K., Wilson, S. J., & Howarth, P. H. (2011). Airway inflammation in atopic patients: A comparison of the upper and lower airways. *Otolaryngology--Head and Neck Surgery: Official Journal of American Academy of Otolaryngology-Head and Neck Surgery*, *145*(3), 396–400. https://doi.org/10.1177/0194599811410531

Bjermer, L., Lemiere, C., Maspero, J., Weiss, S., Zangrilli, J., & Germinaro, M. (2016). Reslizumab for Inadequately Controlled Asthma With Elevated Blood Eosinophil Levels. *Chest*, *150*(4), 789–798. https://doi.org/10.1016/j.chest.2016.03.032

Bleecker, E. R., FitzGerald, J. M., Chanez, P., Papi, A., Weinstein, S. F., Barker, P., … Goldman, M. (2016). Efficacy and safety of benralizumab for patients with severe asthma uncontrolled with high-dosage inhaled corticosteroids and long-acting β2-agonists (SIROCCO): A randomised, multicentre, placebo-controlled phase 3 trial. *The Lancet*, *388*(10056), 2115–2127. https://doi.org/10.1016/S0140-6736(16)31324-1

Blighe K. (2019). EnhancedVolcano: Publication-ready volcano plots with enhanced colouring and labeling (Version 3.8). Retrieved from https://github.com/kevinblighe/EnhancedVolcano

Bochenek, G., Kuschill-Dziurda, J., Szafraniec, K., Plutecka, H., Szczeklik, A., & Nizankowska-Mogilnicka, E. (2014). Certain subphenotypes of aspirin-exacerbated respiratory disease distinguished by latent class analysis. *Journal of Allergy and Clinical Immunology*, *133*(1), 98-103.e6. https://doi.org/10.1016/j.jaci.2013.07.004

Borgeat, P., & Samuelsson, B. (1979). Arachidonic acid metabolism in polymorphonuclear leukocytes: Effects of ionophore A23187. *Proceedings of the National Academy of Sciences*, *76*(5), 2148–2152. https://doi.org/10.1073/pnas.76.5.2148

Bouloumie, A., Marumo, T., Lafontan, M., & Busse, R. (1999). Leptin induces oxidative stress in human endothelial cells. *FASEB Journal: Official Publication of the Federation of American Societies for Experimental Biology*, *13*(10), 1231–1238.

Bousquet, J., Khaltaev, N., Cruz, A. A., Denburg, J., Fokkens, W. J., Togias, A., … Williams, D. (2008). Allergic Rhinitis and its Impact on Asthma (ARIA) 2008*: ARIA: 2008 Update. *Allergy*, *63*, 8–160. https://doi.org/10.1111/j.1398-9995.2007.01620.x

Bousquet, Jean, & World Health Organization (Eds.). (2007). *Global surveillance, prevention and control of chronic respiratory diseases: A comprehensive approach*. Geneva: WHO.

Brown, M. S., & Goldstein, J. L. (1986). A Receptor-Mediated Pathway for Cholesterol Homeostasis(Nobel Lecture). *Angewandte Chemie International Edition in English*, *25*(7), 583–602. https://doi.org/10.1002/anie.198605833

Bruno, A., Pace, E., Chanez, P., Gras, D., Vachier, I., Chiappara, G., … Gjomarkaj, M. (2009). Leptin and leptin receptor expression in asthma. *Journal of Allergy and Clinical Immunology*, *124*(2), 230-237.e4. https://doi.org/10.1016/j.jaci.2009.04.032

Buchheit, K. M., Cahill, K. N., Katz, H. R., Murphy, K. C., Feng, C., Lee-Sarwar, K., … Laidlaw, T. M. (2016). Thymic stromal lymphopoietin controls prostaglandin D2 generation in patients with aspirin-exacerbated respiratory disease. *Journal of Allergy and Clinical Immunology*, *137*(5), 1566-1576.e5. https://doi.org/10.1016/j.jaci.2015.10.020

Bureau, M. F., De Clerck, F., Lefort, J., Arreto, C. D., & Vargaftig, B. B. (1992). Thromboxane A2 accounts for bronchoconstriction but not for platelet sequestration and microvascular albumin exchanges induced by fMLP in the guinea pig lung. *The Journal of Pharmacology and Experimental Therapeutics*, *260*(2), 832–840.

Cahill, K. N., & Boyce, J. A. (2017). Aspirin-exacerbated respiratory disease: Mediators and mechanisms of a clinical disease. *Journal of Allergy and Clinical Immunology*, *139*(3), 764–766. https://doi.org/10.1016/j.jaci.2016.09.025

Cahill, K. N., Raby, B. A., Zhou, X., Guo, F., Thibault, D., Baccarelli, A., … Laidlaw, T. M. (2016). Impaired E Prostanoid 2 Expression and Resistance to Prostaglandin E2 in Nasal Polyp Fibroblasts from Subjects with Aspirin-Exacerbated Respiratory Disease. *American Journal of Respiratory Cell and Molecular Biology*, *54*(1), 34–40. https://doi.org/10.1165/rcmb.2014-0486OC

Caldefie-Chezet, F., Poulin, A., & Vasson, M. P. (2003). Leptin regulates functional capacities of polymorphonuclear neutrophils. *Free Radical Research*, *37*(8), 809–814.

Capasso, F., Tavares, I. A., Tsang, R., & Bennett, A. (1985). The role of calcium in eicosanoid production induced by ricinoleic acid or the calcium ionophore A23187. *Prostaglandins*, *30*(1), 119–124. https://doi.org/10.1016/S0090-6980(85)80015-0

Carbon, S., Ireland, A., Mungall, C. J., Shu, S., Marshall, B., Lewis, S., … the Web Presence Working Group. (2009). AmiGO: Online access to ontology and annotation data. *Bioinformatics*, *25*(2), 288–289. https://doi.org/10.1093/bioinformatics/btn615

Carreira, A. C., Ventura, A. E., Varela, A. R. P., & Silva, L. C. (2015). Tackling the biophysical properties of sphingolipids to decipher their biological roles. *Biological Chemistry*, *396*(6–7). https://doi.org/10.1515/hsz-2014-0283

Carroll, R. G., Zasłona, Z., Galván-Peña, S., Koppe, E. L., Sévin, D. C., Angiari, S., … O'Neill, L. A. (2018). An unexpected link between fatty acid synthase and cholesterol synthesis in proinflammatory macrophage activation. *Journal of Biological Chemistry*, *293*(15), 5509–5521. https://doi.org/10.1074/jbc.RA118.001921

Castrillo, A., Joseph, S. B., Vaidya, S. A., Haberland, M., Fogelman, A. M., Cheng, G., & Tontonoz, P. (2003). Crosstalk between LXR and Toll-like Receptor Signaling Mediates Bacterial and Viral Antagonism of Cholesterol Metabolism. *Molecular Cell*, *12*(4), 805–816. https://doi.org/10.1016/S1097-2765(03)00384-8

Chauhan, B. F., & Ducharme, F. M. (2012). Anti-leukotriene agents compared to inhaled corticosteroids in the management of recurrent and/or chronic asthma in adults and children. *Cochrane Database of Systematic Reviews*. https://doi.org/10.1002/14651858.CD002314.pub3

Chawes, B. L. K., Edwards, M. J., Shamji, B., Walker, C., Nicholson, G. C., Tan, A. J., … Hansel, T. T. (2010). A novel method for assessing unchallenged levels of mediators in nasal epithelial lining fluid. *Journal of Allergy and Clinical Immunology*, *125*(6), 1387-1389.e3. https://doi.org/10.1016/j.jaci.2010.01.039

Chen, F., Zuo, K., Guo, Y., Li, Z., Xu, G., Xu, R., & Shi, J. (2014). Long-term results of endoscopic sinus surgery–oriented treatment for chronic rhinosinusitis with asthma. *The Laryngoscope*, *124*(1), 24–28. https://doi.org/10.1002/lary.24196

Chen, H., & Boutros, P. C. (2011). VennDiagram: A package for the generation of highly-customizable Venn and Euler diagrams in R. *BMC Bioinformatics*, *12*(1), 35. https://doi.org/10.1186/1471-2105-12-35

Chen, J., Bardes, E. E., Aronow, B. J., & Jegga, A. G. (2009). ToppGene Suite for gene list enrichment analysis and candidate gene prioritization. *Nucleic Acids Research*, *37*(Web Server), W305–W311. https://doi.org/10.1093/nar/gkp427

Chen, Z., Li, S., Subramaniam, S., Shyy, J. Y.-J., & Chien, S. (2017). Epigenetic Regulation: A New Frontier for Biomedical Engineers. *Annual Review of Biomedical Engineering*, *19*(1), 195–219. https://doi.org/10.1146/annurev-bioeng-071516-044720

Cheong, H. S., Park, S.-M., Kim, M.-O., Park, J.-S., Lee, J. Y., Byun, J. Y., … Park, C.-S. (2011). Genome-wide methylation profile of nasal polyps: Relation to aspirin hypersensitivity in asthmatics: Genome-wide methylation profile of AIA. *Allergy*, *66*(5), 637–644. https://doi.org/10.1111/j.1398-9995.2010.02514.x

Chinetti, G., Zawadski, C., Fruchart, J. C., & Staels, B. (2004). Expression of adiponectin receptors in human macrophages and regulation by agonists of the nuclear receptors PPARα, PPARγ, and LXR. *Biochemical and Biophysical Research Communications*, *314*(1), 151–158. https://doi.org/10.1016/j.bbrc.2003.12.058

Chiurchiù, V., Leuti, A., Dalli, J., Jacobsson, A., Battistini, L., Maccarrone, M., & Serhan, C. N. (2016). Proresolving lipid mediators resolvin D1, resolvin D2, and maresin 1 are critical in modulating T cell responses. *Science Translational Medicine*, *8*(353), 353ra111-353ra111. https://doi.org/10.1126/scitranslmed.aaf7483

Chong, J., Soufan, O., Li, C., Caraus, I., Li, S., Bourque, G., … Xia, J. (2018). MetaboAnalyst 4.0: Towards more transparent and integrative metabolomics analysis. *Nucleic Acids Research*, *46*(W1), W486–W494. https://doi.org/10.1093/nar/gky310

Claria, J., & Serhan, C. N. (1995). Aspirin triggers previously undescribed bioactive eicosanoids by human endothelial cell-leukocyte interactions. *Proceedings of the National Academy of Sciences*, *92*(21), 9475–9479. https://doi.org/10.1073/pnas.92.21.9475

Claycombe, K., King, L. E., & Fraker, P. J. (2008). A role for leptin in sustaining lymphopoiesis and myelopoiesis. *Proceedings of the National Academy of Sciences*, *105*(6), 2017–2021. https://doi.org/10.1073/pnas.0712053105

Colombo, M., Raposo, G., & Théry, C. (2014). Biogenesis, Secretion, and Intercellular Interactions of Exosomes and Other Extracellular Vesicles. *Annual Review of Cell and Developmental Biology*, *30*(1), 255–289. https://doi.org/10.1146/annurev-cellbio-101512-122326

Combs, T. P., Wagner, J. A., Berger, J., Doebber, T., Wang, W.-J., Zhang, B. B., … Moller, D. E. (2002). Induction of Adipocyte Complement-Related Protein of 30 Kilodaltons by PPARγ Agonists: A Potential Mechanism of Insulin Sensitization. *Endocrinology*, *143*(3), 998–1007. https://doi.org/10.1210/endo.143.3.8662

Conrad, D. J., Kuhn, H., Mulkins, M., Highland, E., & Sigal, E. (1992). Specific inflammatory cytokines regulate the expression of human monocyte 15-lipoxygenase. *Proceedings of the National Academy of Sciences*, *89*(1), 217–221. https://doi.org/10.1073/pnas.89.1.217

Considine, R. V., Sinha, M. K., Heiman, M. L., Kriauciunas, A., Stephens, T. W., Nyce, M. R., … Caro, J. F. (1996). Serum Immunoreactive-Leptin Concentrations in Normal-Weight and Obese Humans. *New England Journal of Medicine*, *334*(5), 292–295. https://doi.org/10.1056/NEJM199602013340503

Corrigan, C. J., Napoli, R. L., Meng, Q., Fang, C., Wu, H., Tochiki, K., … Ying, S. (2012). Reduced expression of the prostaglandin E2 receptor E-prostanoid 2 on bronchial mucosal leukocytes in patients with aspirin-sensitive asthma. *Journal of Allergy and Clinical Immunology*, *129*(6), 1636–1646. https://doi.org/10.1016/j.jaci.2012.02.007

Coumans, F. A. W., Brisson, A. R., Buzas, E. I., Dignat-George, F., Drees, E. E. E., El-Andaloussi, S., … Nieuwland, R. (2017). Methodological Guidelines to Study Extracellular Vesicles. *Circulation Research*, *120*(10), 1632–1648. https://doi.org/10.1161/CIRCRESAHA.117.309417

Cowburn, A. S., Sladek, K., Soja, J., Adamek, L., Nizankowska, E., Szczeklik, A., … Sampson, A. P. (1998). Overexpression of leukotriene C4 synthase in bronchial biopsies from patients with aspirin-intolerant asthma. *Journal of Clinical Investigation*, *101*(4), 834–846. https://doi.org/10.1172/JCI620

Daffern, P. J., Muilenburg, D., Hugli, T. E., & Stevenson, D. D. (1999). Association of urinary leukotriene E4 excretion during aspirin challenges with severity of respiratory responses. *Journal of Allergy and Clinical Immunology*, *104*(3), 559–564. https://doi.org/10.1016/S0091-6749(99)70324-6

Dahlén, S. E., Hansson, G., Hedqvist, P., Bjorck, T., Granstrom, E., & Dahlen, B. (1983). Allergen challenge of lung tissue from asthmatics elicits bronchial contraction that correlates with the release of leukotrienes C4, D4, and E4. *Proceedings of the National Academy of Sciences*, *80*(6), 1712–1716. https://doi.org/10.1073/pnas.80.6.1712

Dahlén, S. E., Hedqvist, P., Hammarström, S., & Samuelsson, B. (1980). Leukotrienes are potent constrictors of human bronchi. *Nature*, *288*(5790), 484–486.

Dahlén, S.-E., MalmströM, K., Nizankowska, E., DahléN, B., Kuna, P., Kowalski, M., … Szczeklik, A. (2002). Improvement of Aspirin-Intolerant Asthma by Montelukast, a Leukotriene Antagonist: A Randomized, Double-Blind, Placebo-Controlled Trial. *American Journal of Respiratory and Critical Care Medicine*, *165*(1), 9–14. https://doi.org/10.1164/ajrccm.165.1.2010080

Dahlin, A., & Weiss, S. T. (2016). Genetic and Epigenetic Components of Aspirin-Exacerbated Respiratory Disease. *Immunology and Allergy Clinics of North America*, *36*(4), 765–789. https://doi.org/10.1016/j.iac.2016.06.010

De Rosa, V., Procaccini, C., Calì, G., Pirozzi, G., Fontana, S., Zappacosta, S., … Matarese, G. (2007). A Key Role of Leptin in the Control of Regulatory T Cell Proliferation. *Immunity*, *26*(2), 241–255. https://doi.org/10.1016/j.immuni.2007.01.011

Dhariwal, J., Cameron, A., Trujillo-Torralbo, M.-B., del Rosario, A., Bakhsoliani, E., Paulsen, M., … Walton, R. P. (2017). Mucosal Type 2 Innate Lymphoid Cells Are a Key Component of the Allergic Response to Aeroallergens. *American Journal of Respiratory and Critical Care Medicine*, *195*(12), 1586–1596. https://doi.org/10.1164/rccm.201609-1846OC

Dietz, K., de los Reyes Jiménez, M., Gollwitzer, E. S., Chaker, A. M., Zissler, U. M., Rådmark, O. P., … Esser-von Bieren, J. (2017). Age dictates a steroid-resistant cascade of Wnt5a, transglutaminase 2, and leukotrienes in inflamed airways. *Journal of Allergy and Clinical Immunology*, *139*(4), 1343-1354.e6. https://doi.org/10.1016/j.jaci.2016.07.014

Ding, D. J., Martin, J. G., & Macklem, P. T. (1987). Effects of lung volume on maximal methacholine-induced bronchoconstriction in normal humans. *Journal of Applied Physiology*, *62*(3), 1324–1330. https://doi.org/10.1152/jappl.1987.62.3.1324

Dixon, R. A. F., Diehl, R. E., Opas, E., Rands, E., Vickers, P. J., Evans, J. F., … Miller, D. K. (1990). Requirement of a 5-lipoxygenase-activating protein for leukotriene synthesis. *Nature*, *343*(6255), 282–284. https://doi.org/10.1038/343282a0

Dobin, A., Davis, C. A., Schlesinger, F., Drenkow, J., Zaleski, C., Jha, S., … Gingeras, T. R. (2013). STAR: Ultrafast universal RNA-seq aligner. *Bioinformatics*, *29*(1), 15–21. https://doi.org/10.1093/bioinformatics/bts635

Dominiczak, M. H., & Caslake, M. J. (2011). Apolipoproteins: Metabolic role and clinical biochemistry applications. *Annals of Clinical Biochemistry*, *48*(6), 498–515. https://doi.org/10.1258/acb.2011.011111

Dougherty, R. H., Sidhu, S. S., Raman, K., Solon, M., Solberg, O. D., Caughey, G. H., … Fahy, J. V. (2010). Accumulation of intraepithelial mast cells with a unique protease phenotype in TH2-high asthma. *Journal of Allergy and Clinical Immunology*, *125*(5), 1046-1053.e8. https://doi.org/10.1016/j.jaci.2010.03.003

Draijer, C., Boorsma, C. E., Reker-Smit, C., Post, E., Poelstra, K., & Melgert, B. N. (2016). PGE2-treated macrophages inhibit development of allergic lung inflammation in mice. *Journal of Leukocyte Biology*, *100*(1), 95–102. https://doi.org/10.1189/jlb.3MAB1115-505R

Du, P., Zhang, X., Huang, C.-C., Jafari, N., Kibbe, W. A., Hou, L., & Lin, S. M. (2010). Comparison of Beta-value and M-value methods for quantifying methylation levels by microarray analysis. *BMC Bioinformatics*, *11*(1), 587. https://doi.org/10.1186/1471-2105-11-587

Duewell, P., Kono, H., Rayner, K. J., Sirois, C. M., Vladimer, G., Bauernfeind, F. G., … Latz, E. (2010). NLRP3 inflammasomes are required for atherogenesis and activated by cholesterol crystals. *Nature*, *464*(7293), 1357–1361. https://doi.org/10.1038/nature08938

Dumlao, D. S., Buczynski, M. W., Norris, P. C., Harkewicz, R., & Dennis, E. A. (2011). High-throughput lipidomic analysis of fatty acid derived eicosanoids and N-acylethanolamines. *Biochimica et Biophysica Acta (BBA) - Molecular and Cell Biology of Lipids*, *1811*(11), 724–736. https://doi.org/10.1016/j.bbalip.2011.06.005

Durinck, S., Moreau, Y., Kasprzyk, A., Davis, S., De Moor, B., Brazma, A., & Huber, W. (2005). BioMart and Bioconductor: A powerful link between biological databases and microarray data analysis. *Bioinformatics*, *21*(16), 3439–3440. https://doi.org/10.1093/bioinformatics/bti525

Durinck, Steffen, Spellman, P. T., Birney, E., & Huber, W. (2009). Mapping identifiers for the integration of genomic datasets with the R/Bioconductor package biomaRt. *Nature Protocols*, *4*(8), 1184–1191. https://doi.org/10.1038/nprot.2009.97

Dworski, R., & Sheller, J. R. (1997). Differential sensitivities of human blood monocytes and alveolar macrophages to the inhibition of prostaglandin endoperoxide synthase-2 by interleukin-4. *Prostaglandins*, *53*(4), 237–251.

Early, S. B., Barekzi, E., Negri, J., Hise, K., Borish, L., & Steinke, J. W. (2007). Concordant Modulation of Cysteinyl Leukotriene Receptor Expression by IL-4 and IFN-γ on Peripheral Immune Cells. *American Journal of Respiratory Cell and Molecular Biology*, *36*(6), 715–720. https://doi.org/10.1165/rcmb.2006-0252OC

Ekström, M., Nwaru, B. I., Hasvold, P., Wiklund, F., Telg, G., & Janson, C. (2019). Oral corticosteroid use, morbidity and mortality in asthma: A nationwide prospective cohort study in Sweden. *Allergy*. https://doi.org/10.1111/all.13874

El Kebir, D., Gjorstrup, P., & Filep, J. G. (2012). Resolvin E1 promotes phagocytosis-induced neutrophil apoptosis and accelerates resolution of pulmonary inflammation. *Proceedings of the National Academy of Sciences*, *109*(37), 14983–14988. https://doi.org/10.1073/pnas.1206641109

El Kebir, D., Jozsef, L., Khreiss, T., Pan, W., Petasis, N. A., Serhan, C. N., & Filep, J. G. (2007). Aspirin-Triggered Lipoxins Override the Apoptosis-Delaying Action of Serum Amyloid A in Human Neutrophils: A Novel Mechanism for Resolution of Inflammation. *The Journal of Immunology*, *179*(1), 616–622. https://doi.org/10.4049/jimmunol.179.1.616

El Kebir, Driss, József, L., Pan, W., Wang, L., Petasis, N. A., Serhan, C. N., & Filep, J. G. (2009). 15-Epi-lipoxin A 4 Inhibits Myeloperoxidase Signaling and Enhances Resolution of Acute Lung Injury. *American Journal of Respiratory and Critical Care Medicine*, *180*(4), 311–319. https://doi.org/10.1164/rccm.200810-1601OC

Eliopoulos, A. G. (2002). Induction of COX-2 by LPS in macrophages is regulated by Tpl2-dependent CREB activation signals. *The EMBO Journal*, *21*(18), 4831–4840. https://doi.org/10.1093/emboj/cdf478

Ellen, A. F., Albers, S.-V., Huibers, W., Pitcher, A., Hobel, C. F. V., Schwarz, H., … Driessen, A. J. M. (2009). Proteomic analysis of secreted membrane vesicles of archaeal Sulfolobus species reveals the presence of endosome sorting complex components. *Extremophiles*, *13*(1), 67–79. https://doi.org/10.1007/s00792-008-0199-x

Enooku, K., Nakagawa, H., Fujiwara, N., Kondo, M., Minami, T., Hoshida, Y., … Koike, K. (2019). Altered serum acylcarnitine profile is associated with the status of nonalcoholic fatty liver disease (NAFLD) and NAFLD-related hepatocellular carcinoma. *Scientific Reports*, *9*(1). https://doi.org/10.1038/s41598-019-47216-2

Esser, J., Gehrmann, U., D'Alexandri, F. L., Hidalgo-Estévez, A. M., Wheelock, C. E., Scheynius, A., … Rådmark, O. (2010). Exosomes from human macrophages and dendritic cells contain enzymes for leukotriene biosynthesis and promote granulocyte migration. *Journal of Allergy and Clinical Immunology*, *126*(5), 1032-1040.e4. https://doi.org/10.1016/j.jaci.2010.06.039

European Medicines Agency (EMA), C. for M. P. for H. U. (Ed.). (2011). *Guideline on bioanalytical method validation*. . EMEA/CHMP/EWP/192217/2009 Rev. 1 Corr. 2, 21 July 2011.

Fahy, J. V. (2015). Type 2 inflammation in asthma—Present in most, absent in many. *Nature Reviews Immunology*, *15*(1), 57–65. https://doi.org/10.1038/nri3786

Feltis, B. N., Wignarajah, D., Reid, D. W., Ward, C., Harding, R., & Walters, E. H. (2007). Effects of inhaled fluticasone on angiogenesis and vascular endothelial growth factor in asthma. *Thorax*, *62*(4), 314–319. https://doi.org/10.1136/thx.2006.069229

Ferreri, N. R., Howland, W. C., Stevenson, D. D., & Spiegelberg, H. L. (1988). Release of Leukotrienes, Prostaglandins, and Histamine into Nasal Secretions of Aspirin-sensitive Asthmatics during Reaction to Aspirin. *American Review of Respiratory Disease*, *137*(4), 847–854. https://doi.org/10.1164/ajrccm/137.4.847

Finney-Hayward, T. K., Bahra, P., Li, S., Poll, C. T., Nicholson, A. G., Russell, R. E. K., … Donnelly, L. E. (2009). Leukotriene B4 release by human lung macrophages via receptor- not voltage-operated Ca2+ channels. *European Respiratory Journal*, *33*(5), 1105–1112. https://doi.org/10.1183/09031936.00062708

Fischer, C., Milting, H., Fein, E., Reiser, E., Lu, K., Seidel, T., … Dendorfer, A. (2019). Long-term functional and structural preservation of precision-cut human myocardium under continuous electromechanical stimulation in vitro. *Nature Communications*, *10*(1). https://doi.org/10.1038/s41467-018-08003-1

Flamand, N. (2002). Cyclic AMP-Mediated Inhibition of 5-Lipoxygenase Translocation and Leukotriene Biosynthesis in Human Neutrophils. *Molecular Pharmacology*, *62*(2), 250–256. https://doi.org/10.1124/mol.62.2.250

Fokkens, W. J., Lund, V. J., Mullol, J., Bachert, C., Alobid, I., Baroody, F., … Wormald, P. J. (2012). EPOS 2012: European position paper on rhinosinusitis and nasal polyps 2012. A summary for otorhinolaryngologists. *Rhinology Journal*, *50*(1), 1–12. https://doi.org/10.4193/Rhino50E2

Frankenberger, M., Eder, C., Hofer, T. P. J., Heimbeck, I., Skokann, K., Kaßner, G., … Ziegler-Heitbrock, L. (2011). Chemokine Expression by Small Sputum Macrophages in COPD. *Molecular Medicine*, *17*(7–8), 762–770. https://doi.org/10.2119/molmed.2010.00202

Freire-de-Lima, C. G., Xiao, Y. Q., Gardai, S. J., Bratton, D. L., Schiemann, W. P., & Henson, P. M. (2006). Apoptotic Cells, through Transforming Growth Factor-β, Coordinately Induce Anti-inflammatory and Suppress Pro-inflammatory Eicosanoid and NO Synthesis in Murine Macrophages. *Journal of Biological Chemistry*, *281*(50), 38376–38384. https://doi.org/10.1074/jbc.M605146200

Gaber, F., Daham, K., Higashi, A., Higashi, N., Gulich, A., Delin, I., … Dahlen, B. (2008). Increased levels of cysteinyl-leukotrienes in saliva, induced sputum, urine and blood from patients with aspirin-intolerant asthma. *Thorax*, *63*(12), 1076–1082. https://doi.org/10.1136/thx.2008.101196

Gardner, J. C., Wu, H., Noel, J. G., Ramser, B. J., Pitstick, L., Saito, A., … McCormack, F. X. (2016). Keratinocyte growth factor supports pulmonary innate immune defense through maintenance of alveolar antimicrobial protein levels and macrophage function. *American Journal of Physiology. Lung Cellular and Molecular Physiology*, *310*(9), L868-879. https://doi.org/10.1152/ajplung.00363.2015

Gauvreau, G. M., Watson, R. M., & O'Byrne, P. M. (1999). Protective Effects of Inhaled PGE2 on Allergen-induced Airway Responses and Airway Inflammation. *American Journal of Respiratory and Critical Care Medicine*, *159*(1), 31–36. https://doi.org/10.1164/ajrccm.159.1.9804030

Gevaert, P., Calus, L., Van Zele, T., Blomme, K., De Ruyck, N., Bauters, W., … Bachert, C. (2013). Omalizumab is effective in allergic and nonallergic patients with nasal

polyps and asthma. *Journal of Allergy and Clinical Immunology*, *131*(1), 110-116.e1. https://doi.org/10.1016/j.jaci.2012.07.047

Gevaert, P., Van Bruaene, N., Cattaert, T., Van Steen, K., Van Zele, T., Acke, F., … Bachert, C. (2011). Mepolizumab, a humanized anti–IL-5 mAb, as a treatment option for severe nasal polyposis. *Journal of Allergy and Clinical Immunology*, *128*(5), 989-995.e8. https://doi.org/10.1016/j.jaci.2011.07.056

Godson, C., Mitchell, S., Harvey, K., Petasis, N. A., Hogg, N., & Brady, H. R. (2000). Cutting Edge: Lipoxins Rapidly Stimulate Nonphlogistic Phagocytosis of Apoptotic Neutrophils by Monocyte-Derived Macrophages. *The Journal of Immunology*, *164*(4), 1663–1667. https://doi.org/10.4049/jimmunol.164.4.1663

Gómez-Muñoz, A., Kong, J. Y., Parhar, K., Wang, S. W., Gangoiti, P., González, M., … Steinbrecher, U. P. (2005). Ceramide-1-phosphate promotes cell survival through activation of the phosphatidylinositol 3-kinase/protein kinase B pathway. *FEBS Letters*, *579*(17), 3744–3750. https://doi.org/10.1016/j.febslet.2005.05.067

Grotta, M. B., Squebola-Cola, D. M., Toro, A. A., Ribeiro, M. A. G., Mazon, S. B., Ribeiro, J. D., & Antunes, E. (2013). Obesity increases eosinophil activity in asthmatic children and adolescents. *BMC Pulmonary Medicine*, *13*(1). https://doi.org/10.1186/1471-2466-13-39

Gruen, M. L., Hao, M., Piston, D. W., & Hasty, A. H. (2007). Leptin requires canonical migratory signaling pathways for induction of monocyte and macrophage chemotaxis. *American Journal of Physiology-Cell Physiology*, *293*(5), C1481–C1488. https://doi.org/10.1152/ajpcell.00062.2007

Gupta, P., Vijayan, V. K., & Bansal, S. K. (2010). Sphingomyelin metabolism in erythrocyte membrane in asthma. *Journal of Asthma*, *47*(9), 966–971. https://doi.org/10.1080/02770903.2010.517590

Haack, T. B., Kopajtich, R., Freisinger, P., Wieland, T., Rorbach, J., Nicholls, T. J., … Prokisch, H. (2013). ELAC2 Mutations Cause a Mitochondrial RNA Processing Defect Associated with Hypertrophic Cardiomyopathy. *The American Journal of Human Genetics*, *93*(2), 211–223. https://doi.org/10.1016/j.ajhg.2013.06.006

Hackett, T.-L. (2012). Epithelial–mesenchymal transition in the pathophysiology of airway remodelling in asthma: *Current Opinion in Allergy and Clinical Immunology*, *12*(1), 53–59. https://doi.org/10.1097/ACI.0b013e32834ec6eb

Hait, N. C., Allegood, J., Maceyka, M., Strub, G. M., Harikumar, K. B., Singh, S. K., … Spiegel, S. (2009). Regulation of Histone Acetylation in the Nucleus by Sphingosine-1-Phosphate. *Science*, *325*(5945), 1254–1257. https://doi.org/10.1126/science.1176709

Haj-Salem, I., Plante, S., Gounni, A. S., Rouabhia, M., & Chakir, J. (2018). Fibroblast-derived exosomes promote epithelial cell proliferation through TGF-β2 signalling pathway in severe asthma. *Allergy*, *73*(1), 178–186. https://doi.org/10.1111/all.13234

Halberg, N., Wernstedt-Asterholm, I., & Scherer, P. E. (2008). The Adipocyte as an Endocrine Cell. *Endocrinology and Metabolism Clinics of North America*, *37*(3), 753–768. https://doi.org/10.1016/j.ecl.2008.07.002

Hanania, N. A., Alpan, O., Hamilos, D. L., Condemi, J. J., Reyes-Rivera, I., Zhu, J., … Busse, W. (2011). Omalizumab in Severe Allergic Asthma Inadequately Controlled With Standard Therapy: A Randomized Trial. *Annals of Internal Medicine*, *154*(9), 573. https://doi.org/10.7326/0003-4819-154-9-201105030-00002

Hannun, Y. A., & Obeid, L. M. (2018). Sphingolipids and their metabolism in physiology and disease. *Nature Reviews Molecular Cell Biology*, *19*(3), 175–191. https://doi.org/10.1038/nrm.2017.107

Hart, P. H., Vitti, G. F., Burgess, D. R., Whitty, G. A., Piccoli, D. S., & Hamilton, J. A. (1989). Potential antiinflammatory effects of interleukin 4: Suppression of human monocyte tumor necrosis factor alpha, interleukin 1, and prostaglandin E2. *Proceedings of the National Academy of Sciences*, *86*(10), 3803–3807. https://doi.org/10.1073/pnas.86.10.3803

Hastan, D., Fokkens, W. J., Bachert, C., Newson, R. B., Bislimovska, J., Bockelbrink, A., … Burney, P. (2011). Chronic rhinosinusitis in Europe - an underestimated disease. A GA2LEN study: Chronic rhinosinusitis in Europe. *Allergy*, *66*(9), 1216–1223. https://doi.org/10.1111/j.1398-9995.2011.02646.x

Heise, C. E., O'Dowd, B. F., Figueroa, D. J., Sawyer, N., Nguyen, T., Im, D.-S., … Evans, J. F. (2000). Characterization of the Human Cysteinyl Leukotriene 2 Receptor. *Journal of Biological Chemistry*, *275*(39), 30531–30536. https://doi.org/10.1074/jbc.M003490200

Henderson, W. R., Chiang, G. K. S., Tien, Y., & Chi, E. Y. (2006). Reversal of Allergen-induced Airway Remodeling by CysLT 1 Receptor Blockade. *American Journal of Respiratory and Critical Care Medicine*, *173*(7), 718–728. https://doi.org/10.1164/rccm.200501-088OC

Henderson, W. R., Tang, L.-O., Chu, S.-J., Tsao, S.-M., Chiang, G. K. S., Jones, F., … Chi, E. Y. (2002). A Role for Cysteinyl Leukotrienes in Airway Remodeling in a Mouse Asthma Model. *American Journal of Respiratory and Critical Care Medicine*, *165*(1), 108–116. https://doi.org/10.1164/ajrccm.165.1.2105051

Henkel, F. D. R., Friedl, A., Haid, M., Thomas, D., Bouchery, T., Haimerl, P., … Esser-von Bieren, J. (2018). House dust mite drives pro-inflammatory eicosanoid reprogramming and macrophage effector functions. *Allergy*. https://doi.org/10.1111/all.13700

Herishanu, Y., Rogowski, O., Polliack, A., & Marilus, R. (2006). Leukocytosis in obese individuals: Possible link in patients with unexplained persistent neutrophilia. *European Journal of Haematology*, *76*(6), 516–520. https://doi.org/10.1111/j.1600-0609.2006.00658.x

Hirai, H., Tanaka, K., Yoshie, O., Ogawa, K., Kenmotsu, K., Takamori, Y., … Nagata, K. (2001). Prostaglandin D2 Selectively Induces Chemotaxis in T Helper Type 2 Cells, Eosinophils, and Basophils via Seven-Transmembrane Receptor Crth2. *The Journal of Experimental Medicine*, *193*(2), 255–262. https://doi.org/10.1084/jem.193.2.255

Hirsch, A. G., Stewart, W. F., Sundaresan, A. S., Young, A. J., Kennedy, T. L., Scott Greene, J., … Schwartz, B. S. (2017). Nasal and sinus symptoms and chronic rhinosinusitis in a population-based sample. *Allergy*, *72*(2), 274–281. https://doi.org/10.1111/all.13042

Hoek, R. M., Ruuls, S. R., Murphy, C. A., Wright, G. J., Goddard, R., Zurawski, S. M., … Sedgwick, J. D. (2000). Down-regulation of the macrophage lineage through interaction with OX2 (CD200). *Science (New York, N.Y.)*, *290*(5497), 1768–1771. https://doi.org/10.1126/science.290.5497.1768

Hoffman, M., Pizzo, S. V., & Weinberg, J. B. (1988). Alpha 2 macroglobulin-proteinase complexes stimulate prostaglandin E2 synthesis by peritoneal macrophages. *Agents and Actions*, *25*(3–4), 360–367.

Holguin, F., Bleecker, E. R., Busse, W. W., Calhoun, W. J., Castro, M., Erzurum, S. C., … Wenzel, S. E. (2011). Obesity and asthma: An association modified by age of asthma onset. *Journal of Allergy and Clinical Immunology*, *127*(6), 1486-1493.e2. https://doi.org/10.1016/j.jaci.2011.03.036

Holguin, F., Rojas, M., Brown, L. anne, & Fitzpatrick, A. M. (2011). Airway and Plasma Leptin and Adiponectin in Lean and Obese Asthmatics and Controls. *Journal of Asthma*, *48*(3), 217–223. https://doi.org/10.3109/02770903.2011.555033

Holland, W. L., Miller, R. A., Wang, Z. V., Sun, K., Barth, B. M., Bui, H. H., … Scherer, P. E. (2011). Receptor-mediated activation of ceramidase activity initiates the pleiotropic actions of adiponectin. *Nature Medicine*, *17*(1), 55–63. https://doi.org/10.1038/nm.2277

Hong, S., Gronert, K., Devchand, P. R., Moussignac, R.-L., & Serhan, C. N. (2003). Novel Docosatrienes and 17S-Resolvins Generated from Docosahexaenoic Acid in Murine Brain, Human Blood, and Glial Cells: Autacoids in anti-inflammation. *Journal of Biological Chemistry*, *278*(17), 14677–14687. https://doi.org/10.1074/jbc.M300218200

Hope, A. P., Woessner, K. A., Simon, R. A., & Stevenson, D. D. (2009). Rational approach to aspirin dosing during oral challenges and desensitization of patients with aspirin-exacerbated respiratory disease. *Journal of Allergy and Clinical Immunology*, *123*(2), 406–410. https://doi.org/10.1016/j.jaci.2008.09.048

Hosogai, N., Fukuhara, A., Oshima, K., Miyata, Y., Tanaka, S., Segawa, K., … Shimomura, I. (2007). Adipose Tissue Hypoxia in Obesity and Its Impact on Adipocytokine Dysregulation. *Diabetes*, *56*(4), 901–911. https://doi.org/10.2337/db06-0911

Hosono, K., Isonaka, R., Kawakami, T., Narumiya, S., & Majima, M. (2016). Signaling of Prostaglandin E Receptors, EP3 and EP4 Facilitates Wound Healing and Lymphangiogenesis with Enhanced Recruitment of M2 Macrophages in Mice. *PLOS ONE*, *11*(10), e0162532. https://doi.org/10.1371/journal.pone.0162532

Hossain, F., Al-Khami, A. A., Wyczechowska, D., Hernandez, C., Zheng, L., Reiss, K., … Ochoa, A. C. (2015). Inhibition of Fatty Acid Oxidation Modulates Immunosuppressive Functions of Myeloid-Derived Suppressor Cells and Enhances Cancer Therapies. *Cancer Immunology Research*, *3*(11), 1236–1247. https://doi.org/10.1158/2326-6066.CIR-15-0036

Hough, K. P., Wilson, L. S., Trevor, J. L., Strenkowski, J. G., Maina, N., Kim, Y.-I., … Deshane, J. S. (2018). Unique Lipid Signatures of Extracellular Vesicles from the Airways of Asthmatics. *Scientific Reports*, *8*(1). https://doi.org/10.1038/s41598-018-28655-9

Hovi, T., Mosher, D., & Vaheri, A. (1977). Cultured human monocytes synthesize and secrete alpha2-macroglobulin. *The Journal of Experimental Medicine*, *145*(6), 1580–1589. https://doi.org/10.1084/jem.145.6.1580

Hsiao, Y.-W., Li, C.-F., Chi, J.-Y., Tseng, J. T., Chang, Y., Hsu, L.-J., … Wang, J.-M. (2013). CCAAT/Enhancer Binding Protein in Macrophages Contributes to Immunosuppression and Inhibits Phagocytosis in Nasopharyngeal Carcinoma. *Science Signaling*, *6*(284), ra59–ra59. https://doi.org/10.1126/scisignal.2003648

Hua, Y., Liang, C., Zhu, J., Miao, C., Yu, Y., Xu, A., … Wang, Z. (2017). Expression of lactate dehydrogenase C correlates with poor prognosis in renal cell carcinoma. *Tumor Biology*, *39*(3), 101042831769596. https://doi.org/10.1177/1010428317695968

Huang, J. T., Welch, J. S., Ricote, M., Binder, C. J., Willson, T. M., Kelly, C., … Glass, C. K. (1999). Interleukin-4-dependent production of PPAR-gamma ligands in macrophages by 12/15-lipoxygenase. *Nature*, *400*(6742), 378–382. https://doi.org/10.1038/22572

Huang, S. C.-C., Everts, B., Ivanova, Y., O'Sullivan, D., Nascimento, M., Smith, A. M., … Pearce, E. J. (2014). Cell-intrinsic lysosomal lipolysis is essential for alternative activation of macrophages. *Nature Immunology*, *15*(9), 846–855. https://doi.org/10.1038/ni.2956

Huang, S. K., Wettlaufer, S. H., Hogaboam, C. M., Flaherty, K. R., Martinez, F. J., Myers, J. L., … Peters-Golden, M. (2008). Variable Prostaglandin E2 Resistance in Fibroblasts from Patients with Usual Interstitial Pneumonia. *American Journal of Respiratory and Critical Care Medicine*, *177*(1), 66–74. https://doi.org/10.1164/rccm.200706-963OC

Hulse, K. E., Norton, J. E., Suh, L., Zhong, Q., Mahdavinia, M., Simon, P., … Schleimer, R. P. (2013). Chronic rhinosinusitis with nasal polyps is characterized by B-cell inflammation and EBV-induced protein 2 expression. *Journal of Allergy and Clinical Immunology*, *131*(4), 1075-1083.e7. https://doi.org/10.1016/j.jaci.2013.01.043

Hunter, J. A., Finkbeiner, W. E., Nadel, J. A., Goetzl, E. J., & Holtzman, M. J. (1985). Predominant generation of 15-lipoxygenase metabolites of arachidonic acid by epithelial cells from human trachea. *Proceedings of the National Academy of Sciences*, *82*(14), 4633–4637. https://doi.org/10.1073/pnas.82.14.4633

Idle, J. R., & Gonzalez, F. J. (2007). Metabolomics. *Cell Metabolism*, *6*(5), 348–351. https://doi.org/10.1016/j.cmet.2007.10.005

Ishizuka, Kawakami, Hidaka, Matsuki, Takamizawa, Suzuki, … Nakamura. (1998). Stimulation with thromboxane A2 (TXA2) receptor agonist enhances ICAM-1, VCAM-1 or ELAM-1 expression by human vascular endothelial cells. *Clinical and Experimental Immunology*, *112*(3), 464–470. https://doi.org/10.1046/j.1365-2249.1998.00614.x

Isobe, Y., Arita, M., Matsueda, S., Iwamoto, R., Fujihara, T., Nakanishi, H., … Arai, H. (2012). Identification and Structure Determination of Novel Anti-inflammatory Mediator Resolvin E3, 17,18-Dihydroxyeicosapentaenoic Acid. *Journal of Biological Chemistry*, *287*(13), 10525–10534. https://doi.org/10.1074/jbc.M112.340612

Israel, E., & Reddel, H. K. (2017). Severe and Difficult-to-Treat Asthma in Adults. *New England Journal of Medicine*, *377*(10), 965–976. https://doi.org/10.1056/NEJMra1608969

Ivanova, J. I., Bergman, R., Birnbaum, H. G., Colice, G. L., Silverman, R. A., & McLaurin, K. (2012). Effect of asthma exacerbations on health care costs among asthmatic patients with moderate and severe persistent asthma. *Journal of Allergy and Clinical Immunology*, *129*(5), 1229–1235. https://doi.org/10.1016/j.jaci.2012.01.039

Jakschik, B. A., Harper, T., & Murphy, R. C. (1982). Leukotriene C4 and D4 formation by particulate enzymes. *The Journal of Biological Chemistry*, *257*(10), 5346–5349.

Jarvis, D., Newson, R., Lotvall, J., Hastan, D., Tomassen, P., Keil, T., … Burney, P. (2012). Asthma in adults and its association with chronic rhinosinusitis: The

GA2LEN survey in Europe: Asthma and chronic rhinosinusitis. *Allergy*, *67*(1), 91–98. https://doi.org/10.1111/j.1398-9995.2011.02709.x

Jenkins, C., Costello, J., & Hodge, L. (2004). Systematic review of prevalence of aspirin induced asthma and its implications for clinical practice. *BMJ*, *328*(7437), 434. https://doi.org/10.1136/bmj.328.7437.434

Jenkins, R. W., Clarke, C. J., Canals, D., Snider, A. J., Gault, C. R., Heffernan-Stroud, L., … Hannun, Y. A. (2011). Regulation of CC Ligand 5/RANTES by Acid Sphingomyelinase and Acid Ceramidase. *Journal of Biological Chemistry*, *286*(15), 13292–13303. https://doi.org/10.1074/jbc.M110.163378

Jha, A. K., Huang, S. C.-C., Sergushichev, A., Lampropoulou, V., Ivanova, Y., Loginicheva, E., … Artyomov, M. N. (2015). Network Integration of Parallel Metabolic and Transcriptional Data Reveals Metabolic Modules that Regulate Macrophage Polarization. *Immunity*, *42*(3), 419–430. https://doi.org/10.1016/j.immuni.2015.02.005

Jinnai, N., Sakagami, T., Sekigawa, T., Kakihara, M., Nakajima, T., Yoshida, K., … Inoue, I. (2004). Polymorphisms in the prostaglandin E2 receptor subtype 2 gene confer susceptibility to aspirin-intolerant asthma: A candidate gene approach. *Human Molecular Genetics*, *13*(24), 3203–3217. https://doi.org/10.1093/hmg/ddh332

Johnston, S. L., Freezer, N. J., Ritter, W., O'Toole, S., & Howarth, P. H. (1995). Prostaglandin D2-induced bronchoconstriction is mediated only in part by the thromboxane prostanoid receptor. *European Respiratory Journal*, *8*(3), 411–415. https://doi.org/10.1183/09031936.95.08030411

Jostarndt, K., Gellert, N., Rubic, T., Weber, C., Kühn, H., Johansen, B., … Neuzil, J. (2002). Dissociation of Apoptosis Induction and CD36 Upregulation by Enzymatically Modified Low-Density Lipoprotein in Monocytic Cells. *Biochemical and Biophysical Research Communications*, *290*(3), 988–993. https://doi.org/10.1006/bbrc.2001.6290

Jozsef, L., Zouki, C., Petasis, N. A., Serhan, C. N., & Filep, J. G. (2002). Lipoxin A4 and aspirin-triggered 15-epi-lipoxin A4 inhibit peroxynitrite formation, NF- B and AP-1 activation, and IL-8 gene expression in human leukocytes. *Proceedings of the National Academy of Sciences*, *99*(20), 13266–13271. https://doi.org/10.1073/pnas.202296999

Kanaoka, Y., Maekawa, A., & Austen, K. F. (2013). Identification of GPR99 Protein as a Potential Third Cysteinyl Leukotriene Receptor with a Preference for Leukotriene E4 Ligand. *Journal of Biological Chemistry*, *288*(16), 10967–10972. https://doi.org/10.1074/jbc.C113.453704

Kelly, M. M., Chakir, J., Vethanayagam, D., Boulet, L.-P., Laviolette, M., Gauldie, J., & O'Byrne, P. M. (2006). Montelukast Treatment Attenuates the Increase in Myofibroblasts Following Low-Dose Allergen Challenge. *Chest*, *130*(3), 741–753. https://doi.org/10.1378/chest.130.3.741

Kerstjens, H. A. M., Moroni-Zentgraf, P., Tashkin, D. P., Dahl, R., Paggiaro, P., Vandewalker, M., … Bateman, E. D. (2016). Tiotropium improves lung function, exacerbation rate, and asthma control, independent of baseline characteristics including age, degree of airway obstruction, and allergic status. *Respiratory Medicine*, *117*, 198–206. https://doi.org/10.1016/j.rmed.2016.06.013

Kim, Sang-Heon, Kim, Y.-K., Park, H.-W., Jee, Y.-K., Kim, S.-H., Bahn, J.-W., … Min, K.-U. (2007). Association between polymorphisms in prostanoid receptor genes

and aspirin-intolerant asthma: *Pharmacogenetics and Genomics*, *17*(4), 295–304. https://doi.org/10.1097/01.fpc.0000239977.61841.fe

Kim, S.-H., Bae, J.-S., Suh, C.-H., Nahm, D.-H., Holloway, J. W., & Park, H.-S. (2005). Polymorphism of tandem repeat in promoter of 5-lipoxygenase in ASA-intolerant asthma: A positive association with airway hyperresponsiveness. *Allergy*, *60*(6), 760–765. https://doi.org/10.1111/j.1398-9995.2005.00780.x

Kim, S.-H., Oh, J.-M., Kim, Y.-S., Palmer, L. J., Suh, C.-H., Nahm, D.-H., & Park, H.-S. (2006). Cysteinyl leukotriene receptor 1 promoter polymorphism is associated with aspirin-intolerant asthma in males. *Clinical Experimental Allergy*, *36*(4), 433–439. https://doi.org/10.1111/j.1365-2222.2006.02457.x

Koch, A., Grammatikos, G., Trautmann, S., Schreiber, Y., Thomas, D., Bruns, F., … Penna-Martinez, M. (2017). Vitamin D Supplementation Enhances C18(dihydro)ceramide Levels in Type 2 Diabetes Patients. *International Journal of Molecular Sciences*, *18*(7), 1532. https://doi.org/10.3390/ijms18071532

Kolesnikov, N., Hastings, E., Keays, M., Melnichuk, O., Tang, Y. A., Williams, E., … Brazma, A. (2015). ArrayExpress update—Simplifying data submissions. *Nucleic Acids Research*, *43*(Database issue), D1113-1116. https://doi.org/10.1093/nar/gku1057

Kowal, K., Żebrowska, E., & Chabowski, A. (2019). Altered Sphingolipid Metabolism Is Associated With Asthma Phenotype in House Dust Mite-Allergic Patients. *Allergy, Asthma & Immunology Research*, *11*(3), 330. https://doi.org/10.4168/aair.2019.11.3.330

Kowalski, M. L., Lewandowska-Polak, A., Wozniak, J., Ptasinska, A., Jankowski, A., Wagrowska-Danilewicz, M., … Pawliczak, R. (2005). Association of stem cell factor expression in nasal polyp epithelial cells with aspirin sensitivity and asthma. *Allergy*, *60*(5), 631–637. https://doi.org/10.1111/j.1398-9995.2005.00753.x

Kowalski, Marek L., Pawliczak, R., Wozniak, J., Siuda, K., Poniatowska, M., Iwaszkiewicz, J., … Kaliner, M. A. (2000). Differential Metabolism of Arachidonic Acid in Nasal Polyp Epithelial Cells Cultured from Aspirin-sensitive and Aspirin-tolerant Patients. *American Journal of Respiratory and Critical Care Medicine*, *161*(2), 391–398. https://doi.org/10.1164/ajrccm.161.2.9902034

Kratchmarova, I., Kalume, D. E., Blagoev, B., Scherer, P. E., Podtelejnikov, A. V., Molina, H., … Pandey, A. (2002). A Proteomic Approach for Identification of Secreted Proteins during the Differentiation of 3T3-L1 Preadipocytes to Adipocytes. *Molecular & Cellular Proteomics*, *1*(3), 213–222. https://doi.org/10.1074/mcp.M200006-MCP200

Kucukural, A., Yukselen, O., Ozata, D. M., Moore, M. J., & Garber, M. (2019). DEBrowser: Interactive differential expression analysis and visualization tool for count data. *BMC Genomics*, *20*(1). https://doi.org/10.1186/s12864-018-5362-x

Kulshreshtha, A., Ahmad, T., Agrawal, A., & Ghosh, B. (2013). Proinflammatory role of epithelial cell–derived exosomes in allergic airway inflammation. *Journal of Allergy and Clinical Immunology*, *131*(4), 1194-1203.e14. https://doi.org/10.1016/j.jaci.2012.12.1565

Kunikata, T., Yamane, H., Segi, E., Matsuoka, T., Sugimoto, Y., Tanaka, S., … Narumiya, S. (2005). Suppression of allergic inflammation by the prostaglandin E receptor subtype EP3. *Nature Immunology*, *6*(5), 524–531. https://doi.org/10.1038/ni1188

Lachowicz-Scroggins, M. E., Dunican, E. M., Charbit, A. R., Raymond, W., Looney, M. R., Peters, M. C., … Fahy, J. V. (2019). Extracellular DNA, Neutrophil Extracellular Traps, and Inflammasome Activation in Severe Asthma. *American Journal of Respiratory and Critical Care Medicine*, *199*(9), 1076–1085. https://doi.org/10.1164/rccm.201810-1869OC

Laidlaw, T. M., Kidder, M. S., Bhattacharyya, N., Xing, W., Shen, S., Milne, G. L., … Boyce, J. A. (2012). Cysteinyl leukotriene overproduction in aspirin-exacerbated respiratory disease is driven by platelet-adherent leukocytes. *Blood*, *119*(16), 3790–3798. https://doi.org/10.1182/blood-2011-10-384826

Laidlaw, Tanya M., Cutler, A. J., Kidder, M. S., Liu, T., Cardet, J. C., Chhay, H., … Boyce, J. A. (2014). Prostaglandin E2 resistance in granulocytes from patients with aspirin-exacerbated respiratory disease. *Journal of Allergy and Clinical Immunology*, *133*(6), 1692-1701.e3. https://doi.org/10.1016/j.jaci.2013.12.1034

Laidlaw, Tanya M., Fuentes, D. J., & Wang, Y. (2017). Efficacy of Zileuton in Patients with Asthma and History of Aspirin Sensitivity: A Retrospective Analysis of Data from Two Phase 3 Studies. *Journal of Allergy and Clinical Immunology*, *139*(2), AB384. https://doi.org/10.1016/j.jaci.2016.12.924

Larsson, A.-K., Hagfjärd, A., Dahlén, S.-E., & Adner, M. (2011). Prostaglandin D2 induces contractions through activation of TP receptors in peripheral lung tissue from the guinea pig. *European Journal of Pharmacology*, *669*(1–3), 136–142. https://doi.org/10.1016/j.ejphar.2011.07.046

Lässer, C., O'Neil, S. E., Ekerljung, L., Ekström, K., Sjöstrand, M., & Lötvall, J. (2011). RNA-containing Exosomes in Human Nasal Secretions. *American Journal of Rhinology & Allergy*, *25*(2), 89–93. https://doi.org/10.2500/ajra.2011.25.3573

Lässer, C., O'Neil, S. E., Shelke, G. V., Sihlbom, C., Hansson, S. F., Gho, Y. S., … Lötvall, J. (2016). Exosomes in the nose induce immune cell trafficking and harbour an altered protein cargo in chronic airway inflammation. *Journal of Translational Medicine*, *14*(1). https://doi.org/10.1186/s12967-016-0927-4

Lässer, C., Seyed Alikhani, V., Ekström, K., Eldh, M., Torregrosa Paredes, P., Bossios, A., … Valadi, H. (2011). Human saliva, plasma and breast milk exosomes contain RNA: Uptake by macrophages. *Journal of Translational Medicine*, *9*(1), 9. https://doi.org/10.1186/1479-5876-9-9

Lee, C. W., Lewis, R. A., Corey, E. J., & Austen, K. F. (1983). Conversion of leukotriene D4 to leukotriene E4 by a dipeptidase released from the specific granule of human polymorphonuclear leucocytes. *Immunology*, *48*(1), 27–35.

Lee, H. Y., Ye, Y. M., Kim, S. H., Ban, G. Y., Kim, S. C., Kim, J. H., … Park, H. S. (2017). Identification of phenotypic clusters of nonsteroidal anti-inflammatory drugs exacerbated respiratory disease. *Allergy*, *72*(4), 616–626. https://doi.org/10.1111/all.13075

Lee, J., Walsh, M. C., Hoehn, K. L., James, D. E., Wherry, E. J., & Choi, Y. (2014). Regulator of Fatty Acid Metabolism, Acetyl Coenzyme A Carboxylase 1, Controls T Cell Immunity. *The Journal of Immunology*, *192*(7), 3190–3199. https://doi.org/10.4049/jimmunol.1302985

Lee, Y.-J., Shin, Y.-H., Kim, J.-K., Shim, J.-Y., Kang, D.-R., & Lee, H.-R. (2010). Metabolic syndrome and its association with white blood cell count in children and adolescents in Korea: The 2005 Korean National Health and Nutrition Examination Survey. *Nutrition, Metabolism and Cardiovascular Diseases*, *20*(3), 165–172. https://doi.org/10.1016/j.numecd.2009.03.017

Lemanske, R. F., & Busse, W. W. (2003). 6. Asthma. *Journal of Allergy and Clinical Immunology*, *111*(2), S502–S519. https://doi.org/10.1067/mai.2003.94

Levänen, B., Bhakta, N. R., Torregrosa Paredes, P., Barbeau, R., Hiltbrunner, S., Pollack, J. L., … Wheelock, Å. M. (2013). Altered microRNA profiles in bronchoalveolar lavage fluid exosomes in asthmatic patients. *Journal of Allergy and Clinical Immunology*, *131*(3), 894-903.e8. https://doi.org/10.1016/j.jaci.2012.11.039

Levy, B. D., & Serhan, C. N. (2003). Exploring new approaches to the treatment of asthma: Potential roles for lipoxins and aspirin-triggered lipid mediators. *Drugs of Today (Barcelona, Spain: 1998)*, *39*(5), 373–384.

Lewis, A., Torvinen, S., Dekhuijzen, P. N. R., Chrystyn, H., Watson, A. T., Blackney, M., & Plich, A. (2016). The economic burden of asthma and chronic obstructive pulmonary disease and the impact of poor inhalation technique with commonly prescribed dry powder inhalers in three European countries. *BMC Health Services Research*, *16*(1). https://doi.org/10.1186/s12913-016-1482-7

Liao, Y., Smyth, G. K., & Shi, W. (2014). featureCounts: An efficient general purpose program for assigning sequence reads to genomic features. *Bioinformatics*, *30*(7), 923–930. https://doi.org/10.1093/bioinformatics/btt656

Liu, T., Laidlaw, T. M., Feng, C., Xing, W., Shen, S., Milne, G. L., & Boyce, J. A. (2012). Prostaglandin E2 deficiency uncovers a dominant role for thromboxane A2 in house dust mite-induced allergic pulmonary inflammation. *Proceedings of the National Academy of Sciences*, *109*(31), 12692–12697. https://doi.org/10.1073/pnas.1207816109

Liu, T., Laidlaw, T. M., Katz, H. R., & Boyce, J. A. (2013). Prostaglandin E2 deficiency causes a phenotype of aspirin sensitivity that depends on platelets and cysteinyl leukotrienes. *Proceedings of the National Academy of Sciences*, *110*(42), 16987–16992. https://doi.org/10.1073/pnas.1313185110

Liu, Tao, Zhao, F., Xie, C., Liu, A.-M., Li, T.-L., Chen, X., … Yang, P.-C. (2011). Role of Thymic Stromal Lymphopoietin in the Pathogenesis of Nasal Polyposis. *The American Journal of the Medical Sciences*, *341*(1), 40–47. https://doi.org/10.1097/MAJ.0b013e3181f20489

Lohia, S., Schlosser, R. J., & Soler, Z. M. (2013). Impact of intranasal corticosteroids on asthma outcomes in allergic rhinitis: A meta-analysis. *Allergy*, *68*(5), 569–579. https://doi.org/10.1111/all.12124

Lord, G. M., Matarese, G., Howard, J. K., Baker, R. J., Bloom, S. R., & Lechler, R. I. (1998). Leptin modulates the T-cell immune response and reverses starvation-induced immunosuppression. *Nature*, *394*(6696), 897–901. https://doi.org/10.1038/29795

Love, M. I., Huber, W., & Anders, S. (2014). Moderated estimation of fold change and dispersion for RNA-seq data with DESeq2. *Genome Biology*, *15*(12). https://doi.org/10.1186/s13059-014-0550-8

Lovren, F., Pan, Y., Quan, A., Szmitko, P. E., Singh, K. K., Shukla, P. C., … Verma, S. (2010). Adiponectin primes human monocytes into alternative anti-inflammatory M2 macrophages. *American Journal of Physiology-Heart and Circulatory Physiology*, *299*(3), H656–H663. https://doi.org/10.1152/ajpheart.00115.2010

Lumeng, C. N., Bodzin, J. L., & Saltiel, A. R. (2007). Obesity induces a phenotypic switch in adipose tissue macrophage polarization. *Journal of Clinical Investigation*, *117*(1), 175–184. https://doi.org/10.1172/JCI29881

Lynch, K. R., O'Neill, G. P., Liu, Q., Im, D.-S., Sawyer, N., Metters, K. M., … Evans, J. F. (1999). Characterization of the human cysteinyl leukotriene CysLT1 receptor. *Nature*, *399*(6738), 789–793. https://doi.org/10.1038/21658

Mahdavinia, M., Carter, R. G., Ocampo, C. J., Stevens, W., Kato, A., Tan, B. K., … Schleimer, R. P. (2014). Basophils are elevated in nasal polyps of patients with chronic rhinosinusitis without aspirin sensitivity. *Journal of Allergy and Clinical Immunology*, *133*(6), 1759–1763. https://doi.org/10.1016/j.jaci.2013.12.1092

Majumdar, R., Tameh, A. T., & Parent, C. A. (2016). Exosomes Mediate LTB 4 Release during Neutrophil Chemotaxis. *PLOS Biol*, *14*(1), e1002336. https://doi.org/10.1371/journal.pbio.1002336

Makowska, J. S., Burney, P., Jarvis, D., Keil, T., Tomassen, P., Bislimovska, J., … Kowalski, M. L. (2016). Respiratory hypersensitivity reactions to NSAIDs in Europe: The global allergy and asthma network (GA ^{2} LEN) survey. *Allergy*, *71*(11), 1603–1611. https://doi.org/10.1111/all.12941

Maksimovic, J., Gordon, L., & Oshlack, A. (2012). SWAN: Subset-quantile Within Array Normalization for Illumina Infinium HumanMethylation450 BeadChips. *Genome Biology*, *13*(6), R44. https://doi.org/10.1186/gb-2012-13-6-r44

Mancuso, P., Canetti, C., Gottschalk, A., Tithof, P. K., & Peters-Golden, M. (2004). Leptin augments alveolar macrophage leukotriene synthesis by increasing phospholipase activity and enhancing group IVC iPLA $_{2}$ (cPLA $_{2}$ γ) protein expression. *American Journal of Physiology-Lung Cellular and Molecular Physiology*, *287*(3), L497–L502. https://doi.org/10.1152/ajplung.00010.2004

Martin-Urdiroz, M., Deeks, M. J., Horton, C. G., Dawe, H. R., & Jourdain, I. (2016). The Exocyst Complex in Health and Disease. *Frontiers in Cell and Developmental Biology*, *4*. https://doi.org/10.3389/fcell.2016.00024

Mascia, K., Haselkorn, T., Deniz, Y. M., Miller, D. P., Bleecker, E. R., & Borish, L. (2005). Aspirin sensitivity and severity of asthma: Evidence for irreversible airway obstruction in patients with severe or difficult-to-treat asthma. *Journal of Allergy and Clinical Immunology*, *116*(5), 970–975. https://doi.org/10.1016/j.jaci.2005.08.035

Mastalerz, L., Celejewska-Wójcik, N., Wójcik, K., Gielicz, A., Januszek, R., Cholewa, A., … Sanak, M. (2014). Induced sputum eicosanoids during aspirin bronchial challenge of asthmatic patients with aspirin hypersensitivity. *Allergy*, *69*(11), 1550–1559. https://doi.org/10.1111/all.12512

Mattioli, B., Straface, E., Quaranta, M. G., Giordani, L., & Viora, M. (2005). Leptin Promotes Differentiation and Survival of Human Dendritic Cells and Licenses Them for Th1 Priming. *The Journal of Immunology*, *174*(11), 6820–6828. https://doi.org/10.4049/jimmunol.174.11.6820

Maycock, A. L., Anderson, M. S., DeSousa, D. M., & Kuehl, F. A. (1982). Leukotriene A4: Preparation and enzymatic conversion in a cell-free system to leukotriene B4. *The Journal of Biological Chemistry*, *257*(23), 13911–13914.

Mazzeo, C., Cañas, J. A., Zafra, M. P., Rojas Marco, A., Fernández-Nieto, M., Sanz, V., … del Pozo, V. (2015). Exosome secretion by eosinophils: A possible role in asthma pathogenesis. *Journal of Allergy and Clinical Immunology*, *135*(6), 1603–1613. https://doi.org/10.1016/j.jaci.2014.11.026

McCartney, D. L., Walker, R. M., Morris, S. W., McIntosh, A. M., Porteous, D. J., & Evans, K. L. (2016). Identification of polymorphic and off-target probe binding

sites on the Illumina Infinium MethylationEPIC BeadChip. *Genomics Data*, *9*, 22–24. https://doi.org/10.1016/j.gdata.2016.05.012

McCartney-Francis, N. L., & Wahl, S. M. (2001). TGF-β and macrophages in the rise and fall of inflammation. In S. N. Breit & S. M. Wahl (Eds.), *TGF-β and Related Cytokines in Inflammation* (pp. 65–90). Retrieved from http://link.springer.com/10.1007/978-3-0348-8354-2_4

Meana, C., Peña, L., Lordén, G., Esquinas, E., Guijas, C., Valdearcos, M., … Balboa, M. A. (2014). Lipin-1 Integrates Lipid Synthesis with Proinflammatory Responses during TLR Activation in Macrophages. *The Journal of Immunology*, *193*(9), 4614–4622. https://doi.org/10.4049/jimmunol.1400238

Mechtcheriakova, D., Sobanov, Y., Holtappels, G., Bajna, E., Svoboda, M., Jaritz, M., … Jensen-Jarolim, E. (2011). Activation-Induced Cytidine Deaminase (AID)-Associated Multigene Signature to Assess Impact of AID in Etiology of Diseases with Inflammatory Component. *PLoS ONE*, *6*(10), e25611. https://doi.org/10.1371/journal.pone.0025611

Mellor, E. A., Frank, N., Soler, D., Hodge, M. R., Lora, J. M., Austen, K. F., & Boyce, J. A. (2003). Expression of the type 2 receptor for cysteinyl leukotrienes (CysLT2R) by human mast cells: Functional distinction from CysLT1R. *Proceedings of the National Academy of Sciences*, *100*(20), 11589–11593. https://doi.org/10.1073/pnas.2034927100

Mellor, Elizabeth A., Austen, K. F., & Boyce, J. A. (2002). Cysteinyl Leukotrienes and Uridine Diphosphate Induce Cytokine Generation by Human Mast Cells Through an Interleukin 4–regulated Pathway that Is Inhibited by Leukotriene Receptor Antagonists. *The Journal of Experimental Medicine*, *195*(5), 583–592. https://doi.org/10.1084/jem.20020044

Mi, H., Huang, X., Muruganujan, A., Tang, H., Mills, C., Kang, D., & Thomas, P. D. (2017). PANTHER version 11: Expanded annotation data from Gene Ontology and Reactome pathways, and data analysis tool enhancements. *Nucleic Acids Research*, *45*(D1), D183–D189. https://doi.org/10.1093/nar/gkw1138

Micheletto, C., Visconti, M., Trevisan, F., Tognella, S., Bertacco, S., & Dal Negro, R. W. (2010). The prevalence of nasal polyps and the corresponding urinary LTE4 levels in severe compared to mild and moderate asthma. *European Annals of Allergy and Clinical Immunology*, *42*(3), 120–124.

Miljkovic, D., Bassiouni, A., Cooksley, C., Ou, J., Hauben, E., Wormald, P.-J., & Vreugde, S. (2014). Association between Group 2 Innate Lymphoid Cells enrichment, nasal polyps and allergy in Chronic Rhinosinusitis. *Allergy*, *69*(9), 1154–1161. https://doi.org/10.1111/all.12440

Miller, M., Cho, J. Y., Pham, A., Ramsdell, J., & Broide, D. H. (2009). Adiponectin and Functional Adiponectin Receptor 1 Are Expressed by Airway Epithelial Cells in Chronic Obstructive Pulmonary Disease. *The Journal of Immunology*, *182*(1), 684–691. https://doi.org/10.4049/jimmunol.182.1.684

Mita, H., Endoh, S., Kudoh, M., Kawagishi, Y., Kobayashi, M., Taniguchi, M., & Akiyama, K. (2001). Possible involvement of mast-cell activation in aspirin provocation of aspirin-induced asthma. *Allergy*, *56*(11), 1061–1067.

Mittelbrunn, M., Gutiérrez-Vázquez, C., Villarroya-Beltri, C., González, S., Sánchez-Cabo, F., González, M. Á., … Sánchez-Madrid, F. (2011). Unidirectional transfer of microRNA-loaded exosomes from T cells to antigen-presenting cells. *Nature Communications*, *2*(1). https://doi.org/10.1038/ncomms1285

Moffatt, M. F., Kabesch, M., Liang, L., Dixon, A. L., Strachan, D., Heath, S., … Cookson, W. O. C. (2007). Genetic variants regulating ORMDL3 expression contribute to the risk of childhood asthma. *Nature*, *448*(7152), 470–473. https://doi.org/10.1038/nature06014

Moore, W. C., Meyers, D. A., Wenzel, S. E., Teague, W. G., Li, H., Li, X., … Bleecker, E. R. (2010). Identification of Asthma Phenotypes Using Cluster Analysis in the Severe Asthma Research Program. *American Journal of Respiratory and Critical Care Medicine*, *181*(4), 315–323. https://doi.org/10.1164/rccm.200906-0896OC

Mostafa, M. M., Rider, C. F., Shah, S., Traves, S. L., Gordon, P. M. K., Miller-Larsson, A., … Newton, R. (2019). Glucocorticoid-driven transcriptomes in human airway epithelial cells: Commonalities, differences and functional insight from cell lines and primary cells. *BMC Medical Genomics*, *12*(1). https://doi.org/10.1186/s12920-018-0467-2

Mueller, S. K., Nocera, A. L., Dillon, S. T., Gu, X., Wendler, O., Otu, H. H., … Bleier, B. S. (2019). Noninvasive exosomal proteomic biosignatures, including cystatin SN, peroxiredoxin-5, and glycoprotein VI, accurately predict chronic rhinosinusitis with nasal polyps: Noninvasive proteomic exosomal biosignature. *International Forum of Allergy & Rhinology*, *9*(2), 177–186. https://doi.org/10.1002/alr.22226

Murphy, A. J., Akhtari, M., Tolani, S., Pagler, T., Bijl, N., Kuo, C.-L., … Tall, A. R. (2011). ApoE regulates hematopoietic stem cell proliferation, monocytosis, and monocyte accumulation in atherosclerotic lesions in mice. *Journal of Clinical Investigation*, *121*(10), 4138–4149. https://doi.org/10.1172/JCI57559

Murphy, R. C., & Gijón, M. A. (2007). Biosynthesis and metabolism of leukotrienes. *Biochemical Journal*, *405*(3), 379–395. https://doi.org/10.1042/BJ20070289

Murray, C. S. (2006). Study of modifiable risk factors for asthma exacerbations: Virus infection and allergen exposure increase the risk of asthma hospital admissions in children. *Thorax*, *61*(5), 376–382. https://doi.org/10.1136/thx.2005.042523

Nagarkar, D. R., Poposki, J. A., Tan, B. K., Comeau, M. R., Peters, A. T., Hulse, K. E., … Kato, A. (2013). Thymic stromal lymphopoietin activity is increased in nasal polyps of patients with chronic rhinosinusitis. *Journal of Allergy and Clinical Immunology*, *132*(3), 593-600.e12. https://doi.org/10.1016/j.jaci.2013.04.005

Nasser, S. M., Pfister, R., Christie, P. E., Sousa, A. R., Barker, J., Schmitz-Schumann, M., & Lee, T. H. (1996). Inflammatory cell populations in bronchial biopsies from aspirin-sensitive asthmatic subjects. *American Journal of Respiratory and Critical Care Medicine*, *153*(1), 90–96. https://doi.org/10.1164/ajrccm.153.1.8542168

Navratil, A. R., Vozenilek, A. E., Cardelli, J. A., Green, J. M., Thomas, M. J., Sorci-Thomas, M. G., … Woolard, M. D. (2015). Lipin-1 contributes to modified low-density lipoprotein-elicited macrophage pro-inflammatory responses. *Atherosclerosis*, *242*(2), 424–432. https://doi.org/10.1016/j.atherosclerosis.2015.08.012

Neeland, I. J., Ayers, C. R., Rohatgi, A. K., Turer, A. T., Berry, J. D., Das, S. R., … de Lemos, J. A. (2013). Associations of visceral and abdominal subcutaneous adipose tissue with markers of cardiac and metabolic risk in obese adults: Abdominal Fat and Cardiometabolic Risk. *Obesity*, n/a-n/a. https://doi.org/10.1002/oby.20135

Nutku, E. (2003). Ligation of Siglec-8: A selective mechanism for induction of human eosinophil apoptosis. *Blood*, *101*(>12), 5014–5020. https://doi.org/10.1182/blood-2002-10-3058

Obeid, L., Linardic, C., Karolak, L., & Hannun, Y. (1993). Programmed cell death induced by ceramide. *Science*, *259*(5102), 1769–1771. https://doi.org/10.1126/science.8456305

O'Byrne, P. M., Barnes, P. J., Rodriguez-Roisin, R., Runnerstrom, E., Sandstrom, T., Svensson, K., & Tattersfield, A. (2001). Low Dose Inhaled Budesonide and Formoterol in Mild Persistent Asthma: The OPTIMA Randomized Trial. *American Journal of Respiratory and Critical Care Medicine*, *164*(8), 1392–1397. https://doi.org/10.1164/ajrccm.164.8.2104102

Odegaard, J. I., Ricardo-Gonzalez, R. R., Goforth, M. H., Morel, C. R., Subramanian, V., Mukundan, L., … Chawla, A. (2007). Macrophage-specific PPARγ controls alternative activation and improves insulin resistance. *Nature*, *447*(7148), 1116–1120. https://doi.org/10.1038/nature05894

Oh, S. F., Dona, M., Fredman, G., Krishnamoorthy, S., Irimia, D., & Serhan, C. N. (2012). Resolvin E2 Formation and Impact in Inflammation Resolution. *The Journal of Immunology*, *188*(9), 4527–4534. https://doi.org/10.4049/jimmunol.1103652

Ohashi, K., Parker, J. L., Ouchi, N., Higuchi, A., Vita, J. A., Gokce, N., … Walsh, K. (2010). Adiponectin Promotes Macrophage Polarization toward an Anti-inflammatory Phenotype. *Journal of Biological Chemistry*, *285*(9), 6153–6160. https://doi.org/10.1074/jbc.M109.088708

O'Neill, S., Sweeney, J., Patterson, C. C., Menzies-Gow, A., Niven, R., Mansur, A. H., … on behalf of the British Thoracic Society Difficult Asthma Network. (2015). The cost of treating severe refractory asthma in the UK: An economic analysis from the British Thoracic Society Difficult Asthma Registry. *Thorax*, *70*(4), 376–378. https://doi.org/10.1136/thoraxjnl-2013-204114

Ono, E., Dutile, S., Kazani, S., Wechsler, M. E., Yang, J., Hammock, B. D., … Levy, B. D. (2014). Lipoxin Generation Is Related to Soluble Epoxide Hydrolase Activity in Severe Asthma. *American Journal of Respiratory and Critical Care Medicine*, *190*(8), 886–897. https://doi.org/10.1164/rccm.201403-0544OC

Oyeniran, C., Sturgill, J. L., Hait, N. C., Huang, W.-C., Avni, D., Maceyka, M., … Spiegel, S. (2015). Aberrant ORM (yeast)–like protein isoform 3 (ORMDL3) expression dysregulates ceramide homeostasis in cells and ceramide exacerbates allergic asthma in mice. *Journal of Allergy and Clinical Immunology*, *136*(4), 1035-1046.e6. https://doi.org/10.1016/j.jaci.2015.02.031

Palikhe, N. S., Kim, S.-H., Cho, B.-Y., Ye, Y.-M., Choi, G.-S., & Park, H.-S. (2010). Genetic variability in CRTH2 polymorphism increases eotaxin-2 levels in patients with aspirin exacerbated respiratory disease. *Allergy*, *65*(3), 338–346. https://doi.org/10.1111/j.1398-9995.2009.02158.x

Palmblad, J., Malmsten, C. L., Udén, A. M., Rådmark, O., Engstedt, L., & Samuelsson, B. (1981). Leukotriene B4 is a potent and stereospecific stimulator of neutrophil chemotaxis and adherence. *Blood*, *58*(3), 658–661.

Park, J. E., Dutta, B., Tse, S. W., Gupta, N., Tan, C. F., Low, J. K., … Sze, S. K. (2019). Hypoxia-induced tumor exosomes promote M2-like macrophage polarization of infiltrating myeloid cells and microRNA-mediated metabolic shift. *Oncogene*, *38*(26), 5158–5173. https://doi.org/10.1038/s41388-019-0782-x

Park, S.-Y., Jung, M.-Y., Kim, H.-J., Lee, S.-J., Kim, S.-Y., Lee, B.-H., … Kim, I.-S. (2008). Rapid cell corpse clearance by stabilin-2, a membrane phosphatidylserine receptor. *Cell Death & Differentiation*, *15*(1), 192–201. https://doi.org/10.1038/sj.cdd.4402242

Parolini, I., Federici, C., Raggi, C., Lugini, L., Palleschi, S., De Milito, A., … Fais, S. (2009). Microenvironmental pH is a key factor for exosome traffic in tumor cells. *The Journal of Biological Chemistry*, *284*(49), 34211–34222. https://doi.org/10.1074/jbc.M109.041152

Passalacqua, G. (2000). United airways disease: Therapeutic aspects. *Thorax*, *55*(90002), 26S – 27. https://doi.org/10.1136/thorax.55.suppl_2.S26

Pauwels, R. A., Pedersen, S., Busse, W. W., Tan, W. C., Chen, Y.-Z., Ohlsson, S. V., … O'Byrne, P. M. (2003). Early intervention with budesonide in mild persistent asthma: A randomised, double-blind trial. *The Lancet*, *361*(9363), 1071–1076. https://doi.org/10.1016/S0140-6736(03)12891-7

Payne, S. G., Milstien, S., & Spiegel, S. (2002). Sphingosine-1-phosphate: Dual messenger functions. *FEBS Letters*, *531*(1), 54–57. https://doi.org/10.1016/s0014-5793(02)03480-4

Peachell, P. T., MacGlashan, D. W., & Lichtenstein, L. M. (1988). Regulation of human basophil and lung mast cell function by cyclic adenosine monophosphate. *J Immunol*, *140*(2), 571–579.

Pendergraft, T. B., Stanford, R. H., Beasley, R., Stempel, D. A., Roberts, C., & McLaughlin, T. (2004). Rates and characteristics of intensive care unit admissions and intubations among asthma-related hospitalizations. *Annals of Allergy, Asthma & Immunology*, *93*(1), 29–35. https://doi.org/10.1016/S1081-1206(10)61444-5

Peters, T. J., Buckley, M. J., Statham, A. L., Pidsley, R., Samaras, K., V Lord, R., … Molloy, P. L. (2015). De novo identification of differentially methylated regions in the human genome. *Epigenetics & Chromatin*, *8*(1), 6. https://doi.org/10.1186/1756-8935-8-6

Peters-Golden, M. (2006). Influence of body mass index on the response to asthma controller agents. *European Respiratory Journal*, *27*(3), 495–503. https://doi.org/10.1183/09031936.06.00077205

Peters-Golden, Marc, & Henderson, W. R. (2007). Leukotrienes. *New England Journal of Medicine*, *357*(18), 1841–1854. https://doi.org/10.1056/NEJMra071371

Philip, G., Nayak, A. S., Berger, W. E., Leynadier, F., Vrijens, F., Dass, S. B., & Reiss, T. F. (2004). The effect of montelukast on rhinitis symptoms in patients with asthma and seasonal allergic rhinitis. *Current Medical Research and Opinion*, *20*(10), 1549–1558. https://doi.org/10.1185/030079904X3348

Picado, C., Ramis, I., Rosellò, J., Prat, J., Bulbena, O., Plaza, V., … Gelpí, E. (1992). Release of Peptide Leukotriene into Nasal Secretions after Local Instillation of Aspirin in Aspirin-sensitive Asthmatic Patients. *American Review of Respiratory Disease*, *145*(1), 65–69. https://doi.org/10.1164/ajrccm/145.1.65

Picado, CéSar, Fernandez-Morata, J. C., Juan, M., Roca-Ferrer, J., Fuentes, M., Xaubet, A., & Mullol, J. (1999). Cyclooxygenase-2 mRNA Is Downexpressed in Nasal Polyps from Aspirin-sensitive Asthmatics. *American Journal of Respiratory and Critical Care Medicine*, *160*(1), 291–296. https://doi.org/10.1164/ajrccm.160.1.9808048

Pillai, S. G., Cousens, D. J., Barnes, A. A., Buckley, P. T., Chiano, M. N., Hosking, L. K., … Investigators of the GAIN Network. (2004). A coding polymorphism in the

CYSLT2 receptor with reduced affinity to LTD4 is associated with asthma. *Pharmacogenetics*, *14*(9), 627–633.

Pipkorn, U., & Karlsson, G. (1988). Methods for obtaining specimens from the nasal mucosa for morphological and biochemical analysis. *European Respiratory Journal*, *1*, 856–862.

Ponikau, J. U., Sherris, D. A., Kephart, G. M., Kern, E. B., Gaffey, T. A., Tarara, J. E., & Kita, H. (2003). Features of airway remodeling and eosinophilic inflammation in chronic rhinosinusitis. *Journal of Allergy and Clinical Immunology*, *112*(5), 877–882. https://doi.org/10.1016/j.jaci.2003.08.009

Poole, J. A., Barnes, C. S., Demain, J. G., Bernstein, J. A., Padukudru, M. A., Sheehan, W. J., … Nel, A. E. (2019). Impact of weather and climate change with indoor and outdoor air quality in asthma: A Work Group Report of the AAAAI Environmental Exposure and Respiratory Health Committee. *Journal of Allergy and Clinical Immunology*, *143*(5), 1702–1710. https://doi.org/10.1016/j.jaci.2019.02.018

Poposki, J. A., Uzzaman, A., Nagarkar, D. R., Chustz, R. T., Peters, A. T., Suh, L. A., … Kato, A. (2011). Increased expression of the chemokine CCL23 in eosinophilic chronic rhinosinusitis with nasal polyps. *Journal of Allergy and Clinical Immunology*, *128*(1), 73-81.e4. https://doi.org/10.1016/j.jaci.2011.03.017

Prado, N., Marazuela, E. G., Segura, E., Fernandez-Garcia, H., Villalba, M., Thery, C., … Batanero, E. (2008). Exosomes from Bronchoalveolar Fluid of Tolerized Mice Prevent Allergic Reaction. *The Journal of Immunology*, *181*(2), 1519–1525. https://doi.org/10.4049/jimmunol.181.2.1519

Price, M. M., Oskeritzian, C. A., Falanga, Y. T., Harikumar, K. B., Allegood, J. C., Alvarez, S. E., … Spiegel, S. (2013). A specific sphingosine kinase 1 inhibitor attenuates airway hyperresponsiveness and inflammation in a mast cell–dependent murine model of allergic asthma. *Journal of Allergy and Clinical Immunology*, *131*(2), 501-511.e1. https://doi.org/10.1016/j.jaci.2012.07.014

Prieto, P., Cuenca, J., Través, P. G., Fernández-Velasco, M., Martín-Sanz, P., & Boscá, L. (2010). Lipoxin A4 impairment of apoptotic signaling in macrophages: Implication of the PI3K/Akt and the ERK/Nrf-2 defense pathways. *Cell Death & Differentiation*, *17*(7), 1179–1188. https://doi.org/10.1038/cdd.2009.220

Prieur, X., Mok, C. Y. L., Velagapudi, V. R., Núñez, V., Fuentes, L., Montaner, D., … Vidal-Puig, A. (2011). Differential Lipid Partitioning Between Adipocytes and Tissue Macrophages Modulates Macrophage Lipotoxicity and M2/M1 Polarization in Obese Mice. *Diabetes*, *60*(3), 797–809. https://doi.org/10.2337/db10-0705

Proud, D., Sanders, S. P., & Wiehler, S. (2004). Human Rhinovirus Infection Induces Airway Epithelial Cell Production of Human -Defensin 2 Both In Vitro and In Vivo. *The Journal of Immunology*, *172*(7), 4637–4645. https://doi.org/10.4049/jimmunol.172.7.4637

Pundir, V., Pundir, J., Lancaster, G., Kirkland, P., Cornet, M., Lourijsen, E. S., … Fokkens, W. J. (2016). Role of corticosteroids in Functional Endoscopic Sinus Surgery—A systematic review and meta-analysis. *Rhinology Journal*, *54*(1), 3–19. https://doi.org/10.4193/Rhin15.079

R Core Team. (2017). R: A Language and Environment for Statistical Computing (Version 3.4.3). Retrieved from https://www.R-project.org/

Rajan, J. P., Wineinger, N. E., Stevenson, D. D., & White, A. A. (2015). Prevalence of aspirin-exacerbated respiratory disease among asthmatic patients: A meta-analysis of the literature. *Journal of Allergy and Clinical Immunology*, *135*(3), 676-681.e1. https://doi.org/10.1016/j.jaci.2014.08.020

Ramirez-Yañez, G. O., Hamlet, S., Jonarta, A., Seymour, G. J., & Symons, A. L. (2006). Prostaglandin E2 enhances transforming growth factor-beta 1 and TGF-beta receptors synthesis: An in vivo and in vitro study. *Prostaglandins, Leukotrienes and Essential Fatty Acids*, *74*(3), 183–192. https://doi.org/10.1016/j.plefa.2006.01.003

Raso, G. M., Pacilio, M., Esposito, E., Coppola, A., Di Carlo, R., & Meli, R. (2002). Leptin potentiates IFN-γ-induced expression of nitric oxide synthase and cyclo-oxygenase-2 in murine macrophage J774A.1. *British Journal of Pharmacology*, *137*(6), 799–804. https://doi.org/10.1038/sj.bjp.0704903

Reddel, H. K., Bateman, E. D., Becker, A., Boulet, L.-P., Cruz, A. A., Drazen, J. M., … FitzGerald, J. M. (2015). A summary of the new GINA strategy: A roadmap to asthma control. *European Respiratory Journal*, *46*(3), 622–639. https://doi.org/10.1183/13993003.00853-2015

Reinke, S. N., Gallart-Ayala, H., Gómez, C., Checa, A., Fauland, A., Naz, S., … Wheelock, C. E. (2017). Metabolomics analysis identifies different metabotypes of asthma severity. *European Respiratory Journal*, *49*(3), 1601740. https://doi.org/10.1183/13993003.01740-2016

Remes Lenicov, F., Paletta, A. L., Gonzalez Prinz, M., Varese, A., Pavillet, C. E., Lopez Malizia, Á., … Ceballos, A. (2018). Prostaglandin E2 Antagonizes TGF-β Actions During the Differentiation of Monocytes Into Dendritic Cells. *Frontiers in Immunology*, *9*. https://doi.org/10.3389/fimmu.2018.01441

Ricote, M., Welch, J. S., & Glass, C. K. (2000). Regulation of Macrophage Gene Expression by the Peroxisome Proliferator-Activated Receptor-gamma. *Horm Res*, 8. https://doi.org/10.1159/000053271

Rigotti, A., Miettinen, H. E., & Krieger, M. (2003). The Role of the High-Density Lipoprotein Receptor SR-BI in the Lipid Metabolism of Endocrine and Other Tissues. *Endocrine Reviews*, *24*(3), 357–387. https://doi.org/10.1210/er.2001-0037

Rijkers, E. S. K., de Ruiter, T., Baridi, A., Veninga, H., Hoek, R. M., & Meyaard, L. (2008). The inhibitory CD200R is differentially expressed on human and mouse T and B lymphocytes. *Molecular Immunology*, *45*(4), 1126–1135. https://doi.org/10.1016/j.molimm.2007.07.013

Ritchie, M. E., Phipson, B., Wu, D., Hu, Y., Law, C. W., Shi, W., & Smyth, G. K. (2015). Limma powers differential expression analyses for RNA-sequencing and microarray studies. *Nucleic Acids Research*, *43*(7), e47–e47. https://doi.org/10.1093/nar/gkv007

Rivera, J., Cordero, R. J. B., Nakouzi, A. S., Frases, S., Nicola, A., & Casadevall, A. (2010). Bacillus anthracis produces membrane-derived vesicles containing biologically active toxins. *Proceedings of the National Academy of Sciences*, *107*(44), 19002–19007. https://doi.org/10.1073/pnas.1008843107

Rix, I., Håkansson, K., Larsen, C. G., Frendø, M., & von Buchwald, C. (2015). Management of Chronic Rhinosinusitis with Nasal Polyps and Coexisting Asthma: A Systematic Review. *American Journal of Rhinology & Allergy*, *29*(3), 193–201. https://doi.org/10.2500/ajra.2015.29.4178

Rizk, A. K., Lavoie, K. L., Pepin, V., Wright, A., & Bacon, S. L. (2012). Sex Differences in the Effects of Inhaled Corticosteroids on Weight Gain among Patients with Asthma. *ISRN Pulmonology*, *2012*, 1–7. https://doi.org/10.5402/2012/138326

Roberts-Dalton, H. D., Cocks, A., Falcon-Perez, J. M., Sayers, E. J., Webber, J. P., Watson, P., … Jones, A. T. (2017). Fluorescence labelling of extracellular vesicles using a novel thiol-based strategy for quantitative analysis of cellular delivery and intracellular traffic. *Nanoscale*, *9*(36), 13693–13706. https://doi.org/10.1039/C7NR04128D

Roca-Ferrer, J., Garcia-Garcia, F. J., Pereda, J., Perez-Gonzalez, M., Pujols, L., Alobid, I., … Picado, C. (2011). Reduced expression of COXs and production of prostaglandin E2 in patients with nasal polyps with or without aspirin-intolerant asthma. *Journal of Allergy and Clinical Immunology*, *128*(1), 66-72.e1. https://doi.org/10.1016/j.jaci.2011.01.065

Rogerio, A. P., Haworth, O., Croze, R., Oh, S. F., Uddin, M., Carlo, T., … Levy, B. D. (2012). Resolvin D1 and Aspirin-Triggered Resolvin D1 Promote Resolution of Allergic Airways Responses. *The Journal of Immunology*, *189*(4), 1983–1991. https://doi.org/10.4049/jimmunol.1101665

Römisch-Margl, W., Prehn, C., Bogumil, R., Röhring, C., Suhre, K., & Adamski, J. (2012). Procedure for tissue sample preparation and metabolite extraction for high-throughput targeted metabolomics. *Metabolomics*, *8*(1), 133–142. https://doi.org/10.1007/s11306-011-0293-4

Rubinow, K. B., Wall, V. Z., Nelson, J., Mar, D., Bomsztyk, K., Askari, B., … Bornfeldt, K. E. (2013). Acyl-CoA Synthetase 1 Is Induced by Gram-negative Bacteria and Lipopolysaccharide and Is Required for Phospholipid Turnover in Stimulated Macrophages. *Journal of Biological Chemistry*, *288*(14), 9957–9970. https://doi.org/10.1074/jbc.M113.458372

Rutkowsky, J. M., Knotts, T. A., Ono-Moore, K. D., McCoin, C. S., Huang, S., Schneider, D., … Hwang, D. H. (2014). Acylcarnitines activate proinflammatory signaling pathways. *American Journal of Physiology-Endocrinology and Metabolism*, *306*(12), E1378–E1387. https://doi.org/10.1152/ajpendo.00656.2013

Ryo, M., Nakamura, T., Kihara, S., Kumada, M., Shibazaki, S., Takahashi, M., … Funahashi, T. (2004). Adiponectin as a biomarker of the metabolic syndrome. *Circulation Journal: Official Journal of the Japanese Circulation Society*, *68*(11), 975–981.

Saklayen, M. G. (2018). The Global Epidemic of the Metabolic Syndrome. *Current Hypertension Reports*, *20*(2). https://doi.org/10.1007/s11906-018-0812-z

Salimi, M., Stöger, L., Liu, W., Go, S., Pavord, I., Klenerman, P., … Xue, L. (2017). Cysteinyl leukotriene E 4 activates human group 2 innate lymphoid cells and enhances the effect of prostaglandin D 2 and epithelial cytokines. *Journal of Allergy and Clinical Immunology*, *140*(4), 1090-1100.e11. https://doi.org/10.1016/j.jaci.2016.12.958

Sampey, B. P., Freemerman, A. J., Zhang, J., Kuan, P.-F., Galanko, J. A., O'Connell, T. M., … Makowski, L. (2012). Metabolomic Profiling Reveals Mitochondrial-Derived Lipid Biomarkers That Drive Obesity-Associated Inflammation. *PLoS ONE*, *7*(6), e38812. https://doi.org/10.1371/journal.pone.0038812

Samter, M., & Beers, R. F. (1968). Intolerance to aspirin. Clinical studies and consideration of its pathogenesis. *Annals of Internal Medicine*, *68*(5), 975–983.

Sanak, M., Pierzchalska, M., Bazan-Socha, S., & Szczeklik, A. (2000). Enhanced Expression of the Leukotriene C4 Synthase Due to Overactive Transcription of an Allelic Variant Associated with Aspirin-Intolerant Asthma. *American Journal of Respiratory Cell and Molecular Biology*, *23*(3), 290–296. https://doi.org/10.1165/ajrcmb.23.3.4051

Sanin, D. E., Matsushita, M., Klein Geltink, R. I., Grzes, K. M., van Teijlingen Bakker, N., Corrado, M., … Pearce, E. J. (2018). Mitochondrial Membrane Potential Regulates Nuclear Gene Expression in Macrophages Exposed to Prostaglandin E2. *Immunity*, *49*(6), 1021-1033.e6. https://doi.org/10.1016/j.immuni.2018.10.011

Santos-Alvarez, J., Goberna, R., & Sánchez-Margalet, V. (1999). Human Leptin Stimulates Proliferation and Activation of Human Circulating Monocytes. *Cellular Immunology*, *194*(1), 6–11. https://doi.org/10.1006/cimm.1999.1490

Saradna, A., Do, D. C., Kumar, S., Fu, Q.-L., & Gao, P. (2018). Macrophage polarization and allergic asthma. *Translational Research*, *191*, 1–14. https://doi.org/10.1016/j.trsl.2017.09.002

Satoh, N., Ogawa, Y., Katsuura, G., Numata, Y., Masuzaki, H., Yoshimasa, Y., & Nakao, K. (1998). Satiety effect and sympathetic activation of leptin are mediated by hypothalamic melanocortin system. *Neuroscience Letters*, *249*(2–3), 107–110.

Savas, M., Wester, V. L., Staufenbiel, S. M., Koper, J. W., van den Akker, E. L. T., Visser, J. A., … van Rossum, E. F. C. (2017). Systematic Evaluation of Corticosteroid Use in Obese and Non-obese Individuals: A Multi-cohort Study. *International Journal of Medical Sciences*, *14*(7), 615–621. https://doi.org/10.7150/ijms.19213

Sawicka, E., Zuany-Amorim, C., Manlius, C., Trifilieff, A., Brinkmann, V., Kemeny, D. M., & Walker, C. (2003). Inhibition of Th1- and Th2-Mediated Airway Inflammation by the Sphingosine 1-Phosphate Receptor Agonist FTY720. *The Journal of Immunology*, *171*(11), 6206–6214. https://doi.org/10.4049/jimmunol.171.11.6206

Schäfer, D., Schmid, M., Göde, U. C., & Baenkler, H.-W. (1999). Dynamics of eicosanoids in peripheral blood cells during bronchial provocation in aspirin-intolerant asthmatics. *European Respiratory Journal*, *13*(3), 638–646. https://doi.org/10.1183/09031936.99.13363899

Schindelin, J., Arganda-Carreras, I., Frise, E., Kaynig, V., Longair, M., Pietzsch, T., … Cardona, A. (2012). Fiji: An open-source platform for biological-image analysis. *FOCUS ON BIOIMAGE INFORMATICS*, 7.

Schleimer, R. P. (2017). Immunopathogenesis of Chronic Rhinosinusitis and Nasal Polyposis. *Annual Review of Pathology: Mechanisms of Disease*, *12*(1), 331–357. https://doi.org/10.1146/annurev-pathol-052016-100401

Senior, B. A., Kennedy, D. W., Tanabodee, J., Kroger, H., Hassab, M., & Lanza, D. (1998). Long-term Results of Functional Endoscopic Sinus Surgery. *The Laryngoscope*, *108*(2), 151–157. https://doi.org/10.1097/00005537-199802000-00001

Serhan, C. N., Hamberg, M., & Samuelsson, B. (1984). Lipoxins: Novel series of biologically active compounds formed from arachidonic acid in human leukocytes. *Proceedings of the National Academy of Sciences*, *81*(17), 5335–5339. https://doi.org/10.1073/pnas.81.17.5335

Serhan, C. N., & Reardon, E. (1989). 15-Hydroxyeicosatetraenoic acid inhibits superoxide anion generation by human neutrophils: Relationship to lipoxin production. *Free Radical Research Communications*, *7*(3–6), 341–345.

Serhan, C N, & Sheppard, K. A. (1990). Lipoxin formation during human neutrophil-platelet interactions. Evidence for the transformation of leukotriene A4 by platelet 12-lipoxygenase in vitro. *Journal of Clinical Investigation*, *85*(3), 772–780. https://doi.org/10.1172/JCI114503

Serhan, Charles N., Clish, C. B., Brannon, J., Colgan, S. P., Chiang, N., & Gronert, K. (2000). Novel Functional Sets of Lipid-Derived Mediators with Antiinflammatory Actions Generated from Omega-3 Fatty Acids via Cyclooxygenase 2–Nonsteroidal Antiinflammatory Drugs and Transcellular Processing. *The Journal of Experimental Medicine*, *192*(8), 1197–1204. https://doi.org/10.1084/jem.192.8.1197

Sestini, P., Armetti, L., Gambaro, G., Pieroni, M. G., Refini, R. M., Sala, A., … Robuschi, M. (1996). Inhaled PGE2 prevents aspirin-induced bronchoconstriction and urinary LTE4 excretion in aspirin-sensitive asthma. *American Journal of Respiratory and Critical Care Medicine*, *153*(2), 572–575. https://doi.org/10.1164/ajrccm.153.2.8564100

Settipane, G., & Chafee, F. (1977). Nasal polyps in asthma and rhinitis A review of 6,037 patients. *Journal of Allergy and Clinical Immunology*, *59*(1), 17–21. https://doi.org/10.1016/0091-6749(77)90171-3

Shamsuddin, M., Hsueh, W., & Smith, L. J. (1992). Production of leukotrienes and thromboxane by resident and activated rat alveolar macrophages: A possible role of protein kinase C. *The Journal of Laboratory and Clinical Medicine*, *120*(3), 434–443.

Sharma, S. T., & Nieman, L. K. (2011). Cushing's Syndrome: All Variants, Detection, and Treatment. *Endocrinology and Metabolism Clinics of North America*, *40*(2), 379–391. https://doi.org/10.1016/j.ecl.2011.01.006

Sheedy, F. J., Grebe, A., Rayner, K. J., Kalantari, P., Ramkhelawon, B., Carpenter, S. B., … Moore, K. J. (2013). CD36 coordinates NLRP3 inflammasome activation by facilitating intracellular nucleation of soluble ligands into particulate ligands in sterile inflammation. *Nature Immunology*, *14*(8), 812–820. https://doi.org/10.1038/ni.2639

Sher, E. R., Leung, D. Y., Surs, W., Kam, J. C., Zieg, G., Kamada, A. K., & Szefler, S. J. (1994). Steroid-resistant asthma. Cellular mechanisms contributing to inadequate response to glucocorticoid therapy. *Journal of Clinical Investigation*, *93*(1), 33–39. https://doi.org/10.1172/JCI116963

Shimizu, S., Ogawa, T., Seno, S., Kouzaki, H., & Shimizu, T. (2013). Pro-Resolution Mediator Lipoxin A4 and its Receptor in Upper Airway Inflammation. *Annals of Otology, Rhinology & Laryngology*, *122*(11), 683–689. https://doi.org/10.1177/000348941312201104

Shimizu, T. (2009). Lipid Mediators in Health and Disease: Enzymes and Receptors as Therapeutic Targets for the Regulation of Immunity and Inflammation. *Annual Review of Pharmacology and Toxicology*, *49*(1), 123–150. https://doi.org/10.1146/annurev.pharmtox.011008.145616

Shore, S. A., Terry, R. D., Flynt, L., Xu, A., & Hug, C. (2006). Adiponectin attenuates allergen-induced airway inflammation and hyperresponsiveness in mice. *Journal*

of Allergy and Clinical Immunology, *118*(2), 389–395. https://doi.org/10.1016/j.jaci.2006.04.021

Sidibeh, C. O., Pereira, M. J., Abalo, X. M., J. Boersma, G., Skrtic, S., Lundkvist, P., … Eriksson, J. W. (2018). FKBP5 expression in human adipose tissue: Potential role in glucose and lipid metabolism, adipogenesis and type 2 diabetes. *Endocrine*, *62*(1), 116–128. https://doi.org/10.1007/s12020-018-1674-5

Silverman, J. M., Clos, J., de'Oliveira, C. C., Shirvani, O., Fang, Y., Wang, C., … Reiner, N. E. (2010). An exosome-based secretion pathway is responsible for protein export from Leishmania and communication with macrophages. *Journal of Cell Science*, *123*(6), 842–852. https://doi.org/10.1242/jcs.056465

Singhania, A., Rupani, H., Jayasekera, N., Lumb, S., Hales, P., Gozzard, N., … Howarth, P. H. (2017). Altered Epithelial Gene Expression in Peripheral Airways of Severe Asthma. *PLOS ONE*, *12*(1), e0168680. https://doi.org/10.1371/journal.pone.0168680

Siow, D. L., & Wattenberg, B. W. (2012). Mammalian ORMDL Proteins Mediate the Feedback Response in Ceramide Biosynthesis. *Journal of Biological Chemistry*, *287*(48), 40198–40204. https://doi.org/10.1074/jbc.C112.404012

Sladek, K., Dworski, R., Soja, J., Sheller, J. R., Nizankowska, E., Oates, J. A., & Szczeklik, A. (1994). Eicosanoids in bronchoalveolar lavage fluid of aspirin-intolerant patients with asthma after aspirin challenge. *American Journal of Respiratory and Critical Care Medicine*, *149*(4), 940–946. https://doi.org/10.1164/ajrccm.149.4.8143059

Slavin, R. G. (2008). The upper and lower airways: The epidemiological and pathophysiological connection. *Allergy and Asthma Proceedings*, *29*(6), 553–556. https://doi.org/10.2500/aap.2008.29.3169

Smith, M. J., Ford-Hutchinson, A. W., & Bray, M. A. (1980). Leukotriene B: A potential mediator of inflammation. *The Journal of Pharmacy and Pharmacology*, *32*(7), 517–518.

Smith, W. L., & Langenbach, R. (2001). Why there are two cyclooxygenase isozymes. *Journal of Clinical Investigation*, *107*(12), 1491–1495. https://doi.org/10.1172/JCI13271

Smyth, E. M., Grosser, T., Wang, M., Yu, Y., & FitzGerald, G. A. (2009). Prostanoids in health and disease. *Journal of Lipid Research*, *50*(Supplement), S423–S428. https://doi.org/10.1194/jlr.R800094-JLR200

Soler Artigas, M., Wain, L. V., Repapi, E., Obeidat, M., Sayers, I., Burton, P. R., … the SpiroMeta Consortium. (2011). Effect of Five Genetic Variants Associated with Lung Function on the Risk of Chronic Obstructive Lung Disease, and Their Joint Effects on Lung Function. *American Journal of Respiratory and Critical Care Medicine*, *184*(7), 786–795. https://doi.org/10.1164/rccm.201102-0192OC

Sommer, D. D., Rotenberg, B. W., Sowerby, L. J., Lee, J. M., Janjua, A., Witterick, I. J., … Nayan, S. (2016). A novel treatment adjunct for aspirin exacerbated respiratory disease: The low-salicylate diet: a multicenter randomized control crossover trial: Low-salicylate diet in patients with AERD. *International Forum of Allergy & Rhinology*, *6*(4), 385–391. https://doi.org/10.1002/alr.21678

Song, J., Wang, H., Zhang, Y.-N., Cao, P.-P., Liao, B., Wang, Z.-Z., … Liu, Z. (2018). Ectopic lymphoid tissues support local immunoglobulin production in patients with chronic rhinosinusitis with nasal polyps. *Journal of Allergy and Clinical Immunology*, *141*(3), 927–937. https://doi.org/10.1016/j.jaci.2017.10.014

Sood, A., Cui, X., Qualls, C., Beckett, W. S., Gross, M. D., Steffes, M. W., … Jacobs, D. R. (2008). Association between asthma and serum adiponectin concentration in women. *Thorax*, *63*(10), 877–882. https://doi.org/10.1136/thx.2007.090803

Sousa, A., Pfister, R., Christie, P. E., Lane, S. J., Nasser, S. M., Schmitz-Schumann, M., & Lee, T. H. (1997). Enhanced expression of cyclo-oxygenase isoenzyme 2 (COX-2) in asthmatic airways and its cellular distribution in aspirin-sensitive asthma. *Thorax*, *52*(11), 940–945. https://doi.org/10.1136/thx.52.11.940

Sousa, A. R., Parikh, A., Scadding, G., Corrigan, C. J., & Lee, T. H. (2002). Leukotriene-Receptor Expression on Nasal Mucosal Inflammatory Cells in Aspirin-Sensitive Rhinosinusitis. *New England Journal of Medicine*, *347*(19), 1493–1499. https://doi.org/10.1056/NEJMoa013508

Spector, A. A. (2009). Arachidonic acid cytochrome P450 epoxygenase pathway. *Journal of Lipid Research*, *50*(Supplement), S52–S56. https://doi.org/10.1194/jlr.R800038-JLR200

Stachler, R. J. (2015). Comorbidities of asthma and the unified airway: Comorbidities of asthma and the unified airway. *International Forum of Allergy & Rhinology*, *5*(S1), S17–S22. https://doi.org/10.1002/alr.21615

Steinke, J. W., Payne, S. C., & Borish, L. (2012). Interleukin-4 in the Generation of the AERD Phenotype: Implications for Molecular Mechanisms Driving Therapeutic Benefit of Aspirin Desensitization. *Journal of Allergy*, *2012*, 1–9. https://doi.org/10.1155/2012/182090

Stępień, M., Stępień, A., Wlazeł, R. N., Paradowski, M., Banach, M., & Rysz, J. (2014). Obesity indices and inflammatory markers in obese non-diabetic normo- and hypertensive patients: A comparative pilot study. *Lipids in Health and Disease*, *13*(1). https://doi.org/10.1186/1476-511X-13-29

Stevens, W. W., Ocampo, C. J., Berdnikovs, S., Sakashita, M., Mahdavinia, M., Suh, L., … Schleimer, R. P. (2015). Cytokines in Chronic Rhinosinusitis. Role in Eosinophilia and Aspirin-exacerbated Respiratory Disease. *American Journal of Respiratory and Critical Care Medicine*, *192*(6), 682–694. https://doi.org/10.1164/rccm.201412-2278OC

Stevens, W. W., Peters, A. T., Hirsch, A. G., Nordberg, C. M., Schwartz, B. S., Mercer, D. G., … Schleimer, R. P. (2017). Clinical Characteristics of Patients with Chronic Rhinosinusitis with Nasal Polyps, Asthma, and Aspirin-Exacerbated Respiratory Disease. *The Journal of Allergy and Clinical Immunology: In Practice*, *5*(4), 1061-1070.e3. https://doi.org/10.1016/j.jaip.2016.12.027

Sturm, E. M., Schratl, P., Schuligoi, R., Konya, V., Sturm, G. J., Lippe, I. T., … Heinemann, A. (2008). Prostaglandin E2 Inhibits Eosinophil Trafficking through E-Prostanoid 2 Receptors. *The Journal of Immunology*, *181*(10), 7273–7283. https://doi.org/10.4049/jimmunol.181.10.7273

Suissa, S., Ernst, P., Benayoun, S., Baltzan, M., & Cai, B. (2000). Low-Dose Inhaled Corticosteroids and the Prevention of Death from Asthma. *New England Journal of Medicine*, *343*(5), 332–336. https://doi.org/10.1056/NEJM200008033430504

Summer, R., Little, F. F., Ouchi, N., Takemura, Y., Aprahamian, T., Dwyer, D., … Walsh, K. (2008). Alveolar macrophage activation and an emphysema-like phenotype in adiponectin-deficient mice. *American Journal of Physiology-Lung Cellular and Molecular Physiology*, *294*(6), L1035–L1042. https://doi.org/10.1152/ajplung.00397.2007

Sutherland, E. R., Goleva, E., Strand, M., Beuther, D. A., & Leung, D. Y. M. (2008). Body Mass and Glucocorticoid Response in Asthma. *American Journal of Respiratory and Critical Care Medicine*, *178*(7), 682–687. https://doi.org/10.1164/rccm.200801-076OC

Sverdlov, E. D. (2012). Amedeo Avogadro's cry: What is 1 μg of exosomes? *BioEssays*, *34*(10), 873–875. https://doi.org/10.1002/bies.201200045

Sweeney, J., Patterson, C. C., Menzies-Gow, A., Niven, R. M., Mansur, A. H., Bucknall, C., … Heaney, L. G. (2016). Comorbidity in severe asthma requiring systemic corticosteroid therapy: Cross-sectional data from the Optimum Patient Care Research Database and the British Thoracic Difficult Asthma Registry. *Thorax*, *71*(4), 339–346. https://doi.org/10.1136/thoraxjnl-2015-207630

Szczeklik, A., Niżankowska, E., Duplaga, M., & the Aiane Investigators, on behalf of. (2000). Natural history of aspirin-induced asthma. *European Respiratory Journal*, *16*(3), 432. https://doi.org/10.1034/j.1399-3003.2000.016003432.x

Szczeklik, W., Sanak, M., & Szczeklik, A. (2004). Functional effects and gender association of COX-2 gene polymorphism G-765C in bronchial asthma. *Journal of Allergy and Clinical Immunology*, *114*(2), 248–253. https://doi.org/10.1016/j.jaci.2004.05.030

Ta, V., & White, A. A. (2015). Survey-Defined Patient Experiences With Aspirin-Exacerbated Respiratory Disease. *The Journal of Allergy and Clinical Immunology: In Practice*, *3*(5), 711–718. https://doi.org/10.1016/j.jaip.2015.03.001

Takabayashi, T., Kato, A., Peters, A. T., Hulse, K. E., Suh, L. A., Carter, R., … Schleimer, R. P. (2013). Excessive Fibrin Deposition in Nasal Polyps Caused by Fibrinolytic Impairment through Reduction of Tissue Plasminogen Activator Expression. *American Journal of Respiratory and Critical Care Medicine*, *187*(1), 49–57. https://doi.org/10.1164/rccm.201207-1292OC

Takabayashi, T., Kato, A., Peters, A. T., Hulse, K. E., Suh, L. A., Carter, R., … Schleimer, R. P. (2013). Increased expression of factor XIII-A in patients with chronic rhinosinusitis with nasal polyps. *Journal of Allergy and Clinical Immunology*, *132*(3), 584-592.e4. https://doi.org/10.1016/j.jaci.2013.02.003

Takabayashi, T., Kato, A., Peters, A. T., Suh, L. A., Carter, R., Norton, J., … Schleimer, R. P. (2012). Glandular mast cells with distinct phenotype are highly elevated in chronic rhinosinusitis with nasal polyps. *Journal of Allergy and Clinical Immunology*, *130*(2), 410-420.e5. https://doi.org/10.1016/j.jaci.2012.02.046

Takemura, Y., Ouchi, N., Shibata, R., Aprahamian, T., Kirber, M. T., Summer, R. S., … Walsh, K. (2007). Adiponectin modulates inflammatory reactions via calreticulin receptor–dependent clearance of early apoptotic bodies. *Journal of Clinical Investigation*, *117*(2), 375–386. https://doi.org/10.1172/JCI29709

Tang, T., Scambler, T. E., Smallie, T., Cunliffe, H. E., Ross, E. A., Rosner, D. R., … Clark, A. R. (2017). Macrophage responses to lipopolysaccharide are modulated by a feedback loop involving prostaglandin E2, dual specificity phosphatase 1 and tristetraprolin. *Scientific Reports*, *7*(1). https://doi.org/10.1038/s41598-017-04100-1

Telenga, E. D., Tideman, S. W., Kerstjens, H. A. M., Hacken, N. H. T. ten, Timens, W., Postma, D. S., & van den Berge, M. (2012). Obesity in asthma: More neutrophilic inflammation as a possible explanation for a reduced treatment response. *Allergy*, *67*(8), 1060–1068. https://doi.org/10.1111/j.1398-9995.2012.02855.x

The Gene Ontology Consortium. (2019). The Gene Ontology Resource: 20 years and still GOing strong. *Nucleic Acids Research*, *47*(D1), D330–D338. https://doi.org/10.1093/nar/gky1055

Thivierge, M., Stankova, J., & Rola-Pleszczynski, M. (2001). IL-13 and IL-4 Up-Regulate Cysteinyl Leukotriene 1 Receptor Expression in Human Monocytes and Macrophages. *The Journal of Immunology*, *167*(5), 2855–2860. https://doi.org/10.4049/jimmunol.167.5.2855

Tomassen, P., Vandeplas, G., Van Zele, T., Cardell, L.-O., Arebro, J., Olze, H., … Bachert, C. (2016). Inflammatory endotypes of chronic rhinosinusitis based on cluster analysis of biomarkers. *Journal of Allergy and Clinical Immunology*, *137*(5), 1449-1456.e4. https://doi.org/10.1016/j.jaci.2015.12.1324

Tomlinson, G. S., Booth, H., Petit, S. J., Potton, E., Towers, G. J., Miller, R. F., … Noursadeghi, M. (2012). Adherent Human Alveolar Macrophages Exhibit a Transient Pro-Inflammatory Profile That Confounds Responses to Innate Immune Stimulation. *PLoS ONE*, *7*(6), e40348. https://doi.org/10.1371/journal.pone.0040348

Torregrosa Paredes, P., Esser, J., Admyre, C., Nord, M., Rahman, Q. K., Lukic, A., … Gabrielsson, S. (2012). Bronchoalveolar lavage fluid exosomes contribute to cytokine and leukotriene production in allergic asthma. *Allergy*, *67*(7), 911–919. https://doi.org/10.1111/j.1398-9995.2012.02835.x

Tost, J., & Gut, I. G. (2007). DNA methylation analysis by pyrosequencing. *Nature Protocols*, *2*(9), 2265–2275. https://doi.org/10.1038/nprot.2007.314

Trajkovic, K., Hsu, C., Chiantia, S., Rajendran, L., Wenzel, D., Wieland, F., … Simons, M. (2008). Ceramide Triggers Budding of Exosome Vesicles into Multivesicular Endosomes. *Science*, *319*(5867), 1244–1247. https://doi.org/10.1126/science.1153124

Triche, T. J., Weisenberger, D. J., Van Den Berg, D., Laird, P. W., & Siegmund, K. D. (2013). Low-level processing of Illumina Infinium DNA Methylation BeadArrays. *Nucleic Acids Research*, *41*(7), e90–e90. https://doi.org/10.1093/nar/gkt090

Trinh, H. K. T., Kim, S.-C., Cho, K., Kim, S.-J., Ban, G.-Y., Yoo, H.-J., … Kim, S.-H. (2016). Exploration of the Sphingolipid Metabolite, Sphingosine-1-phosphate and Sphingosine, as Novel Biomarkers for Aspirin-exacerbated Respiratory Disease. *Scientific Reports*, *6*(1). https://doi.org/10.1038/srep36599

Trusca, V. G., Fuior, E. V., Fenyo, I. M., Kardassis, D., Simionescu, M., & Gafencu, A. V. (2017). Differential action of glucocorticoids on apolipoprotein E gene expression in macrophages and hepatocytes. *PLOS ONE*, *12*(3), e0174078. https://doi.org/10.1371/journal.pone.0174078

Turk, J., Maas, R. L., Brash, A. R., Roberts, L. J., & Oates, J. A. (1982). Arachidonic acid 15-lipoxygenase products from human eosinophils. *The Journal of Biological Chemistry*, *257*(12), 7068–7076.

Ualiyeva, S., Hallen, N., Kanaoka, Y., Barrett, N. A., & Bankova, L. (2019). Nasal Epithelial Brush Cells Generate Cysteinyl Leukotrienes in Response to Aeroallergens and Stress Signals. *Journal of Allergy and Clinical Immunology*, *143*(2), AB89. https://doi.org/10.1016/j.jaci.2018.12.274

Ubhi, B. K., Conner, A., Duchoslav, E., Evans, A., Robinson, R., Baker, P. R. S., & Watkins, S. (2016). *A Novel Lipid Screening Platform that Provides a Complete Solution for Lipidomics Research*. SCIEX Technical Application Note.

Uematsu, S., Matsumoto, M., Takeda, K., & Akira, S. (2002). Lipopolysaccharide-Dependent Prostaglandin E2 Production Is Regulated by the Glutathione-Dependent Prostaglandin E2 Synthase Gene Induced by the Toll-Like Receptor 4/MyD88/NF-IL6 Pathway. *The Journal of Immunology*, *168*(11), 5811–5816. https://doi.org/10.4049/jimmunol.168.11.5811

Valadi, H., Ekström, K., Bossios, A., Sjöstrand, M., Lee, J. J., & Lötvall, J. O. (2007). Exosome-mediated transfer of mRNAs and microRNAs is a novel mechanism of genetic exchange between cells. *Nature Cell Biology*, *9*(6), 654–659. https://doi.org/10.1038/ncb1596

van Ree, R., Hummelshøj, L., Plantinga, M., Poulsen, L. K., & Swindle, E. (2014). Allergic sensitization: Host-immune factors. *Clinical and Translational Allergy*, *4*(1), 12. https://doi.org/10.1186/2045-7022-4-12

Van Zele, T., Gevaert, P., Holtappels, G., Beule, A., Wormald, P. J., Mayr, S., … Bachert, C. (2010). Oral steroids and doxycycline: Two different approaches to treat nasal polyps. *Journal of Allergy and Clinical Immunology*, *125*(5), 1069-1076.e4. https://doi.org/10.1016/j.jaci.2010.02.020

Vandanmagsar, B., Youm, Y.-H., Ravussin, A., Galgani, J. E., Stadler, K., Mynatt, R. L., … Dixit, V. D. (2011). The NLRP3 inflammasome instigates obesity-induced inflammation and insulin resistance. *Nature Medicine*, *17*(2), 179–188. https://doi.org/10.1038/nm.2279

Varga, E. m., Jacobson, M. r., Masuyama, K., Rak, S., Till, S. j., Darby, Y., … Durham, S. r. (1999). Inflammatory cell populations and cytokine mRNA expression in the nasal mucosa in aspirin-sensitive rhinitis. *European Respiratory Journal*, *14*(3), 610. https://doi.org/10.1034/j.1399-3003.1999.14c21.x

Vento-Tormo, R., Company, C., Rodríguez-Ubreva, J., de la Rica, L., Urquiza, J. M., Javierre, B. M., … Ballestar, E. (2016). IL-4 orchestrates STAT6-mediated DNA demethylation leading to dendritic cell differentiation. *Genome Biology*, *17*(1). https://doi.org/10.1186/s13059-015-0863-2

Virchow, J. C., Backer, V., Kuna, P., Prieto, L., Nolte, H., Villesen, H. H., … de Blay, F. (2016). Efficacy of a House Dust Mite Sublingual Allergen Immunotherapy Tablet in Adults With Allergic Asthma: A Randomized Clinical Trial. *JAMA*, *315*(16), 1715. https://doi.org/10.1001/jama.2016.3964

Wadsworth, S., Sin, D., & Dorscheid. (2011). Clinical update on the use of biomarkers of airway inflammation in the management of asthma. *Journal of Asthma and Allergy*, 77. https://doi.org/10.2147/JAA.S15081

Wakil, S. J., Stoops, J. K., & Joshi, V. C. (1983). Fatty Acid Synthesis and its Regulation. *Annual Review of Biochemistry*, *52*(1), 537–579. https://doi.org/10.1146/annurev.bi.52.070183.002541

Wang, K., Liu, C.-T., Wu, Y.-H., Feng, Y.-L., & Bai, H. (2008). Budesonide/formoterol decreases expression of vascular endothelial growth factor (VEGF) and VEGF receptor 1 within airway remodelling in asthma. *Advances in Therapy*, *25*(4), 342–354. https://doi.org/10.1007/s12325-008-0048-4

Wang, X., Collins, H. L., Ranalletta, M., Fuki, I. V., Billheimer, J. T., Rothblat, G. H., … Rader, D. J. (2007). Macrophage ABCA1 and ABCG1, but not SR-BI, promote macrophage reverse cholesterol transport in vivo. *Journal of Clinical Investigation*, *117*(8), 2216–2224. https://doi.org/10.1172/JCI32057

Wang, Y., Mitchell, J., Sharma, M., Gabriel, A., Moriyama, K., & Palmer, P. P. (2004). Leukotrienes mediate 5-hydroxytryptamine-induced plasm extravasation in the

rat knee joint via CysLT-type receptors. *Inflammation Research*, *53*(2), 66–71. https://doi.org/10.1007/s00011-003-1224-2

Wang, Z.-C., Yao, Y., Wang, N., Liu, J.-X., Ma, J., Chen, C.-L., … Liu, Z. (2018). Deficiency in interleukin-10 production by M2 macrophages in eosinophilic chronic rhinosinusitis with nasal polyps: IL-10 $^{+}$ M2 macrophages in CRSwNP. *International Forum of Allergy & Rhinology*, *8*(11), 1323–1333. https://doi.org/10.1002/alr.22218

Weisberg, S. P., Hunter, D., Huber, R., Lemieux, J., Slaymaker, S., Vaddi, K., … Jr., A. W. F. (2006). CCR2 modulates inflammatory and metabolic effects of high-fat feeding. *Journal of Clinical Investigation*, *116*(1), 115–124. https://doi.org/10.1172/JCI24335

Wenzel, S., Castro, M., Corren, J., Maspero, J., Wang, L., Zhang, B., … Teper, A. (2016). Dupilumab efficacy and safety in adults with uncontrolled persistent asthma despite use of medium-to-high-dose inhaled corticosteroids plus a long-acting β2 agonist: A randomised double-blind placebo-controlled pivotal phase 2b dose-ranging trial. *The Lancet*, *388*(10039), 31–44. https://doi.org/10.1016/S0140-6736(16)30307-5

Wenzel, S. E., Larsen, G. L., Johnston, K., Voelkel, N. F., & Westcott, J. Y. (1990). Elevated Levels of Leukotriene C $_{4}$ in Bronchoalveolar Lavage Fluid from Atopic Asthmatics after Endobronchial Allergen Challenge. *American Review of Respiratory Disease*, *142*(1), 112–119. https://doi.org/10.1164/ajrccm/142.1.112

Wenzel, S. E., Schwartz, L. B., Langmack, E. L., Halliday, J. L., Trudeau, J. B., Gibbs, R. L., & Chu, H. W. (1999). Evidence That Severe Asthma Can Be Divided Pathologically into Two Inflammatory Subtypes with Distinct Physiologic and Clinical Characteristics. *American Journal of Respiratory and Critical Care Medicine*, *160*(3), 1001–1008. https://doi.org/10.1164/ajrccm.160.3.9812110

White, A. A., & Doherty, T. A. (2018). Role of Group 2 Innate Lymphocytes in Aspirin-exacerbated Respiratory Disease Pathogenesis. *American Journal of Rhinology & Allergy*, *32*(1), 7–11. https://doi.org/10.2500/ajra.2018.32.4498

Widal, F., Abrami, P., & Lermoyez, J. (1987). First complete description of the aspirin idiosyncrasy-asthma-nasal polyposis syndrome (plus urticaria)—1922 (with a note on aspirin desensitization). By F. Widal, P. Abrami, J. Lermoyez. *The Journal of Asthma: Official Journal of the Association for the Care of Asthma*, *24*(5), 297–300.

Wiggins, R. C., Glatfelter, A., Kshirsagar, B., & Brukman, J. (1986). Procoagulant activity in normal human urine associated with subcellular particles. *Kidney International*, *29*(2), 591–597.

Wilk, S., Scheibenbogen, C., Bauer, S., Jenke, A., Rother, M., Guerreiro, M., … Skurk, C. (2011). Adiponectin is a negative regulator of antigen-activated T cells. *European Journal of Immunology*, *41*(8), 2323–2332. https://doi.org/10.1002/eji.201041349

Wong, C. K., Cheung, P. F.-Y., & Lam, C. W. K. (2007). Leptin-mediated cytokine release and migration of eosinophils: Implications for immunopathophysiology of allergic inflammation. *European Journal of Immunology*, *37*(8), 2337–2348. https://doi.org/10.1002/eji.200636866

Woodruff, P. G., Boushey, H. A., Dolganov, G. M., Barker, C. S., Yang, Y. H., Donnelly, S., … Fahy, J. V. (2007). Genome-wide profiling identifies epithelial cell genes associated with asthma and with treatment response to corticosteroids.

Proceedings of the National Academy of Sciences, *104*(40), 15858–15863. https://doi.org/10.1073/pnas.0707413104

Worgall, T. S., Veerappan, A., Sung, B., Kim, B. I., Weiner, E., Bholah, R., … Worgall, S. (2013). Impaired Sphingolipid Synthesis in the Respiratory Tract Induces Airway Hyperreactivity. *Science Translational Medicine*, *5*(186), 186ra67-186ra67. https://doi.org/10.1126/scitranslmed.3005765

World Health Organization. (2018). *Fact Sheet on Obesity and Overweight*. Retrieved from https://www.who.int/news-room/fact-sheets/detail/obesity-and-overweight

Wu, T. D., & Nacu, S. (2010). Fast and SNP-tolerant detection of complex variants and splicing in short reads. *Bioinformatics*, *26*(7), 873–881. https://doi.org/10.1093/bioinformatics/btq057

Wung, P. K., Anderson, T., Fontaine, K. R., Hoffman, G. S., Specks, U., Merkel, P. A., … Wegener's Granulomatosis Etanercept Trial Research Group. (2008). Effects of glucocorticoids on weight change during the treatment of Wegener's granulomatosis. *Arthritis & Rheumatism*, *59*(5), 746–753. https://doi.org/10.1002/art.23561

Xia, J., & Wishart, D. S. (2011). Metabolomic Data Processing, Analysis, and Interpretation Using MetaboAnalyst. *Current Protocols in Bioinformatics*, *34*(1), 14.10.1-14.10.48. https://doi.org/10.1002/0471250953.bi1410s34

Xia, P., Wang, L., Moretti, P. A. B., Albanese, N., Chai, F., Pitson, S. M., … Vadas, M. A. (2002). Sphingosine Kinase Interacts with TRAF2 and Dissects Tumor Necrosis Factor-α Signaling. *Journal of Biological Chemistry*, *277*(10), 7996–8003. https://doi.org/10.1074/jbc.M111423200

Xue, L., Fergusson, J., Salimi, M., Panse, I., Ussher, J. E., Hegazy, A. N., … Klenerman, P. (2015). Prostaglandin D2 and leukotriene E4 synergize to stimulate diverse TH2 functions and TH2 cell/neutrophil crosstalk. *Journal of Allergy and Clinical Immunology*, *135*(5), 1358-1366.e11. https://doi.org/10.1016/j.jaci.2014.09.006

Yaghi, L., Poras, I., Simoes, R. T., Donadi, E. A., Tost, J., Daunay, A., … Moreau, P. (2016). Hypoxia inducible factor-1 mediates the expression of the immune checkpoint HLA-G in glioma cells through hypoxia response element located in exon 2. *Oncotarget*, *7*(39). https://doi.org/10.18632/oncotarget.11628

Yamauchi, T., Kamon, J., Ito, Y., Tsuchida, A., Yokomizo, T., Kita, S., … Kadowaki, T. (2003). Cloning of adiponectin receptors that mediate antidiabetic metabolic effects. *Nature*, *423*(6941), 762–769. https://doi.org/10.1038/nature01705

Yang, H.-W., Lee, S.-A., Shin, J.-M., Park, I.-H., & Lee, H.-M. (2017). Glucocorticoids ameliorate TGF-β1-mediated epithelial-to-mesenchymal transition of airway epithelium through MAPK and Snail/Slug signaling pathways. *Scientific Reports*, *7*(1). https://doi.org/10.1038/s41598-017-02358-z

Yang, Y., Sadri, H., Prehn, C., Adamski, J., Rehage, J., Dänicke, S., … Sauerwein, H. (2019). Acylcarnitine profiles in serum and muscle of dairy cows receiving conjugated linoleic acids or a control fat supplement during early lactation. *Journal of Dairy Science*, *102*(1), 754–767. https://doi.org/10.3168/jds.2018-14685

Yao, X., Fredriksson, K., Yu, Z.-X., Xu, X., Raghavachari, N., Keeran, K. J., … Levine, S. J. (2010). Apolipoprotein E Negatively Regulates House Dust Mite–induced Asthma via a Low-Density Lipoprotein Receptor–mediated Pathway. *American Journal of Respiratory and Critical Care Medicine*, *182*(10), 1228–1238. https://doi.org/10.1164/rccm.201002-0308OC

Yeh, Y.-L., Su, M.-W., Chiang, B.-L., Yang, Y.-H., Tsai, C.-H., & Lee, Y. L. (2018). Genetic profiles of transcriptomic clusters of childhood asthma determine specific severe subtype. *Clinical & Experimental Allergy*, *48*(9), 1164–1172. https://doi.org/10.1111/cea.13175

Ying, S., Meng, Q., Scadding, G., Parikh, A., Corrigan, C. J., & Lee, T. H. (2006). Aspirin-sensitive rhinosinusitis is associated with reduced E-prostanoid 2 receptor expression on nasal mucosal inflammatory cells. *Journal of Allergy and Clinical Immunology*, *117*(2), 312–318. https://doi.org/10.1016/j.jaci.2005.10.037

Yoshimine, F., Hasegawa, T., Suzuki, E., Terada, M., Koya, T., Kondoh, A., … Gejyo, F. (2005). Contribution of aspirin-intolerant asthma to near fatal asthma based on a questionnaire survey in Niigata Prefecture, Japan. *Respirology*, *10*(4), 477–484. https://doi.org/10.1111/j.1440-1843.2005.00740.x

Yoshimura, T., Yoshikawa, M., Otori, N., Haruna, S., & Moriyama, H. (2008). Correlation between the Prostaglandin D2/E2 Ratio in Nasal Polyps and the Recalcitrant Pathophysiology of Chronic Rhinosinusitis Associated with Bronchial Asthma. *Allergology International*, *57*(4), 429–436. https://doi.org/10.2332/allergolint.O-08-545

Yvan-Charvet, L., Welch, C., Pagler, T. A., Ranalletta, M., Lamkanfi, M., Han, S., … Tall, A. R. (2008). Increased Inflammatory Gene Expression in ABC Transporter–Deficient Macrophages: Free Cholesterol Accumulation, Increased Signaling via Toll-Like Receptors, and Neutrophil Infiltration of Atherosclerotic Lesions. *Circulation*, *118*(18), 1837–1847. https://doi.org/10.1161/CIRCULATIONAHA.108.793869

Zabeo, D., Cvjetkovic, A., Lässer, C., Schorb, M., Lötvall, J., & Höög, J. (2016). Exosomes purified from a single cell type have diverse morphology and composition. *BioRxiv*. https://doi.org/10.1101/094045

Zerbino, D. R., Achuthan, P., Akanni, W., Amode, M. R., Barrell, D., Bhai, J., … Flicek, P. (2018). Ensembl 2018. *Nucleic Acids Research*, *46*(D1), D754–D761. https://doi.org/10.1093/nar/gkx1098

Zhang, F., Wang, H., Wang, X., Jiang, G., Liu, H., Zhang, G., … Du, J. (2016). TGF-beta induces M2-like macrophage polarization via SNAIL-mediated suppression of a pro-inflammatory phenotype. *Oncotarget*, *7*(32). https://doi.org/10.18632/oncotarget.10561

Zhang, J., Fu, M., Cui, T., Xiong, C., Xu, K., Zhong, W., … Chen, Y. E. (2004). Selective disruption of PPAR 2 impairs the development of adipose tissue and insulin sensitivity. *Proceedings of the National Academy of Sciences*, *101*(29), 10703–10708. https://doi.org/10.1073/pnas.0403652101

Zhang, W., Zhang, J., Cheng, L., Ni, H., You, B., Shan, Y., … Chen, J. (2018). A disintegrin and metalloprotease 10-containing exosomes derived from nasal polyps promote angiogenesis and vascular permeability. *Molecular Medicine Reports*. https://doi.org/10.3892/mmr.2018.8634

Zhang, X., Biagini Myers, J. M., Yadagiri, V. K., Ulm, A., Chen, X., Weirauch, M. T., … Ji, H. (2017). Nasal DNA methylation differentiates corticosteroid treatment response in pediatric asthma: A pilot study. *PLOS ONE*, *12*(10), e0186150. https://doi.org/10.1371/journal.pone.0186150

Zhou, W., Toki, S., Zhang, J., Goleniewksa, K., Newcomb, D. C., Cephus, J. Y., … Peebles, R. S. (2016). Prostaglandin I2 Signaling and Inhibition of Group 2 Innate

Lymphoid Cell Responses. *American Journal of Respiratory and Critical Care Medicine*, *193*(1), 31–42. https://doi.org/10.1164/rccm.201410-1793OC

Zimmer, B., Angioni, C., Osthues, T., Toewe, A., Thomas, D., Pierre, S. C., … Sisignano, M. (2018). The oxidized linoleic acid metabolite 12,13-DiHOME mediates thermal hyperalgesia during inflammatory pain. *Biochimica et Biophysica Acta (BBA) - Molecular and Cell Biology of Lipids*, *1863*(7), 669–678. https://doi.org/10.1016/j.bbalip.2018.03.012

Zissler, U. M., Ulrich, M., Jakwerth, C. A., Rothkirch, S., Guerth, F., Weckmann, M., … Chaker, A. M. (2018). Biomatrix for upper and lower airway biomarkers in patients with allergic asthma. *Journal of Allergy and Clinical Immunology*, *142*(6), 1980–1983. https://doi.org/10.1016/j.jaci.2018.07.027

Zukunft, S., Sorgenfrei, M., Prehn, C., Möller, G., & Adamski, J. (2013). Targeted Metabolomics of Dried Blood Spot Extracts. *Chromatographia*, *76*(19–20), 1295–1305. https://doi.org/10.1007/s10337-013-2429-3

8 Supplemental data

Table 8.1 Lipid mediator profiles of PGE_2/IL4-stimulated aMDM

Lipid mediator	Mean lipid mediator concentrations (ng/mL)								
	Healthy			NT CRSwNP			N-ERD		
	Control	PGE_2	IL4	Control	PGE_2	IL4	Control	PGE_2	IL4
11-HDHA	0.027	0.041	0.043	0.020	0.033	0.027	0.042	0.033	0.045
11,12-DHET	0.040	0.050	0.044	0.069	0.089	0.088	0.101	0.059	0.069
13-HDHA	0.032	0.041	0.043	0.031	0.040	0.049	0.061	0.054	0.053
18-HEPE	0.014	0.035	0.017	0.016	0.025	0.020	0.025	0.031	0.030
5-HEPE	2.426	2.748	2.810	1.689	2.277	2.764	4.359	3.567	4.600
5-HETE	21.067	25.092	26.688	15.509	21.801	24.653	34.500	28.619	37.173
5-oxoETE	0.727	0.830	0.700	0.553	0.700	0.680	1.018	0.854	0.871
LTB_4	40.289	46.076	50.993	34.870	41.050	48.950	66.792	54.218	66.148
LTC_4	0.407	0.586	0.540	0.294	0.565	0.374	0.467	0.456	0.495
LTD_4	0.127	0.197	0.157	0.117	0.170	0.131	0.142	0.138	0.152
LTE_4	0.003	0.003	0.003	0.004	0.004	0.002	0.045	0.037	0.045
cysLTs	0.537	0.785	0.700	0.415	0.739	0.508	0.655	0.632	0.692
LXA_4	0.099	0.160	0.140	0.104	0.122	0.106	0.112	0.114	0.101
PGD_2	0.014	0.013	0.080	0.009	0.014	0.111	0.037	0.020	0.134
PGE_2	0.174	0.000	3.925	0.000	0.253	4.835	0.605	0.000	5.793
$PGF_{2\alpha}$	0.053	0.047	0.062	0.044	0.069	0.079	0.074	0.061	0.081
TXB_2	0.184	0.220	0.236	0.176	0.364	0.257	0.344	0.333	0.423

Mean concentrations of all successfully measured lipid mediators in the SN of aMDM from N-ERD (n = 15), NT CRSwNP (n = 10) and healthy (n = 10) individuals after *in vitro*-stimulation with PGE_2 or IL4 for 24 h.

Table 8.2 Baseline aMDM chemokine/cytokine profile

Analyte	Mean concentration (pg/mL)			p value			log2 Fold Change		
	Healthy	CRSwNP	N-ERD	N *vs.* H	N *vs.* C	C *vs.* H	N *vs.* H	N *vs.* C	C *vs.* H
CXCL1	682.9	649.2	657.4	> 0.999	> 0.999	> 0.999	-0.055	0.018	-0.073
CXCL2	40.4	26.3	31.6	> 0.999	> 0.999	> 0.999	-0.356	0.266	-0.622
CXCL8	1080.2	1012.4	1334.2	> 0.999	> 0.999	> 0.999	0.305	0.398	-0.093
CXCL9	761.6	764.6	761.6	> 0.999	> 0.999	> 0.999	0.000	-0.006	0.006
CXCL10	131.3	27.7	39.7	> 0.999	> 0.999	> 0.999	-1.727	0.519	-2.246
CXCL11	198.8	244.9	137.3	N/A	N/A	N/A	-0.534	-0.835	0.301
CCL5	21.9	24.4	19.9	0.699	> 0.999	> 0.999	-0.141	-0.297	0.156
CCL11	84.1	82.7	83.4	> 0.999	> 0.999	> 0.999	-0.012	0.012	-0.024
CCL17	2650.4	175.5	171.2	> 0.999	0.502	0.558	-3.953	-0.036	-3.917
TNF	8.6	10.5	11.6	> 0.999	> 0.999	> 0.999	0.431	0.135	0.296
IL-1β	61.1	72.0	74.5	> 0.999	> 0.999	> 0.999	0.285	0.049	0.235
IL-6	75.1	66.2	68.6	> 0.999	> 0.999	> 0.999	-0.130	0.053	-0.182
IL-12p70	363.2	331.7	198.1	> 0.999	0.302	0.182	-0.875	-0.744	-0.131
IL-18	36.3	36.6	34.1	> 0.999	> 0.999	> 0.999	-0.090	-0.103	0.012
IL-33	35.5	35.2	35.3	0.908	> 0.999	> 0.999	-0.010	0.002	-0.012
IL-10	6.2	5.3	5.4	> 0.999	> 0.999	> 0.999	-0.196	0.047	-0.243
IL-27	N/A	N/A	N/A	N/A	N/A	N/A	N/A	N/A	N/A

Mean baseline chemokine/cytokine concentrations in PMN SN of N-ERD (n = 15), NT CRSwNP (n = 10) and healthy (n = 8) individuals. cysLTs, sum of LTC_4, LTD_4 and LTE_4; H, healthy; C, NT CRSwNP; N, N-ERD. Data were analyzed with the Kruskal-Wallis test with Dunn's correction: $p < 0.05$.

Table 8.3 Lipid mediator profile of PGE_2/IL4-stimulated aMDM – statistical analysis

Lipid mediator	2-way ANOVA: intergroup stimulations (adjusted *p* value)									2-way ANOVA: intragroup stimulations (adjusted *p* value)					
	Control			PGE_2			IL4			Control *vs.* PGE_2			Control *vs.* IL4		
	N *vs.* H	N *vs.* C	C *vs.* H	N *vs.* H	N *vs.* C	C *vs.* H	N *vs.* H	N *vs.* C	C *vs.* H	Healthy	CRSwNP	N-ERD	Healthy	CRSwNP	N-ERD
11-HDHA	0.365	0.126	0.836	0.984	0.257	0.384	0.751	> 0.999	0.777	0.163	0.668	0.913	0.236	0.296	0.456
11,12-DHET	**0.036**	0.383	0.505	0.576	0.712	0.217	0.918	0.442	0.285	0.966	0.504	0.090	0.838	0.469	**0.023**
13-HDHA	**0.043**	**0.036**	0.998	0.673	0.938	0.881	0.492	0.457	0.998	0.430	0.124	0.506	0.547	0.538	0.643
18-HEPE	0.593	0.697	0.987	0.509	0.670	0.968	0.939	0.829	0.662	0.902	0.844	0.767	0.058	0.551	0.668
5-HEPE	0.158	**0.032**	0.784	0.204	0.189	0.999	0.713	0.434	0.905	0.524	**0.016**	0.710	0.629	0.242	**0.047**
5-HETE	0.203	**0.044**	0.782	0.375	0.249	0.967	0.894	0.658	0.917	0.170	**0.015**	0.563	0.381	0.115	0.088
5-oxoETE	0.307	0.053	0.687	0.663	0.599	0.995	0.992	0.717	0.811	0.955	0.381	0.204	0.523	0.285	0.142
LTB_4	0.232	0.123	0.946	0.616	0.537	0.992	0.869	0.693	0.954	0.205	0.076	0.991	0.602	0.563	0.070
LTC_4	0.985	0.882	0.954	0.992	0.941	0.904	0.933	0.952	0.998	0.489	0.760	0.956	0.292	0.074	0.993
LTD_4	0.987	0.966	0.996	0.999	0.976	0.968	0.826	0.947	0.964	0.591	0.891	0.927	0.083	0.231	0.988
LTE_4	0.241	0.255	> 0.999	0.247	0.234	> 0.999	0.388	0.425	0.998	> 0.999	0.954	0.998	> 0.999	0.987	0.262
cysLTs	0.966	0.868	0.968	> 0.999	0.919	0.922	0.944	0.972	0.995	0.507	0.795	0.951	0.229	0.093	0.981
LXA_4	0.924	0.969	0.990	0.505	0.989	0.631	0.406	0.973	0.579	0.198	0.997	0.821	**0.039**	0.699	0.994
PGD_2	0.432	0.303	0.972	**0.013**	0.421	0.282	0.927	0.943	0.999	**< 0.001**	**< 0.001**	**< 0.001**	0.998	0.934	0.342
PGE_2	N/A	N/A	N/A	N/A	N/A	N/A	N/A	N/A	N/A	N/A	N/A	N/A	N/A	N/A	N/A
$PGF_{2\alpha}$	0.541	0.311	0.922	0.635	0.994	0.730	0.768	0.931	0.583	0.786	0.068	0.869	0.911	0.234	0.544
TXB_2	0.470	0.436	0.998	0.361	0.448	0.988	0.683	0.973	0.582	0.756	0.520	0.458	0.875	0.051	0.984

Statistical analysis of all successfully measured lipid mediators in the SN of aMDM *in vitro*-stimulated with PGE_2 or IL4 for 24 h. H, healthy; C, NT CRSwNP; N, N-ERD; N/A, not available (due to not detectable lipid mediators in some conditions). Significance threshold by 2-way ANOVA: $p < 0.05$.

Table 8.4 Chemokine/cytokine profile of PGE_2/IL4-stimulated aMDM – statistical analysis

Analyte	2-way ANOVA: intergroup stimulations (adjusted *p* value)									2-way ANOVA: intragroup stimulations (adjusted *p* value)					
	Control			PGE_2			IL4			Control *vs.* PGE_2			Control *vs.* IL4		
	N *vs.* H	N *vs.* C	C *vs.* H	N *vs.* H	N *vs.* C	C *vs.* H	N *vs.* H	N *vs.* C	C *vs.* H	Healthy	CRSwNP	N-ERD	Healthy	CRSwNP	N-ERD
CXCL1	0.996	> 0.999	0.993	0.998	> 0.999	0.998	0.125	0.197	0.962	0.090	0.989	0.905	> 0.999	0.999	> 0.999
CXCL2	0.991	0.997	0.976	0.967	> 0.999	0.968	0.181	0.486	0.776	**0.035**	0.701	0.287	0.998	0.994	0.975
CXCL8	0.954	0.928	0.997	> 0.999	0.999	> 0.999	0.989	0.789	0.706	0.109	0.147	**0.017**	0.737	0.846	0.297
CXCL9	> 0.999	0.972	0.972	0.892	0.892	> 0.999	> 0.999	**0.035**	**0.035**	0.592	0.457	0.177	0.870	0.738	> 0.999
CXCL10	0.701	0.994	0.636	0.745	0.998	0.712	0.218	0.201	0.999	0.324	0.974	0.842	0.919	0.992	0.970
CXCL11	N/A	N/A	N/A	N/A	N/A	N/A	N/A	N/A	N/A	N/A	N/A	N/A	N/A	N/A	N/A
CCL5	0.934	0.718	0.903	0.364	0.739	0.796	0.702	0.953	0.866	0.460	0.793	0.972	0.854	0.979	0.127
CCL11	0.858	0.858	0.550	0.934	0.657	0.447	0.448	0.550	0.082	0.068	**0.043**	> 0.999	0.827	0.953	0.664
CCL17	> 0.999	> 0.999	> 0.999	0.285	0.760	0.101	0.930	0.869	0.986	0.504	0.574	0.659	0.984	0.079	0.207
TNF	0.632	0.945	0.819	0.208	0.313	0.962	0.996	0.991	0.999	0.420	0.123	0.059	0.664	0.903	0.177
IL-1β	0.884	0.996	0.921	0.999	0.799	0.776	0.602	0.892	0.864	**0.001**	0.415	0.766	0.502	**0.009**	0.441
IL-6	0.992	0.999	0.985	0.839	0.913	0.986	0.888	0.998	0.916	0.975	0.603	0.898	> 0.999	> 0.999	0.235
IL-12 p70	0.369	0.514	0.962	0.362	0.822	0.709	0.891	0.908	0.659	0.930	0.891	0.753	0.994	0.766	0.992
IL-18	0.835	0.792	0.996	0.788	0.913	0.965	0.588	0.563	0.999	0.198	0.134	0.987	> 0.999	0.459	0.947
IL-33	0.684	0.985	0.582	0.784	> 0.999	0.783	0.392	0.985	0.482	0.745	0.926	0.350	0.744	0.533	0.637
IL-10	0.759	0.987	0.665	0.849	0.840	0.518	0.214	0.445	0.867	0.256	0.727	0.969	0.987	0.851	0.811
IL-27	N/A	N/A	N/A	N/A	N/A	N/A	N/A	N/A	N/A	N/A	N/A	N/A	N/A	N/A	N/A

Statistical analysis of 17 chemokines/cytokines in the SN of aMDM *in vitro*-stimulated with PGE_2 or IL4 for 24 h. H, healthy; C, NT CRSwNP; N, N-ERD; N/A, not available (due to not detectable chemokines/cytokines in some conditions). Significance threshold by 2-way ANOVA: $p < 0.05$.

Table 8.5 Targeted methylomics - PMN

Target genes	Target CpG site	Targeted methylation (%)			Kruskal-Wallis with Dunn's correction (*p* value)		
		Healthy	CRSwNP	N-ERD	N *vs.* H	N *vs.* C	C *vs.* H
PGDS	cg12554857	4.54	5.57	3.79	0.957	0.562	> 0.999
	CpG 3	3.26	4.32	2.88	0.632	0.151	> 0.999
	median	3.90	4.95	3.34	0.804	0.278	> 0.999
LTB4	CpG4	1.58	3.12	2.06	> 0.999	0.428	0.124
	CpG3	2.94	3.57	3.30	> 0.999	> 0.999	> 0.999
	CpG2	0.46	0.47	0.45	> 0.999	> 0.999	> 0.999
	cg20542800	1.38	1.91	1.26	0.784	**0.040**	0.653
	median	1.48	2.22	1.57	> 0.999	0.208	0.260
ALOX5AP	CpG1	0.81	0.84	0.47	0.555	0.434	> 0.999
	cg08529529	2.63	2.70	2.15	0.682	0.497	> 0.999
	median	1.72	1.77	1.31	0.535	0.323	> 0.999
PTGES	CpG3	82.27	80.24	81.05	> 0.999	0.958	> 0.999
	CpG4	76.42	75.93	75.38	> 0.999	> 0.999	> 0.999
	cg26672426	62.36	57.93	62.06	> 0.999	0.624	0.550
	CpG6	76.79	71.50	73.41	0.836	0.764	0.127
	CpG7	79.57	80.50	79.90	> 0.999	> 0.999	> 0.999
	CpG8	85.72	85.51	84.13	> 0.999	> 0.999	> 0.999
	CpG9	89.60	84.83	85.33	0.744	> 0.999	0.266
	CpG10	84.52	84.29	82.25	> 0.999	> 0.999	> 0.999
	CpG11	60.81	57.06	54.86	> 0.999	> 0.999	0.826
	CpG12	70.12	70.93	68.01	> 0.999	> 0.999	> 0.999
	median	78.38	76.86	76.35	> 0.999	> 0.999	0.594

Targeted methylomics analysis of PMN DNA from N-ERD (n = 15), NT CRSwNP (n = 10) and healthy (n = 10) individuals. N, N-ERD; C, NT CRSwNP, H, healthy. Data shown as mean percentage of CpG sites or *median* of all CpG sites (gene region) of one gene. Significance threshold by Kruskal-Wallis with Dunn's correction: $p < 0.05$.

Table 8.6 Targeted methylomics - monocytes

Target genes	Target CpG site	Targeted methylation (%)			Kruskal-Wallis with Dunn's correction (*p value*)		
		Healthy	CRSwNP	N-ERD	N *vs.* H	N *vs.* C	C *vs.* H
PGDS	cg12554857	1.85	2.45	1.52	> 0.999	> 0.999	> 0.999
	CpG 3	1.26	2.38	2.73	0.193	> 0.999	0.656
	median	1.55	2.41	2.12	0.949	> 0.999	0.645
LTB4	CpG4	2.59	2.62	2.40	> 0.999	> 0.999	> 0.999
	CpG3	3.02	3.75	4.23	0.170	0.928	> 0.999
	CpG2	0.32	1.78	1.04	> 0.999	0.708	0.192
	cg20542800	1.29	1.40	1.36	> 0.999	> 0.999	> 0.999
	median	1.38	2.20	1.98	0.245	> 0.999	0.229
ALOX5AP	CpG1	0.91	0.27	0.62	> 0.999	> 0.999	> 0.999
	cg08529529	3.57	4.74	4.68	> 0.999	> 0.999	0.961
	median	2.24	2.51	2.65	> 0.999	> 0.999	> 0.999
PTGES	CpG3	82.42	80.92	84.09	> 0.999	> 0.999	> 0.999
	CpG4	80.59	80.36	80.92	> 0.999	> 0.999	> 0.999
	cg26672426	61.90	58.24	59.91	> 0.999	> 0.999	> 0.999
	CpG6	70.77	75.46	73.21	> 0.999	> 0.999	> 0.999
	CpG7	85.98	80.29	83.84	> 0.999	0.992	0.275
	CpG8	89.23	90.09	90.57	> 0.999	> 0.999	> 0.999
	CpG9	88.89	91.98	89.44	> 0.999	> 0.999	> 0.999
	CpG10	76.35	83.61	88.96	0.098	0.362	> 0.999
	CpG11	61.82	62.75	62.66	> 0.999	> 0.999	> 0.999
	CpG12	64.53	73.21	68.52	0.499	> 0.999	0.122
	median	79.17	78.07	79.88	> 0.999	0.751	> 0.999

Targeted methylomics analysis of monocyte DNA from N-ERD (n = 15), NT CRSwNP (n = 10) and healthy (n = 10) individuals. N, N-ERD; C, NT CRSwNP, H, healthy. Data shown as mean percentage of CpG sites or *median* of all CpG sites (gene region) of one gene. Significance threshold by Kruskal-Wallis with Dunn's correction: $p < 0.05$.

Table 8.7 Targeted methylomics – methylation % of stimulated aMDM

Target gene	Target CpG sites	Targeted methylation (%)								
		Healthy (n = 10)			NT CRSwNP (n = 8)			N-ERD (n = 13)		
		Control	PGE_2	IL4	Control	PGE_2	IL4	Control	PGE_2	IL4
PGDS	cg12554857	3.25	2.58	2.27	2.26	1.10	3.17	3.61	2.82	2.18
	CpG 3	3.45	3.86	4.88	2.94	3.86	2.85	2.80	2.92	3.42
	median	3.35	3.22	3.57	2.60	2.48	3.01	3.21	2.87	2.80
LTB4R	CpG4	3.85	2.29	1.49	2.66	1.99	4.31	1.60	2.41	3.00
	CpG3	4.09	3.58	4.77	3.24	4.55	4.95	4.02	3.27	4.70
	CpG2	1.66	1.59	0.81	2.79	1.63	1.47	1.79	1.30	1.34
	cg20542800	1.95	1.92	1.90	1.59	1.26	1.38	1.15	1.18	1.48
	median	2.76	2.29	1.76	2.65	1.97	2.84	1.88	1.94	1.97
ALOX 5AP	CpG1	1.06	0.03	0.96	1.50	1.41	1.27	1.12	2.07	0.12
	cg08529529	2.20	3.51	3.39	3.18	3.68	3.92	3.98	4.44	4.74
	median	1.63	1.77	2.17	2.34	2.55	2.59	2.55	3.26	2.43
PTGES	CpG3	86.71	84.42	84.48	83.73	85.53	83.45	80.57	85.29	85.88
	CpG4	84.85	83.89	84.39	82.66	80.37	79.71	84.51	86.90	80.14
	cg26672426	62.10	64.17	61.37	67.21	63.20	53.32	63.94	61.08	61.29
	CpG6	81.75	75.56	77.42	75.44	78.30	71.80	70.48	72.96	73.47
	CpG7	92.75	88.24	85.67	83.04	83.71	83.75	86.80	89.87	86.43
	CpG8	95.08	85.02	92.28	90.72	90.88	82.74	88.09	88.67	87.30
	CpG9	88.40	93.12	92.18	89.18	88.08	84.28	83.77	88.51	89.90
	CpG10	90.60	93.24	91.73	78.72	83.27	76.94	82.35	82.30	80.36
	CpG11	67.73	62.28	61.58	61.42	65.97	64.08	60.59	63.99	60.83
	CpG12	73.70	70.00	70.88	69.40	72.47	70.66	66.94	68.78	69.83
	median	84.69	83.50	83.22	80.06	79.25	75.90	78.57	82.39	79.52

Targeted methylomics analysis of aMDM DNA from N-ERD, NT CRSwNP and healthy individuals stimulated with PGE_2 or IL4 for 24 h. N, N-ERD; C, NT CRSwNP, H, healthy. Data shown as mean percentage of CpG sites or *median* of all CpG sites (gene region) of one gene.

Table 8.8 Targeted methylomics – statistical analysis of stimulated aMDM

Target gene	Target CpG site	2-way ANOVA: intergroup stimulations (adjusted p value)								
		Control			PGE_2			IL4		
		N *vs.* H	N *vs.* C	C *vs.* H	N *vs.* H	N *vs.* C	C *vs.* H	N *vs.* H	N *vs.* C	C *vs.* H
PGDS	cg12554857	0.997	0.661	0.732	0.931	0.976	0.826	0.988	0.569	0.691
	CpG 3	0.972	0.997	0.960	0.423	0.586	0.922	0.848	0.858	> 0.999
	median	0.996	0.819	0.798	0.885	0.769	0.985	0.976	0.930	0.855
LTB4R	CpG4	**0.043**	0.603	0.388	**0.015**	0.198	0.367	0.936	0.793	0.953
	CpG3	0.996	0.703	0.777	> 0.999	0.957	0.966	0.906	0.367	0.646
	CpG2	0.951	0.462	0.360	0.741	0.777	0.988	0.931	0.917	0.999
	cg20542800	0.274	0.777	0.731	0.587	0.612	0.987	0.457	0.992	0.603
	median	0.109	0.224	0.958	0.083	0.897	0.142	0.700	0.997	0.790
ALOX 5AP	CpG1	0.822	0.955	0.696	0.980	0.566	0.463	0.067	0.733	0.373
	cg08529529	0.209	0.603	0.796	0.706	0.225	0.728	0.641	0.755	0.988
	median	0.194	0.847	0.534	0.731	0.829	0.969	0.064	0.526	0.544
PTGES	CpG3	0.308	0.830	0.718	0.998	0.855	0.895	0.985	0.999	0.981
	CpG4	0.951	0.888	0.765	0.728	0.740	0.994	0.713	0.234	0.693
	cg26672426	0.804	0.853	0.541	0.550	0.980	0.390	0.858	0.935	0.988
	CpG6	0.094	0.675	0.516	0.649	0.764	0.956	0.891	0.636	0.902
	CpG7	0.642	0.802	0.352	0.978	0.969	0.894	0.956	0.554	0.760
	CpG8	0.428	0.876	0.787	0.295	0.705	0.670	0.760	0.910	0.570
	CpG9	0.706	0.555	0.966	0.418	0.951	0.529	0.631	0.996	0.646
	CpG10	0.540	0.880	0.349	0.183	0.286	0.893	0.295	0.991	0.443
	CpG11	0.168	0.983	0.313	0.861	0.990	0.765	0.923	0.905	0.743
	CpG12	0.427	0.884	0.776	0.990	0.946	0.986	0.968	0.758	0.899
	median	0.214	0.932	0.468	0.352	0.790	0.662	0.958	0.734	0.615

Targeted methylomics analysis of aMDM DNA from N-ERD, NT CRSwNP and healthy individuals stimulated with PGE_2 or IL4 for 24 h. N, N-ERD; C, NT CRSwNP, H, healthy. Significance threshold by 2-way ANOVA: $p < 0.05$.

Table 8.9 Genome-wide methylomics – monocytes and aMDM

Overlapping promoters	Chromosome			Number of CpGs	aMDM		Monocyte	
	number	start	end		Stouffer	mean Δβ FC	Stouffer	mean Δβ FC
CPT1A	chr11	68607068	68607257	2	**0.031**	-0.023	N/A	N/A
CPT1B	chr22	51016385	51017162	14	**0.008**	0.056	**< 0.001**	0.066
ACACA	chr17	35715685	35716004	3	**0.029**	-0.015	N/A	N/A
PF4	chr4	74847099	74848667	10	**0.001**	-0.160	**< 0.001**	-0.187
CXCL2	chr4	74964855	74965262	5	**0.009**	-0.027	N/A	N/A
FGF7	chr15	49715341	49716270	5	**< 0.001**	-0.161	**< 0.001**	-0.161

Statistics of overlapping gene promoters of DMRs from monocytes and aMDM of N-ERD (n = 15) and healthy (n = 8) individuals. Δβ, delta beta; FC, Fold Change. Significance threshold by Stouffer: < 0.05.

Table 8.10 Top functional pathways altered between N-ERD sMac and aMDM

Pathway	Analysis	q value Bonferroni	DEGs in pathway	Total genes in pathway
chemokine activity	Molecular function	**< 0.001**	22	48
cytokine activity		**< 0.001**	61	222
cytokine receptor activity		**0.003**	31	90
chemokine receptor binding		**0.010**	23	60
nucleotide receptor activity		**0.029**	12	22
purinergic nucleotide receptor activity		**0.029**	12	22
extracellular matrix binding		**0.037**	21	56
defense response	Biological process	**7.68E-31**	416	1651
inflammatory response		**1.87E-28**	223	711
immune response		**1.06E-27**	392	1572
regulation of immune system process		**8.07E-20**	355	1506
positive regulation of immune system process		**1.68E-18**	252	976
cytokine production		**3.81E-17**	194	700
regulation of inflammatory response		**1.95E-16**	116	341
adaptive immune response		**1.26E-15**	128	402
regulation of response to wounding		**3.92E-15**	142	472
innate immune response		**9.20E-15**	216	846
regulation of cytokine production		**1.92E-14**	173	631
regulation of defense response		**2.00E-14**	210	820
regulation of immune response		**2.13E-14**	225	899
cell activation		**2.42E-14**	244	1001
leukocyte activation		**3.02E-14**	211	828

ToppGene molecular function and biological process analysis results of DEGs between N-ERD sMac and aMDM as revealed by RNAseq. All significant molecular function and the top 15 significant biological process pathways are shown. Significance threshold by Bonferroni: q < 0.05.

Table 8.11 Hierarchical clusters of analytes in targeted metabolomics

Analysis	Analyte group	Cluster analysis – number and % of analytes									
		I	%	II	%	III	%	IV	%	V	%
Sputum	Acylcarnitine	0	0	**38**	**95.0**	2	5.0				
	Sphingomyeline	5	33.3	1	6.7	9	**60.0**				
	Amino acid / biogenic amine	0	0.0	13	39.4	**20**	**60.6**				
	Phosphatidylcholine aa/ae	**35**	**38.9**	23	25.6	**32**	**35.6**				
	Sum of carbohydrates	0	0	**1**	**100**	0	0				
NLF	Acylcarnitine	**38**	**95.0**	2	5.0	0	0	0	0		
	Sphingomyeline	2	13.3	1	6.7	**11**	**73.3**	1	6.7		
	Amino acid / biogenic amine	**13**	**35.1**	**13**	**35.1**	5	13.5	6	16.2		
	Phosphatidylcholine aa/ae	**31**	**34.4**	4	4.4	25	27.8	**30**	**33.3**		
	Sum of carbohydrates	0	0	0	0	0	0	**1**	**100.0**		
Plasma	Acylcarnitine	6	15.0	4	10.0	9	22.5	6	15.0	**15**	**37.5**
	Sphingomyeline	0	0	0	0	1	6.7	2	13.3	**12**	**80.0**
	Amino acid / biogenic amine	9	28.1	**11**	**34.4**	8	25.0	1	3.1	3	9.4
	Phosphatidylcholine aa/ae	**24**	**26.7**	12	13.3	15	16.7	14	15.6	**25**	**27.8**
	Sphingolipid metabolomics (II)	0	0	2	8.3	**10**	**41.7**	6	25.0	6	25.0
	Sum of carbohydrates	**1**	**100.0**	0	0	0	0	0	0	0	0

Targeted metabolomics hierarchical clustering analysis of sputum, NLF and plasma in healthy (n = 3-9), NT CRSwNP (n = 0-10) and N-ERD (n = 5-13) individuals. Number and percentage of analytes per analyte group in each cluster are shown. Clusters with highest percentages are marked as bold for each analyte group.

Table 8.12 Lipid mediator profile of NLF

Lipid mediator progenitor	Lipid mediator	Concentration (ng/µL NLF)		p value	log2 Fold Change
		Healthy	N-ERD		
EPA	12-HEPE	0.0086	0	**0.048**	N/A
	15-HEPE	0.0816	0.0169	0.111	-2.270
LA	9-HODE	0.1058	0.0079	**0.032**	-3.746
	9,10-DiHOME	0.0321	0.0157	0.286	-1.033
	12,13-DiHOME	0.0263	0.0121	0.064	-1.126
	13-HODE	3.2617	0.4399	**0.016**	-2.890
AA	8,9-EET	0.0046	0	**0.029**	N/A
	9-HETE	0.0031	0.0007	0.103	-2.057
	12-oxoETE	0.0676	0.0561	0.657	-0.267
	12-HETE	0.0861	0.0453	0.373	-0.926
	15-HETE	0.6711	0.2817	0.286	-1.252
	15-HETrE	0.0560	0.0195	0.286	-1.521
	15-oxoETE	0.1038	0.0606	0.556	-0.775
	LTB_4	0.0157	0.0071	0.343	-1.149
	LTE_4	0.0003	0.0041	0.543	3.981
	PGD_2	0.0292	0.0002	**0.016**	-7.367
	PGE_2	0.0513	0.0404	0.714	-0.347
	$PGF_{2\alpha}$	0.0199	0.0148	0.413	-0.426
	TXB_2	0.0048	0.0016	0.365	-1.594
DHA	17-HDHA	0.2162	0.0570	**0.016**	-1.924
	RvD_2	0.0084	N/A	N/A	N/A

Lipid mediator concentrations in NLF of N-ERD (n = 5) and healthy (n = 4) individuals. EPA, eicosapentaenoic acid; LA, linoleic acid; AA, arachidonic acid; DHA, docosahexaenoic acid. Data were analyzed with the Mann-Whitney test: $p < 0.05$.

Table 8.13 Chemokine/cytokine profile of hBECs stimulated with sputum-derived exosomes

Analyte	Concentration in exosome isolations (pg/mL)			Concentration in SN of stimulated hBECs (pg/mL)			hBECs stimulations: *p* value			log2 Fold Change		
	qPBS	H exos	N exos	qPBS	H exos	N exos	H *vs.* qPBS	N *vs.* qPBS	N *vs.* H	H *vs.* qPBS	N *vs.* qPBS	N *vs.* H
GM-CSF	0	0	0	81.36	108.9	143.5	> 0.999	**0.040**	0.232	0.421	0.819	0.398
Periostin	6760	7219	7219	7171	7215	7170	> 0.999	> 0.999	> 0.999	0.009	0.000	-0.009
CXCL8	0	1.239	10.5	39.56	92.59	249	0.342	**0.005**	0.342	1.227	2.654	1.427
CCL2	38.79	38.79	36.02	40.38	41.39	42.13	> 0.999	> 0.999	> 0.999	0.036	0.061	0.026
CCL26	23.06	23.06	22.34	23.88	24.98	25.85	0.120	**0.022**	> 0.999	0.065	0.114	0.049
IL25	0	131.4	131.4	151	129.7	110.3	0.618	0.342	> 0.999	-0.219	-0.453	-0.234
IL33	8.74	11.99	7.083	9.718	10.04	10.19	> 0.999	> 0.999	> 0.999	0.047	0.068	0.021
TSLP	0	0	0	0	0	0	N/A	N/A	N/A	N/A	N/A	N/A

Concentrations and statistical analysis of 8 chemokines/cytokines in exosome isolations from sputum and the SN of hBECs *in vitro*-stimulated with exosomes isolations (qPBS, healthy, N-ERD) for 24 h. qPBS, qEV SEC-processed PBS; H, healthy; N, N-ERD; N/A, not available (due to not detectable analytes in some conditions). Data were analyzed with the Friedman test with Dunn's correction test: $p < 0.05$.

Table 8.14 Chemokine/cytokine profile of aMDM stimulated with sputum-derived exosomes

Analyte	Concentration in exosome isolations (pg/mL)			Concentration in SN of stimulated aMDM (pg/mL)			aMDM stimulations: *p* value			log2 Fold Change		
	qPBS	H exos	N exos	qPBS	H exos	N exos	H *vs.* qPBS	N *vs.* qPBS	N *vs.* H	H *vs.* qPBS	N *vs.* qPBS	N *vs.* H
CXCL1	209.62	389.06	244.31	248.94	6354.71	976.15	**< 0.001**	0.401	0.073	4.674	1.971	-2.703
CXCL2	0	0	0	21.97	2158.28	195.56	N/A	N/A	**0.008***	6.618	3.154	-3.464
CXCL8	0	4.42	11.30	7028.23	75757.28	45743.45	**0.001**	0.240	0.240	3.430	2.702	-0.728
CXCL9	1429.28	1535.81	1485.81	1448.15	1512.36	1462.29	**< 0.001**	0.313	0.137	0.063	0.014	-0.049
CXCL10	0	3.29	1.00	5.98	5.13	14.05	> 0.999	> 0.999	> 0.999	-0.222	1.233	1.455
CXCL11	0	14.92	0	41.07	187.85	115.10	**< 0.001**	0.401	0.073	2.193	1.487	-0.707
CCL5	24.07	26.31	25.11	34.14	354.09	51.61	**< 0.001**	0.401	0.073	3.375	0.596	-2.779
CCL11	155.02	204.39	169.93	179.38	205.68	175.70	0.507	0.507	**0.018**	0.197	-0.030	-0.227
CCL17	160.09	272.71	189.40	1636.04	1808.98	1805.95	**0.018**	**0.037**	> 0.999	0.145	0.143	-0.002
TNF	1.01	25.43	7.46	30.38	5108.39	133.13	**< 0.001**	0.401	0.073	7.394	2.132	-5.262
IL1β	7.11	19.05	10.45	16.33	459.37	44.77	**< 0.001**	0.401	0.073	4.814	1.455	-3.359
IL6	4.04	7.15	5.38	146.03	15885.25	1435.80	**< 0.001**	0.401	0.073	6.765	3.298	-3.468
IL12p70	0	318.42	42.38	5.30	222.20	27.90	N/A	N/A	**0.016***	5.390	2.397	-2.994
IL18	0	42.52	12.12	12.07	262.59	51.89	**< 0.001**	0.401	0.073	4.444	2.105	-2.339
IL33	9.52	28.14	15.70	12.61	28.15	16.67	**< 0.001**	0.240	0.101	1.159	0.403	-0.756
IL10	0	0	0	0	27.52	0.13	N/A	N/A	N/A	N/A	N/A	-7.695
IL27	293.93	1034.42	415.50	362.23	611.44	434.70	**< 0.001**	0.401	0.073	0.755	0.263	-0.492

Concentrations and statistical analysis of 17 chemokines/cytokines in exosome isolations from sputum and the SN of aMDM *in vitro*-stimulated with exosomes isolations (qPBS, healthy, N-ERD) for 24 h. qPBS, qEV SEC-processed PBS; H, healthy; N, N-ERD; N/A, not available (due to not detectable analytes in some conditions). Data were analyzed with the Friedman test with Dunn's correction or Mann-Whitney-Wilcoxon* test (H *vs.* N: CXCL2, IL12p70): $p < 0.05$.

Appendix

Appendix I: Permission to reuse content (Figure 1.1, Figure 1.2)

Annual review of pathology

Order detail ID: 71976494
Order License Id: 4644961009829

ISSN: 1553-4014
Publication Type: e-Journal
Volume:
Issue:
Start page:
Publisher: ANNUAL REVIEWS

Permission Status: Granted

Permission type: Republish or display content
Type of use: Thesis/Dissertation

Hide details

Requestor type	Academic institution
Format	Print, Electronic
Portion	chart/graph/table/figure
Number of charts/graphs/tables/figures	2
The requesting person/organization	Pascal Haimerl
Title or numeric reference of the portion(s)	Figure 1, Figure 4
Title of the article or chapter the portion is from	Immunopathogenesis of Chronic Rhinosinusitis and Nasal Polyposis
Editor of portion(s)	N/A
Author of portion(s)	Robert P. Schleimer
Volume of serial or monograph	12
Page range of portion	333, 343
Publication date of portion	December 5, 2016
Rights for	Main product and any product related to main product
Duration of use	Life of current and all future editions
Creation of copies for the disabled	no
With minor editing privileges	yes
For distribution to	Worldwide
In the following language(s)	Original language of publication
With incidental promotional use	no
Lifetime unit quantity of new product	Up to 499
Title	Multi-omics characterization of NSAID-exacerbated respiratory disease: Altered lipid metabolism and macrophage activation
Institution name	Technical University of Munich (TUM)
Expected presentation date	Dec 2019

Note: This item will be invoiced or charged separately through CCC's **RightsLink** service. More info **$ 0.00**

Appendix II: Permission to reuse content (Figure 1.3)

REVIEW ARTICLE FREE PREVIEW

Severe and Difficult-to-Treat Asthma in Adults

Elliot Israel, M.D., and Helen K. Reddel, M.B., B.S., Ph.D.

Adults with severe asthma consume substantial human and financial resources. This review examines the biology, current diagnosis, and treatment of this multifaceted condition.

September 7, 2017
N Engl J Med 2017; 377:965-976
DOI: 10.1056/NEJMra1608969

Reuse of Content Within a Thesis or Dissertation

Content (full-text or portions thereof) may be used in print and electronic versions of a dissertation or thesis without formal permission from the Massachusetts Medical Society (MMS), Publisher of the *New England Journal of Medicine*.

The following credit line must be printed along with the copyrighted material:

> Reproduced with permission from (scientific reference citation), Copyright Massachusetts Medical Society.

J Asthma Allergy. 2011; 4: 77–86.
Published online 2011 Jun 30. doi: 10.2147/JAA.S15081
PMCID: PMC3140298
PMID: 21792321

Clinical update on the use of biomarkers of airway inflammation in the management of asthma

SJ Wadsworth,[1,2] DD Sin,[1,2] and DR Dorscheid[1,2]

▸ Author information ▾ Copyright and License information Disclaimer

Appendix III: Permission to reuse content (Figure 1.4)

ELSEVIER LICENSE
TERMS AND CONDITIONS

Aug 09, 2019

This Agreement between Pascal Haimerl ("You") and Elsevier ("Elsevier") consists of your license details and the terms and conditions provided by Elsevier and Copyright Clearance Center.

License Number	4644971401380
License date	Aug 09, 2019
Licensed Content Publisher	Elsevier
Licensed Content Publication	Journal of Allergy and Clinical Immunology
Licensed Content Title	Aspirin-exacerbated respiratory disease: Mediators and mechanisms of a clinical disease
Licensed Content Author	Katherine N. Cahill,Joshua A. Boyce
Licensed Content Date	Mar 1, 2017
Licensed Content Volume	139
Licensed Content Issue	3
Licensed Content Pages	3
Start Page	764
End Page	766
Type of Use	reuse in a thesis/dissertation
Intended publisher of new work	other
Portion	figures/tables/illustrations
Number of figures/tables/illustrations	1
Format	both print and electronic
Are you the author of this Elsevier article?	No
Will you be translating?	No
Original figure numbers	Figure 1
Title of your thesis/dissertation	Multi-omics characterization of NSAID-exacerbated respiratory disease: Altered lipid metabolism and macrophage activation
Publisher of new work	Technical University of Munich (TUM)
Expected completion date	Dec 2019
Estimated size (number of pages)	1
Requestor Location	Pascal Haimerl Biedersteinerstraße 29 Munich, other Germany Attn:
Publisher Tax ID	GB 494 6272 12
Total	0.00 EUR

Appendix IV: Permission to reuse content (Figure 1.5)

Annual review of pharmacology and toxicology

Order detail ID: 71976566
Order License Id: 4644980672553

ISSN: 1545-4304
Publication Type: e-Journal
Volume:
Issue:
Start page:
Publisher: ANNUAL REVIEWS

Permission Status: Granted

Permission type: Republish or display content
Type of use: Thesis/Dissertation

Hide details

Requestor type	Academic institution
Format	Print, Electronic
Portion	chart/graph/table/figure
Number of charts/graphs/tables/figures	1
The requesting person/organization	Pascal Haimerl
Title or numeric reference of the portion(s)	Figure 2
Title of the article or chapter the portion is from	Lipid Mediators in Health and Disease: Enzymes and Receptors as Therapeutic Targets for the Regulation of Immunity and Inflammation
Editor of portion(s)	N/A
Author of portion(s)	Takao Shimizu
Volume of serial or monograph	49
Page range of portion	127
Publication date of portion	October 3, 2008
Rights for	Main product and any product related to main product
Duration of use	Life of current and all future editions
Creation of copies for the disabled	no
With minor editing privileges	yes
For distribution to	Worldwide
In the following language(s)	Original language of publication
With incidental promotional use	no
Lifetime unit quantity of new product	Up to 499
Title	Multi-omics characterization of NSAID-exacerbated respiratory disease: Altered lipid metabolism and macrophage activation
Institution name	Technical University of Munich (TUM)
Expected presentation date	Dec 2019

Note: This item will be invoiced or charged separately through CCC's **RightsLink** service. More info **$ 0.00**

Appendix V: Permission to reuse content (Figure 1.6)

SPRINGER NATURE LICENSE TERMS AND CONDITIONS	
Aug 09, 2019	
This Agreement between Pascal Haimerl ("You") and Springer Nature ("Springer Nature") consists of your license details and the terms and conditions provided by Springer Nature and Copyright Clearance Center.	
License Number	4644981420310
License date	Aug 09, 2019
Licensed Content Publisher	Springer Nature
Licensed Content Publication	Nature Reviews Molecular Cell Biology
Licensed Content Title	Sphingolipids and their metabolism in physiology and disease
Licensed Content Author	Yusuf A. Hannun, Lina M. Obeid
Licensed Content Date	Nov 22, 2017
Licensed Content Volume	19
Licensed Content Issue	3
Type of Use	Thesis/Dissertation
Requestor type	academic/university or research institute
Format	print and electronic
Portion	figures/tables/illustrations
Number of figures/tables/illustrations	1
High-res required	no
Will you be translating?	no
Circulation/distribution	<501
Author of this Springer Nature content	no
Title	Multi-omics characterization of NSAID-exacerbated respiratory disease: Altered lipid metabolism and macrophage activation
Institution name	Technical University of Munich (TUM)
Expected presentation date	Dec 2019
Portions	Figure 1
Requestor Location	Pascal Haimerl Biedersteinerstraße 29 Munich, other Germany Attn:
Total	0.00 EUR

Appendix VI: Permission to reuse content (Figure 1.7)

Annual review of cell and developmental biology

Order detail ID:	71976726
Order License Id:	4645200892798
ISSN:	1530-8995
Publication Type:	e-Journal
Volume:	
Issue:	
Start page:	
Publisher:	ANNUAL REVIEWS
Author/Editor:	ANNUAL REVIEWS, INC

Permission Status: Granted

Permission type: Republish or display content
Type of use: Thesis/Dissertation

Hide details

Requestor type	Academic institution
Format	Print, Electronic
Portion	chart/graph/table/figure
Number of charts/graphs/tables/figures	1
The requesting person/organization	Pascal Haimerl
Title or numeric reference of the portion(s)	Figure 1
Title of the article or chapter the portion is from	Biogenesis, Secretion, and Intercellular Interactions of Exosomes and Other Extracellular Vesicles
Editor of portion(s)	N/A
Author of portion(s)	Marina Colombo, Graça Raposo and Clotilde Théry
Volume of serial or monograph	30
Page range of portion	258
Publication date of portion	August 21, 2014
Rights for	Main product and any product related to main product
Duration of use	Life of current and all future editions
Creation of copies for the disabled	no
With minor editing privileges	yes
For distribution to	Worldwide
In the following language(s)	Original language of publication
With incidental promotional use	no
Lifetime unit quantity of new product	Up to 499
Title	Multi-omics characterization of NSAID-exacerbated respiratory disease: Altered lipid metabolism and macrophage activation
Institution name	Technical University of Munich (TUM)
Expected presentation date	Dec 2019

Note: This item will be invoiced or charged separately through CCC's **RightsLink** service. More info **$ 0.00**

Acknowledgements

First, I would like to thank my main supervisor and mentor **PD Dr. Julia Esser-von Bieren** for her tremendous support throughout my whole PhD, starting even before my very first day at ZAUM and even now in "overtime"! I really appreciate your leadership style and enormous financial backing, which allows all of us PhD students to advance forward in this complex world of science on our own, but always with excellent guidance whenever we need it. Even in times when experimental outcomes looked dim, you showed me new ways of how to interpret the data – encouraging me to push forward and ultimately become the scientist I am today. You have my deepest respect for your endurance, expertise, creativity, writing and grant winning skills as well as work-life-balance mentality. I wish you to achieve all your scientific goals and hope that I have been able to satisfactorily contribute to them :)!

Next, I want to thank my thesis advisors **Prof. Dr. Carsten Schmidt-Weber**, head of ZAUM/IAF, and **Prof. Dr. Matthias Feige** for their critical and supportive guidance that enhanced the quality of this study.

PD Dr. Adam Chaker – the. best. ENT. physician. – you have been a major key to everything. I want to thank you very much for all your effort in providing critical, scarce samples, scientific and medical expertise and several invitations to symposia and the clinic itself! Thanks to you, I have been able to get to know and work with Jana and Ulrike, which was challenging, fun and educating at the same time.

Thus, I want to thank you, **Ulrike**, for surviving being "my" MD student, your hard work in recruiting and sampling patients and your eagerness for knowledge and strong support in the lab. I really liked working with you and wish you all the best!

Major parts of this study could not have been performed without the support of collaboration partners: **Prof. Dr. Jerzy Adamski, Conny, Mark, Alex, Silke** from the GAC HGMU, **Rachel** from the EMBL, **Susi** and **Stephie** from AG Feige TUM, **Dominique** from the ZAFES, **PD Dr. Simone Moertl, Lisa M.** and **Rosi** from the ISB HGMU.

I have been really fortunate to work at ZAUM, a particularly excellent institute with top class scientists in the field of allergy, immunology, airway and skin diseases and pollen, but comfortable and happy-to-be-employed-here working environment. I enjoyed working at ZAUM a lot and want to hereby thank everyone that supported me non- and scientifically throughout my PhD: **Uli Z., Constanze, Lynn, Lisa, Antonia, Marlene, Steffi, Manja, Jenny, Felix, Natalie, Jana, Kerstin W., Kerstin P., Veronika, Caro, Alex, David, Francesca, Evelyn, Jeroen, Jose, Gudrun, Elke, Christine, Cordula, Yi-Ting, Caspar, Renske, Anna-Lena, Johanna, Joana + Ferdi, Sabrina, Katharina, Danijel, Myriam** and **Frau Pilz**! (Since this list is not doing you justice, I will thank you all personally after my defense.)

Right at the end of my study, I was granted the opportunity to dive into the world of R and bioinformatics thanks to **Xavier**. It was fun to work with and getting mentored by you – a great and rewarding experience indeed!

AG EvB and office 0.05: **Julia, Sonja, Toni, Marta, Fiona, Sina, Uli and Shu**… …it definitely was **N I C E** :)! And since some sentences on page 170 of a thesis that will rarely be read cannot express my gratitude for all of you, I already have a better ending for us in mind. Time will tell!

Zu guter Letzt möchte ich meiner Familie (**MaPaOlRe + Martha-Mücke-Combo**) und dir, **Lisa – 愛してるよ！**, von Herzen für Eure Unterstützung und Geduld danken! Ohne Euch wäre alles doch ziemlich doof!

In Gedenken an **Omi**.